



Eveline Brodl, BSc MSc

**A short story of living lights:
Functional studies on the role of LuxF and flavin derivatives in
bacterial bioluminescence**

DISSERTATION

zur Erlangung des akademischen Grades

Doktorin der Naturwissenschaften

eingereicht an der

Technischen Universität Graz

Betreuer

Univ.-Prof. Mag. rer. nat. Dr. rer. nat. Peter Macheroux

Institut für Biochemie

EIDESSTATTLICHE ERKLÄRUNG

Ich erkläre an Eides statt, dass ich die vorliegende Arbeit selbstständig verfasst, andere als die angegebenen Quellen/Hilfsmittel nicht benutzt, und die den benutzten Quellen wörtlich und inhaltlich entnommenen Stellen als solche kenntlich gemacht habe. Das in TUGRAZonline hochgeladene Textdokument ist mit der vorliegenden Dissertation identisch.

Datum

Unterschrift

Abstract

Bioluminescence is the production of light by living organisms. The enzymes encoded by the *lux* operon, with the gene order *luxCDABE(G)*, catalyze a cascade of reactions enabling cold light emission. The *luxA* and *luxB* genes encode the α - and β -subunits, respectively, of the enzyme luciferase. *LuxC*, *luxD* and *luxE* constitute the fatty acid reductase complex, responsible for the synthesis of the long-chain aliphatic aldehyde substrate and *luxG* encodes a flavin reductase. In bioluminescent bacteria, the heterodimeric luciferase catalyzes the monooxygenation of long-chain aliphatic aldehydes to the corresponding acids utilizing reduced flavin mononucleotide (FMNH₂) and molecular oxygen. The energy released as a photon results from an excited state flavin-4a-hydroxide, emitting light centered around 490 nm. Some photobacterial strains carry the additional gene *luxF* with the altered gene order *luxCDABFEG*. The exact role of *luxF* and its encoded protein LuxF is still uncertain. However, crystallographic analysis of LuxF revealed the presence of four molecules of a flavin derivative, *i.e.* 6-(3'-(R)-myristyl) FMN (myrFMN), non-covalently bound to the homodimer. This molecule combines two components of the bioluminescent reaction, FMN and a long-chain aliphatic acid.

The elucidation of the role of *luxF* and LuxF and its bound flavin derivative in light emission was the main focus of my work. As a first step, I have evaluated the substrate scope of a bacterial luciferase and tried to relate substrate preferences as a potential determinant for myrFMN formation. Even numbered saturated and α,β -unsaturated aldehydes with eight, ten, twelve and fourteen carbon atoms were examined as potential substrates *in vitro*. Both saturated and unsaturated aldehydes were accepted as substrates, while those with longer chain lengths had higher activity in terms of total bioluminescent light emission than shorter chain lengths. Nevertheless, the mechanism of the flavin derivative formation remained obscure. Further in-depth analysis revealed that myrFMN is produced as a side product of the luciferase-catalyzed reaction. Based on these findings a reaction mechanism for generation of this flavin derivative was postulated. Additionally, it was elucidated that apo-LuxF captures myrFMN and thereby relieves the inhibitory effect on luciferase activity. This suggested that LuxF acts as a scavenger of myrFMN in bioluminescent bacteria. Novel insights into the role of LuxF in bioluminescent light emission were gained via application of an *E. coli* based *lux-rib* expression system where the *lux-rib* operon of *Photobacterium leiognathi* subsp. *mandapamensis* 27561 was cloned into a single expression vector, which allowed the heterologous expression of the complete *lux* operon. To evaluate this novel bioluminescence expression system, a plate reader assay that combines recording of cell growth and bioluminescent light emission intensity over time was developed. Comparing *E. coli* based *lux-rib* expression system with or without *luxF* revealed that the presence of *luxF* enhances light intensity by a factor of 1.5. Furthermore, isolation and analysis by UV/Vis absorption and NMR spectroscopy as well as mass spectrometry of the flavin derivative revealed the presence of more than just the previously investigated myrFMN and led to the discovery of three different flavin derivatives with different alkyl chains.

Zusammenfassung

Biolumineszenz ist die enzymatische Lichtproduktion durch lebende Organismen. Die Enzyme, welche im *lux* Operon kodiert sind und die Genabfolge *luxCDABE(G)* besitzen, katalysieren eine Kaskade von Reaktionen, um die sogenannte „kalte Lichtemission“ zu ermöglichen. Die Gene *luxA* und *luxB* kodieren für die α - und β -Untereinheiten des Enzymes Luziferase. *LuxC*, *luxD* und *luxE* bilden den Fettsäuresynthetekomplex, der für die Bereitstellung der langkettigen, aliphatischen Aldehyde als Substrate zuständig ist. *LuxG* kodiert für die Flavinreduktase. In biolumineszenten Bakterien katalysiert die heterodimere Luziferase die Oxidation von langkettigen, aliphatischen Aldehyden zu den korrespondierenden Säuren. Dafür wird reduziertes Flavinmononucleotid (FMNH₂) und molekularer Sauerstoff benötigt. Die Energie, die als Photon frei wird, kommt von einem Flavin-4a-hydroxid im angeregten Zustand. Das emittierte Licht hat sein Maximum bei 490 nm. Manche Photobakteriumstämme besitzen das zusätzliche Gen *luxF* und daher eine geänderte Genabfolge von *luxCDABFEG*. Die genaue Funktion dieses Gens und des kodierten Proteins LuxF ist noch unbekannt. Jedoch zeigte die röntgenkristallographische Struktur von LuxF, dass vier Moleküle eines Flavinderivates, nämlich 6-(3'-(R)-myristyl) FMN (myrFMN), nicht kovalent im LuxF-Homodimer gebunden sind. Dieses Molekül kombiniert zwei Komponenten der biolumineszenten Reaktion, FMN und eine langkettige, aliphatische Säure.

Das Hauptaugenmerk meiner Arbeit war der Aufklärung der Funktion des Gens *luxF*, dem Protein LuxF und dem von LuxF gebundenen Flavinderivat gewidmet. Zu Beginn wurde die Luziferase auf ihre Substratspezifität getestet, um Hinweise über die Entstehung dieses Flavinderivates zu erhalten. Geradzahlige, gesättigte und ungesättigte Aldehyde mit acht, zehn, zwölf und vierzehn Kohlenstoffatomen wurden als potentielle Substrate *in vitro* getestet. Sowohl gesättigte als auch ungesättigte Aldehyde wurden als Substrate akzeptiert, wobei jene mit einer längeren Kettenlänge höhere Aktivität bezüglich der absoluten Lichtemission zeigten, als jene mit kürzerer Kettenlänge. Dennoch blieb der Reaktionsmechanismus zur Bildung des Flavinderivates ungeklärt. Weitere ausführliche Analysen zeigten, dass myrFMN als Nebenprodukt der Luziferase-katalysierten Reaktion entsteht. Aufgrund dessen wurde ein möglicher Reaktionsmechanismus für die Entstehung von myrFMN postuliert. Zusätzlich konnte eruiert werden, dass apo-LuxF in der Lage ist, frei vorliegendes myrFMN zu binden und damit einhergehend die Inhibierung der Luziferaseaktivität durch dieses Molekül unterbunden werden kann. Neue Erkenntnisse zu LuxF konnten durch die Etablierung eines *E. coli* basierenden *lux-rib* Expressionssystems gewonnen werden. Dabei wurde das *lux-rib* Operon von *Photobacterium leiognathi* subsp. *mandapamensis* 27561 in einen Expressionsvektor kloniert, welcher die heterologe Expression aller *lux* Operon Gene ermöglichte. Um dieses neue Expressionssystem evaluieren zu können, wurde eine Messmethode für ein Plattenlesegerät entwickelt, welche Messungen der Zelldichte und der Lichtintensität über einen längeren Zeitraum koppelt. Bei dem Vergleich zweier *E. coli* basierenden *lux-rib* Operon Expressionssysteme, eines mit *luxF* und eines ohne *luxF*, konnte bei Anwesenheit von *luxF* eine Steigerung der Lichtintensität um das 1.5-fache beobachtet werden. Nachfolgende Analysen der isolierten Flavinderivate

mittels UV/Vis Absorptions- und NMR-Spektroskopie als auch Massenspektrometrie zeigten nicht nur die Präsenz des bereits untersuchten myrFMNs, sondern auch insgesamt drei verschiedene Flavinderivate mit unterschiedlicher Länge beziehungsweise Struktur der Alkylkette.

Acknowledgement

Zu aller erst möchte ich mich bei Peter Macheroux bedanken, da er mir einerseits die Möglichkeit gegeben hat an seinem Institut meine Doktorarbeit zu diesem spannenden und abwechslungsreichen Thema der bakteriellen Biolumineszenz durchzuführen und andererseits ein Umfeld geschaffen hat, wo man wachsen und lernen kann, sich immer wieder neuen Herausforderungen stellt und stets den nächsten Schritt wagt. Seine konstruktive Kritik und hilfreichen Kommentare lassen einen über sich hinaus wachsen.

Großer Dank gebührt auch allen Kooperationspartnern, die mich auf meinem Weg die letzten viereinhalb Jahre begleitet haben und mir immer wieder geholfen und mich unterstützt haben. In diesem Zusammenhang möchte ich mich bei Rolf Breinbauer, Karl Gruber, Stefan Schild und Hans-Jörg Weber herzlich bedanken. Das Doktoratskolleg „Molecular Enzymology“ hat es mir durch die großzügige, finanzielle Unterstützung unter anderen ermöglicht viele unterschiedliche Konferenzen zu besuchen und vor Ort meine Daten zu präsentieren und meinen Horizont zu erweitern.

Dieses Projekt wäre natürlich nicht so weit fortgeschritten ohne die Vorarbeit und Hilfe von Steve Stipsits, Thomas Bergner und Chaitanya Tabib. In diesem Zusammenhang möchte ich auch Andreas Winkler danken, der das Projekt schon länger begleitet und regelmäßig Hilfestellungen gibt und vor allem beim kürzlich publizierten Review Pionierarbeit geleistet hat. Für die Unterstützung im Labor und bei Fragen, die vor allem die organische Synthese und Analyse betreffen, möchte ich mich bei Jakov Ivkovic, Kathrin Heckenbichler und Gernot Strohmeier bedanken.

Ohne die große Unterstützung von meinen zwei überaus motivierten Studentinnen Christina Horn und Alexandra Csamay wäre ich vor allem im letzten Jahr meiner Dissertation nicht so weit gekommen und daher ein großes Dankeschön an die beiden. Wir hatten und haben immer sehr viel Spaß im Labor und ich wünsche euch das Beste, nicht nur für eure wissenschaftliche Zukunft, und möge euch die Freude an der Forschung erhalten bleiben.

Ich möchte mich natürlich für die Unterstützung aller Arbeitsgruppen bedanken, die früher oder später Teil des Institutes waren oder sind: AG Hermetter, AG Daum, AG Straganz, AG Murkovic, AG Winkler, AG Oberdorfer und natürlich im Speziellen AG Macheroux.

Bei all der Unterstützung im und rund um das Labor, möchte ich auf keinen Fall die Personen missen, die mich vor allem abseits des Arbeitstrubels unterstützt und aufgebaut haben. Meine Freunde und Studienkollegen, bei denen ich mir den Frust von der Seele reden konnte, mich auf andere Gedanken brachten und bei denen ich immer Rat suchen konnte: vielen Dank an Birgit, Christoph, Marko, Wolfi, Mitch, Vera, Flo, Daniela, Stefan und David!

Ein riesengroßes Dankeschön geht an Johannes. Wir haben gemeinsam ein Projekt verwirklicht, das meine Arbeit einen großen Schritt vorwärts brachte. Vielen Dank für die tolle Zusammenarbeit und deine Hilfsbereitschaft in und abseits der Arbeit. Danke für die Geduld, die vielen Erklärungen und Diskussionen zu wissenschaftlichen Themen und die Unterstützung vor allem auch auf den letzten Schritten zu dieser Arbeit.

Besonderer Dank gilt meinen Eltern, die immer für mich da sind und alle Höhen und Tiefen hautnah miterlebten. Danke für die Geduld, Hilfsbereitschaft und Toleranz. Danke, dass ich immer das machen durfte, was ich wollte und mir Spaß gemacht hat und dass mir alle Lebenswege offen standen und noch immer stehen. Im Zuge dessen möchte ich mich auch bei meinen Großeltern bedanken, die diese Einstellung teilen und mittragen und mich auch immer unterstützt haben.

In der Hoffnung niemanden vergessen zu haben, vielen Dank an alle!

Preface and Thesis Outline

Bioluminescence has mesmerized scientists over decades and still has not lost its fascination. Especially bacterial bioluminescence has a very long history in scientific research. Nevertheless, many questions remain to be answered. This PhD thesis tries to elucidate a small part of the mechanism behind cold light emission. The focus lies on LuxF and its tightly bound 6-(3'-(*R*)-myristyl) flavin adenine mononucleotide (myrFMN). The role of this homodimeric protein and attached flavin derivative will be discussed in further detail in the following chapters. This PhD thesis is written in a cumulative fashion. The first four chapters are already published or accepted in peer-reviewed journals. The last chapter represents an exception and was prepared as a manuscript for possible publication in the near future.

Chapter I provides an introduction to the field of bacterial bioluminescence. It gives a general overview on genetic, ecologic, phylogenetic, mechanistic and structural level of the complex machinery enabling cold light emission in bioluminescent bacteria. Furthermore, a theoretical model of the fatty acid reductase complex was established.

Chapter II deals with the synthesis of unsaturated long chain fatty aldehydes and their application as possible substrates for various bacterial luciferases. It is well established that various chain lengths are accepted by bacterial luciferases but only even numbered saturated aliphatic aldehydes gave high light intensities. This chapter tries to elucidate the activity achieved with unsaturated aldehydes as substrates for bacterial luciferase.

Chapter III analyzes the putative side product of the bacterial bioluminescent reaction, namely myrFMN. Combining *in vivo* and *in vitro* measurements revealed its function as inhibitor of the luciferase. Additionally, the first HPLC-MS analysis of this uncommon flavin derivative confirmed the structure of the molecule.

Chapter IV describes the development of a dual measurement of cell density and bioluminescence intensity over longer time periods in a plate reader. Additionally, a *lux* gene expression system in *E. coli* combining all ten genes of the *lux-rib* operon in one vector was established. This enables easy and simple comparison of different *lux* operons of bacterial bioluminescent strains and their growth behavior and light intensity.

Chapter V summarizes the last results collected in the laboratory. Focusing on the *luxF* gene and its possible influence on light intensity, the established *lux* gene expression system in *E. coli* was utilized. Preparing one strain containing *luxF* and one strain without *luxF* enabled the direct comparison of this gene on growth behavior and light production of bioluminescent bacteria. Furthermore, these *E. coli* cultures were analyzed concerning their amount of produced side product myrFMN and made isolation of the flavin derivative applicable. Subsequent HPLC and NMR analyses confirmed the structure of myrFMN and even revealed two other flavin derivatives.

List of contents

ABSTRACT	I
ZUSAMMENFASSUNG	II
ACKNOWLEDGEMENT	IV
PREFACE AND THESIS OUTLINE	VI
LIST OF CONTENTS	VII
I. MOLECULAR MECHANISMS OF BACTERIAL BIOLUMINESCENCE	2
1.1. ABSTRACT	2
1.2. INTRODUCTION	3
1.3. ECOLOGY	4
1.4. PHYLOGENY	6
1.5. THE <i>LUX</i> OPERON	7
1.6. ENZYMES AND REACTION MECHANISMS IN BACTERIAL BIOLUMINESCENCE	8
1.7. STRUCTURE-FUNCTION RELATIONSHIPS	14
1.8. CONCLUSIONS	31
1.9. REFERENCES	33
1.10. SUPPLEMENTARY INFORMATION	42
II. SYNTHESIS OF α,β-UNSATURATED ALDEHYDES AS POTENTIAL SUBSTRATES FOR BACTERIAL LUCIFERASES	45
2.1. ABSTRACT	45
2.2. INTRODUCTION	46
2.3. MATERIALS AND METHODS	49
2.4. RESULTS	58
2.5. DISCUSSION	64
2.6. CONCLUSION	65
2.7. REFERENCES	66
2.8. SUPPLEMENTARY DATA	68
III. EVIDENCE FOR THE GENERATION OF MYRISTYLATED FMN BY BACTERIAL LUCIFERASE	85
3.1. ABSTRACT	85
3.2. INTRODUCTION	86
3.3. EXPERIMENTAL PROCEDURES	88
3.4. RESULTS	92

3.5. DISCUSSION	98
3.6. REFERENCES	102
3.7. SUPPORTING INFORMATION	104
<u>IV. <i>IN SITU</i> MEASUREMENT AND CORRELATION OF CELL DENSITY AND LIGHT EMISSION OF BIOLUMINESCENT BACTERIA</u>	109
4.1. ABSTRACT	110
4.2. INTRODUCTION	111
4.3. PROTOCOL	113
4.4. REPRESENTATIVE RESULTS	117
4.5. DISCUSSION	125
4.6. REFERENCES	128
4.7. SUPPLEMENTAL MATERIAL	130
<u>V. THE IMPACT OF LUXF ON LIGHT INTENSITY IN BACTERIAL BIOLUMINESCENCE</u>	134
5.1. ABSTRACT	134
5.2. INTRODUCTION	135
5.3. MATERIALS AND METHODS	136
5.4. RESULTS	139
5.5. DISCUSSION	144
5.6. CONCLUSION	145
5.7. REFERENCES	147
5.8. SUPPLEMENT	151
<u>VI. CONCLUSION AND OUTLOOK</u>	158
<u>VII. LIST OF ABBREVIATIONS</u>	162
<u>VIII. CONTRIBUTIONS</u>	164
<u>IX. LIST OF PUBLICATIONS</u>	166
<u>X. CURRICULUM VITAE</u>	168

Chapter I

Molecular Mechanism of Bacterial Bioluminescence

Parts of this chapter were submitted for a special issue on Biochemistry and Biophysics in the Computational and Structural Biotechnology Journal, volume 16, pages 551-564 and this review article is available online since November 15th, 2018 (<https://doi.org/10.1016/j.csbj.2018.11.003>).

I. MOLECULAR MECHANISMS OF BACTERIAL BIOLUMINESCENCE

*Eveline Brodl, Andreas Winkler and Peter Macheroux**

Institute of Biochemistry, Graz University of Technology, Graz, Austria

* Corresponding Author: Peter Macheroux, Institute of Biochemistry, Graz University of Technology. Email: peter.macheroux@tugraz.at.

Keywords

bacterial bioluminescence, luciferase, *lux* operon, structure-function relationships, fatty acid reductase complex, luciferin, FMN

1.1. ABSTRACT

Bioluminescence refers to the production of light by living organisms. Bioluminescent bacteria with a variety of bioluminescence emission characteristics have been identified in *Vibrionaceae*, *Shewanellaceae* and *Enterobacteriaceae*. Bioluminescent bacteria are mainly found in marine habitats and they are either free-floating, sessile or have specialized to live in symbiosis with other marine organisms. On the molecular level, bioluminescence is enabled by a cascade of chemical reactions catalyzed by enzymes encoded by the *lux* operon with the gene order *luxCDABEG*. The *luxA* and *luxB* genes encode the α - and β -subunits, respectively, of the enzyme luciferase producing the light emitting species. *LuxC*, *luxD* and *luxE* constitute the fatty acid reductase complex, responsible for the synthesis of the long-chain aldehyde substrate and *luxG* encodes a flavin reductase. In bacteria, the heterodimeric luciferase catalyzes the monooxygenation of long-chain aliphatic aldehydes to the corresponding acids utilizing reduced FMN and molecular oxygen. The energy released as a photon results from an excited state flavin-4a-hydroxide, emitting light centered around 490 nm. Advances in the mechanistic understanding of bacterial bioluminescence have been spurred by the structural characterization of proteins encoded by the *lux* operon. However, the number of available crystal structures is limited to LuxAB (*Vibrio harveyi*), LuxD (*Vibrio harveyi*) and LuxF (*Photobacterium leiognathi*). Based on the crystal structure of LuxD and homology models of LuxC and LuxE, we provide a hypothetical model of the overall structure of the LuxCDE fatty acid reductase complex that is in line with biochemical observations. Although, bacterial bioluminescence has been studied for a long time, several issues remain elusive. Therefore, further investigations of proteins involved in this fascinating process shall shed light on these remaining enigmas.

1.2. INTRODUCTION

Bioluminescence is the phenomenon of light emission that results from an enzyme-catalyzed oxidation reaction in living organisms. Bioluminescence can be found in nearly all kingdoms of life with a variety of luciferases and luciferins, the enzymes and light-emitting molecule involved in light emission, respectively. Consequently, the spectral range of light emission of bioluminescent organisms spans from ca. 400 to 700 nm, *i.e.* from blue to red light. Varieties of blue are the most common colors in light emission followed by green. Only very few species emit violet, yellow, orange or red light. The reason for this color preference relates to the predominant environment of bioluminescent organisms, mainly living in the seawater, which can best be penetrated by blue light (λ_{\max} ca. 475 nm) [1].

One component that nearly all bioluminescent reactions have in common is the dependence on oxygen. While molecular oxygen is used as an oxidizing agent in all cases, different biochemical reactions are catalyzed and various molecules are employed as luciferins. In fact, the enzymes involved in formation of excited state luciferins, the luciferases from evolutionary distant organisms, are neither related at the gene nor the protein sequence level [2]. As the individual mechanisms of the various bioluminescent systems strongly differ from each other, this review is focussed on bacterial bioluminescence.

In principle, the biological functions of bioluminescence can be categorized into four major groups: defense, counterillumination, prey attraction and intraspecific communication [1,3]. There are several known strategies for utilizing bioluminescence as defense mechanism. A bright flash of light can startle predators, causing them to hesitate. Some animals produce clouds or particles of light that distract or blind a predator. Bioluminescence can be used as burglar alarm marking their predators with luminescent slime, making them easy targets for secondary predators. In general, glowing tissue in the deep sea can draw attention to predators, making it risky to consume bioluminescent prey. Counterillumination is a special form of camouflage. Many predators in the midwater have upwardly directed eyes to search for silhouettes. Animals that are producing light that is comparable in color, intensity and angular distribution to down welling ambient light are disappearing from the predator's vision. Prey attraction is most prominent in fish, especially the diverse anglerfishes, which have bacterial cultures in their light organs. By altering the conditions in the light organ they control the bacteria leading to emission of light. Communication within species is another well-known function of bioluminescence to attract a mate [1,3].

However, the purpose of bioluminescence for marine bacteria is still obscure. The possible biological advantages of light emission can be diverse, since bioluminescent bacteria can be free-floating, colonizing the skin of marine animals as saprophytes, living in their intestine as commensal enteric symbionts or in their tissues and body fluids as parasites. One observation revealed that luminous bacteria associated with fecal pellets in the mid-depths of the ocean are involved in nutrition turnover. Various fishes are attracted to the luminous fecal debris, which is then consumed. The bacteria are ingested and transferred to the gut

where they find a nutrition rich environment to proliferate. After excretion, the luminous bacterial culture is associated with fecal pellets again, restarting the proliferation-cycle [1,4,5].

Another observation showed that some bioluminescent bacteria form a specific symbiosis with several families of marine fish or squids colonizing extracellular light organs [2]. For luminous bacteria living in symbiosis, the fish has the advantage of using the light emission for its purposes while the bacteria are provided with nutrition and an ideal growth environment [1]. In contrast, only few species were found in freshwater (*e.g.*, *V. albensis*) or terrestrial habitats (*e.g.*, *Photorhabdus* species as symbionts of entomopathogenic nematodes) [2,6]. Although the habitat and the main function of light emission might be different, all luminous bacteria are gram negative, motile, rod-shaped and facultative anaerobic [7]. Beijerinck was the first to categorize them into the genus *Photobacterium* [8]. With new bioluminescent bacteria being isolated and due to the advancements in analyzing and determining various genera, a new taxonomy and phylogeny was necessary [9].

1.3. ECOLOGY

As mentioned above bioluminescent bacteria can live in symbiosis with certain marine fish or squids in so called light organs. Light organs or photophores are composed of specialized cells called photocytes [1,11]. The cell density in light organs of host fishes is very high (up to 10^9 to 10^{11} cells per mL) leading to limitations in oxygen and nutrition consumption following a very slow growth rate but high luminescence levels of bioluminescent bacteria [2,4]. Different physiological adaptations, complex optical components or specialized muscles in hosts help them to use the light emission properly and adjust the waveband and angular distribution by reflection, refraction, filtering or scattering [1,4]. So far, only three species of *Aliivibrio* (*A. fischeri*, *A. sp. thorii*, *A. wodanis*) and three species of *Photobacterium* (*P. leiognathi*, *P. mandapamensis*, *P. kishitanii*) and a newly investigated symbiont of flashlight fishes (*Candidatus Photodesmus katoptron*) were found to form bioluminescent symbiosis with marine organisms [12–14].

In this context, the hypothesis of “host family bacterial species specificity” was analyzed in more detail. Fishes and squids that are living in symbioses with bacterial cultures were believed to constantly harbor the same bacterial species in their light organs and that even coevolution and codivergence was involved in their further development. However, it has to be taken into account that bioluminescent symbiosis is very different from other symbiotic associations or even endosymbiotic relationships. Endosymbiosis is an obligate association of the symbiont with the host leading to coevolutionary events and reduction and loss in the genome of the symbiont and bacterial cultures are maternally transferred to the next generation. Luminous bacteria that undergo symbiosis are not dependent on their animal hosts; they can survive in various habitats, as mentioned above, even as free-living bacteria. Another major difference concerns the selection and acquirement of the bacterial species by

the respective host where each new generation takes up bacteria from the environment externally. Strict host-symbiont specificity would favor coevolution and a genetic basis of the host in selecting its “native” symbiont. However, the analysis of various host symbiont species has not provided any evidence for codivergence. Alternatively, it was hypothesized that the environment, the depth, the geographic location, the temperature and the relative density of symbiotic bacterial cultures in the surrounding of an aposymbiotic juvenile host plays a major role in the acquisition of bacterial species colonizing the nascent light organ. This environmental congruence would correlate with the species distribution in the ocean depending on the temperature, salinity, nutrition availability and incident light intensity [4]. Furthermore, there seems to be a correlation between the habitat of host fishes and the optimal growth temperatures of symbiotic bioluminescent bacteria leading to symbiosis when both partners are living in the same depth of the sea [2,9,15–17].

Additional evidence for this concept arose with the determination of cosymbiosis in light organs. Cosymbiosis of two species within the same light organ of a host fish was rarely observed, but one of these rare examples is the coexistence of *P. leiognathi* and *P. mandapamensis*, which were found to be symbionts in *Acropoma japonicum*, *Photopectoralis bindus* and *Photopectoralis panayensis*. The absence of codivergence indicated that animals from the same species can accumulate different bacterial species in their light organ [9,15].

More recently, a possible exception to this concept was reported. The bacterium *Candidatus Photodesmus katoptron* from the flashlight fish *Anomalops katoptron* seems to be an obligate mutualistic symbiont. Genome sequence analysis of this bacterium revealed a reduced genome size and loss of various essential genes, especially involved in amino acid synthesis and energy metabolism, correlating with the obligate host dependence hypothesis [13,14]. Another exception might be the light organ symbionts of *Secutor indicus*. This fish harbors mainly *Photobacterium leiognathi* in its light organ with a single *lux-rib* operon, excluding species with two *lux-rib* operons. This discrimination between symbionts seems to rely rather on the exclusion of some species than a positive selection of a specific strain [18]. In the future, for a more detailed analysis of this unique symbiosis behavior, further bioluminescent symbiotic bacteria have to be extracted, cultivated and classified.

1.4. PHYLOGENY

With every new bioluminescent bacterium discovered, isolated and characterized, reclassification, new taxonomy and phylogeny was necessary [9]. So far, luminous bacteria have been found among three families, namely *Vibrionaceae*, *Shewanellaceae* and *Enterobacteriaceae*, within five main genera *Vibrio*, *Photobacterium*, *Aliivibrio*, *Photorhabdus* and *Shewanella* [2,6,10]. New genomic and phylogenetic characterizations and classifications of various bioluminescent strains in the last two decades have been achieved by Dunlap, Ast, Urbanczyk and coworkers. Genomic profiling with repetitive element palindromic PCR (rep-PCR) and the multilocus phylogenetic analysis of 16S *rRNA*, *gyrB*, *gapA*, *pyrH*, *recA*, *rpoA* and many more proved to be effective methods for determining phylogeny of closely related bacteria. Additionally, sequence analysis of *lux* genes and their intergenic spacer regions provided higher resolution in phylogenetic analyses. These classifications led to the introduction of new clades for bioluminescent bacteria.

Analysis of various strains represented in three species, *Aliivibrio*, *Photobacterium* and *Vibrio*, indicated that horizontal gene transfer (HGT) of *lux* genes is rare and therefore not contributing to species variation. Thus, vertical gene transfer with multiple losses of *lux* genes is a more likely scenario. There are only a few exceptions reported, where horizontal gene transfer might explain phylogenetic relationships of different strains [10]. Some of them will be listed here. Only very few *Vibrio cholerae* strains possess the *lux* genes and are luminous. In the species of *Vibrio vulnificus*, a human pathogen, only one single strain, *V. vulnificus* VVL1 (ATCC 43382), possesses the *lux* genes and thus is capable of producing light. Another species with only a few bioluminescent representatives is *Vibrio chagasii*. Only *V. chagasii* 21N-12 and *V. chagasii* SB-52 are luminous and their *lux* genes are closely related to *V. harveyi* and *V. splendidus*, respectively. *Vibrio damsela* BT-6 seems to have gained the *lux* gene via horizontal gene transfer of the *lux-rib₂* operon of *P. leiognathi*. Furthermore, the second *lux-rib* operon of *P. mandapamensis* is highly related to *P. leiognathi* [10].

Establishing new clades and taxonomical categorization of new bacteria leads to a better understanding of relationships and origins in bioluminescent bacteria. However, the reclassification and renaming of various bioluminescent strains may lead to confusion as previously collected data of one strain and newly determined characteristics of another strain may in fact become features of the same bacterium. One of the largest reclassifications was undertaken in 2009. The *Vibrio fischeri* clade was renamed *Aliivibrio* with four species, namely *Aliivibrio fischeri*, *Aliivibrio logei*, *Aliivibrio salmonicidas* and *Aliivibrio wodanis* [12,19]. As a next step complete genome sequencing and comparative genomic analysis led to further comparison of relationships and reclassifications of strains [20–22]. As a matter of fact, establishment of new clades and reclassification of luminous bacteria is still ongoing.

1.5. THE *LUX* OPERON

Despite classification into three families, all bioluminescent bacteria share the genes coding for the proteins responsible for light emission. The enzymes involved in bacterial bioluminescence are encoded in an operon with a single promoter. The gene order is conserved over various bacterial strains with the core sequence *luxCDABE* [2]. Due to various species harboring the *lux* operon and being capable of cold light emission, it was assumed that bioluminescence evolved independently at least 40 times [1,3]. Another hypothesis is that the *lux* operon arose once in the evolutionary past and that all genes have a common ancestor. Due to vertical gene transfer, gene duplications, losses and new recruitments, the constellations found today have evolved [2,6,9]. A schematic representation of different *lux* operons summarizes the gene architectures, where sequence information is available so far (Figure 1).

Additionally, Supplementary Table 1 lists all bioluminescent bacterial strains, where DNA and protein sequences of most genes of the *lux* operon are available. Starting from *Photobacterium leiognathi* subsp. *mandapamensis* ATCC 27561, where the gene sequence of the whole *lux-rib* operon is known, extensive BLAST searches on NCBI were performed to find all obtainable bioluminescent bacterial strains with the core genes *luxCDABE*. All obtained strains were reanalyzed in order to identify all related sequences and after rigorous evaluation, 49 bioluminescent bacterial strains remained, as listed in Supplementary Table 1. The bioluminescent bacterial strains given in Supplementary Table 1 were the basis for sequence alignments to calculate conservation scores with the ConSurf server [23] for all structural models of the luciferase (Figure 3) and the fatty acid reductase complex (Figures 4-8).

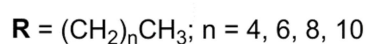
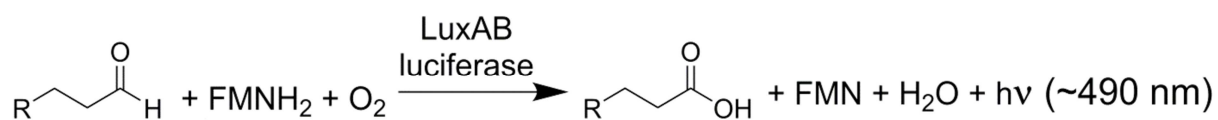


Figure 1. Examples of *lux* gene order of bioluminescent bacterial strains (adapted from Figure 2 in Dunlap P. *Bioluminescence: Fundamentals and Applications in Biotechnology - Volume 1*. 2014 [6]). According to Supplementary Table 1 and available gene sequences and orders, the five most divergent bacterial strains (*Vibrio harveyi*, *Aliivibrio fischeri*, *Photobacterium mandapamensis*, *Photobacterium leiognathi* and *Photobacterium luminescens*) were chosen to represent *lux* operon constellations. The color code of individual genes is also used for the corresponding protein models in Figures 3-8. The arrow above *luxR* indicates that its reading frame is oriented in the opposite direction (individual operon not directly linked to the *lux* operon).

The genes *luxA* and *luxB* encode the heterodimeric luciferase; *luxC*, *luxD*, and *luxE* are part of the fatty acid reductase complex and *luxG* encodes a flavin reductase. Next to the core genes *luxCDABE(G)*, additional genes are found within the *lux* operon (*luxF*; *ribEBHA*; *luxI*) or in a separate operon (*luxR*) adjacent to the *lux* operon, where the reading frame is in the opposite direction (Figure 1).

1.6. ENZYMES AND REACTION MECHANISMS IN BACTERIAL BIOLUMINESCENCE

The core genes, *luxCDABE(G)*, code for all enzymes involved in a complex machinery enabling bioluminescence. In bioluminescent bacteria, the heterodimeric enzyme luciferase (LuxAB) catalyzes the monooxygenation of aliphatic aldehydes to the corresponding acids utilizing reduced flavin mononucleotide (FMNH₂) as redox cofactor. Tetradecanal is postulated to be the natural substrate of bacterial luciferases, however long-chain aliphatic aldehydes with carbon chain lengths of 8 to 16 are also potential substrates [24]. From an excited state FMN-4a-hydroxide the energy is released as light, thus this intermediate serves as the light emitting luciferin [25,26]. According to the structures of the luciferase, the active site enabling light emission is located in the α -subunit, while the β -subunit is presumably responsible for stability, folding and quantum yield. The two subunits share approximately 30% sequence identity suggesting that *luxB* arose by gene duplication of *luxA* [27]. The overall reaction mechanism of bacterial bioluminescence is depicted in Scheme 1.

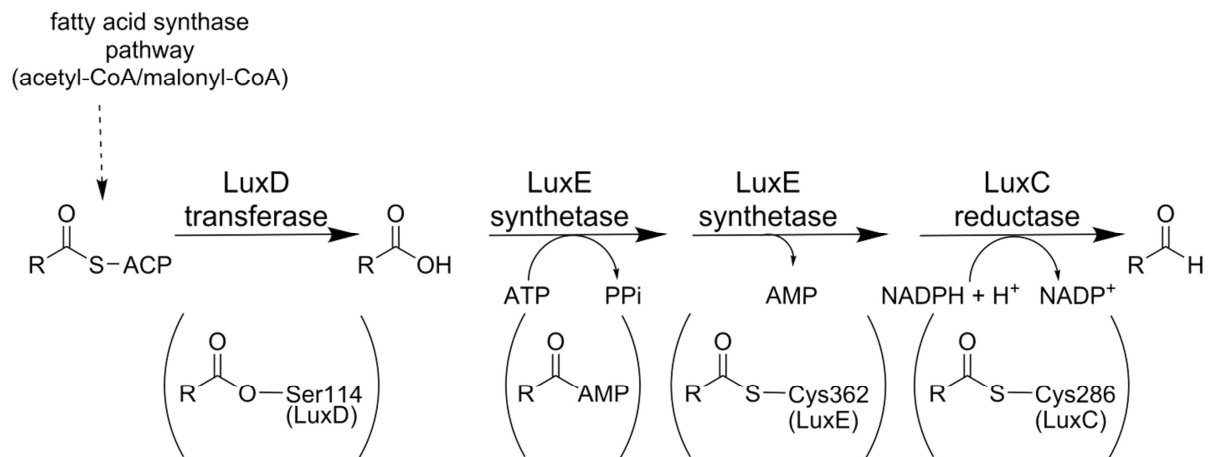


Scheme 1. General reaction mechanism of bacterial bioluminescence. Long-chain aldehydes (CH₃(CH₂)_nCHO), reduced flavin mononucleotide (FMNH₂) and molecular oxygen (O₂) are converted by the enzyme luciferase (LuxAB) to the corresponding long-chain acids (CH₃(CH₂)_nCOOH), oxidized flavin mononucleotide (FMN), water (H₂O) and light emission (hν) with an approximate maximum at 490 nm.

The bacterial bioluminescent reaction belongs to the group of two component systems since reduced FMN is necessary for the reaction to proceed and has to be supplied by another enzyme than the luciferase itself [28,29]. Due to its high similarity to Fre, a flavin reductase in *E. coli*, it was assumed that the protein LuxG has a similar function in bioluminescent bacteria [30–32]. In 2008, Nijvipakul *et al.* determined the function of LuxG as a NAD(P)H-dependent flavin reductase. LuxG converts free flavin mononucleotide (FMN) to reduced flavin mononucleotide (FMNH₂) that can be used by the luciferase for bacterial

bioluminescence [33,34]. Because the product FMNH₂ is prone to oxidation by molecular oxygen, it is still a matter of debate whether FMNH₂ is released by the reductase and freely diffuses to be sequestered by the luciferase or if a LuxG – LuxAB complex is formed in order to directly transfer reduced FMN from the reductase to the luciferase. A separate paragraph is dedicated to provide some more details related to this question.

To supply the long-chain aldehyde substrates to the luciferase, the proteins LuxC, LuxD, and LuxE constitute a fatty acid reductase complex [25]. The gene *luxC* encodes a NADPH-dependent acyl protein reductase (approximately 54 kDa), *luxD* specifies an acyl-transferase (approximately 33 kDa) and *luxE* encodes an acyl-protein synthetase (approximately 42 kDa). A schematic overview of the reactions catalyzed by this complex is shown in Scheme 2.



Scheme 2. Overview of individual reactions catalyzed by the LuxCDE fatty acid reductase complex. Intermediate species covalently linked to individual enzymes are shown in brackets beneath the corresponding reaction steps. The reaction cascade is initiated by the myristoyl transferase LuxD via unloading of myristic acid (R = (CH₂)₁₂CH₃) bound to the acyl carrier protein (ACP). Covalently linked to Ser114 (*Vibrio harveyi* numbering) the acyl moiety is transported to the LuxCE complex and released as the free fatty acid that interacts with the LuxE synthetase. At the expense of ATP the fatty acid is activated by LuxE to acyl-AMP and in a second step covalently attached to Cys362. This intermediate is then channeled directly to the active site of the LuxC reductase, where it is initially transferred to Cys286 of LuxC. The latter intermediate is then reduced by NADPH resulting in aldehyde formation and dissociation of the product. Details of the individual processes are provided in the section - *The fatty acid reductase complex (luxCDE)*.

In addition to the canonical *luxCDABE(G)* gene cluster, a number of bioluminescent *Photobacteria* carry an additional *luxF* gene. Natural occurring nonsense mutations in this gene revealed that the strains carrying this inactivated *luxF* are luminous but to a lower degree. This would support the hypothesis that LuxF is somehow involved in regulating light intensity [15]. The additional gene *luxF* in the *lux* operon of photobacterial strains, led to the differentiation of two subgroups of *Photobacterium leiognathi*, *Photobacterium leiognathi* subsp. *leiognathi* (without *luxF*) and *Photobacterium leiognathi* subsp. *mandapamensis* (with *luxF*). Additional phenotypic characterization led to further discrimination of the two groups. *P. leiognathi* subsp. *leiognathi* shows higher light intensities at low salt concentrations and a more intense blue color, while *P. leiognathi* subsp. *mandapamensis* shows higher light intensities at high salt concentrations and blue-green color. Ast and Dunlap speculated that *luxF* arose through a gene duplication event of *luxB* in an ancestor of *Photobacterium*, which was lost again in the lineage leading to subsp. *leiognathi* in accordance with the observation that only *Photobacterium leiognathi* subsp. *mandapamensis* and *Photobacterium phosphoreum* contain *luxF* [35].

During the structural characterization of the homodimeric protein LuxF, an unusual flavin derivative - 6-(3'-(R)-myristyl)-flavin mononucleotide (myrFMN) - was discovered in keeping with the observed electron density (PDB 1FVP) [36–38]. More recently, it was reported that LuxF binding to myrFMN is important to prevent inhibition of the luciferase by this putative side product of the luciferase reaction. LuxF is thereby acting as a scavenger of myrFMN [39,40]. The chemical nature of this side product of the bioluminescent reaction also provides insights into the mechanism of the luciferase reaction, described in more detail later in this review.

Recently, bacterial bioluminescence has been utilized as a reporter system in plant protoplasts as well as for single-cell imaging [41,42]. Toward this end, Cui *et al.*, have constructed a fusion of *luxA* and *luxB* from *Photobacterium luminescens* that was further optimized by directed evolution. This resulted in five amino acid exchanges of which four were found in the domain that harbors the active site of the enzyme (corresponding to the α -subunit in the heterodimeric luciferase). However, the amino acid replacements are not in or near the active site and thus their effect on the activity and efficiency of the fused luciferase is unclear [42]. Furthermore, Gregor *et al.* have subjected the entire *lux* operon, *i.e.* including the genes encoding the fatty acid reductase complex as well as the flavin reductase, for optimization using directed evolution. Several beneficial mutations in *luxA*, *luxB*, *luxC* and *frp* could be identified that led to a seven-fold increase of brightness when expressed in *Escherichia coli* [41]. As before, the molecular reasons for enhanced light emission remain undetermined and may include several factors such as enhanced gene expression or increased enzyme activity/efficiency. Although, these examples demonstrate the utility of bacterial bioluminescence for further applications, for example in the field of imaging, unfortunately they have failed to provide additional information on critical issues such as the population of the excited state and the involvement of amino acid residues in the active site as well as the dynamic interaction of the α - and β -subunits.

1.6.1. Genes associated with the *lux* operon

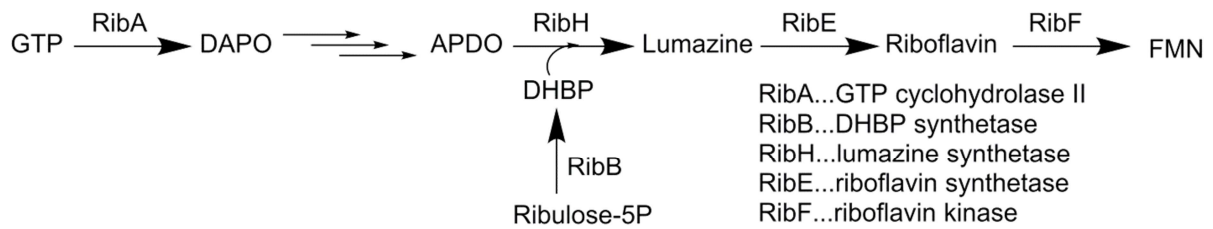
Apart from the core genes *luxCDABE(G)*, various other genes are coregulated, coexpressed or linked to the *lux* operon. Having a closer look on these additional genes revealed their importance for fine tuning of light emission.

For some luminous bacteria, bioluminescence is regulated via cell density dependent induction or derepression of luciferase-gene expression, so called quorum sensing regulation. Small secondary metabolite levels, *e.g.* acyl homoserine lactones, reflect the cell density of bioluminescent bacteria. Especially for two bacterial strains, *Aliivibrio fischeri* and *Vibrio harveyi*, this regulatory mechanism was investigated in detail. Among many other regulatory factors, the genes *luxI*, within the *lux* operon before *luxC*, and *luxR*, directly adjacent to the operon with the reading frame in the opposite direction (Figure 1), are involved in quorum sensing regulation. Furthermore, levels of autoinducers and their synthetases, transcriptional regulators, kinases involved in phosphorylation/dephosphorylation cascades and signal transduction cascades and even small quorum-regulatory RNAs play a role in this complex regulatory mechanism and influence the expression levels of the genes in the *lux* operon [2,6,45,46].

1.6.2. Riboflavin Synthesis Genes – *ribE*, *ribB*, *ribH*, *ribA*

In strains of the genus *Photobacterium*, the genes *ribEBHA* may play a role in bioluminescence. These genes are involved in riboflavin biosynthesis and are an example for gene recruitment, constituting together with the *lux* genes the *lux-rib* operon – *luxCDAB(F)EG – ribEBHA*. These *rib* genes might facilitate light production as they provide a part of the FMN substrate. Depending on the strain none, one or more of these *rib* genes are cotranscribed with the *lux* genes. Interestingly, there is no transcriptional stop or other regulatory terminator between *lux* and *rib* genes indicating coexpression [6,43].

In Scheme 3 the synthesis pathway of riboflavin/FMN is depicted with the involved *rib* proteins highlighted. DNA sequence analysis and alignment to homologous genes identified the *rib* genes and the corresponding function of the proteins. The gene *ribE* encodes a riboflavin synthetase (RibE) converting lumazine to riboflavin; *ribB* encodes 3,4-dihydroxyl-2-butanone 4-phosphate (DHBP) synthetase (RibB); *ribH* encodes the lumazine synthetase (RibH) and *ribA* encodes a GTP cyclohydrolase II (RibA) [43].



Scheme 3. Schematic representation of the synthesis pathway of riboflavin (adapted from Figure 2 in Sung, Lee, *J. Photosci.*, 2004 [44]). Guanosine triphosphate (GTP) is converted to 2,5-diamino-6-(5'-phosphoribosylamino)-4-pyrimidineone (DAPO) by RibA, which is further converted in three steps to 5-amino-6-(D-ribitylamino)uracil (APDO). Another route starts from ribulose 5-phosphate, which is converted to 3,4-dihydroxy-2-butanone 4-phosphate (DHBP) by RibB. The enzyme RibH produces the product 6,7-dimethyl-8-ribityllumazine (lumazine) from DHBP and APDO. Lumazine is converted to riboflavin by RibE, which is subsequently transformed into flavin mononucleotide (FMN) by a riboflavin kinase RibF.

1.6.3. Color change in light emission

One of the first descriptions of a bioluminescent bacterial strain emitting light in a different color than blue-green was *Photobacterium fischeri* Y-1 (later *V. fischeri*). This strain emits yellow light and was isolated from seawater in 1977 [47]. The yellow fluorescent protein YFP binds FMN and shifts the light emission from around 490 nm to 545 nm. Interestingly, this color change was temperature dependent, where cells grown above 22 °C will emit blue-green light and cells grown below 18 °C will emit yellow light (Figure 2) [47–49].

At the same time as YFP was discovered, another shift in light emission towards blue color was reported. The blue fluorescent protein (BFP, later termed lumazine protein) was isolated from *Photobacterium phosphoreum*, *Photobacterium fischeri* and *Photobacterium leiognathi* (later reclassified as *P. mandapamensis*) [50–53]. The isolation of BFP from *P. phosphoreum* and the identification of its ligand as 6,7-dimethyl-8-ribityllumazine (lumazine), a precursor of riboflavin biosynthesis (Scheme 3), led to the renaming to lumazine protein (LumP) [54]. Comparing *in vivo* and *in vitro* analysis revealed that *in vivo* the bioluminescence maximum is at 475 nm, while *in vitro* the maximum lies at 490 nm. After addition of BFP to the *in vitro* reaction, the maximum shifts to 475 nm as in the *in vivo* result. The fluorescence spectrum matches the *in vivo* bioluminescence spectrum, but the BFP spectrum can be easily altered by temperature, dilution, pH, ionic strength and urea (due to an increase of free lumazine). Both antenna proteins (BFP/LumP and YFP) are species specific and can influence the kinetics by enhancing the light intensity and the decay rate [51,52,55–57].

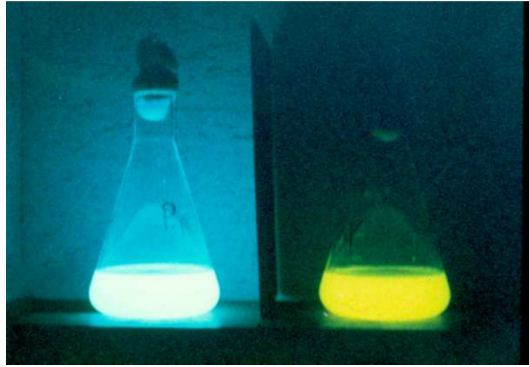


Figure 2. Bacterial cultures of *Photobacterium phosphoreum* on the left and *Vibrio fischeri* Y-1 on the right. The light emission in blue and yellow, respectively, shows nicely the effect of LumP and YFP [58].

These first analyses led to vigorous discussions about the primary emitter of the bioluminescent reaction and the possible reaction mechanisms behind the energy transfer to the antenna proteins [51,52,55,59,60]. It was speculated that LumP and YFP form a complex with the luciferase enabling weak dipole-dipole Förster-type coupling of the high energy intermediate of the bioluminescent reaction with the antenna transitions. To make FRET (Förster resonance energy transfer) possible, a spectral overlap of the fluorescence spectrum of the donor and the absorption spectrum of the acceptor is needed [59,60]. It was further suggested that the aldehyde substrate holds the two proteins (luciferase and antenna protein) in place. The complex formation has to take place before the excited state intermediate is formed to ensure the energy transfer in time [52,53,56,59,60].

For LumP, X-ray analyses provided further insight in the mechanism. The crystal structure of the L49N variant of the lumazine protein of *P. leiognathi* in complex with riboflavin (PDB 3DDY) gave first structural information on the binding site. The crystal structure has high similarity with the riboflavin synthase of *Schizosaccharomyces pombe* and *Escherichia coli*. However, a closer comparison of riboflavin synthase and lumazine protein revealed certain differences, as the latter is a monomer in solution and binds only one molecule of 6,7-dimethyl-8-ribityllumazine (or riboflavin) in the N-terminal domain [61]. The crystal structure of LumP of *Photobacterium kishitanii* in complex with lumazine, riboflavin and FMN (PDB 3A3G, 3A35; 3A3B) confirmed one single binding site at the N-terminal region. Computational docking of LumP-Lumazine (PDB 3A3G) with luciferase of *V. harveyi* (PDB 3FGC) predicts complex formation, which is supported by complementary charge distributions on the surfaces of the luciferase and LumP. This suggests a possible direct energy transfer between those two proteins, as the ring system of lumazine is located in close proximity (approximately 10 Å) to the isoalloxazine ring [59,62]. However, the overlap of the absorption spectrum of the lumazine with the emission spectrum of the luciferase is very small and, moreover, the shift in light emission is to higher energy (for color change towards blue at 475 nm). The question of how energy transfer is achieved remains unanswered [51,55,63]. Recent studies and reviews failed to provide deeper insight into the

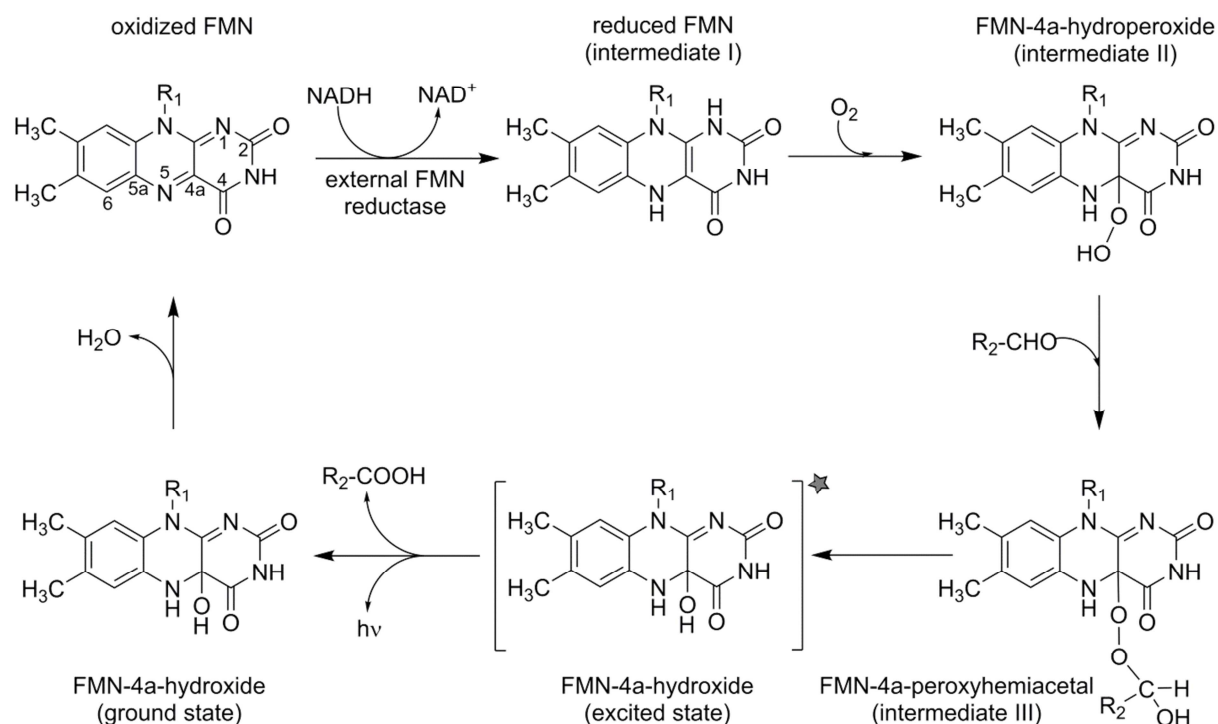
exact mechanism of the color change of bioluminescent emission [59,64,65] and thus this phenomenon remains puzzling.

Each enzyme presented above contributes to the core machinery of the *lux* operon enabling light emission, or even modulation of light intensity and color or regulation of bacterial bioluminescence. While the schemes provided above represent the overall reaction, they are simplified representations of complex molecular mechanisms. Using structural information from individual enzymes of the Lux family and addressing evolutionary conserved areas within these structures, allows a better understanding of the underlying core reaction mechanisms. Especially in combination with the comparison of so far not crystallized members of the *lux* operon with closely related enzyme families and homology modeling, molecular mechanisms and structure function relationships of the enzymes involved in bacterial bioluminescence can be described.

1.7. STRUCTURE-FUNCTION RELATIONSHIPS

1.7.1. The mechanism of bacterial bioluminescence

Bacterial bioluminescence is based on a classical two-component system consisting of an enzyme (termed luciferase) that catalyzes the bioluminescent reaction, and a small molecule that acts as the light-emitting species in the course of the reaction (termed the luciferin, reviewed in [4,66]). In the case of bacterial bioluminescence, the luciferin is derived from flavin mononucleotide (FMN), which undergoes a sequence of reactions as shown in Scheme 4. FMN is widely used in nature as a versatile cofactor in a plethora of biochemical reactions involving the handling of electrons, *i.e.* oxidation-reduction reactions (EC class 1: oxidoreductases) [67]. The energy required to populate the excited state of the luciferin is derived from the oxidation of a long-chain fatty aldehyde, which is synthesized in bioluminescent bacteria from myristoyl-ACP (see *Introduction* and *The fatty acid reductase complex, below*), to the corresponding long-chain fatty acid.



Scheme 4. Reaction cycle of FMN during bacterial bioluminescence. Oxidized flavin mononucleotide (FMN; R₁: ribityl monophosphate) is reduced by an external FMN reductase employing NAD(P)H as the reducing agent. Reduced FMN (intermediate I) reacts with dioxygen and forms the FMN-4a-hydroperoxide (intermediate II). The addition of long-chain aldehydes (*e.g.* R₂: (CH₂)₁₂CH₃) leads to the formation of the FMN-4a-peroxyhemiacetal (intermediate III). After mono-oxygenation of the long-chain aldehyde to the corresponding acid, an excited state FMN-4a-hydroxide is formed, which is the luciferin in the bacterial bioluminescent reaction. As this luciferin relaxes to the ground state, the free energy is released as light with an emission maximum at 490 nm. After release of one water molecule the catalytic cycle is completed and FMN returned to its oxidized ground state.

In addition to the wealth of biochemical experiments addressing mechanistic aspects of bacterial bioluminescence, the elucidation of the crystal structure of a functional luciferase was a major milestone in understanding the involvement of individual amino acids and specific structural elements. Molecular details of the luciferase from *Vibrio harveyi* have shown that the *luxA* and *luxB* gene products form a heterodimer consisting of two (β α)₈ barrels [68,69]. The active site of the luciferase that needs to accommodate all substrates, shown in Scheme 1 (*Introduction*), was speculated to be present only in the LuxA-subunit. Subsequent crystal structures that have the oxidized FMN cofactor bound to the α -subunit confirmed this assignment of the active site and further demonstrated the importance of the β -subunit in stabilizing the active conformation of the α protomer via specific contacts between conserved residues in the β -subunit and an α -subunit loop region close to the active site (Figure 3 panels A and B) [27]. Thus far, no structural information on the spatial orientation of the FMN and the aldehyde (or intermediates of the reaction) is available, preventing a more detailed interpretation of how the excited state is generated in the course of the overall reaction.

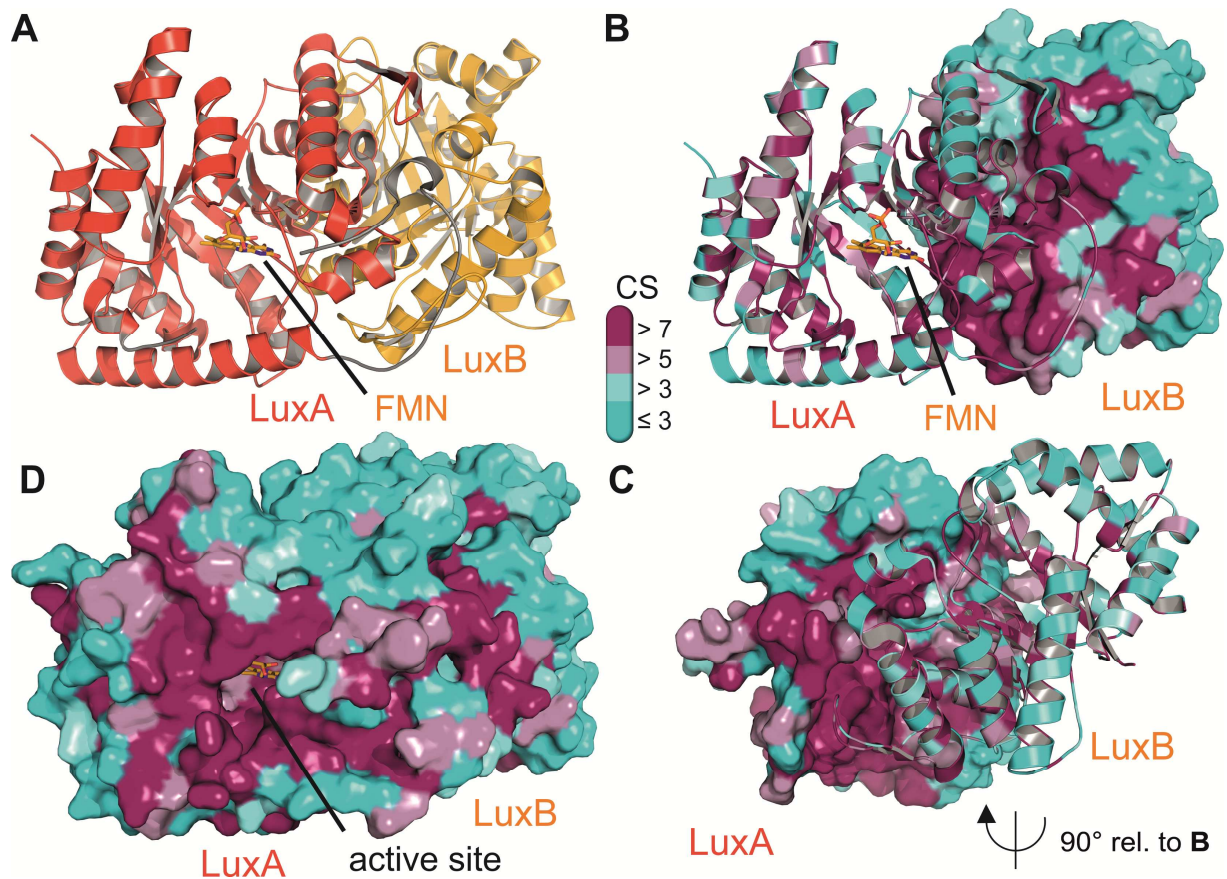


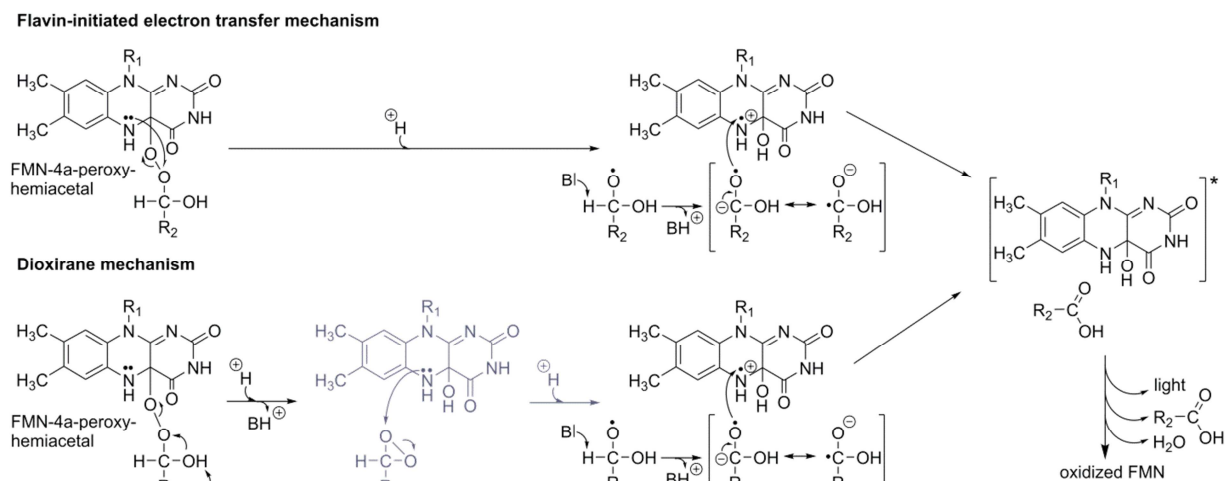
Figure 3. Crystal structure of the bacterial luciferase from *Vibrio harveyi* (PDB 3FGC). Panel A shows the characteristic heterodimer of LuxA (red) and LuxB (orange) in cartoon representation. The FMN cofactor in the active site is shown as yellow stick model. The characteristic loop region that mediates the contact between the α - and β -subunits is shown in grey [27]. Panels B, C and D feature the same luciferase dimer colored according to the conservation of residues among the members of bioluminescent bacteria (details of which sequences are aligned are shown in Supplementary Table 1). Conservation scores from 1 to 9 correspond to an increase in evolutionary conservation and are colored according to the bar legend in the middle of the figure with higher scores (purple) indicating higher conservation. Panels B and C show the high conservation of residues at the heterodimer interface. Either LuxB or LuxA are shown in surface representation in panels B and C, respectively, and panel C features a 90° out of plane rotation of the dimer for better visibility of the highly conserved LuxA interface. Panel D shows both protomers in surface representation and highlights the strict conservation of residues in the open active site as well as its entrance. Conservation scores were computed with the ConSurf server [23].

The central question in understanding any bioluminescent process revolves around two issues: (i) what is the structure of the excited state and (ii) how is it populated during the bioluminescent reaction? In order to tackle these questions, research efforts focused initially on the identification of reaction intermediates. A milestone toward a better understanding of the bioluminescent reaction was the identification of the FMN-4a-hydroperoxide (also referred to as intermediate II) that forms upon reaction of luciferase-bound reduced FMN with dioxygen (Scheme 4) [70,71]. This intermediate is fairly stable in the absence of aldehyde substrates, with half-lives of up to 41 min at 4 °C [71,72] and decays to oxidized FMN and hydrogen peroxide. Its stability also enabled characterization by UV-Vis absorption and NMR-spectroscopy lending further support to its chemical structure [71,73]. Interestingly, the same flavin intermediate is involved in the hydroxylation of aromatic substrates, *e.g.* *p*-hydroxybenzoate hydroxylase and phenol hydroxylase, which also carry out monooxygenation reactions [74]. However, none of these flavin-dependent aromatic hydroxylases produce light during the reaction of their respective substrates suggesting that fundamental mechanistic differences exist between these enzymatic systems. Following the identification of the FMN-4a-hydroperoxide as an intermediate of the bioluminescent reaction, the actual light-emitting species could be identified as the FMN-4a-hydroxide, which forms as a result of the reaction of the FMN-4a-hydroperoxide and the long-chain fatty aldehyde (Scheme 4) [26]. The chemical identity of the FMN-4a-hydroxide as the bioluminophore was also confirmed by a recent theoretical study [75]. These two intermediates are in fact linked by the FMN-4a-peroxyhemiacetal that forms by the reaction of the FMN-4a-hydroperoxide and the long-chain fatty aldehyde (Scheme 4, bottom right). Since the FMN-4a-peroxyhemiacetal is less stable than the hydroperoxide, it could thus far only be detected by absorption spectroscopy [76]. After light emission the FMN-4a-hydroxide splits off water and returns into the oxidized state (Scheme 4, left), thus closing the catalytic cycle. Bacterial luciferases are not capable of reducing the oxidized flavin to the reduced state, in fact oxidized FMN binds rather weakly to the enzyme [77], and therefore reduced FMN needs to be provided by other enzymes, such as NAD(P)H-dependent flavin reductases such as LuxG mentioned above (Scheme 4).

Although the sequence of chemical events shown in Scheme 4 is generally agreed upon, the generation of the excited FMN-4a-hydroxide from the FMN-4a-peroxyhemiacetal remains a matter of debate [78,79]. Based on the overall bioluminescent reaction, Eberhard and Hastings proposed a Baeyer-Villiger mechanism for the bacterial luciferase reaction [80]. Although in keeping with the stoichiometry of the overall reaction, it does not *per se* explain how the excited state of the FMN-4a-hydroxide is populated. In fact, enzymes that reportedly follow a Baeyer-Villiger reaction mechanism, such as cyclohexanone monooxygenase, lack the production of light entirely [74]. Moreover, cyclohexanone monooxygenase converts boronic to boric acids in a Baeyer-Villiger reaction mechanism, whereas bacterial luciferase fails to catalyze these oxidation reactions [72,81]. This inconsistency led to the development of alternative mechanistic models that better explain the generation of the excited state of the luciferin [82–84]. Based on kinetic studies using

flavin analogs bearing different substituents at the 8-position of the isoalloxazine ring, it was proposed that a single electron transfer from the isoalloxazine moiety of the flavin to the distal oxygen atom of the peroxide initiates bond cleavage and the concomitant formation of a radical pair consisting of the FMN-4a-hydroxide radical cation and the substrate-derived carboxylic acid radical anion, as shown in Scheme 5 [82]. The transfer of an electron from the carboxylic acid radical anion to the FMN-4a-hydroxide radical cation eventually leads to the generation of the excited state of the FMN-4a-hydroxide. This mechanism, reminiscent of the so-called chemically initiated electron exchange luminescence (CIEEL) mechanism [85], has received additional support from the observation that the electron transfer from the carboxylic acid radical anion to the FMN-4a-hydroxide radical cation provides sufficient energy (ca. 90 kcal/mol) to populate the excited state [83]. In a variation of this mechanism, the FMN-4a-peroxyhemiacetal directly decays to the FMN-4a-hydroxide and a dioxirane intermediate (Scheme 5, lower reaction path). This step is followed by an electron transfer, in this case from the FMN-4a-hydroxide rather than the FMN-4a-peroxyhemiacetal, yielding the same radical pair as before (Scheme 5). However, the dioxirane mechanism suffers from a major drawback: the FMN-4a-hydroxide appears twice in the reaction sequence, before and after the rate-limiting step that populates the excited state. This is in contrast to experimental findings that have demonstrated its occurrence only as a result of the relaxation of the excited state FMN-4a-hydroxide, *i.e.* after the rate-limiting step [26,86].

As mentioned above, the flavin-initiated electron transfer mechanism is conceptually derived from the CIEEL mechanism originally proposed by Schuster and was applied to rationalize the generation of a high energy intermediate in firefly bioluminescence [85,87]. However, redetermination of chemiexcitation efficiencies yielded much lower values than originally reported and have led to a critical reevaluation of the validity of the CIEEL mechanism [88]. Since the classical CIEEL mechanism involves the transfer of an electron from the donor to the peroxide followed by back-transfer of an electron to generate the excited state of the fluorophore (or in the case of bioluminescence the excited state of the luciferin), it has been argued that a charge transfer, *i.e.* not a “full” electron, may be sufficient to trigger the decomposition of the peroxide and subsequently leads to the generation of an excited state [88–91]. Although most theoretical studies in the field of bioluminescence have focused on the firefly [89–91] and Cypridina bioluminescence [92,93], it is conceivable that an equivalent charge-transfer process occurs in the bacterial bioluminescent reaction. Taking this into consideration, the mechanism depicted in Scheme 5 (top) represents the extreme case of a “full” electron transfer but may in fact only involve the transfer of charge from the flavin to the peroxide bond to trigger the events leading to the generation of the excited state FMN-4a-hydroxide.

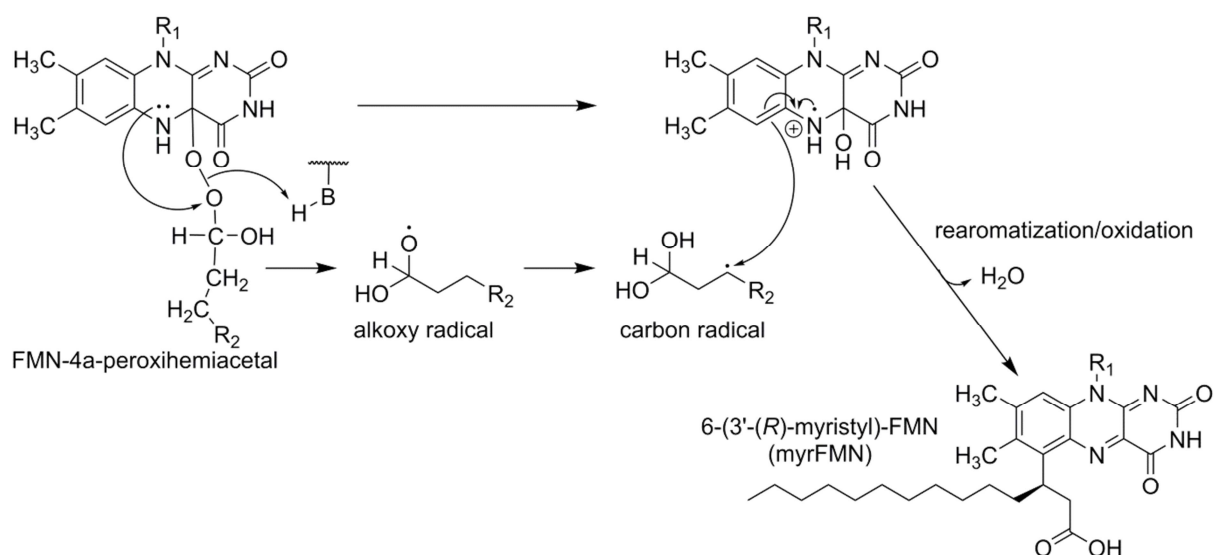


Scheme 5. Mechanistic details of the flavin-initiated electron transfer and the dioxirane mechanism. In the former mechanism (upper reaction path), electron transfer from N5 of the isoalloxazine ring to the distal oxygen atom of the flavin-4a-peroxyhemiactal (R_1 : ribityl monophosphate) leads to the formation of a substrate-derived alkoxy radical (e.g. R_2 : $(\text{CH}_2)_{12}\text{CH}_3$) and the flavin-4a-hydroxy radical cation. Deprotonation of the alkoxy radical generates a resonance stabilized anion radical, which transfers an electron back to the flavin-4a-hydroxy radical cation thus leading to the population of the excited state of the flavin-4a-hydroxide. In an alternative route to this mechanism, the dioxirane mechanism (lower reaction path), the flavin-4a-peroxyhemiactal forms a dioxirane intermediate, which then receives an electron from the flavin-4a-hydroxide (depicted in dark grey). As before, this leads to the flavin-4a-hydroxide radical cation and the subsequent generation of the excited state similar to the mechanism in the flavin-initiated electron transfer mechanism. In both reactions the rate limiting step is the electron donation from the reduced flavin moiety to the substrate moiety.

In mechanistic terms it is also important to consider in which step the carbon-hydrogen bond at C1 of the aldehyde substrate is broken. As shown in Scheme 5, electron transfer is presumably followed by carbon-hydrogen bond cleavage. In order to assess whether this step is rate-limiting, kinetic isotope effects, using deuterated $[1-^2\text{H}]$ -aldehyde substrates, were determined. The moderate kinetic isotope effects of 1.4-1.9 [84,94] suggested that carbon-hydrogen bond breakage is only partially rate-limiting and thus supports the electron transfer mechanism depicted in Scheme 5. More recently, a computational study suggested that the excited state is populated by a charge-transfer rather than an electron transfer mechanism [78]. In the proposed mechanism, carbon-hydrogen bond cleavage is directly connected to the generation of the excited state and thus a strong kinetic isotope effect should be observed, which is arguably not the case. On the other hand, it is also unclear how charge-transfer coupled to carbon-hydrogen bond cleavage results in the population of the excited state of the FMN-4a-hydroxide.

The transient occurrence of radicals during the bioluminescent reaction received further support by studies aiming to understand the origin of a mysterious flavin adduct, the so-called myristylated FMN derivative, *i.e.* 6-(3'-(*R*)-myristyl)-flavin mononucleotide (myrFMN) first discovered in bioluminescent *Photobacteria* [37,39,95]. In addition, it was shown that some bioluminescent marine bacteria have an additional gene, *luxF*, which encodes a

protein (LuxF) that specifically binds four molecules of myrFMN per dimer [37]. *LuxF* presumably evolved by gene duplication of *luxB* and while LuxF retained parts of the overall fold, specific elements were removed and replaced by myrFMN specific binding elements [39]. This led to the hypothesis that LuxF acts as a scavenger of myrFMN to prevent the observed inhibitory effect on the luciferase reaction. However, the origin of myrFMN remained unclear until it was shown recently that myrFMN is in fact a side product of the luciferase reaction [40]. Based on this discovery, a mechanism was postulated that rationalizes the formation of myrFMN (Scheme 6). This mechanism invokes the rearrangement of the transient substrate-derived radical anion to a carbon radical that subsequently recombines with the FMN-4a-hydroxide radical cation to form the covalent myrFMN adduct (Scheme 6).



Scheme 6. Proposed mechanism for myrFMN formation (adapted from Scheme 3 in Tabib, Brodl, Macheroux, *Mol. Microbiol.* 2017 [40]). As shown in Scheme 5, an electron is transferred from the N5 of the flavin to the distal oxygen atom of the peroxy moiety. A hydrogen rearrangement of the alkoxy radical (R_2 : $(CH_2)_{10}CH_3$) intermediate leads to a C3 carbon radical. This combines with the flavin-4a-hydroxide radical cation forming a covalent bond between the C6 of the isoalloxazine ring and the C3 carbon of the myristyl aldehyde. After rearomatization and the oxidation of the aldehyde to the acid followed by release of water, 6-(3'-(R)-myristyl)-FMN (myrFMN) is formed.

In our view, the formation of a carbon-carbon bond between the C6 position of the isoalloxazine ring and the C3 carbon of the aliphatic substrate molecule requires radical chemistry thus providing indirect support for an electron transfer mechanism being in operation in bacterial luciferase. In conclusion, the available data indicate the involvement of electron transfer as a central step on the reaction path to the excited state of the FMN-4a-hydroxide as postulated in flavin-initiated electron transfer mechanism (Scheme 5, top line).

1.7.2. Generation of reduced FMN

As mentioned above and indicated in Scheme 4, bacterial luciferase is a flavin-dependent monooxygenase and thus requires the supply of reduced FMN in order to initiate the bioluminescent reaction. This task is carried out by flavin reductases, which may use NADH and/or NADPH as reducing agents [28,29]. Flavin reductases are either flavin-dependent (class 1) or independent (class 2) [79] and thus exhibit different properties in terms of the formation of binary and ternary enzyme substrate complexes. A central point in this context revolves around the question whether the reduced flavin (FMNH₂) is directly transferred from the flavin reductase to the luciferase or simply released and subsequently sequestered by luciferase. Since free reduced flavin may rapidly react with dioxygen to yield oxidized flavin and hydrogen peroxide, the latter mechanism is potentially wasteful and thus the direct transfer of reduced FMN to the luciferase presents an attractive alternative mechanism that avoids this complication. Indeed, *in vitro* studies have provided evidence for such a direct transfer of reduced FMN between the flavin reductase and luciferase from *V. fischeri* [96]. In contrast, a recent study using LuxG and the luciferase from *P. leiognathi* TH1 indicated that the acquisition of reduced FMN by luciferase occurs by free diffusion [97]. Clearly, direct transfer of reduced flavin from the reductase to the luciferase requires the formation of a stable protein complex in which the reduced flavin is “handed over”. However, attempts to establish the formation of such a reductase-luciferase complex have been unsuccessful thus far. Similarly, it was shown that light emission by *V. harveyi* luciferase in transgenic *Escherichia coli* is supported by Fre, which is an oxidoreductase similar to LuxG from *P. leiognathi* [98]. Although it cannot be ruled out entirely, it appears unlikely that Fre (from *E. coli*) forms a protein complex with a luciferase from *V. harveyi* thus adding further support to the free diffusion mechanism. In agreement with this assessment, Campbell and Baldwin found no evidence for the existence of a Fre-luciferase complex [98]. From a structural perspective it should be noted that Fre from *E. coli* and LuxG from *V. harveyi* share about 40% sequence identity. Therefore, their molecular architecture is expected to be very similar and the mechanistic details involving substrate specificity and NAD(P)H binding can be inferred from the crystal structure of *E. coli* Fre [30]. With respect to the potential direct interaction of LuxG with the luciferase, the structural information cannot provide a direct answer. It should, however, be emphasized that during evolution the same flavin reductase fold has frequently been used to increase specificity for certain biochemical pathways by altering side chain functionalities in loop regions or by directly fusing the reductase domain with other functionalities such as ferredoxin units, FMN-flavodoxin modules or heme domains. Therefore, the inclusion of *luxG* in the *lux* operon might indicate some specialization of LuxG for enhanced light production, even though reduced FMN provided by other flavin reducing enzymes is also accepted by the luciferase. In conclusion, LuxG is an important NAD(P)H-dependent flavin reductase providing the luciferase with reduced FMN via free diffusion.

1.7.3. The fatty acid reductase complex (*luxCDE*)

Three enzymes are required for the production of the fatty aldehyde substrate of luciferase, a transferase, a synthetase and a reductase. Initially, the transferase (encoded by *luxD*) takes over the acyl moiety from acyl-ACP or acyl-CoA using the alcohol group of a serine residue to form an ester derivative, which is eventually hydrolyzed to the free acid [99], a step that is greatly enhanced by interaction with the LuxE synthetase [100]. Subsequent elucidation of the crystal structure of LuxD from *Vibrio harveyi* and biochemical experiments showed that Ser114, which is part of a classical catalytic triad, is the acylated residue (Figure 4) [101]. In addition, a flexible β -hairpin element is observed close to the catalytic serine that might control activation and/or release of the fatty acid in the appropriate environment of the LuxCDE reductase complex. Strikingly, the relatively flat triangular surface of LuxD featuring the catalytic residues is lined mostly by evolutionary conserved residues, suggesting that this part of the molecule is involved in formation of a specific complex with the remaining subunits of the fatty acid reductase complex [102].

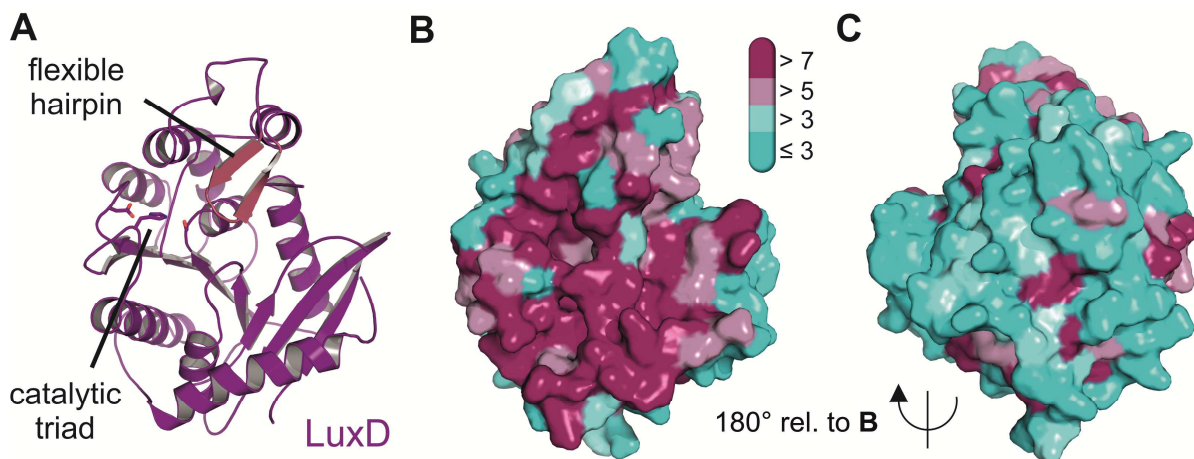


Figure 4. Crystal structure of LuxD, the myristoyl-ACP-specific thioesterase from *V. harveyi* (PDB 1THT). Panel A shows the cartoon representation of LuxD in purple color with residues of the catalytic triad as stick models. The flexible hairpin element above the catalytic serine residue is colored in light red. Panels B and C feature the same coloration according to evolutionary conservation of residues introduced in Figure 3. Highly conserved residues of the whole surface region around the fatty acid binding site support its involvement in complex formation with LuxE and/or LuxC (see below).

The synthetase subunit (encoded by *luxE*) activates the free acid at the expense of ATP, leading to the formation of acyl-AMP. This reacts with an invariant C-terminal cysteine residue to the corresponding thioester [103]. No structural information is available for LuxE, however, the close relationship with acyl-CoA synthetases provides an opportunity to generate homology models of LuxE. Even though sequence identities to the closest homologs are below 18%, the core regions of the synthetase units feature highly conserved residues with structural implications indicating the conservation of the overall protein fold. Also, the ATP binding site features full conservation of residues involved in base recognition and phosphate binding as well as the magnesium coordination shell close to the triphosphate of ATP. Interesting differences can be observed in the C-terminal part of the proteins where a flexible subdomain is involved in coenzyme A coordination and formation of the CoA derivatives [104]. For LuxE this subdomain is missing and replaced by a hairpin element that contains the acylated C-terminal cysteine residue (Cys362, [103]). Based upon open and closed structures of acyl-CoA synthetases, we generated models of LuxE in the two states using the structures of acyl-CoA ligase from *Bacteroides thetaiotaomicron* (PDB 4R1L) and phenylacetate-CoA ligase from *Burkholderia cenocepacia* [105], respectively (Figure 5). Importantly, while biochemical data suggested LuxE to be monomeric [102], the modeling approach strongly supports a dimeric LuxE species. This is supported by the observation of untypical elution behavior during gel filtration considering monomeric LuxE and the fact that the monomer was assigned based on the absence of lysine specific crosslinking experiments [102] – Lysines that are absent near the interface of the dimeric models. The dimeric assembly is further supported by the high degree of evolutionary conservation of residues at the corresponding molecular interface (Figure 5 C).

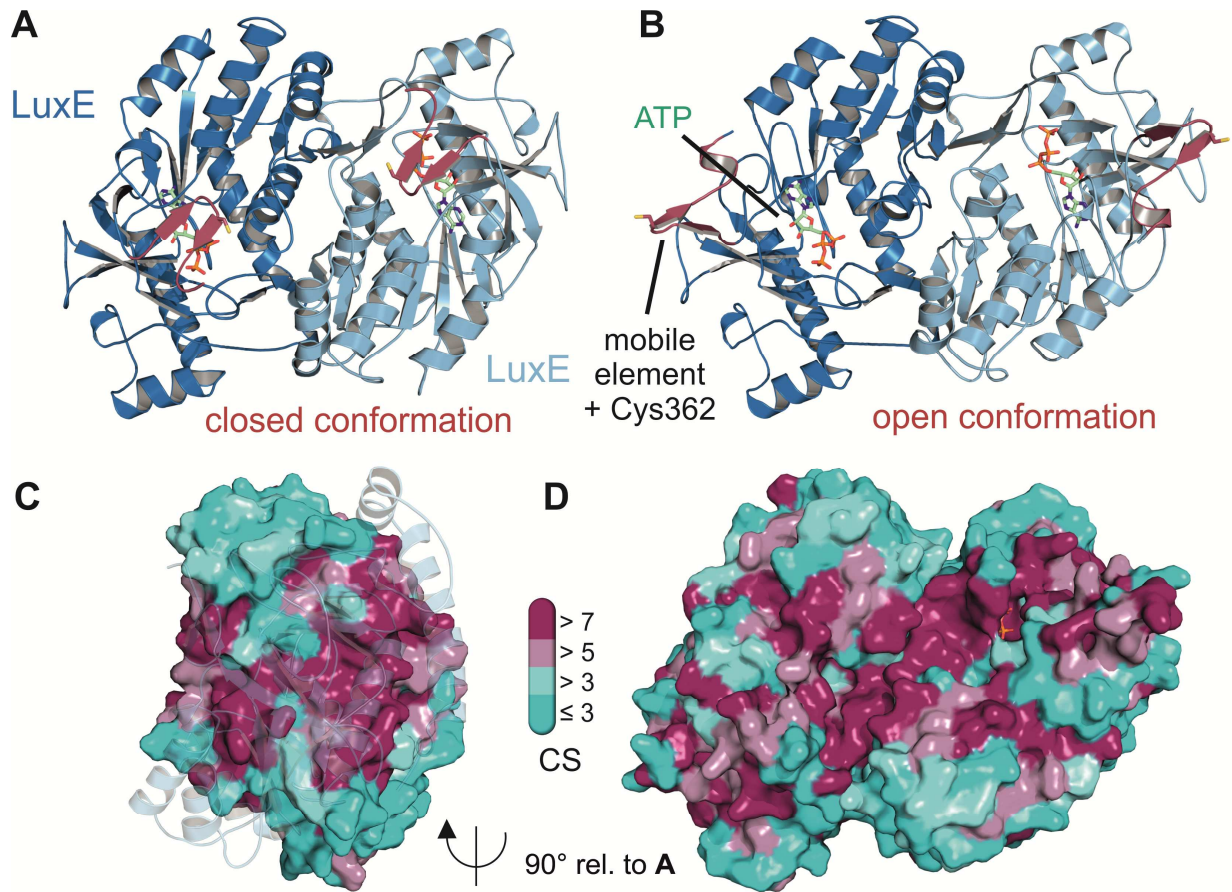


Figure 5. Homology models of LuxE from *V. harveyi*. Panels A and B correspond to homology models generated with the SWISS-MODEL server [106] based on PDB 2Y4O and PDB 4R1L, respectively, in the closed and open conformations. The mobile element is depicted in red color and the cysteine residue that can be acylated present in this region is shown as stick model. For reasons of clarity individual functional elements and cofactors are only labeled once in both panels A and B. Nevertheless, all red beta hairpins correspond to the same mobile element and all green stick models correspond to ATP. The overall LuxE dimer is shown in cartoon representation with one protomer colored in blue and the other in light blue. The ATP moiety overlaid from the cofactor bound form of the closed LuxE model template (PDB 2Y27) is shown as green stick model and its proximity to Cys362 further supports the relevance of the closed LuxE state. The open conformation is relevant for the LuxE-LuxC interaction as described before. Panels C and D show the evolutionary conservation of residues according to the ConSurf generated conservation scores (CS – bar legend in the middle). Panel C shows the conservation of the dimer interface in a rotated view relative to panel A and with the light blue protomer shown in transparency. Panel D shows the same view as panels A and B to illustrate the high conservation of residues at a specific surface of the dimer, which is therefore likely involved in the interaction with the LuxC reductase component (*cf.* Figure 7) [103].

The flexibility and surface exposure of the catalytically important cysteine residue located at the C-terminus of LuxE allows it to reach into the active site of the reductase (encoded by *luxC*) where the thioester is reduced by NADPH to the aldehyde with concomitant release of the free fatty aldehyde. Several studies have confirmed the interaction between LuxC and LuxE and it has been shown that their interaction greatly stimulates their respective activities [100,102,103,107–109]. In order to rationalize the interaction on a molecular level, we employed a similar homology modeling approach as for LuxE. Although the sequence identity of LuxC to aldehyde dehydrogenases is rather low (around 18%), we could generate homology models that nicely confirm the tetrameric assembly of LuxC, as indicated by biochemical experiments [102,109] (Figure 6). In addition, an overlay of the model with a substrate bound indole-3-acetaldehyde dehydrogenase (PDB 5IUW) [110] supports the biochemical observation of Cys286 being the active site residue that is acylated prior to reduction by the NADPH cofactor [108] (Figure 6 A). Also, the high evolutionary conservation of residues at the tetrameric interfaces as well as the substrate and cofactor binding sites further demonstrate the validity of the overall LuxC model (Figure 6 B-D).

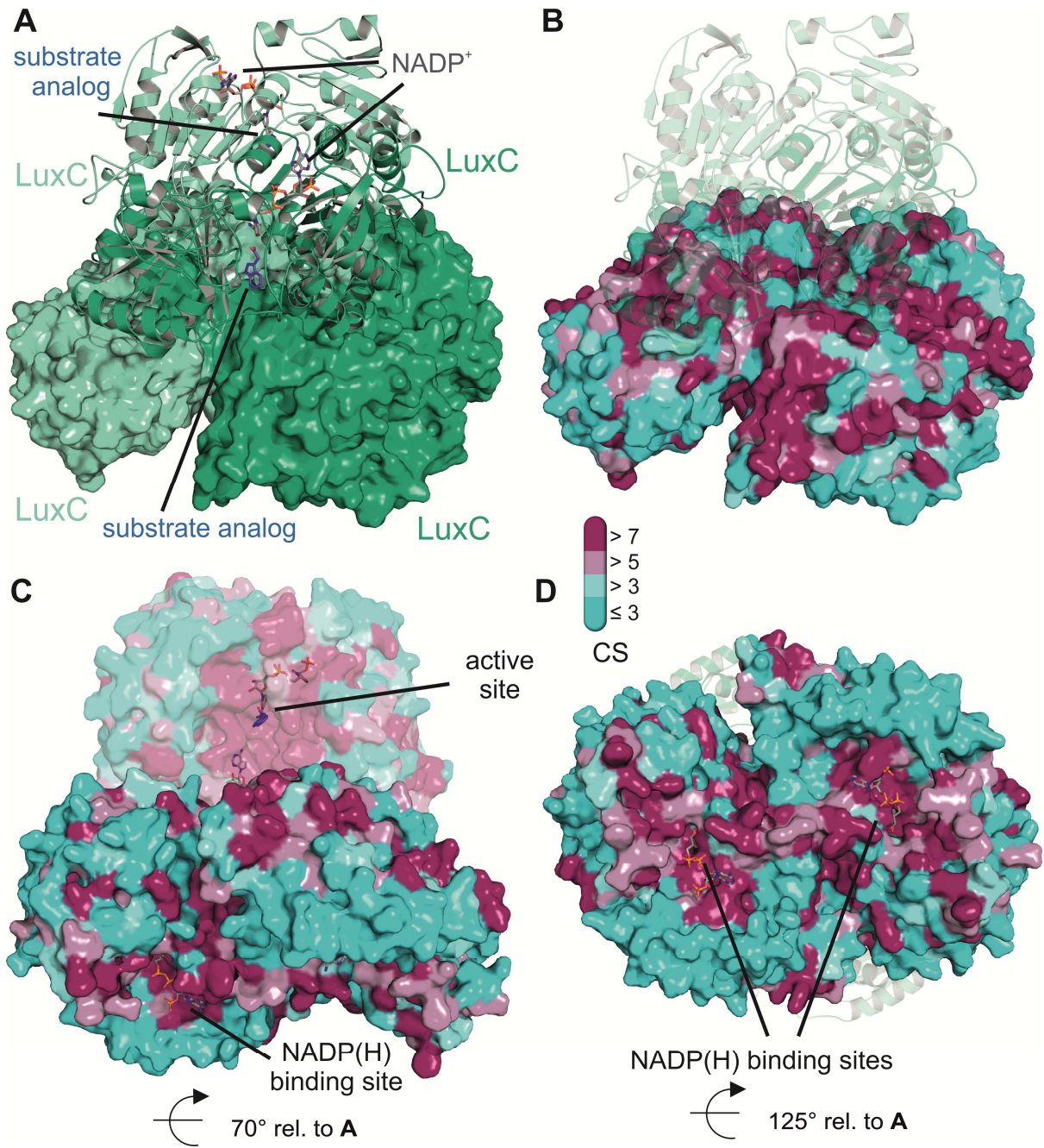


Figure 6. Homology model of LuxC from *V. harveyi*. Panel A features the tetrameric assembly of LuxC obtained from the SWISS-MODEL server [106] using the crystal structure of methylmalonate semialdehyde dehydrogenase from *Bacillus subtilis* as template (PDB 1T90). The tetramer corresponds to a dimer of dimers, which are shown once as cartoon representation and once as molecular surface. Individual protomers of each dimer are colored in green and light green. For the dimer in cartoon representation, we also show stick models of the substrate analog (indole-3-acetaldehyde – blue) and the cofactor (NADP⁺ – grey) in the respective binding sites obtained from the superposition of the LuxC model with indole-3-acetaldehyde dehydrogenase from *Pseudomonas syringae* (PDB 5IUW) and from the structure of an aldehyde dehydrogenase from *Burkholderia multivorans* (PDB 5JRY), respectively. Panels B, C and D provide an overview of the evolutionary conservation of residues according to the ConSurf server [23] and computed conservation scores (CS – bar legend). Panel B highlights the conserved residues at the interface of the individual LuxC dimers in the same orientation as panel A. For clarity, the dimer in cartoon representation is shown in transparent mode. Panel C shows a different orientation of the tetrameric assembly, to demonstrate the high degree of conservation in the active site generated at the interface of two subdomains of each LuxC protomer. Importantly, the substrate and the NADPH cofactor approach the active site from opposite sides. Panel D shows another view of one LuxC dimer highlighting the conservation of residues around the NADP⁺ binding site. For better visibility loop regions covering the NADP⁺ binding site are not shown in this figure. Similar to the observations for LuxE, patches of strongly conserved residues can be found at surface elements near the active site that are not involved in LuxC oligomerization and are therefore likely involved in complex formation with the LuxE synthetase subunits.

It is well established that LuxD, LuxE and LuxC form a large multifunctional complex consisting of four reductase, four synthetase and two to four transferase subunits with an overall molecular mass of ca. 500 kDa [102]. It was demonstrated that the LuxD transferase subunit is readily lost during purification of the complex, but that the maximum stimulation of activity was observed for equimolar concentrations of all components [102]. Therefore, we have attempted the reconstruction of a LuxC₄LuxD₄LuxE₄ complex based on our homology models in combination with available functional data and conservation of residues among LuxCDE containing organisms. The complex is highly specific for the processing of myristoyl-ACP in agreement with reports that myristyl aldehyde (tetradecanal) is the main substrate in the luciferase reaction [24,99]. In this context, it should be noted that other acyl-CoA derivatives are accepted by the reductase and thus aldehydes with different chain length may be used by the luciferase for light production. Considering the overall good agreement of the homology models of LuxC and LuxE with biochemical data, we had a closer look at the complementarity of individual interfaces. Based on the evolutionary conservation of residues and distance restraints between individual active sites in the high affinity complex of LuxC and LuxE, we observed a tantalizing molecular interface for their direct interaction. As shown in Figure 7, the distance between two active sites present in LuxC and their relative orientation perfectly matches the distance and orientation of the mobile LuxE element that harbors the acylated cysteine residue. It is known that the interaction between LuxC and LuxE is important for stimulating the acylation of LuxE [108] and even though molecular details of the presented structural models should be considered with caution, the observed interaction of the open LuxE conformation with LuxC might correspond to a functional state where the transfer of the acyl group between LuxE and LuxC can be realized.

Considering, however, the importance of protein dynamics in forming open and closed conformations in the synthetase family [104] as well as in the reductase family [111], it should be stressed that the manually placed model of the LuxC-LuxE complex presented here is an approximation and will require experimental support from crystallographic data or potentially reconstructions from electron micrographs.

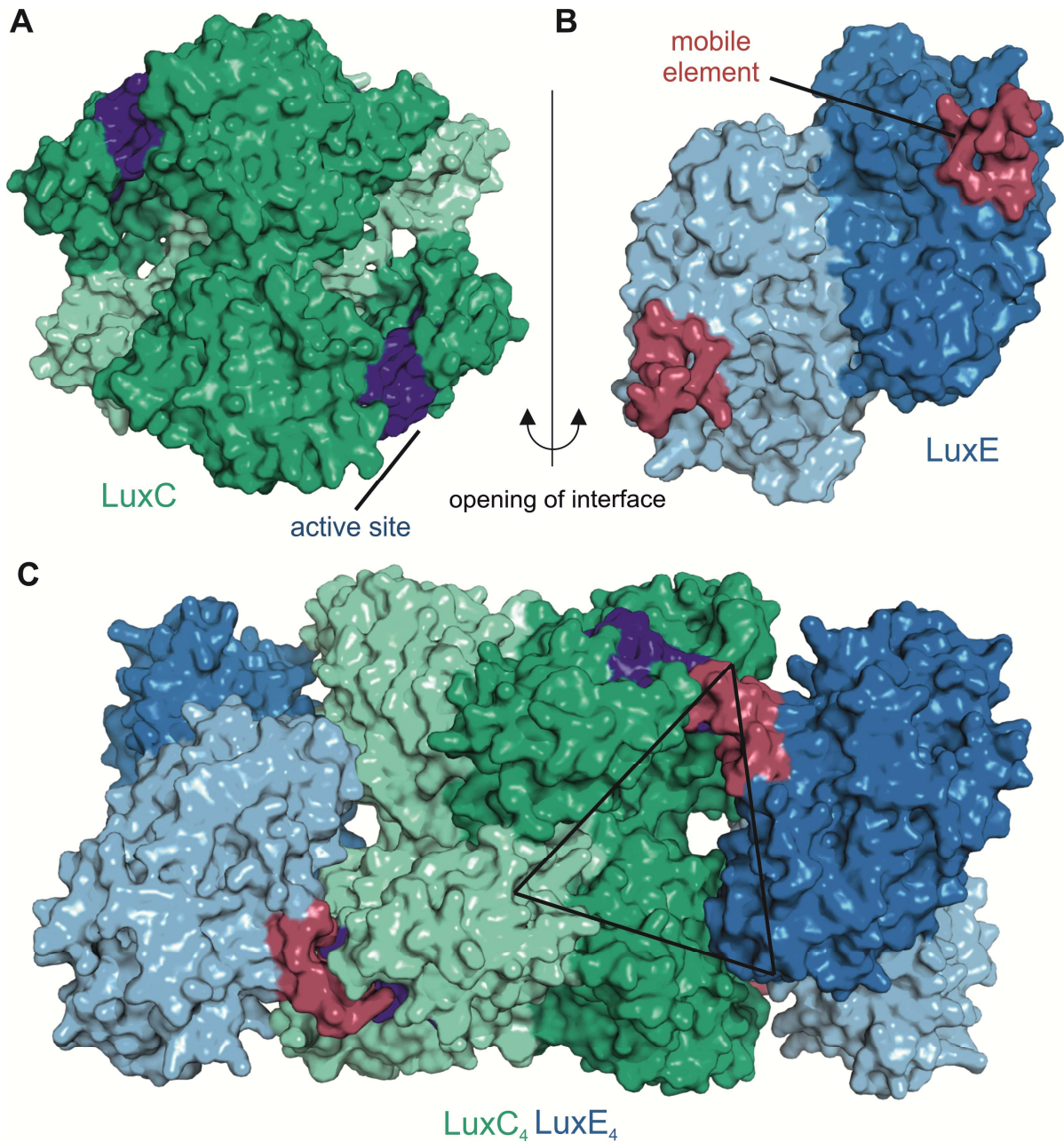


Figure 7. Model of the LuxC - LuxE interaction. Panels A and B show surface representations of LuxC and LuxE, respectively, colored according to the details presented in Figures 5 and 6. The active site region of LuxC is highlighted in dark blue and the mobile element of LuxE containing the acylated residue is colored in red. The central region of complementarity at the LuxC₂-LuxE₂ interface is lined by many highly conserved residues at specific surfaces of the respective oligomeric structures that have been highlighted in Figure 5D (LuxE) and Figure 6B (LuxC). Their complementarity is illustrated by the opening of the interface (right side interface of the complex in panel C) by opposite 90° rotations of LuxC and LuxE. Panel C also shows the second LuxE dimer bound to the opposite side of the LuxC tetramer resulting in an overall LuxC₄LuxE₄ stoichiometry. The architecture around the active site reveals an interesting triangular complementarity to the LuxD structure (Figure 4). For generation of the LuxC-LuxE complex we used a different template for homology modeling of LuxC to better reflect the open apo-conformation that might be needed for the initial interaction with LuxE. This model was again generated with the SWISS-MODEL server [106] based on the apo form of the indole-3-acetaldehyde dehydrogenase (PDB 5IUU). The apo form is characterized by a modest opening of the active site accompanied by unstructured loop regions involved in substrate coordination.

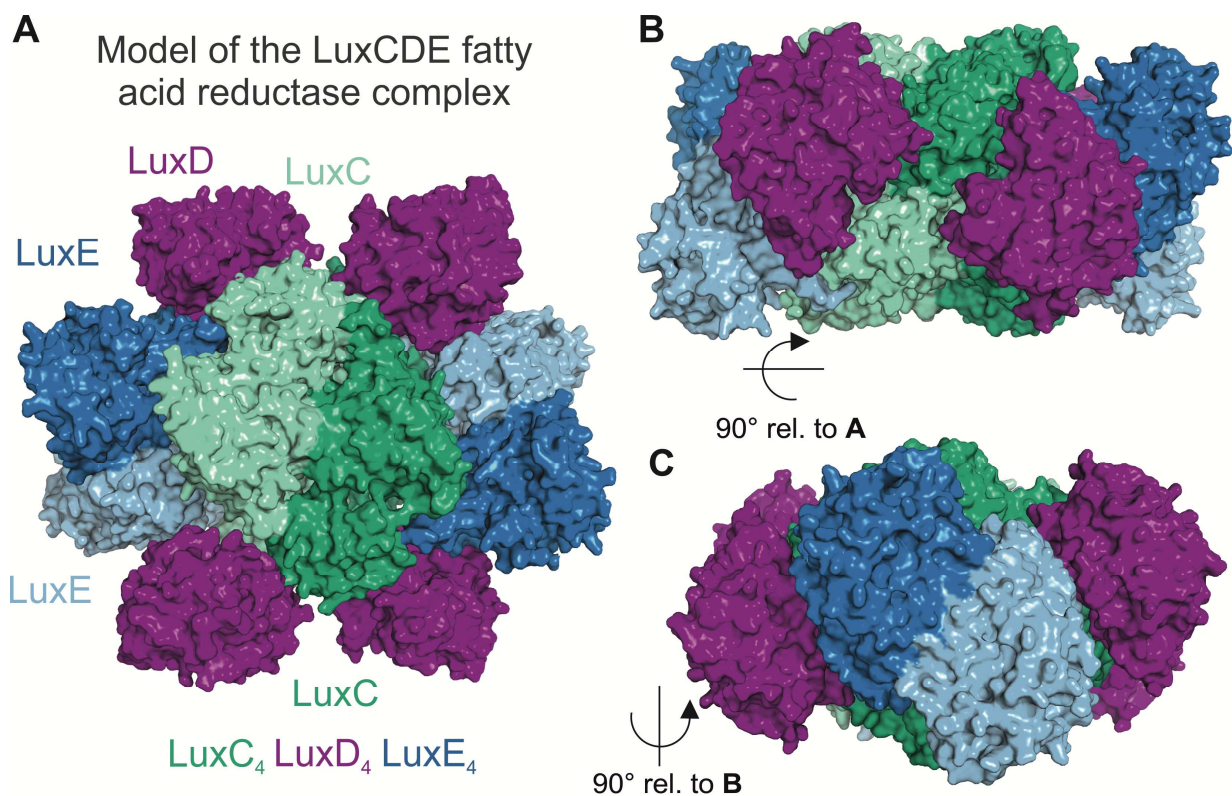


Figure 8. Tentative model of the LuxCDE fatty acid reductase complex. Panels A, B and C show different views of the LuxC₄LuxD₄LuxE₄ complex. Individual subunits are colored according to their individual presentations in Figures 4, 5 and 6. Dark and light colors correspond to individual protomers of the dimeric LuxC and LuxE subspecies. Monomeric LuxD protomers shield off individual active sites of the complex and can readily dissociate [102] to allow release of the final fatty aldehyde product and reassociate to deliver new fatty acid substrates after unloading them from the ACP.

Based on biochemical data and crosslinking experiments also LuxD is implicated to be involved in complex formation with LuxE and LuxC [100,102]. Considering the relatively open active site and the triangular shape needed to shield the active site from bulk solvent (Figure 7 C) we noticed that the outline of LuxD (Figure 4) perfectly matches this substrate access route. Since the active site serine of LuxD carrying the acyl moiety is positioned centrally at the triangular interacting surface and the LuxCE access route is relatively open, the exact rotational position of LuxD is difficult to address based on our LuxC₄E₄ model. Nevertheless, the elongated triangular shape of LuxD and its surface complementarity to the complex model (Figure 7) allowed a manual placement of four LuxD protomers to obtain a symmetric LuxC₄D₄E₄ complex (Figure 8) that is in line with biochemical observations and the evolutionary conservation of residues at the molecular surfaces of individual subunits. In fact, this model also supports the idea that the active site cavity formed at the interface of a LuxCDE complex is used for substrate channeling from LuxD to LuxE and further to LuxC, preventing unwanted dissociation of free fatty acids or unwanted side reactions of the acyl-AMP moiety. The final product of the reductase subunit, the aldehyde, can eventually be transferred to the luciferase for initiating light production.

1.8. CONCLUSIONS

The mesmerizing phenomenon of light emission by living organisms has attracted many scientists of various fields for many decades. As described in this review and summarized in Figure 9, bacterial bioluminescence is a wonderful showcase for the tantalizing complexity of bioluminescence. Although the enzyme luciferase catalyzes a rather trivial oxidation of an aldehyde to the corresponding acid, the mechanism that leads to the population of an excited state remains a major challenge for mechanistic and structural biochemists in particular as sound high-resolution data on reaction intermediates is still lacking. On the organismic level, many questions revolving around the putative functions of bioluminescence for bacteria are still unanswered. Despite the progress achieved over the last decades, the fascination with bioluminescence will surely prompt many more research efforts to challenge the current frontiers of our knowledge.

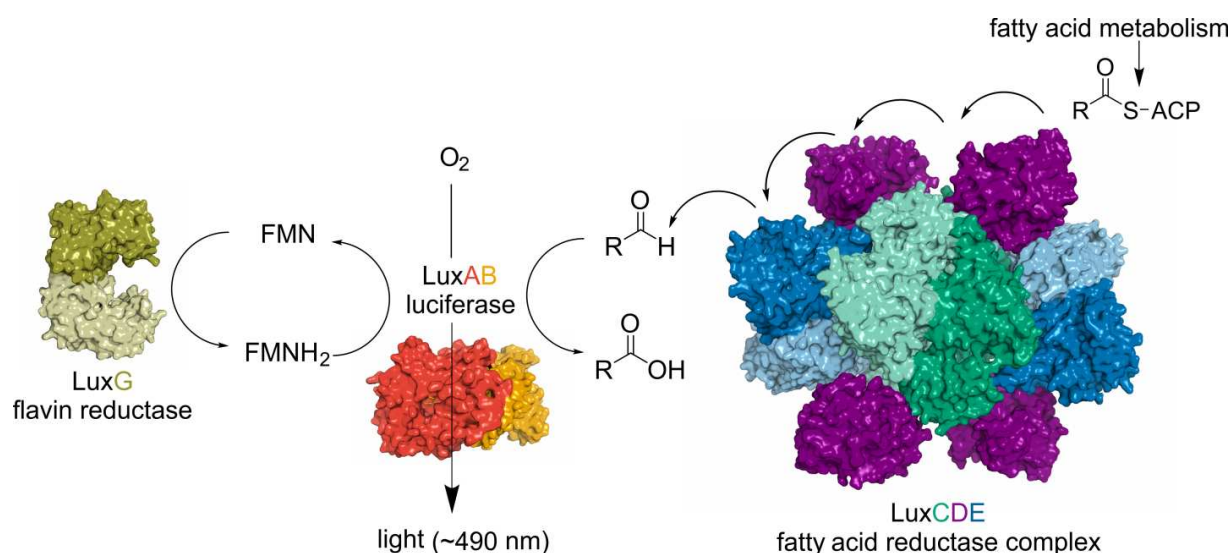


Figure 9. Bacterial bioluminescence in a nutshell. The central player in bacterial bioluminescence is the heterodimeric luciferase (red/orange; see Figure 3), which carries out the oxidation of long-chain fatty aldehydes to the corresponding acid accompanied by light emission (see Scheme 1). The required reduced FMN is provided by an NAD(P)H-dependent FMN reductase (LuxG, on the left side the structure of the closely related enzyme Fre of *E. coli* is shown in olive; PDB 1QFJ [30]) and the fatty aldehyde is synthesized through the multifunctional complex consisting of LuxCDE (green, violet and blue model on the right; see Figure 8).

Author contribution

EB, AW and PM wrote this manuscript together. EB concentrated on the chapters introduction, ecology, phylogeny, enzymes and reaction mechanisms in bacterial bioluminescence, genes associated with the *lux* operon and conclusion. Furthermore, EB did extensive BLAST searches on NCBI, evaluated all bioluminescent strains containing the core genes of the *lux* operon and established Supplementary Table 1. Additionally, all figures in those subchapters mentioned above and all schemes were prepared by EB. AW concentrated on the chapter structure-function relationships, especially on the fatty acid reductase complex, prepared homology models and sequence alignments based on Supplementary Table 1 (Supplementary Figure 1) to calculate conservation scores with the ConSurf server. AW further compiled all structural models of the luciferase (Figure 5) and the fatty acid reductase complex (Figures 6-10). PM focused on the chapters concerning the mechanism of bacterial bioluminescence and the generation of reduced FMN.

Acknowledgements

We are grateful to the Austrian Fonds zur Förderung der Wissenschaftlichen Forschung (FWF) for financial support through the Ph.D. program Molecular Enzymology to P.M. (W901).

Conflict of interest

The authors declare no conflict of interest.

1.9. REFERENCES

- [1] Widder EA. Bioluminescence in the ocean: Origins of biological, chemical, and ecological diversity. *Science* (80-) 2010;328:704–8. doi:10.1126/science.1174269.
- [2] Dunlap P. Bioluminescence, Microbial. In: Schaechter M, editor. *Encycl. Microbiol.*, Oxford: Elsevier; 2009, p. 45–61.
- [3] Haddock SHD, Moline MA, Case JF. Bioluminescence in the sea. *Ann Rev Mar Sci* 2010;2:443–93. doi:10.1146/annurev-marine-120308-081028.
- [4] Hastings JW, Potrikus CJ, Gupta SC, Kurfürst M, Makemson JC. Biochemistry and physiology of bioluminescent bacteria. *Adv Microb Physiol* 1985;26:235–91. doi:10.1016/S0065-2911(08)60398-7.
- [5] Zarubin M, Belkin S, Ionescu M, Genin A. Bacterial bioluminescence as a lure for marine zooplankton and fish. *Proc Natl Acad Sci* 2012;109:853–7. doi:10.1073/pnas.1116683109.
- [6] Dunlap P. Biochemistry and genetics of bacterial bioluminescence. In: Thouand G, Marks R, editors. *Biolumin. Fundam. Appl. Biotechnol.* - Vol. 1, vol. 144, Berlin, Heidelberg: Springer Berlin Heidelberg; 2014, p. 37–64. doi:10.1007/978-3-662-43385-0_2.
- [7] Meighen EA. Molecular biology of bacterial bioluminescence. *Microbiol Rev* 1991;55:123–42. doi:10.1146/annurev.bi.47.070178.001115.
- [8] Robertson LA, Figge MJ, Dunlap P V. Beijerinck and the bioluminescent bacteria: Microbiological experiments in the late 19th and early 20th centuries. *FEMS Microbiol Ecol* 2011;75:185–94. doi:10.1111/j.1574-6941.2010.01004.x.
- [9] Urbanczyk H, Ast JC, Dunlap P V. Phylogeny, genomics, and symbiosis of *Photobacterium*. *FEMS Microbiol Rev* 2011;35:324–42. doi:10.1111/j.1574-6976.2010.00250.x.
- [10] Urbanczyk H, Ast JC, Kaeding AJ, Oliver JD, Dunlap P V. Phylogenetic analysis of the incidence of *lux* gene horizontal transfer in *Vibrionaceae*. *J Bacteriol* 2008;190:3494–504. doi:10.1128/JB.00101-08.
- [11] Lee J. Bioluminescence. In: Smith KC, editor. *Sci. Photobiol.*, Plenum Press; 1989, p. 391–417.
- [12] Ast JC, Urbanczyk H, Dunlap P V. Multi-gene analysis reveals previously unrecognized phylogenetic diversity in *Aliivibrio*. *Syst Appl Microbiol* 2009;32:379–86. doi:10.1016/j.syapm.2009.04.005.
- [13] Hendry TA, Dunlap P V. The uncultured luminous symbiont of *Anomalops katoptron* (Beryciformes: Anomalopidae) represents a new bacterial genus. *Mol Phylogenet Evol* 2011;61:834–43. doi:10.1016/j.ympev.2011.08.006.

- [14] Hendry TA, de Wet JR, Dunlap P V. Genomic signatures of obligate host dependence in the luminous bacterial symbiont of a vertebrate. *Environ Microbiol* 2014;16:2611–22. doi:10.1111/1462-2920.12302.
- [15] Kaeding AJ, Ast JC, Pearce MM, Urbanczyk H, Kimura S, Endo H, et al. Phylogenetic diversity and cosymbiosis in the bioluminescent symbioses of “*Photobacterium mandapamensis*.” *Appl Environ Microbiol* 2007;73:3173–82. doi:10.1128/AEM.02212-06.
- [16] Ast JC, Dunlap P V. Phylogenetic resolution and habitat specificity of members of the *Photobacterium phosphoreum* species group. *Environ Microbiol* 2005;7:1641–54. doi:10.1111/j.1462-2920.2005.00859.x.
- [17] Dunlap P V., Ast JC, Kimura S, Fukui A, Yoshino T, Endo H. Phylogenetic analysis of host-symbiont specificity and codivergence in bioluminescent symbioses. *Cladistics* 2007;23:507–32. doi:10.1111/j.1096-0031.2007.00157.x.
- [18] Urbanczyk H, Kiwaki N, Furukawa T, Iwatsuki Y. Limited geographic distribution of certain strains of the bioluminescent symbiont *Photobacterium leiognathi*. *FEMS Microbiol Ecol* 2012;81:355–63. doi:10.1111/j.1574-6941.2012.01353.x.
- [19] Urbanczyk H, Ast JC, Higgins MJ, Carson J, Dunlap P V. Reclassification of *Vibrio fischeri*, *Vibrio logei*, *Vibrio salmonicida* and *Vibrio wodanis* as *Aliivibrio fischeri* gen. nov., comb. nov., *Aliivibrio logei* comb. nov., *Aliivibrio salmonicida* comb. nov. and *Aliivibrio wodanis* comb. nov. *Int J Syst Evol Microbiol* 2007;57:2823–9. doi:10.1099/ijs.0.65081-0.
- [20] Ruby EG, Urbanowski M, Campbell J, Dunn A, Faini M, Gunsalus R, et al. Complete genome sequence of *Vibrio fischeri*: A symbiotic bacterium with pathogenic congeners. *Proc Natl Acad Sci* 2005;102:3004–9. doi:10.1073/pnas.0409900102.
- [21] Lin B, Wang Z, Malanoski AP, O’Grady EA, Wimpee CF, Vuddhakul V, et al. Comparative genomic analyses identify the *Vibrio harveyi* genome sequenced strains BAA-1116 and HY01 as *Vibrio campbellii*. *Environ Microbiol Rep* 2010;2:81–9. doi:10.1111/j.1758-2229.2009.00100.x.
- [22] Urbanczyk H, Ogura Y, Hendry TA, Gould AL, Kiwaki N, Atkinson JT, et al. Genome sequence of *Photobacterium mandapamensis* strain svers.1.1, the bioluminescent symbiont of the cardinal fish *Siphamia versicolor*. *J Bacteriol* 2011;193:3144–5. doi:10.1128/JB.00370-11.
- [23] Ashkenazy H, Abadi S, Martz E, Chay O, Mayrose I, Pupko T, et al. ConSurf 2016: an improved methodology to estimate and visualize evolutionary conservation in macromolecules. *Nucleic Acids Res* 2016;44:344–50. doi:10.1093/nar/gkw408.
- [24] Ulitzur S, Hastings JW. Evidence for tetradecanal as the natural aldehyde in bacterial bioluminescence. *Proc Natl Acad Sci USA* 1979;76:265–7.
- [25] Meighen EA. Bacterial bioluminescence: organization, regulation, and application of the *lux* genes. *FASEB J* 1993;7:1016–22.

- [26] Kurfürst M, Ghisla S, Hastings JW. Characterization and postulated structure of the primary emitter in the bacterial luciferase reaction. *Proc Natl Acad Sci USA* 1984;81:2990–4.
- [27] Campbell ZT, Weichsel A, Montfort WR, Baldwin TO. Crystal structure of the bacterial luciferase/flavin complex provides insight into the function of the β subunit. *Biochemistry* 2009;48:6085–94. doi:10.1021/bi900003t.
- [28] Ellis HR. The FMN-dependent two-component monooxygenase systems. *Arch Biochem Biophys* 2010;497:1–12. doi:10.1016/j.abb.2010.02.007.
- [29] van Berkel WJH, Kamerbeek NM, Fraaije MW. Flavoprotein monooxygenases, a diverse class of oxidative biocatalysts. *J Biotechnol* 2006;124:670–89. doi:10.1016/j.jbiotec.2006.03.044.
- [30] Ingelman M, Ramaswamy S, Nivière V, Fontecave M, Eklund H. Crystal structure of NAD(P)H:flavin oxidoreductase from *Escherichia coli*. *Biochemistry* 1999;38:7040–9. doi:10.1021/bi982849m.
- [31] Zenno S, Saigo K. Identification of the genes encoding NAD(P)H-flavin oxidoreductases that are similar in sequence to *Escherichia coli* Fre in four species of luminous bacteria: *Photobacterium luminescens*, *Vibrio fischeri*, *Vibrio harveyi*, and *Vibrio orientalis*. *J Bacteriol* 1994;176:3544–51. doi:10.1128/jb.176.12.3544-3551.1994.
- [32] Lin JW, Chao YF, Weng SF. Characteristic analysis of the *luxG* gene encoding the probable flavin reductase that resides in the *lux* operon of *Photobacterium leiognathi*. *Biochem Biophys Res Commun* 1998;246:446–52. doi:10.1006/bbrc.1998.8641.
- [33] Nijvipakul S, Wongratana J, Suadee C, Entsch B, Ballou DP, Chaiyen P. LuxG is a functioning flavin reductase for bacterial luminescence. *J Bacteriol* 2008;190:1531–8. doi:10.1128/JB.01660-07.
- [34] Nijvipakul S, Ballou DP, Chaiyen P. Reduction kinetics of a flavin oxidoreductase LuxG from *Photobacterium leiognathi* (TH1): half-sites reactivity. *Biochemistry* 2010;49:9241–8. doi:10.1021/bi1009985.
- [35] Ast JC, Dunlap P V. Phylogenetic analysis of the *lux* operon distinguishes two evolutionarily distinct clades of *Photobacterium leiognathi*. *Arch Microbiol* 2004;181:352–61. doi:10.1007/s00203-004-0663-7.
- [36] Moore SA, James MNG, O’Kane DJ, Lee J. Crystallization of *Photobacterium leiognathi* non-fluorescent flavoprotein with limited sequence identity to bacterial luciferase. *J Mol Biol* 1992;224:523–6.
- [37] Moore SA, James MNG, O’Kane DJ, Lee J. Crystal structure of a flavoprotein related to the subunits of bacterial luciferase. *EMBO J* 1993;12:1767–74.
- [38] Moore SA, James MNG. Structural refinement of the non-fluorescent flavoprotein from *Photobacterium leiognathi* at 1.60 Å resolution. *J Mol Biol* 1995;249:195–214.

- [39] Bergner T, Tabib CR, Winkler A, Stipsits S, Kayer H, Lee J, et al. Structural and biochemical properties of LuxF from *Photobacterium leiognathi*. *Biochim Biophys Acta - Proteins Proteomics* 2015;1854:1466–75. doi:10.1016/j.bbapap.2015.07.008.
- [40] Tabib CR, Brodl E, Macheroux P. Evidence for the generation of myristylated FMN by bacterial luciferase. *Mol Microbiol* 2017;104:1027–36. doi:10.1111/mmi.13676.
- [41] Gregor C, Gwosch KC, Sahl SJ, Hell SW. Strongly enhanced bacterial bioluminescence with the *ilux* operon for single-cell imaging. *Proc Natl Acad Sci* 2018. doi:10.1073/pnas.1715946115.
- [42] Cui B, Zhang L, Song Y, Wei J, Li C, Wang T, et al. Engineering an enhanced, thermostable, monomeric bacterial luciferase gene as a reporter in plant protoplasts. *PLoS One* 2014. doi:10.1371/journal.pone.0107885.
- [43] Lin JW, Chao YF, Weng SF. Riboflavin synthesis genes *ribE*, *ribB*, *ribH*, *ribA* reside in the *lux* operon of *Photobacterium leiognathi*. *Biochem Biophys Res Commun* 2001;284:587–95. doi:10.1006/bbrc.2001.5013.
- [44] Sung N-D, Lee CY. The *lux* genes and riboflavin genes in bioluminescent system of *Photobacterium leiognathi* are under common regulation. *J Photoscience* 2004;11:41–5.
- [45] Miyashiro T, Ruby EG. Shedding light on bioluminescence regulation in *Vibrio fischeri*. *Mol Microbiol* 2012;84:795–806. doi:10.1111/j.1365-2958.2012.08065.x.
- [46] Defoirdt T, Boon N, Sorgeloos P, Verstraete W, Bossier P. Quorum sensing and quorum quenching in *Vibrio harveyi*: Lessons learned from *in vivo* work. *ISME J* 2008;2:19–26. doi:10.1038/ismej.2007.92.
- [47] Ruby EG, Nealson KH. A luminous bacterium that emits yellow light. *Science* (80-) 1977;196:432–4. doi:10.1126/science.850787.
- [48] Daubner SC, Astorga AM, Leisman GB, Baldwin TO. Yellow light emission of *Vibrio fischeri* strain Y-1: purification and characterization of the energy-accepting yellow fluorescent protein. *Proc Natl Acad Sci U S A* 1987;84:8912–6. doi:10.1073/pnas.84.24.8912.
- [49] Macheroux P, Schmidt KU, Steinerstauch P, Ghisla S, Colepicolo P, Buntic R, et al. Purification of the yellow fluorescent protein from *Vibrio fischeri* and identity of the flavin chromophore. *Biochem Biophys Res Commun* 1987;146:101–6. doi:10.1016/0006-291X(87)90696-6.
- [50] Gast R, Neering IR, Lee J. Separation of a blue fluorescence protein from bacterial luciferase. *Biochem Biophys Res Commun* 1978;80:14–21. doi:10.1016/0006-291X(78)91097-5.
- [51] O’Kane DJ, Karle VA, Lee J. Purification of lumazine proteins from *Photobacterium leiognathi* and *Photobacterium phosphoreum*: Bioluminescence properties. *Biochemistry* 1985;24:1461–7. doi:10.1021/bi00327a026.

- [52] Lee J, O’Kane DJ, Visser AJWG. Spectral properties and function of two lumazine proteins from *Photobacterium*. *Biochemistry* 1985;24:1476–83. doi:10.1021/bi00327a028.
- [53] Small ED, Koka P, Lee J. Lumazine protein from the bioluminescent bacterium *Photobacterium phosphoreum*. *J Biol Chem* 1980;255:8804–10.
- [54] Koka P, Lee J. Separation and structure of the prosthetic group of the blue fluorescence protein from the bioluminescent bacterium *Photobacterium phosphoreum*. *Proc Natl Acad Sci U S A* 1979;76:3068–72. doi:10.1073/pnas.76.7.3068.
- [55] Gast R, Lee J. Isolation of the *in vivo* emitter in bacterial bioluminescence. *Proc Natl Acad Sci U S A* 1978;75:833–7. doi:10.1073/pnas.75.2.833.
- [56] Petushkov VN, Ketelaars M, Gibson BG, Lee J. Interaction of *Photobacterium leiognathi* and *Vibrio fischeri* Y1 luciferases with fluorescent (antenna) proteins: Bioluminescence effects of the aliphatic additive. *Biochemistry* 1996. doi:10.1021/bi9608931.
- [57] Eckstein JW, Cho KW, Colepicolo P, Ghisla S, Hastings JW, Wilson T. A time-dependent bacterial bioluminescence emission spectrum in an *in vitro* single turnover system: energy transfer alone cannot account for the yellow emission of *Vibrio fischeri* Y-1. *Proc Natl Acad Sci U S A* 1990. doi:10.1073/pnas.87.4.1466.
- [58] Macheroux P. Untersuchungen zum Reaktionsmechanismus der bakteriellen Biolumineszenz. University of Konstanz, 1986.
- [59] Titushin MS, Feng Y, Lee J, Vysotski ES, Liu ZJ. Protein-protein complexation in bioluminescence. *Protein Cell* 2011;2:957–72. doi:10.1007/s13238-011-1118-y.
- [60] Petushkov VN, Gibson BG, Lee J. Direct measurement of excitation transfer in the protein complex of bacterial luciferase hydroxyflavin and the associated yellow fluorescence proteins from *Vibrio fischeri* Y1. *Biochemistry* 1996. doi:10.1021/bi952691v.
- [61] Chatwell L, Illarionova V, Illarionov B, Eisenreich W, Huber R, Skerra A, et al. Structure of lumazine protein, an optical transponder of luminescent bacteria. *J Mol Biol* 2008;382:44–55. doi:10.1016/j.jmb.2008.06.052.
- [62] Sato Y, Shimizu S, Ohtaki A, Noguchi K, Miyatake H, Dohmae N, et al. Crystal structures of the lumazine protein from *Photobacterium kishitanii* in complexes with the authentic chromophore, 6,7-dimethyl-8-(1'-D-ribityl) lumazine, and its analogues, riboflavin and flavin mononucleotide, at high resolution. *J Bacteriol* 2010;192:127–33. doi:10.1128/JB.01015-09.
- [63] Lee J. Lumazine protein and the excitation mechanism in bacterial bioluminescence. *Biophys Chem* 1993;48:149–58. doi:10.1016/0301-4622(93)85006-4.
- [64] Shimomura O. *Bioluminescence - Chemical Principles and Methods*. World Scientific Publishing Co. Pte. Ltd.; 2006. doi:10.1142/9789812773647.

- [65] Wilson T, Hastings JW. Bioluminescence living lights, lights for living. Harvard University Press; 2013.
- [66] Tu SC. Reduced flavin: donor and acceptor enzymes and mechanisms of channeling. *Antioxid Redox Signal* 2001;3:881–97. doi:10.1089/15230860152665046.
- [67] Macheroux P, Kappes B, Ealick SE. Flavogenomics - A genomic and structural view of flavin-dependent proteins. *FEBS J* 2011;278:2625–34. doi:10.1111/j.1742-4658.2011.08202.x.
- [68] Fisher AJ, Rayment I, Raushel FM, Baldwin TO. Three-dimensional structure of bacterial luciferase from *Vibrio harveyi* at 2.4 Å resolution. *Biochemistry* 1995;34:6581–6. doi:10.1021/bi00020a002.
- [69] Fisher AJ, Thompson TB, Thoden JB, Baldwin TO, Rayment I. The 1.5 Å resolution crystal structure of bacterial luciferase in low salt conditions. *J Biol Chem* 1996;271:21956–68. doi:10.1074/jbc.271.36.21956.
- [70] Hastings JW, Balny C. The oxygenated bacterial luciferase-flavin intermediate. Reaction products via the light and dark pathways. *J Biol Chem* 1975;250:7288–93.
- [71] Hastings JW, Balny C, Peuch CL, Douzou P. Spectral properties of an oxygenated luciferase-flavin intermediate isolated by low-temperature chromatography. *Proc Natl Acad Sci U S A* 1973;70:3468–72. doi:066/4.
- [72] Ahrens M, Macheroux P, Eberhard A, Ghisla S, Branchaud BP, Hastings JW. Boronic acids as mechanistic probes for the bacterial luciferase reaction. *Photochem Photobiol* 1991;54:295–9. doi:10.1111/j.1751-1097.1991.tb02019.x.
- [73] Vervoort J, Muller F, van den Berg WAM, Moonen CTW, Lee J. Identifications of the true carbon-13 nuclear magnetic resonance spectrum of the stable intermediate II in bacterial luciferase. *Biochemistry* 1986;25:8062–7. doi:10.1021/bi00372a040.
- [74] Palfey BA, McDonald CA. Control of catalysis in flavin-dependent monooxygenases. *Arch Biochem Biophys* 2010;493:26–36. doi:10.1016/j.abb.2009.11.028.
- [75] Luo Y, Liu YJ. Bioluminophore and Flavin Mononucleotide Fluorescence Quenching of Bacterial Bioluminescence—A Theoretical Study. *Chem - A Eur J* 2016. doi:10.1002/chem.201603314.
- [76] Macheroux P, Ghisla S, Hastings JW. Spectral detection of an intermediate preceding the excited state in the bacterial luciferase reaction. *Biochemistry* 1993;32:14183–6.
- [77] Baldwin TO, Nicoli MZ, Becvar JE, Hastings JW. Bacterial luciferase. Binding of oxidized flavin mononucleotide. *J Biol Chem* 1975;250:2763–8. doi:10.1128/AAC.03728-14.
- [78] Hou C, Liu YJ, Ferré N, Fang WH. Understanding bacterial bioluminescence: A theoretical study of the entire process, from reduced flavin to light emission. *Chem - A Eur J* 2014;20:7979–86. doi:10.1002/chem.201400253.
- [79] Tu SC. Mechanisms of bacterial luciferase and related flavin reductases. In: Hille R, Miller SM, Palfey BA, editors. *Handb. Flavoproteins*, Berlin: De Gruyter; 2013, p. 101–18.

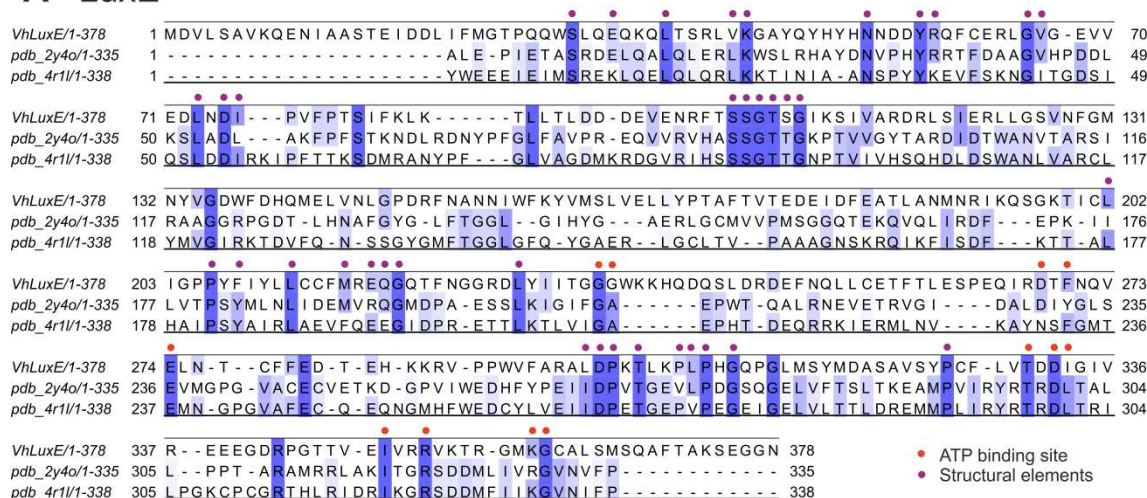
- [80] Eberhard A, Hastings JW. A postulated mechanism for the bioluminescent oxidation of reduced flavin mononucleotide. *Biochem Biophys Res Commun* 1972;47:348–53. doi:10.1016/0006-291X(72)90719-X.
- [81] Branchaud BP, Walsh CT. Functional group diversity in enzymatic oxygenation reactions catalyzed by bacterial flavin-containing cyclohexanone oxygenase. *J Am Chem Soc* 1985;107:2153–61. doi:10.1021/ja00293a054.
- [82] Eckstein JW, Hastings JW, Ghisla S. Mechanism of bacterial bioluminescence: 4a,5-dihydroflavin analogs as models for luciferase hydroperoxide intermediates and the effect of substituents at the 8-position of flavin on luciferase kinetics. *Biochemistry* 1993;32:404–11.
- [83] Merényi G, Lind J, Mager HIX, Tu SC. Properties of 4a-hydroxy-4a,5-dihydroflavin radicals in relation to bacterial bioluminescence. *J Phys Chem* 1992;96:10528–33. doi:10.1021/j100204a074.
- [84] Francisco WA, Abu-Soud HM, DelMonte AJ, Singleton DA, Baldwin TO, Raushel FM. Deuterium kinetic isotope effects and the mechanism of the bacterial luciferase reaction. *Biochemistry* 1998;37:2596–606. doi:10.1021/bi972266x.
- [85] Schuster GB. Chemiluminescence of Organic Peroxides. Conversion of Ground-State Reactants to Excited-State Products by the Chemically Initiated Electron-Exchange Luminescence Mechanism. *Acc Chem Res* 1979. doi:10.1021/ar50142a003.
- [86] Matheson IB, Lee J, Müller F. Bacterial bioluminescence: Spectral study of the emitters in the *in vitro* reaction. *Proc Natl Acad Sci U S A* 1981;78:948–52. doi:10.1021/bi0024310.
- [87] Koo JA, Schmidt SP, Schuster GB. Bioluminescence of the firefly: key steps in the formation of the electronically excited state for model systems. *Proc Natl Acad Sci* 1978. doi:10.1073/pnas.75.1.30.
- [88] Catalani LH, Wilson T. Electron Transfer and Chemiluminescence. Two Inefficient Systems: 1,4-Dimethoxy-9,10-diphenylanthracene Peroxide and Diphenoyl Peroxide. *J Am Chem Soc* 1989. doi:10.1021/ja00189a043.
- [89] Ding BW, Liu YJ. Bioluminescence of firefly squid via mechanism of single electron-transfer oxygenation and charge-transfer-induced luminescence. *J Am Chem Soc* 2017. doi:10.1021/jacs.6b09119.
- [90] Yue L, Liu YJ, Fang WH. Mechanistic insight into the chemiluminescent decomposition of firefly dioxetanone. *J Am Chem Soc* 2012. doi:10.1021/ja302979t.
- [91] Yue L, Lan Z, Liu YJ. The theoretical estimation of the bioluminescent efficiency of the firefly via a nonadiabatic molecular dynamics simulation. *J Phys Chem Lett* 2015. doi:10.1021/jz502305g.
- [92] Pinto Da Silva L, Pereira RFJ, Magalhães CM, Esteves Da Silva JCG. Mechanistic Insight into Cypridina Bioluminescence with a Combined Experimental and Theoretical Chemiluminescent Approach. *J Phys Chem B* 2017. doi:10.1021/acs.jpccb.7b06295.

- [93] Min CG, Ferreira PJO, Pinto da Silva L. Theoretically obtained insight into the mechanism and dioxetanone species responsible for the singlet chemiexcitation of Coelenterazine. *J Photochem Photobiol B Biol* 2017. doi:10.1016/j.jphotobiol.2017.07.012.
- [94] Shannon P, Presswood RB, Spencer R, Becvar JE, Hastings JW, Walsh CT. A study of deuterium isotope effects on the bacterial bioluminescence reaction. In: Singer TP, Ondarza RN, editors. *Mech. Oxid. Enzym.*, North Holland, Amsterdam: Elsevier; 1978, p. 69–78.
- [95] Kasai S, Matsui K, Nakamura T. Purification and some properties of FP390 from *P. phosphoreum*. In: Edmondson DE, McCormick DB, editors. *Flavins and Flavoproteins*, Berlin/New York: Walter de Gruyter; 1987, p. 647–50.
- [96] Jeffers CE, Tu SC. Differential transfers of reduced flavin cofactor and product by bacterial flavin reductase to luciferase. *Biochemistry* 2001;40:1749–54. doi:10.1021/bi0024310.
- [97] Tinikul R, Pitsawong W, Sucharitakul J, Nijvipakul S, Ballou DP, Chaiyen P. The transfer of reduced flavin mononucleotide from LuxG oxidoreductase to luciferase occurs via free diffusion. *Biochemistry* 2013;52:6834–43. doi:10.1021/bi4006545.
- [98] Campbell ZT, Baldwin TO. Fre is the major flavin reductase supporting bioluminescence from *Vibrio harveyi* luciferase in *Escherichia coli*. *J Biol Chem* 2009;284:8322–8. doi:10.1074/jbc.M808977200.
- [99] Ferri SR, Meighen EA. A *lux*-specific myristoyl transferase in luminescent bacteria related to eukaryotic serine esterases. *J Biol Chem* 1991;266:12852–7.
- [100] Carey LM, Rodriguez A, Meighen E. Generation of fatty acids by an acyl esterase in the bioluminescent system of *Photobacterium phosphoreum*. *J Biol Chem* 1984;259:10216–21.
- [101] Lawson DM, Derewenda U, Serre L, Wei Y, Derewend ZS, Ferri S, et al. Structure of a myristoyl-ACP-specific thioesterase from *Vibrio harveyi*. *Biochemistry* 1994;33:9382–8. doi:10.1021/bi00198a003.
- [102] Wall L, Meighen EA. Subunit structure of the fatty acid reductase complex from *Photobacterium phosphoreum*. *Biochemistry* 1986;25:4315–21. doi:10.1021/bi00363a021.
- [103] Soly RR, Meighen EA. Identification of the acyl transfer site of fatty acyl-protein synthetase from bioluminescent bacteria. *J Mol Biol* 1991;219:69–77. doi:10.1016/0022-2836(91)90858-4.
- [104] Li Z, Nair SK. Structural basis for specificity and flexibility in a plant 4-coumarate:CoA ligase. *Structure* 2015;23:2032–42. doi:10.1016/j.str.2015.08.012.
- [105] Law A, Boulanger MJ. Defining a structural and kinetic rationale for paralogous copies of phenylacetate-CoA ligases from the cystic fibrosis pathogen *Burkholderia cenocepacia* J2315. *J Biol Chem* 2011;286:15577–85. doi:10.1074/jbc.M111.219683.

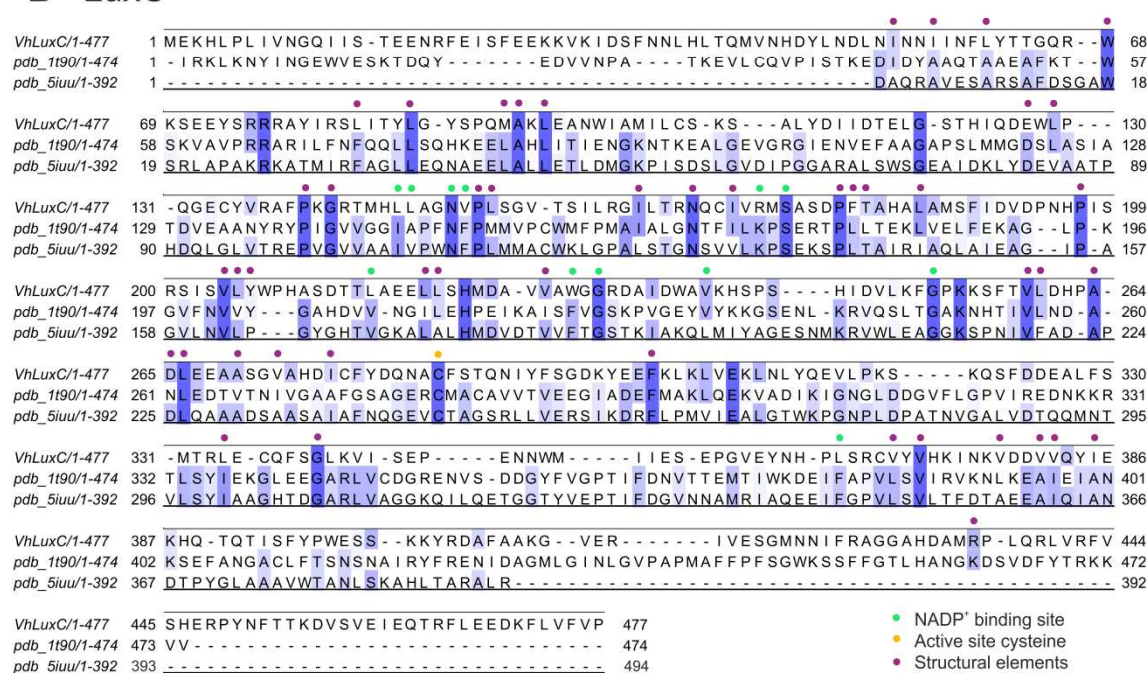
- [106] Biasini M, Bienert S, Waterhouse A, Arnold K, Studer G, Schmidt T, et al. SWISS-MODEL: Modelling protein tertiary and quaternary structure using evolutionary information. *Nucleic Acids Res* 2014;42. doi:10.1093/nar/gku340.
- [107] Wall L, Rodriguez A, Meighen E. Intersubunit transfer of fatty acyl groups during fatty acid reduction. *J Biol Chem* 1986;261:15981–8.
- [108] Lee CY, Meighen EA. Cysteine-286 as the site of acylation of the Lux-specific fatty acyl-CoA reductase. *Biochim Biophys Acta - Protein Struct Mol Enzymol* 1997;1338:215–22. doi:10.1016/S0167-4838(96)00203-8.
- [109] Rodriguez A, Riendeau D, Meighen E. Purification of the acyl coenzyme A reductase component from a complex responsible for the reduction of fatty acids in bioluminescent bacteria. *J Biol Chem* 1983;258:5233–7.
- [110] McClerklin SA, Lee SG, Harper CP, Nwumeh R, Jez JM, Kunkel BN. Indole-3-acetaldehyde dehydrogenase-dependent auxin synthesis contributes to virulence of *Pseudomonas syringae* strain DC3000. *PLoS Pathog* 2018;14. doi:10.1371/journal.ppat.1006811.
- [111] Luo M, Tanner JJ. Structural basis of substrate recognition by aldehyde dehydrogenase 7A1. *Biochemistry* 2015;54:5513–22. doi:10.1021/acs.biochem.5b00754.
- [112] Waterhouse AM, Procter JB, Martin DMA, Clamp M, Barton GJ. Jalview Version 2-A multiple sequence alignment editor and analysis workbench. *Bioinformatics* 2009. doi:10.1093/bioinformatics/btp033.

1.10. Supplementary Information

A LuxE



B LuxC



Supplementary Figure 1: Sequence alignments of LuxE (panel A) and LuxC (panel B) with two templates each that were used for the generation of homology models using the SWISS-MODEL server [106]. The aligned proteins are LuxE from *V. harveyi* (UniProt identifier B2XS33), phenylacetate-CoA ligase from *Burkholderia cenocepacia* (B4EL89, PDB 2Y4O) and acyl-CoA ligase from *Bacteroides thetaiotaomicron* (Q8AAN6, PDB 4R1L) in panel A as well as LuxC from *V. harveyi* (P08639), methylmalonate semialdehyde dehydrogenase from *Bacillus subtilis* (P42412, PDB 1T90) and apo indole-3-acetaldehyde dehydrogenase from *Pseudomonas syringae* (Q88BC5, PDB 5IUU) in panel B. The alignment was performed by the SWISS-MODEL server after selecting the corresponding models and visualized using Jalview [112]. Conserved regions are highlighted in shades of blue, with darker hues indicating higher conservation. Colored dots above these regions indicate the primary reason for conservation and are classified according to the legend in each panel to either structurally important elements or functional regions involved in cofactor binding or active site formation.

Supplementary Table 1: List of bioluminescent bacterial strains with available *lux* operon sequence

No	strain	GenBank accession no	available sequence information
1	<i>Photobacterium leiognathi</i> subsp. <i>mandapamensis</i> ATCC 27561	DQ988878	<i>luxC</i> * <i>DABFEG</i> , <i>ribEBHA</i> *
2a	<i>Photobacterium mandapamensis</i> ajapo.4.20_copy1	EU122285	<i>luxCDABFEG</i> , <i>ribEBHA</i>
2b	<i>Photobacterium mandapamensis</i> ajapo.4.20_copy2	EU122286	<i>luxCDABEG</i> , <i>ribEBHA</i>
3	<i>Photobacterium leiognathi</i> subsp. <i>mandapamensis</i> PL-721	DQ988877.2	<i>luxC</i> * <i>DABFEG</i> , <i>ribEBHA</i> *
4	<i>Photobacterium phosphoreum</i> ATCC 11040	DQ988873	<i>luxCDABFEG</i> , <i>ribBHA</i> *
5	<i>Photobacterium phosphoreum</i> (NBRC 104104)	AB367391.1	<i>luxCDABFEG</i>
6	<i>Photobacterium phosphoreum</i> FS-1.1	AY849486.2	<i>luxC</i> * <i>DABFEG</i> , <i>ribB</i>
7	<i>Photobacterium phosphoreum</i> (NBRC 13896)	AB104437.1	<i>luxCDABFEG</i> , <i>lumP</i>
8	<i>Photobacterium phosphoreum</i>	LC144829.1	<i>luxCDABFEG</i>
9	<i>Photobacterium leiognathi</i> ATCC 25521	M63594	<i>luxCDABEG</i>
10a	<i>Photobacterium leiognathi</i> lelon.2.1_copy1	EF536333.1	<i>luxCDABEG</i> , <i>ribEBHA</i> , <i>lumQ</i>
10b	<i>Photobacterium leiognathi</i> lelon.2.1_copy2	EF536334.1	<i>luxC</i> * <i>DABEG</i> , <i>ribEBHA</i>
11a	<i>Photobacterium leiognathi</i> lnuch.21.1	EF536335.1	<i>luxCDABEG</i> , <i>ribEBHA</i> , <i>lumQ</i>
11b	<i>Photobacterium leiognathi</i> lnuch.21.1	EF536336.1	<i>luxCDABEG</i> , <i>ribEBHA</i>
12	<i>Photobacterium aquimaris</i> (NBRC 104633)	JQ229765.1	<i>luxCDABFEG</i> , <i>ribEBHA</i> *
13	<i>Photobacterium aquimaris</i> BS-1	JQ229766.1	<i>luxCDABFEG</i> , <i>ribEBHA</i> , <i>lumP</i>
14	<i>Photobacterium kishitanii</i> (pjapo.1.1)	DQ988874	<i>luxCDABFEG</i> , <i>ribEBHA</i> *
15	<i>Photobacterium kishitanii</i> (NCIMB 844)	AY341064.2	<i>luxCDABFEG</i> , <i>ribEB</i>
16	<i>Photobacterium damsela</i> BT-6	EU122290.1	<i>luxD</i> * <i>ABE</i>
17a	<i>Photobacterium</i> lnuch.13.1_copy1	EF536338	<i>luxCDABEG</i> , <i>ribEBHA</i> , <i>lumQ</i>
17b	<i>Photobacterium</i> lnuch.13.1_copy2	EF536332	<i>luxCDABEG</i> , <i>ribEBHA</i> , <i>lumQ</i>
18	<i>Aliivibrio salmonicida</i>	AF452135	<i>luxCDABE</i> , <i>luxR</i> , <i>luxI</i> , <i>luxR2</i> , <i>ribG</i>
19	<i>Aliivibrio salmonicida</i> LF1238	FM178380.1	<i>luxCDABEG</i> , <i>luxR</i> , <i>luxI</i>
20	<i>Aliivibrio fischeri</i> ATCC 7744	AY341062.2	<i>luxC</i> * <i>DABE</i> *
21	<i>Aliivibrio fischeri</i> MJ-1	AF170104.1	<i>luxCDABEG</i> , <i>luxR</i> , <i>luxI</i>
22	<i>Aliivibrio fischeri</i> MJ11	CP001133.1	<i>luxCDABEG</i> , <i>luxR</i> , <i>lux</i> , <i>ribG</i>
23	<i>Aliivibrio lojei</i> KCh1	HQ450520.1	<i>luxCDABE</i> , <i>luxR</i> , <i>luxI</i> , <i>luxR2</i>
24	<i>Vibrio vulnificus</i> VVL1 ATCC 43382	EU122289	<i>luxC</i> * <i>DABEG</i>
25	<i>Vibrio orientalis</i> ATCC 33934	EU556495.1	<i>luxCDABEG</i> , <i>luxH</i>
26	<i>Vibrio albensis</i> (NCIMB 41)	AB115761	<i>luxCDABEG</i>
27	<i>Vibrio harveyi</i> ATCC 14126	EU122288	<i>luxCDABEG</i> , <i>ribB</i> *
28	<i>Vibrio harveyi</i> BCB440	EU192082.1	<i>luxCDABEG</i> , <i>luxH</i>
29	<i>Vibrio harveyi</i> ATCC 33843	CP009468.1	<i>luxCDABEG</i>
30	<i>Vibrio chagasii</i> 21N-12	EU122293.1	<i>luxD</i> * <i>ABE</i> *
31	<i>Vibrio chagasii</i> SB-52	EU122294.1	<i>luxD</i> * <i>ABE</i> *
32	<i>Vibrio campbellii</i> ATCC BAA-1116_1	CP006606.1	<i>luxCDABEG</i> , <i>luxH</i>
33	<i>Vibrio campbellii</i> ATCC BAA-1116_2	CP000790.1	<i>luxCDABEG</i> , <i>ribB</i>
34	<i>Vibrio campbellii</i> LA16-V1	CP021146.1	<i>luxCDABEG</i>
35	<i>Vibrio azureus</i> LC2-005 (NBRC 104587)	CP018617.1	<i>luxCDABEG</i>
36	<i>Vibrio</i> sp. BCB494	EU192084.1	<i>luxC</i> * <i>DABEG</i> , <i>luxH</i>
37	<i>Photobacterium luminescens</i> subsp. <i>luminescens</i> ATCC 29999	M90093.1	<i>luxCDABE</i>
38	<i>Photobacterium luminescens</i> Hw	M90092.1	<i>luxCDABE</i>
39	<i>Photobacterium luminescens</i> ZM1	AF403784.1	<i>luxCDABE</i>
40	<i>Photobacterium luminescens</i> HW	M62917.1	<i>luxCDABE</i> *
41	<i>Photobacterium luminescens</i> subsp. <i>laumondii</i> TTO1	BX571866.1	<i>luxCDABE</i>
42	<i>Photobacterium asymbiotica</i> ATCC 43949	FM162591.1	<i>luxCDABE</i>
43	<i>Photobacterium temperata</i> subsp. <i>thracensis</i> (DSM 15199)	CP011104.1	<i>luxCDABE</i>
44	<i>Shewanella hanedai</i> ATCC 33224	AB058949	<i>luxC</i> * <i>DABEG</i>
45	<i>Shewanella hanedai</i> (NCIMB 2157)	AB261992.1	<i>luxCDABEG</i> , <i>luxR</i> , <i>luxI</i>
46	<i>Shewanella woodyi</i>	AB368544.1	<i>luxCDABE</i>
47	<i>Shewanella woodyi</i> ATCC 51908	CP000961.1	<i>luxCDABEG</i>
48	<i>Candidatus Photodesmus katoptron</i> (Akat2007.1.1)	HQ333499.1	<i>luxCDABEG</i>
49	Bacterium symbiont of <i>Cryptosaras couesii</i>	CP020663.1	<i>luxCDABEG</i>

* Indicates partial sequences.

a, b (in numbering) Indicates two copies of the *lux* operon in the same bacterial strain.

Chapter II

Synthesis of α,β -unsaturated aldehydes as potential substrates for bacterial luciferases

This chapter was published in the Journal of Bioorganic and Medicinal Chemistry, volume 25, pages 1487-1495, available online since January 13th, 2017 (<http://dx.doi.org/10.1016/j.bmc.2017.01.013>).

II. Synthesis of α,β -unsaturated aldehydes as potential substrates for bacterial luciferases

Eveline Brodl^a, Jakov Ivkovic^{b,1}, Chaitanya R. Tabib^a, Rolf Breinbauer^b and Peter Macheroux^{a,*}

^aGraz University of Technology, Institute of Biochemistry, Petersgasse 12/2, 8010 Graz, Austria

^bGraz University of Technology, Institute of Organic Chemistry, Stremayrgasse 9, 8010 Graz, Austria

¹current affiliation: University of Lund, Kemiceriet, Center for Analysis and Synthesis, Naturvetarvägen 14, 22100 Lund, Sweden.

*Corresponding author at: Graz University of Technology, Petersgasse 12/2, A-8010 Graz, Austria. Email address: peter.macheroux@tugraz.at

Keywords

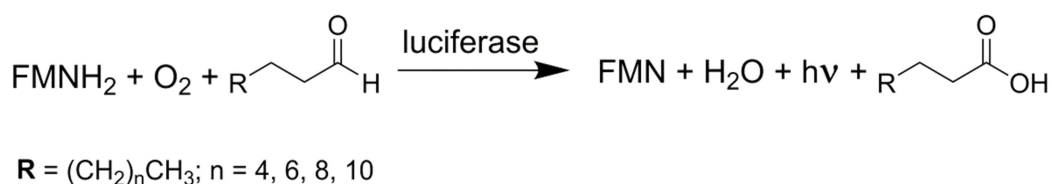
bacterial bioluminescence; luciferase; molecular docking; α , β -unsaturated aldehydes

2.1. Abstract

Bacterial luciferase catalyzes the monooxygenation of long chain aldehydes such as tetradecanal to the corresponding acid accompanied by light emission with a maximum at 490 nm. In this study even numbered aldehydes with eight, ten, twelve and fourteen carbon atoms were compared with analogs having a double bond at the α,β -position. These α,β -unsaturated aldehydes were synthesized in three steps and were examined as potential substrates *in vitro*. The luciferase of *Photobacterium leiognathi* was found to convert these analogs and showed a reduced but significant bioluminescence activity compared to tetradecanal. This study showed the trend that aldehydes, both saturated and unsaturated, with longer chain lengths had higher activity in terms of bioluminescence than shorter chain lengths. The maximal light intensity of (*E*)-tetradec-2-enal was approximately half with luciferase of *P. leiognathi*, compared to tetradecanal. Luciferases of *Vibrio harveyi* and *Aliivibrio fischeri* accepted these newly synthesized substrates but light emission dropped drastically compared to saturated aldehydes. The onset and the decay rate of bioluminescence were much slower, when using unsaturated substrates, indicating a kinetic effect. As a result the duration of the light emission is doubled. These results suggest that the substrate scope of bacterial luciferases is broader than previously reported.

2.2. Introduction

The “cold-light” phenomenon - the enzymatic production of light commonly known as bioluminescence - can be found in prokaryotes and eukaryotes.¹ The involvement of long chain aliphatic aldehydes as substrates in bacterial bioluminescence has been known since 1953 when various chain lengths of the substrates were investigated by Strehler and Cormier.²⁻⁴ In the 1960s, the role of these potential substrates was analyzed concerning the reaction velocity, the initial maximal intensity and the decay of luminescence.^{5,6} In 1963 Spudich and Hastings tested the first unsaturated aldehyde, 2-decenal, and showed complete inactivity with this substrate.⁷ Cormier *et al.* were the first to prove that long chain aldehydes were definitely required for light production.^{8,9} Further investigations focused on the determination of the stoichiometry, the quantum yield and the product of this bioluminescent reaction.¹⁰⁻¹³ It took some more years to identify tetradecanal as the “natural” substrate for bacterial bioluminescence in 1974 by Shimomura.¹⁴ By now it is known, that the luciferase catalyzes the monooxygenation of long chain aliphatic aldehydes to the corresponding acids employing reduced flavin mononucleotide (FMNH₂) as redox cofactor (Scheme 1).¹



Scheme 1: General reaction of bacterial bioluminescence.

The initial step of the reaction is the binding of reduced FMN to luciferase. The enzyme-FMNH₂ complex reacts with molecular oxygen to form flavin-4a-hydroperoxide. This relatively stable enzyme-FMNHOOH complex subsequently reacts with a long chain aliphatic aldehyde to form a flavin-4a-peroxyhemiacetal intermediate.¹⁵ Its slow decay results in the oxidation of the aldehyde to the corresponding acid and the free energy released during this reaction populates an excited state flavin-4a-hydroxide, which in turn serves as the light emitting molecule.¹⁶

Bacterial luciferases are heterodimeric enzymes consisting of an α -subunit and a β -subunit. The two subunits have a sequence identity of approximately 32 % and have evolved from a common ancestor.¹⁷ The active site of the enzyme is exclusively on the α -subunit and also distant from the subunit interface. The exact role of the β -subunit is not clear, but deletion or mutation of this subunit reveals less or complete loss of activity. A mutation of β Tyr151, for instance, has a negative effect on FMNH₂ binding. It seems that the β -subunit is responsible for high quantum yield and protein stability.^{17,18}

Only two crystal structures of bacterial luciferases have been reported, where one of them elucidated the structure of the apo-LuxAB of *Vibrio harveyi*^{17,19} and the other one revealed the apo-LuxAB of *Vibrio harveyi* soaked with FMN.¹⁸ The isoalloxazine ring of the flavin shows a planar conformation and is held in place by mainly backbone contacts. The amino acids involved in the binding of the 5' phosphate are Arg107, Arg125, Glu175, Ser176 and Thr179 (Figure 1).^{18,20} Both structures designate a TIM barrel fold ($\beta\alpha$)₈ for the enzyme. Both subunits have a loop between the β -strand 7 and α -helix 7. The α -subunit, in contrast to the β -subunit, has 29 additional amino acids and a stretch of disordered residues from Lys283 to Arg290. This loop region is the most conserved region of the luciferase sequence. It is highly protease-labile, but binding of FMN or polyvalent anions can prevent proteolytic inactivation.^{17,18} Complete deletion of the loop results in reduction of total quantum yield by two orders of magnitude. It was hypothesized that the mobile loop has a lid-gating mechanism similar to other TIM-barrel enzymes.²¹ This loop is in close proximity to the active center and seems to undergo conformational changes from an open or semi open state to a closed state after flavin binding and before reaction with oxygen.^{17,18,21}

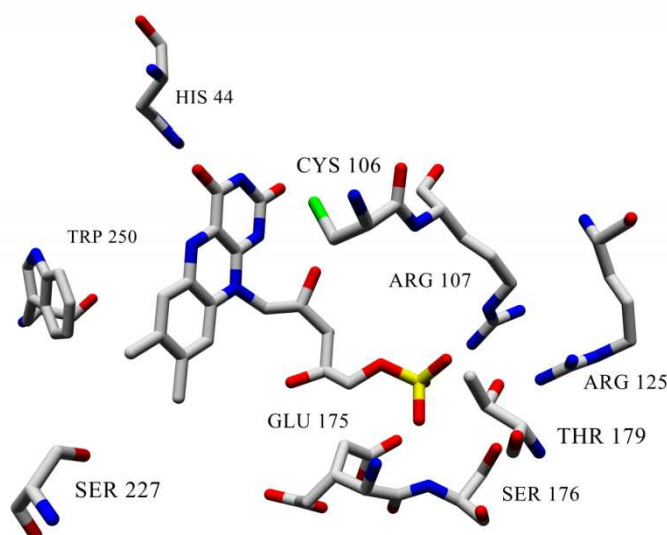


Figure 1: Graphical representation of FMN bound to luciferase of *V. harveyi*. Based on the crystal structure¹⁸, FMN and a few key residues discussed in the text are depicted in stick conformation with according labelling. General color code is used for the atoms. Residues Arg107, Arg125, Glu175, Ser176 and Thr179 are responsible for binding of the 5' phosphate group of FMN. His44, Ser227 and Trp250 might have a role in substrate binding and interaction.

Currently, structural information on the spatial arrangement of FMN and the aldehyde substrate in the active site is lacking, however various mutagenesis and modelling studies were performed in the last years. It was assumed that the flavin binding pocket is large enough to accommodate FMNH₂, O₂ and long chain aldehydes.²² In particular, two amino acids, Cys106 and Ser227, have attracted interest, because their exchange substantially affected enzymatic activity. The former amino acid apparently plays an important catalytic role as alkylation of its reactive thiol led to inactivation of the luciferase (Figure 1).^{17,18} In addition it was found that the Cys106Val variant exhibits decreased aldehyde utilization and reduced stability of the flavin-4a-hydroperoxide intermediate.²⁰ On the other hand, replacement of Ser227 to phenylalanine in the α -subunit led to a steric effect in the well-characterized mutant AK-20 (Figure 1). Generally, replacement of Ser227 by large aromatic amino acids led to a 10-fold decreased binding affinity for aldehyde, smaller amino acids, e.g. alanine had no influence.^{17,23} Modelling studies suggest that the bioluminescent reaction occurs on the *si*-face of the isoalloxazine ring facing the amino acid His44 (Figure 1). The distance of the C4a atom of flavin and the N δ atom of His44 is approximately 7 Å. This distance leaves enough space for functional groups of the intermediates (peroxide, hydroxide) and aldehyde binding. Additionally, a spacious cavity is formed in the active site, which is surrounded by hydrophobic residues. Among those residues is Trp250, which was suggested to interact with the aldehyde substrate (Figure 1).^{20,24} Despite these structural analyses, the exact structure of bacterial luciferases in complex with FMNH₂ and aldehyde substrate is still unknown. A ¹³C and ¹⁵N NMR study by Vervoort *et al.* analyzed the differences of bound FMN and bound FMNH₂ to luciferase of *Vibrio harveyi*. There is clearly a change in electron densities, hydrogen bonding and planarity of the oxidized and reduced state of FMN. The N10 atom of FMNH₂ seems to be slightly out of the molecular plane.²⁵ All these indications prompt speculations about the reaction mechanism as well as the substrate scope.

In this study, α,β -unsaturated aldehydes with chain lengths of eight, ten, twelve and fourteen carbon atoms were synthesized. To investigate the mechanism of bacterial bioluminescence, the recombinant luciferases from *Photobacterium leiognathi*, *Vibrio harveyi* and *Aliivibrio fischeri* were chosen as model systems to test these potential substrates and analyze the substrate specificity of bacterial luciferases.

2.3. Materials and Methods

2.3.1. General experimental information

All commercially available reagents and solvents were purchased from Sigma-Aldrich, Alfa Aesar, Fisher Scientific, Acros Organics, Roth or VWR, and were used without further purification if not stated otherwise. When it was required, non-dry solvents were distilled before use. If reactions were performed under inert conditions, e.g. exclusion of water, oxygen or both, all experiments were carried out using established Schlenk techniques. Herein solvents were dried and/or degassed with common methods and afterwards stored under inert gas atmosphere (argon or N_2) over molecular sieves. In some cases, when explicitly mentioned, dry solvents were received from the listed suppliers. DCM (EtOH stabilized) was distilled first over P_4O_{10} to remove the stabilizer and then over CaH_2 under argon atmosphere and stored over 4 Å molecular sieves in an amber-colored 1000 mL Schlenk bottle.

All reactions were stirred with Teflon-coated magnetic stirring bars. Molecular sieves (Sigma Aldrich, beads with 8-12 mesh) were activated in a round-bottom flask with a gas-inlet adapter by heating them carefully in a heating mantle for approximately 12 h under high vacuum until complete dryness was obtained. These activated molecular sieves were stored at room temperature under argon atmosphere.

Temperatures were measured externally if not otherwise stated. Reactions that were carried out at $-78\text{ }^\circ\text{C}$ were cooled by keeping the reaction vessel immersed in a properly sized Dewar vessel containing acetone/dry ice.

Analytical thin layer chromatography (TLC) was carried out on Merck TLC silica gel 60 F254 aluminum sheets and spots were visualized by UV light ($\lambda = 254$ and/or 366 nm) or by staining with iodide, cerium ammonium molybdate (2.0 g $Ce(SO_4)_2$, 50.0 g $(NH_4)_6Mo_7O_{24}$ and 50 mL conc. H_2SO_4 in 400 mL water) (CAM) or potassium permanganate (0.3 g $KMnO_4$, 20 g K_2CO_3 , 5 mL 5 % aqueous NaOH in 300 mL H_2O) followed by the development of the stains in the heat. Flash column chromatography was performed on silica gel 0.035-0.070 mm, 60 Å (Acros Organics). A 30 to 100 fold excess of silica gel was used with respect to the amount of dry crude product, depending on the separation problem. The dimensions of the column were selected in such a way that the required amount of silica gel formed a pad between 10 cm and 25 cm. The column was equilibrated first with the solvent or solvent mixture, and the crude product diluted with the eluent was applied onto the top of the silica pad. In case when the crude product was insoluble in the eluent, the sample was dissolved in an appropriate solvent (EtOAc or DCM), and the equal amount of diatomaceous earth was added, followed by removal of the solvent under reduced pressure and drying the sample in vacuum, which was then directly loaded onto the top of the silica pad. The mobile phase was forced through the column using a rubber bulb pump.

2.3.2. General procedure GP-1 (Synthesis of α,β -unsaturated ethyl esters)

In a 100 mL single neck round-bottom flask equipped with a magnetic stir bar, 4-(dimethylamino)pyridine (122 mg, 1.00 mmol, 0.10 eq), mono-ethyl malonate (2.36 mL, 20.0 mmol, 2.0 eq) and saturated alkyl aldehyde (10.0 mmol, 1.0 eq) were dissolved in DMF (50 mL). The reaction mixture was stirred at room temperature for 42 h. Subsequently, the mixture was diluted with diethyl ether (50 mL), washed with saturated aqueous NH_4Cl (50 mL), saturated aqueous NaHCO_3 (50 mL), water (50 mL), and concentrated under reduced pressure. Flash chromatography (SiO_2 , 5 % EtOAc in cyclohexane) afforded the desired unsaturated ethyl ester as a colorless liquid.

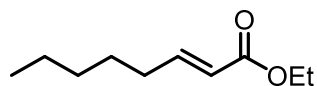
2.3.3. General procedure GP-2 (Synthesis of allyl alcohols)

In a nitrogen-purged 100 mL Schlenk tube equipped with a magnetic stir bar, unsaturated ethyl ester (4.5 mmol, 1.0 eq) was dissolved in dry dichloromethane (18 mL), the vessel was sealed with a glass stopper and cooled to $-78\text{ }^\circ\text{C}$ in an acetone/dry ice bath. 1.0 M solution of diisobutylaluminum hydride in hexanes (10.8 mL, 10.8 mmol, 2.4 eq) was added dropwise via a syringe and a septum throughout 10 min. The reaction was stirred at $-78\text{ }^\circ\text{C}$ until TLC indicated quantitative conversion (3 h). The reaction mixture was quenched by the dropwise addition of MeOH (1 mL). Subsequently, the cooling bath was removed, saturated aqueous potassium sodium tartrate solution (18 mL) was added, and the mixture was stirred vigorously for 2 h. After phase separation the aqueous layer was extracted with dichloromethane (10 mL). The combined organic layers were dried over anhydrous Na_2SO_4 and concentrated under reduced pressure. Flash chromatography (SiO_2 , 20 % EtOAc in cyclohexane) afforded the desired allyl alcohol as a colorless liquid.

2.3.4. General procedure GP-3 (Synthesis of α,β -unsaturated aldehydes)

In a nitrogen-purged 10 mL Schlenk tube equipped with a magnetic stir bar, manganese(IV) oxide (494 mg, 5.0 mmol, 5.0 eq) and activated 4 Å molecular sieves were suspended in dry dichloromethane (4 mL). Allyl alcohol (1.0 mmol, 1.0 eq) was dissolved in dry dichloromethane (3.3 mL), added to the mixture in the Schlenk tube, which was sealed with a glass stopper. After stirring the mixture overnight at room temperature the dark brown reaction mixture was filtered through a compressed pad of diatomaceous earth. The pad was washed with dichloromethane (2 mL), and the filtrate was concentrated under reduced pressure. Flash chromatography (SiO_2 , 10 % EtOAc in cyclohexane) afforded the desired unsaturated aldehyde as a pale yellow liquid.

2.3.5. Ethyl (*E*)-oct-2-enoate (**3d**)



Unsaturated ester **3d** was synthesized and isolated according to the general procedure GP-1 and its stated stoichiometry.

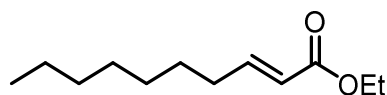
Yield: 940 mg (5.52 mmol, 55 %), colorless liquid.

R_f = 0.35 (cyclohexane/EtOAc 40:1 (v/v); staining: KMnO_4).

^1H NMR (300 MHz, CDCl_3) δ = 6.97 (dt, $^3J = 15.6$ Hz, $^3J = 7.0$ Hz, 1H), 5.81 (d, $^3J = 15.6$ Hz, 1H), 4.18 (q, $^3J = 7.1$ Hz, 2H), 2.25–2.14 (m, 2H), 1.52–1.40 (m, 2H), 1.36–1.25 (m, 7H), 0.82 (t, $^3J = 6.7$ Hz, 3H) ppm.

^{13}C NMR (75 MHz, CDCl_3) δ = 166.9 (s, 1C), 149.6 (s, 1C), 121.4 (s, 1C), 60.2 (s, 1C), 32.3 (s, 1C), 31.4 (s, 1C), 27.8 (s, 1C), 22.6 (s, 1C), 14.4 (s, 1C), 14.1 (s, 1C) ppm.

2.3.6. Ethyl (*E*)-dec-2-enoate (**3c**)



Unsaturated ester **3c** was synthesized and isolated according to the general procedure GP-1 and its stated stoichiometry.

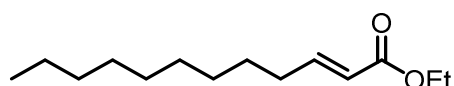
Yield: 1.480 g (7.46 mmol, 75 %), colorless liquid.

R_f = 0.35 (cyclohexane/EtOAc 40:1 (v/v); staining: KMnO_4).

^1H NMR (300 MHz, CDCl_3) δ = 6.96 (dt, $^3J = 15.6$ Hz, $^3J = 7.0$ Hz, 1H), 5.80 (d, $^3J = 15.6$ Hz, 1H), 4.18 (q, $^3J = 7.1$ Hz, 2H), 2.26–2.12 (m, 2H), 1.51–1.39 (m, 2H), 1.35–1.21 (m, 11H), 0.88 (t, $^3J = 6.7$ Hz, 3H) ppm.

^{13}C NMR (75 MHz, CDCl_3) δ = 166.9 (s, 1C), 149.6 (s, 1C), 121.4 (s, 1C), 60.3 (s, 1C), 32.3 (s, 1C), 31.9 (s, 1C), 29.3 (s, 1C), 29.2 (s, 1C), 28.2 (s, 1C), 22.8 (s, 1C), 14.4 (s, 1C), 14.2 (s, 1C) ppm.

2.3.7. Ethyl (*E*)-dodec-2-enoate (**3b**)



Unsaturated ester **3b** was synthesized and isolated according to the general procedure GP-1 and its stated stoichiometry.

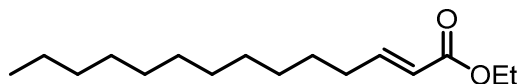
Yield: 1.235 g (5.46 mmol, 55 %), colorless liquid.

R_f = 0.36 (cyclohexane/EtOAc 40:1 (v/v); staining: KMnO_4).

^1H NMR (300 MHz, CDCl_3) δ = 6.96 (dt, 3J = 15.6 Hz, 3J = 7.0 Hz, 1H), 5.80 (d, 3J = 15.6 Hz, 1H), 4.18 (q, 3J = 7.1 Hz, 2H), 2.25–2.13 (m, 2H), 1.51–1.39 (m, 2H), 1.35–1.21 (m, 15H), 0.88 (t, 3J = 6.7 Hz, 3H) ppm.

^{13}C NMR (75 MHz, CDCl_3) δ = 166.9 (s, 1C), 149.6 (s, 1C), 121.3 (s, 1C), 60.2 (s, 1C), 32.3 (s, 1C), 32.0 (s, 1C), 29.6 (s, 1C), 29.5 (s, 1C), 29.4 (s, 1C), 29.3 (s, 1C), 28.2 (s, 1C), 22.8 (s, 1C), 14.4 (s, 1C), 14.2 (s, 1C) ppm.

2.3.8. Ethyl (*E*)-tetradec-2-enoate (**3a**)



Unsaturated ester **3a** was synthesized and isolated according to the general procedure GP-1 and its stated stoichiometry.

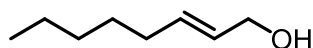
Yield: 1.733 g (6.81 mmol, 68 %), colorless liquid.

R_f = 0.38 (cyclohexane/EtOAc 40:1 (v/v); staining: KMnO_4).

^1H NMR (300 MHz, CDCl_3) δ = 6.96 (dt, 3J = 15.6 Hz, 3J = 7.0 Hz, 1H), 5.80 (d, 3J = 15.6 Hz, 1H), 4.17 (q, 3J = 7.1 Hz, 2H), 2.25–2.12 (m, 2H), 1.51–1.38 (m, 2H), 1.35–1.21 (m, 19H), 0.87 (t, 3J = 6.7 Hz, 3H) ppm.

^{13}C NMR (75 MHz, CDCl_3) δ = 166.9 (s, 1C), 149.6 (s, 1C), 121.3 (s, 1C), 60.2 (s, 1C), 32.3 (s, 1C), 32.0 (s, 1C), 29.8 (m, 2C), 29.7 (s, 1C), 29.5 (s, 1C), 29.4 (s, 1C), 29.3 (s, 1C), 28.2 (s, 1C), 22.8 (s, 1C), 14.4 (s, 1C), 14.2 (s, 1C) ppm.

2.3.9. (*E*)-Oct-2-en-1-ol (**4d**)



Allyl alcohol **4d** was synthesized and isolated according to the general procedure GP-2 and its stated stoichiometry.

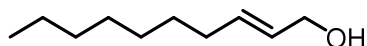
Yield: 449 mg (3.50 mmol, 78 %), colorless liquid.

R_f = 0.57 (cyclohexane/EtOAc 9:1 (v/v); staining: KMnO_4).

^1H NMR (300 MHz, CDCl_3) δ = 5.77–5.54 (m, 2H), 4.08 (br s, 2H), 2.03 (dt, 3J = 6.9 Hz, 3J = 6.6 Hz, 2H), 1.45–1.19 (m, 7H), 0.88 (t, 3J = 6.7 Hz, 3H) ppm.

^{13}C NMR (75 MHz, CDCl_3) δ = 133.8 (s, 1C), 129.0 (s, 1C), 64.0 (s, 1C), 32.3 (s, 1C), 31.5 (s, 1C), 29.0 (s, 1C), 22.7 (s, 1C), 14.2 (s, 1C) ppm.

2.3.10. (*E*)-Dec-2-en-1-ol (4c)



Allyl alcohol **4c** was synthesized and isolated according to the general procedure GP-2 and its stated stoichiometry.

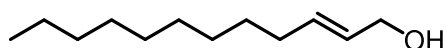
Yield: 605 mg (3.87 mmol, 86 %), colorless liquid.

R_f = 0.57 (cyclohexane/EtOAc 9:1 (v/v); staining: KMnO_4).

^1H NMR (300 MHz, CDCl_3) δ = 5.77–5.55 (m, 2H), 4.07 (br s, 2H), 2.03 (dt, 3J = 6.9 Hz, 3J = 6.5 Hz, 2H), 1.46–1.17 (m, 11H), 0.88 (t, 3J = 6.7 Hz, 3H) ppm.

^{13}C NMR (75 MHz, CDCl_3) δ = 133.7 (s, 1C), 129.0 (s, 1C), 64.0 (s, 1C), 32.3 (s, 1C), 32.0 (s, 1C), 29.3 (s, 3C), 22.8 (s, 1C), 14.2 (s, 1C) ppm.

2.3.11. (*E*)-Dodec-2-en-1-ol (4b)



Allyl alcohol **4b** was synthesized and isolated according to the general procedure GP-2 and its stated stoichiometry.

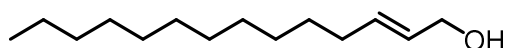
Yield: 617 mg (3.35 mmol, 74 %), colorless liquid.

R_f = 0.57 (cyclohexane/EtOAc 9:1 (v/v); staining: KMnO_4).

^1H NMR (300 MHz, CDCl_3) δ = 5.77–5.56 (m, 2H), 4.08 (br s, 2H), 2.03 (dt, 3J = 6.9 Hz, 3J = 6.6 Hz, 2H), 1.41–1.18 (m, 15H), 0.88 (t, 3J = 6.7 Hz, 3H) ppm.

^{13}C NMR (75 MHz, CDCl_3) δ = 133.8 (s, 1C), 129.0 (s, 1C), 64.0 (s, 1C), 32.4 (s, 1C), 32.1 (s, 1C), 29.8–29.6 (m, 2C), 29.5 (s, 1C), 29.4–29.2 (m, 2C), 22.8 (s, 1C), 14.3 (s, 1C) ppm.

2.3.12. (*E*)-Tetradec-2-en-1-ol (4a)



Allyl alcohol **4a** was synthesized and isolated according to the general procedure GP-2 and its stated stoichiometry.

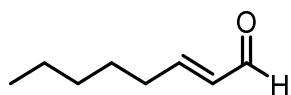
Yield: 641 mg (3.02 mmol, 67 %), colorless liquid.

R_f = 0.57 (cyclohexane/EtOAc 9:1 (v/v); staining: KMnO_4).

^1H NMR (300 MHz, CDCl_3) δ = 5.77–5.56 (m, 2H), 4.08 (br s, 2H), 2.03 (dt, 3J = 6.9 Hz, 3J = 6.6 Hz, 2H), 1.36–1.17 (m, 19H), 0.88 (t, 3J = 6.7 Hz, 3H) ppm.

^{13}C NMR (75 MHz, CDCl_3) δ = 133.8 (s, 1C), 129.0 (s, 1C), 64.0 (s, 1C), 32.4 (s, 1C), 32.1 (s, 1C), 29.9–29.7 (m, 3C), 29.7 (s, 1C), 29.5 (s, 1C), 29.4–29.2 (m, 2C), 22.8 (s, 1C), 14.3 (s, 1C) ppm.

2.3.13. (E)-Oct-2-enal (5d)



Unsaturated aldehyde **5d** was synthesized and isolated according to the general procedure GP-3 and its stated stoichiometry.

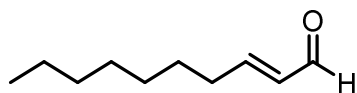
Yield: 103 mg (0.816 mmol, 82 %), pale yellow liquid.

R_f = 0.37 (cyclohexane/EtOAc 9:1 (v/v); staining: KMnO_4).

^1H NMR (300 MHz, CDCl_3) δ = 9.50 (d, 3J = 7.9 Hz, 1H), 6.86 (dt, 3J = 15.6 Hz, 3J = 6.9 Hz, 1H), 6.11 (dd, 3J = 15.6 Hz, 3J = 7.9 Hz, 1H), 2.33 (dt, 3J = 7.2 Hz, 3J = 7.2 Hz, 2H), 1.58–1.42 (m, 2H), 1.37–1.26 (m, 4H), 0.98–0.85 (m, 3H) ppm.

^{13}C NMR (75 MHz, CDCl_3) δ = 194.3 (s, 1C), 159.2 (s, 1C), 133.1 (s, 1C), 32.8 (s, 1C), 31.4 (s, 1C), 27.7 (s, 1C), 22.5 (s, 1C), 14.1 (s, 1C) ppm.

2.3.14. (E)-Dec-2-enal (5c)



Unsaturated aldehyde **5c** was synthesized and isolated according to the general procedure GP-3 and its stated stoichiometry.

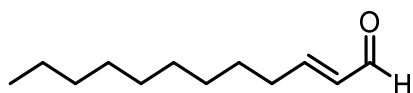
Yield: 122 mg (0.791 mmol, 79 %), pale yellow liquid.

R_f = 0.37 (cyclohexane/EtOAc 9:1 (v/v); staining: KMnO_4).

^1H NMR (300 MHz, CDCl_3) δ = 9.51 (d, 3J = 7.9 Hz, 1H), 6.85 (dt, 3J = 15.6 Hz, 3J = 6.9 Hz, 1H), 6.11 (dd, 3J = 15.6 Hz, 3J = 7.9 Hz, 1H), 2.33 (dt, 3J = 7.2 Hz, 3J = 7.2 Hz, 2H), 1.57–1.44 (m, 2H), 1.40–1.19 (m, 8H), 0.88 (t, 3J = 6.7 Hz, 3H) ppm.

^{13}C NMR (75 MHz, CDCl_3) δ = 194.2 (s, 1C), 159.2 (s, 1C), 133.1 (s, 1C), 32.9 (s, 1C), 31.8 (s, 1C), 29.2 (s, 1C), 29.1 (s, 1C), 28.0 (s, 1C), 22.8 (s, 1C), 14.2 (s, 1C) ppm.

2.3.15. (E)-Dodec-2-enal (5b)



Unsaturated aldehyde **5b** was synthesized and isolated according to the general procedure GP-3 and its stated stoichiometry.

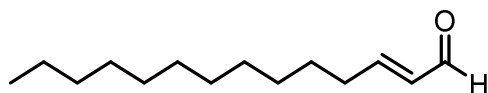
Yield: 136 mg (0.746 mmol, 75 %), pale yellow liquid.

R_f = 0.38 (cyclohexane/EtOAc 9:1 (v/v); staining: KMnO_4).

^1H NMR (300 MHz, CDCl_3) δ = 9.50 (d, 3J = 7.9 Hz, 1H), 6.85 (dt, 3J = 15.6 Hz, 3J = 6.9 Hz, 1H), 6.11 (dd, 3J = 15.6 Hz, 3J = 7.9 Hz, 1H), 2.33 (dt, 3J = 7.2 Hz, 3J = 7.2 Hz, 2H), 1.57–1.43 (m, 2H), 1.39–1.18 (m, 12H), 0.88 (t, 3J = 6.7 Hz, 3H) ppm.

^{13}C NMR (75 MHz, CDCl_3) δ = 194.3 (s, 1C), 159.2 (s, 1C), 133.1 (s, 1C), 32.9 (s, 1C), 32.0 (s, 1C), 29.6 (s, 1C), 29.5 (s, 1C), 29.4 (s, 1C), 29.3 (s, 1C), 28.0 (s, 1C), 22.8 (s, 1C), 14.2 (s, 1C) ppm.

2.3.16. (*E*)-tetradec-2-enal (**5a**)



Unsaturated aldehyde **5a** was synthesized and isolated according to the general procedure GP-3 and its stated stoichiometry.

Yield: 159 mg (0.756 mmol, 76 %), pale yellow liquid.

R_f = 0.40 (cyclohexane/EtOAc 9:1 (v/v); staining: KMnO_4).

^1H NMR (300 MHz, CDCl_3) δ = 9.50 (d, 3J = 7.8 Hz, 1H), 6.85 (dt, 3J = 15.6 Hz, 3J = 6.9 Hz, 1H), 6.11 (dd, 3J = 15.6 Hz, 3J = 7.9 Hz, 1H), 2.33 (dt, 3J = 7.2 Hz, 3J = 7.2 Hz, 2H), 1.57–1.44 (m, 2H), 1.38–1.20 (m, 16H), 0.88 (t, 3J = 6.7 Hz, 3H) ppm.

^{13}C NMR (75 MHz, CDCl_3) δ = 194.3 (s, 1C), 159.2 (s, 1C), 133.1 (s, 1C), 32.9 (s, 1C), 32.0 (s, 1C), 29.8 (s, 2C), 29.6 (s, 1C), 29.5–29.4 (m, 2C), 29.3 (s, 1C), 28.0 (s, 1C), 22.8 (s, 1C), 14.2 (s, 1C) ppm.

2.3.17. Instrumentation

UV/Vis absorption spectra were recorded with a Specord 210 spectrophotometer (Analytic Jena, Jena, Germany). The light emission was measured by a Berthold Technologies Centro LB 960 microplate Luminometer with Mikro Win version 4.16. Gel filtration was performed using a Superdex-200 column (prep grade XK 16/100; GE Healthcare) with an Äktaexplorer 100 Pharmacia Biotech (GE Healthcare).

^1H -, ^{13}C -NMR spectra were recorded on a Bruker AVANCE III 300 spectrometer (^1H : 300.36 MHz; ^{13}C : 75.53 MHz). Chemical shifts were referenced to the residual proton and carbon signal of the deuterated solvent, respectively (CDCl_3 : δ = 7.26 ppm (^1H), 77.16 ppm (^{13}C)). Signal multiplicities are abbreviated as s (singlet), bs (broad singlet), d (doublet), dd (doublet of doublet), t (triplet), q (quadruplet), p (pentet) and m (multiplet). Deuterated solvents for nuclear resonance spectroscopy were purchased from Euriso-top®.

2.3.18. Design, expression and purification of recombinant His-tagged proteins

LuxAB from *Photobacterium leiognathi* (S1; PL_LuxAB) and YcnD from *Bacillus subtilis* were cloned into pET21a vector and transformed into *E. coli* BL21 (DE3) strain for expression as described previously.^{26,27} LuxAB from *Vibrio harveyi* (ATCC 14126; VH_LuxAB) and *Aliivibrio fischeri* (ATCC 7744; AF_LuxAB) were cloned similarly. The genes for VH_LuxAB and AF_LuxAB were integrated into pET24b vector and transformed into *E. coli* Rosetta strain. Both constructs had an additional C-terminal octa-histidine tag. Heterologous expression cultures were grown at 37 °C in LB media containing kanamycin (50 $\mu\text{g}/\text{mL}$) and chloramphenicol (20 $\mu\text{g}/\text{mL}$) as selection markers until an OD (600 nm) of 0.6 was reached. The expression was induced with 0.1 mM IPTG and cells were further grown at 20 °C for 16 h. Cells were harvested by centrifugation (4400g, 10 min, 4 °C) and the wet cell pellets were stored at -20 °C. The cell pellets were resuspended in lysis buffer (50 mM NaH_2PO_4 , 300 mM NaCl, 10 mM imidazole, pH 8), lysed by addition of lysozyme and sonication and after centrifugation the clear supernatant was loaded on 5 mL HisTrap FF/HP columns (GE Healthcare) for purification via Ni-NTA affinity chromatography. The columns were washed with wash buffer (50 mM NaH_2PO_4 , 300 mM NaCl, 20 mM imidazole, pH 8) and the purified protein fractions were gained with elution buffer (50 mM NaH_2PO_4 , 300 mM NaCl, 300 mM imidazole, pH 8). After concentrating and buffer exchange to 45 mM Tris-buffer containing 40 mM MES and 20 mM L-malic acid pH 8, a subsequent gel filtration using a Superdex-200 column was performed. The concentration of the various proteins was determined spectrophotometrically at 280 nm using the extinction coefficients of 82,335 $\text{M}^{-1} \text{cm}^{-1}$ (PL_LuxAB), 84,230 $\text{M}^{-1} \text{cm}^{-1}$ (VH_LuxAB), 83,200 $\text{M}^{-1} \text{cm}^{-1}$ (AF_LuxAB). In the case of YcnD the concentration was determined using an extinction coefficient of 12,190 $\text{M}^{-1} \text{cm}^{-1}$ at 450 nm.

2.3.19. *In vitro* assay

The *in vitro* assay was performed in 96 well white assay plates. For the assay all enzymes and substrates were prepared and/or diluted in 100 mM potassium phosphate buffer pH 7. The reaction mixture contained the enzyme luciferase with either 50 nM for *P. leiognathi* or 200 nM for *V. harveyi* or *A. fischeri*, respectively. YcnD and FMN were adjusted to 1.5 fold of the luciferase concentration, respectively. Additionally 500 nM NADPH and the substrate-buffer suspension were added to make up the final volume of 250 μL . The tested substrates include even chain length (8-14 carbon atoms) saturated and unsaturated aldehydes, respectively. Due to the relatively low solubility of aldehydes in water, concentrated aldehyde suspensions were obtained by adding 5 μL of the substrate to 10 mL of the reaction buffer, respectively (concentration range of 1.94-3.30 mM; Supplementary Data).⁵ The reaction was started by injecting NADPH to the reaction mixture (after a delay of 5 s) and the readings were subsequently taken every 0.01th of a second for a total of 90 s. The light was measured using the luminometer. The light emission was recorded as emission counts. The area under the curve was taken for calculation of the percentage and the total

light emission of luciferase with tetradecanal (**6a**) as substrate was considered as 100 %. The data was calculated to 100 nM of luciferase concentration to compare the results with each other. The values for the conversion of luciferase of *P. leiognathi* are shown by means \pm SD of seven individual measurements for the saturated aldehydes and four individual measurements for the unsaturated aldehydes, respectively. The values for the conversion of luciferase of *V. harveyi* and *A. fischeri* are shown by means \pm SD of four individual measurements, respectively.

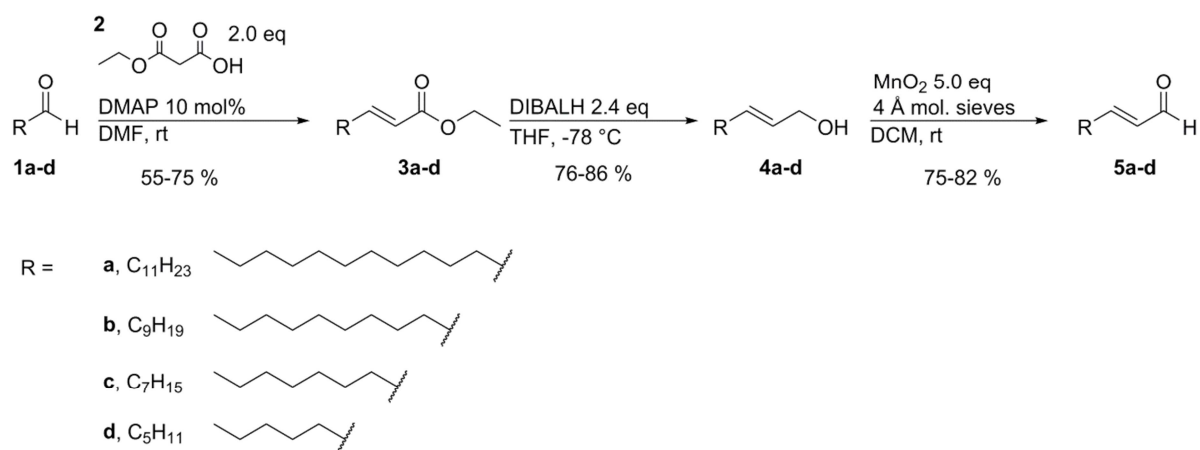
2.3.20. Molecular docking

In silico molecular docking studies were performed using Yasara Structure 13.9.8.²⁸ The crystal structure of the luciferase/flavin complex of *Vibrio harveyi* was retrieved from the Protein Data Bank (PDB entry: 3FGC). Structure preparation and all following experiments were performed within Yasara Structure 13.9.8. All the crystallographic water molecules and the β -subunit of the luciferase were removed before molecular docking. Missing hydrogens were added to the molecules by using the clean mode of Yasara.

For the docking experiments the oxidized flavin structure was modified to the flavin-4a-hydroperoxide intermediate. Therefore, the additional hydrogens and the two oxygens were attached to the molecule and refined by energy minimization using AMBER99 force field, while fixing Lys283 and Arg290 which connect the luciferase backbone with an unstructured and therefore missing loop.¹⁸ The resulting crystal structure was utilized for docking the substrate molecules (**5a-d**, **6a-d**) in flexible mode into the rigid receptor using the plugin Autodock Vina in Yasara Structure 13.9.8.^{29,30} The docking simulation cell was set to 15 Å around the flavin-4a-hydroperoxide intermediate and 500 docking runs with an RMSD cutoff of 2 Å were performed. The docked conformations for each substrate (**5a-d**, **6a-d**) were ranked according to the distance between the C1 atom of the substrate molecule and the terminal oxygen atom of the hydroperoxide functional group. The best-ranked docking pose for each substrate (**5a-d**, **6a-d**) was analyzed in Yasara Structure 13.9.8.

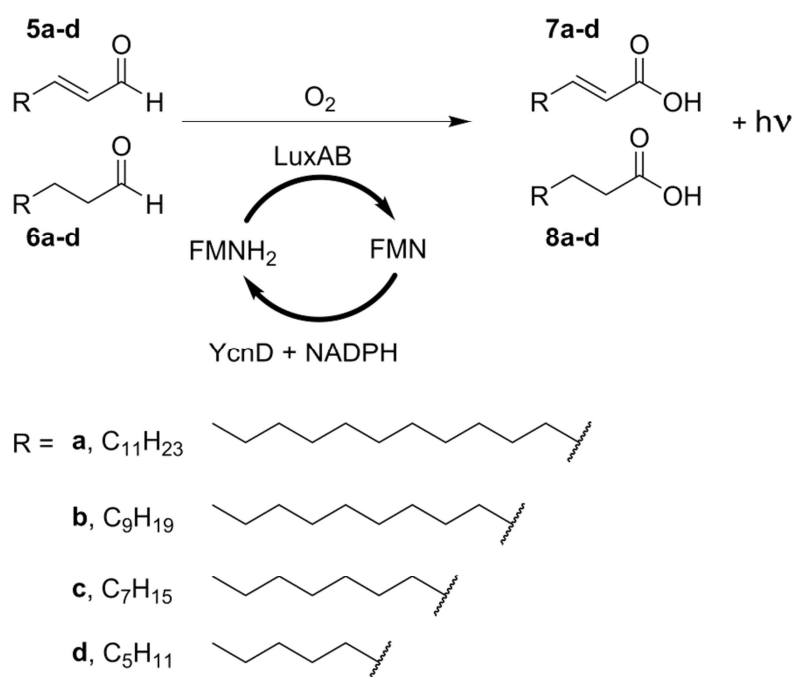
2.4. Results

To obtain new insights into the activity and selectivity of luciferases, unsaturated aldehydes with various chain lengths were synthesized and analyzed. The substrate synthesis was carried out in three steps (Scheme 2). The α,β -unsaturated aldehydes were synthesized starting from commercially available saturated aldehydes with two carbons less in chain length. The starting aldehydes **1a-d** were subjected to a DMAP-catalyzed Knoevenagel condensation with mono-ethyl malonate (**2**) to obtain the corresponding unsaturated esters **3a-d**.³¹ **3a-d** were reduced to the corresponding allyl alcohols **4a-d** using 1.2 equivalents diisobutylaluminum hydride (DIBALH) in DCM at $-78\text{ }^\circ\text{C}$ and were subsequently oxidized with manganese(IV) oxide (MnO_2) to afford the desired α,β -unsaturated aldehydes **5a-d**.



Scheme 2: Synthesis route for aliphatic, unsaturated aldehydes with different chain lengths (C8-C14). Using DMAP-catalyzed Knoevenagel condensation the starting aldehydes **1a-d** were converted to the unsaturated ethyl esters **3a-d**, which were reduced to the corresponding allyl alcohols **4a-d** and were finally oxidized to the α,β -unsaturated aldehydes **5a-d**. The exact equivalents, solvents and temperature conditions are given and the yield for each step is given as percentage.

To test the newly synthesized substrates, an *in vitro* assay was developed (Scheme 3). Briefly, 50 nM recombinant luciferase of *P. leiognathi* (LuxAB) was used in a reaction mixture with 100 mM potassium phosphate buffer pH 7, 75 nM FMN, 75 nM YcnD, 500 nM NADPH and substrate-buffer suspensions of **5a-d** and **6a-d** (see Materials and Methods). YcnD, an NADPH-dependent oxidoreductase from *Bacillus subtilis*, reduces FMN to provide the cosubstrate FMNH₂.²⁷ The luciferase then oxidizes the various substrates to their corresponding acids using the enzyme-bound flavin-4a-hydroperoxide with concomitant emission of light. We assume that saturated aldehydes **6a-d** and unsaturated aldehydes **5a-d** are accepted in a similar way as substrates and converted to the corresponding acids. The photons, emitted during this reaction, were collected by a luminometer for 90 s and the areas under the light emission curve were compared to tetradecanal (**6a**).



Scheme 3: Schematic representation of the *in vitro* assay. The synthesized unsaturated aldehydes **5a-d**, as well as the four saturated aldehydes **6a-d**, were investigated in an *in vitro* assay. The oxidation reaction catalyzed by 50 nM luciferase (LuxAB), employing molecular oxygen (O_2) and reduced FMN ($FMNH_2$), results in long chain aliphatic acids **7a-d** and **8a-d** and the emission of light ($h\nu$). For the reduced FMN, a recycling system was established using the NADPH-dependent oxidoreductase YcnD from *Bacillus subtilis*. The light emission is measured by a luminometer and subsequently converted to total light emission in per cent for comparison and analysis.

As expected, tetradecanal (**6a**) showed the highest light emission and was set to 100 %. The other aldehydes showed lower activity with the luciferase (Figure 2). In the case of dodecanal (**6b**), decanal (**6c**) and (*E*)-tetradec-2-enal (**5a**), light emission was greater than 50 % in comparison to tetradecanal (**6a**). Octanal (**6d**) exhibited the lowest yield of the saturated aldehydes. The unsaturated aldehyde substrates **5b-d**, however, resulted in yields below 10 %. Comparing saturated aldehydes with each other, substrates with longer chain length emit more light than those with shorter chain length and therefore are apparently better substrates for luciferase. This tendency was already observed earlier^{2,6}, however, a clear comparison and definite values were not reported. The same tendency was found for the unsaturated aldehydes, where total light emission decreases with shorter chain length. Thus, saturated and unsaturated aldehydes exhibit a similar chain length dependency but are clearly accepted as substrates for bacterial luciferase.

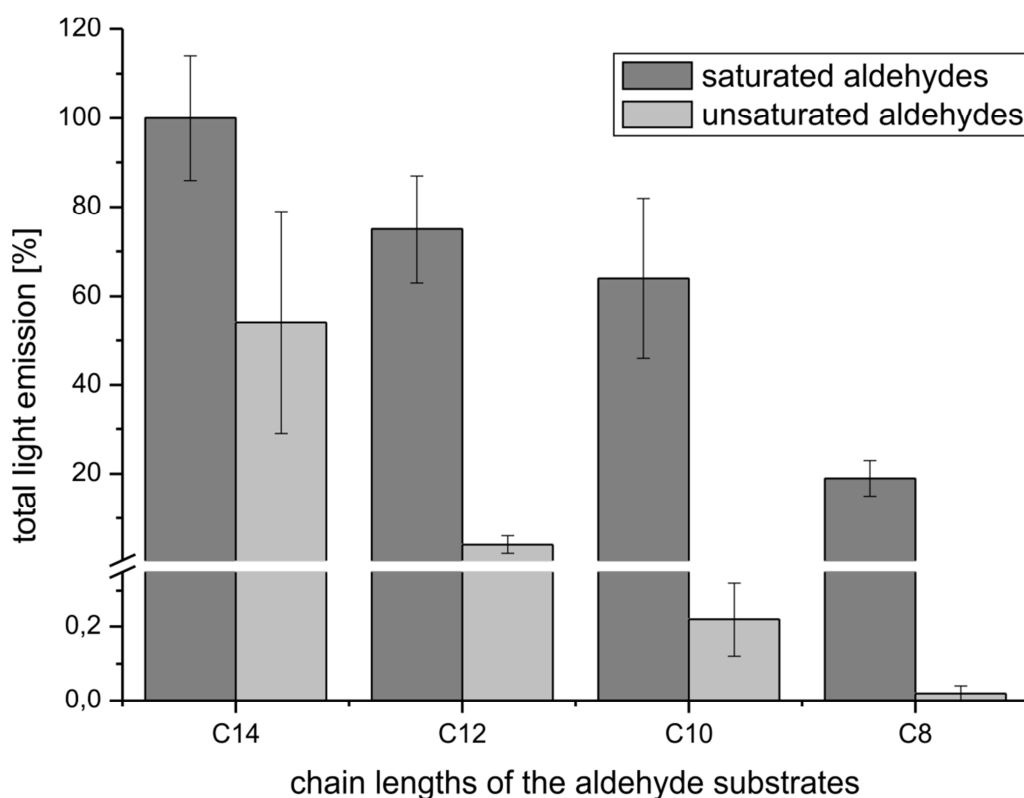


Figure 2: Comparison of saturated and unsaturated aldehydes as potential substrates for the luciferase of *P. leiognathi*. The conversion of unsaturated aldehydes **5a-d** (light grey) and saturated aldehydes **6a-d** (dark grey) by the luciferase during the *in vitro* assay (Scheme 3) can be determined by the total light emission of the reaction measured by the luminometer. The counts of the light emission were converted to percent. The total light emission (as percentage) was plotted against the substrates (here differentiated by their chain lengths). The production of light by the conversion of tetradecanal (**6a**) was set to 100 %. The values are shown by means \pm SD of seven individual measurements for the saturated aldehydes and four individual measurements for the unsaturated aldehydes, respectively.

Next, we analyzed the time course of light emission for unsaturated and saturated aldehydes. As an example, the kinetics of light emission with tetradecanal (**6a**) and (*E*)-tetradec-2-enal (**5a**) as substrates are shown in Figure 3. Generally, the onset as well as the decay of the light emission is faster with saturated aldehydes. In the case of **6a** a maximum light emission is reached after ca. 7 s whereas light emission with **5a** peaks at ca. 10 s. On the other hand, light emission lasted much longer for the unsaturated aldehyde **5a** than for the saturated aldehyde **6a**. A similar kinetic behavior was observed for all other saturated/unsaturated aldehyde pairs. This result indicates that the rate-limiting step (or steps) leading to the population of the excited state luciferin (presumably the flavin-4a-hydroxide³²) is slowed down when unsaturated aldehydes are used as substrates.

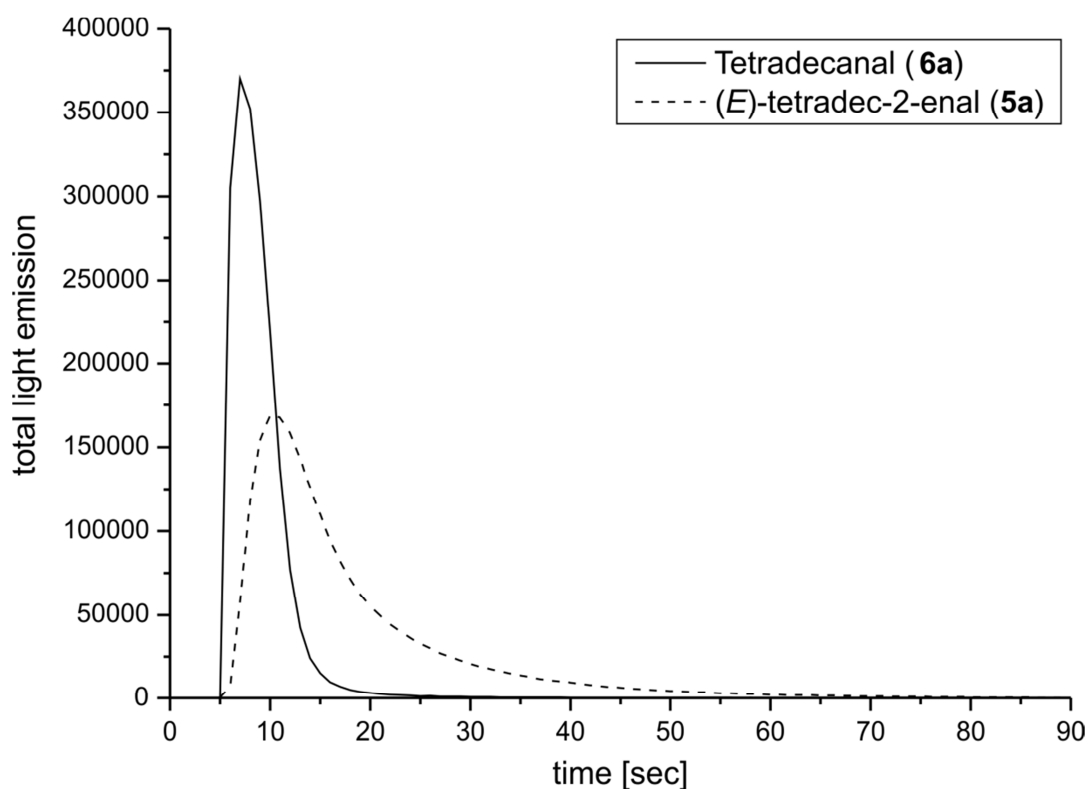


Figure 3: Time course of the total light emission of tetradecanal (6a) and (E)-tetradec-2-enal (5a). The light emission during the conversion of the substrates tetradecanal (6a, solid line) and (E)-tetradec-2-enal (5a, dashed line) was measured as a function of time by the luminometer. The counts of light emission were plotted as per cent, setting the maximal bioluminescence intensity of tetradecanal (6a) as 100 %, against the time (in seconds). This is a representative figure of a single measurement.

Tetradecanal (6a) and (E)-tetradec-2-enal (5a) were chosen as substrates for the *in vitro* assay with luciferases from different genera (*P. leiognathi*, *V. harveyi*, *A. fischeri*) as depicted in Figure 4. The assay conditions were adopted for *V. harveyi* and *A. fischeri*. For the latter, a luciferase concentration of 200 nM was used and the concentrations for FMN and YcnD were set to 300 nM, respectively. Because light emission was highest with the luciferase from *P. leiognathi* it was used as a reference point, *i.e.* set to 100 %. *V. harveyi* and *A. fischeri* accepted both substrates but showed a much lower activity than *P. leiognathi*. Comparison of these two substrates with various luciferases confirms the previous results by depicting a decline of light emission with unsaturated aldehydes. Nevertheless, (E)-tetradec-2-enal (5a) is a substrate for various bacterial luciferases.

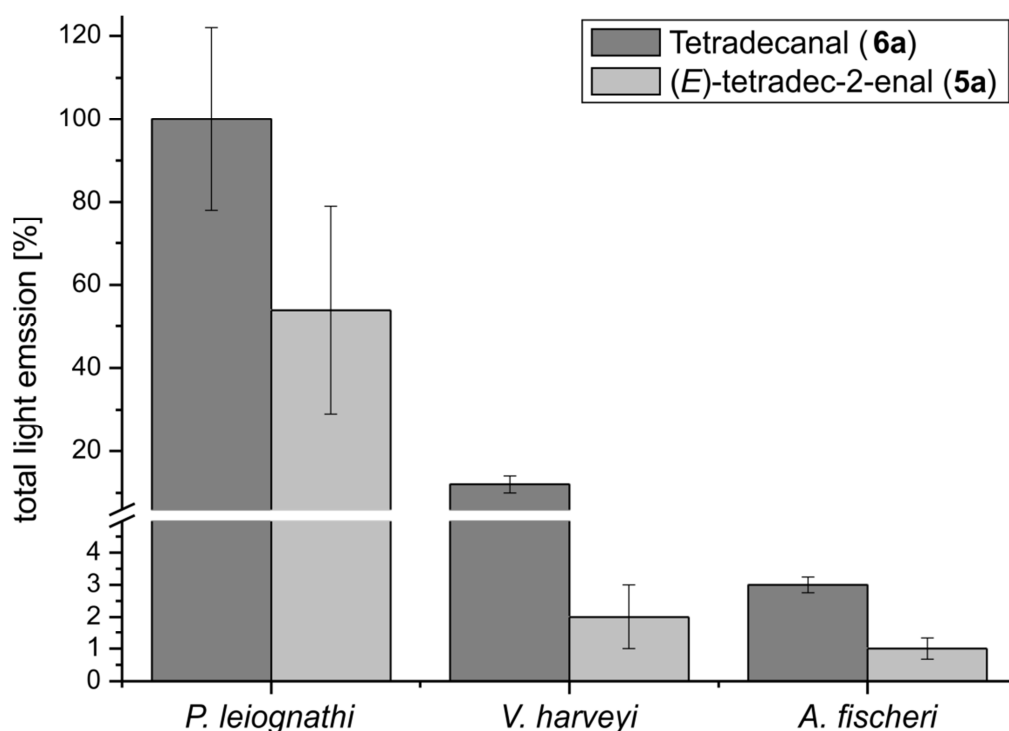


Figure 4: Comparison of the total light emission for luciferases from *P. leiognathi*, *V. harveyi* and *A. fischeri*. Three luciferases of different genera were compared with each other by analyzing the total light emission (as percentage) during conversion of the two potential substrates tetradecanal (**6a**, dark grey) and (*E*)-tetradec-2-enal (**5a**, light grey) in *in vitro* assays. The values are shown by means \pm SD of four individual measurements, respectively.

To evaluate whether the binding of the substrate within the active site might influence the enzyme activity and maximal light intensity, a preliminary docking study was performed. Based on the crystal structure with bound FMN¹⁸, the intermediate state of flavin-4a-hydroperoxide was predicted and the various substrates were docked into the active site. After energy minimization, the structure with the flavin-4a-hydroperoxide in the active site was used for further docking studies with the substrates used in this study, *i.e.* **5a-d** and **6a-d**. The docking results obtained with the saturated and unsaturated aldehydes indicate similar distances of the C1 atom of the respective aldehyde and the distal oxygen atom of the flavin-4a-hydroperoxide (Supplementary Data).

In Figure 5, an overlay of the two docking results with the substrates tetradecanal (**6a**) and (*E*)-tetradec-2-enal (**5a**) is depicted. It appears that the two substrates **5a** and **6a** adopt similar conformations and orientations, except for the position of the oxygen atom of the aldehyde that points in opposite directions. The distance between the C1 of the aldehyde and the distal oxygen of the flavin intermediate is around 3.6-3.7 Å (Supplementary Data).

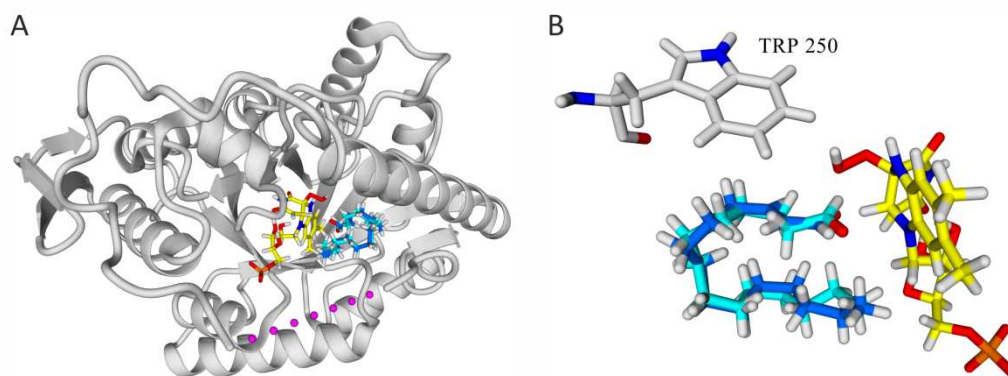


Figure 5: Docking of tetradecanal (6a) and (*E*)-tetradec-2-enal (5a) into the active site of the luciferase of *V. harveyi* with bound flavin-4a-hydroperoxide intermediate. **A:** Crystal structure of the α -subunit of the luciferase of *V. harveyi* with modelled flavin-4a-hydroperoxide intermediate depicted in yellow. The unstructured loop is displayed as pink dots. The two substrates tetradecanal (**6a**, cyan) and (*E*)-tetradec-2-enal (**5a**, blue) are docked into the active site of the luciferase. **B:** Zoom into the active site and overlay of tetradecanal (**6a**, cyan) and (*E*)-tetradec-2-enal (**5a**, blue). The flavin-4a-hydroperoxide intermediate (yellow) is in close proximity to the substrates **6a** and **5a**, having a distance between the distal oxygen of flavin-4a-hydroperoxide to C1 of 3.637 Å and 3.740 Å, respectively.

Thus, our docking results support our experimental findings that unsaturated aldehydes are accepted substrates and indicate that luciferases have a broader substrate range as previously assumed. The different orientation observed for the aldehyde function may be a first hint why unsaturated aldehydes show a substantial difference in kinetics as compared to their saturated counterparts. The hydrophobic pocket, lined for example by Trp250 (Figure 5) within the active site does not allow binding of bulkier or larger substrates, however, replacement of amino acids in the active site of luciferase may help to engineer the putative substrate binding pocket for other aldehyde substrates. Clearly, further structural and computational methods need to be applied to enhance our understanding of the mechanism and substrate scope of bacterial luciferases.

2.5. Discussion

Four different compounds, namely (*E*)-tetradec-2-enal (**5a**), (*E*)-dodec-2-enal (**5b**), (*E*)-dec-2-enal (**5c**) and (*E*)-oct-2-enal (**5d**), were successfully synthesized and analyzed as potential substrates for recombinant luciferases from three different genera. Spudich and Hastings showed in 1963 that 2-decenal (referring to (*E*)-dec-2-enal (**5c**)) is completely inactive in the production of light with the luciferase of *Achromobacter fischeri*. On the contrary, this compound was found to be a potent competitive inhibitor in bioluminescence with decanal in the reaction inhibited by decenal. Strangely enough, they have reported similar quantum yields for the reaction with saturated and unsaturated substrate.⁷ Additionally, Lei and coworkers proposed an inhibitory effect of a postulated “luciferase-aldehyde dead end complex”. In this case the sequence of substrate binding (aldehyde and FMNH₂) to the luciferase seems to be essential for activity or inhibition.³³ Thus, it was assumed that all α, β -unsaturated aldehydes exert an inhibitory effect and were therefore not considered as possible substrates. In contrast to that, we show here that unsaturated aldehydes are accepted as substrates by various recombinant luciferases from the genera *Photobacterium*, *Vibrio* and *Aliivibrio*, although the light emission yield was lower with the unsaturated aldehydes.

In light of our observations, the previously observed inhibitory effect⁷ seems to be a kinetic one. The time course of the light emission is strongly influenced by the various substrates. Unfortunately, substrate-buffer suspensions had to be used for the assays; therefore, it was not possible to conduct more detailed kinetic measurements. Studies with organic co-solvents were attempted, but led to denaturation of the luciferases (data not shown). The solubility of the aldehydes corresponds to the aldehyde chain length according to molar solubility values (Supplementary Data). Octanal (**6d**), for instance, should presumably give better results than tetradecanal (**6a**), as its solubility in aqueous buffer is higher. However, the reverse dependency was observed, as aldehydes with longer chain length are more efficient in light emission in our *in vitro* assay system.

As mentioned in the introduction, structural information on the active site of luciferase is still scarce in particular in regard of the positioning of the aldehyde substrate. Current mechanistic considerations are based on the crystal structure of luciferase of *V. harveyi* with bound FMN.¹⁸ Modelling studies suggested several amino acids that may play an important role for binding or interacting with the aldehyde substrate, as for example His44 and Trp250. Additionally, a spacious hydrophobic cavity was postulated as potential substrate binding position.²⁰ Nevertheless, a structure of the ternary complex of luciferase, FMNH₂ and aldehyde is still lacking leading to speculations concerning substrate binding and the reaction mechanism.

2.6. Conclusion

Bacterial bioluminescence is a fascinating phenomenon and the structure-function relationships responsible for the population of an excited state remains a scientific challenge even after decades of research. Here, we have demonstrated that the scope of substrates utilized by bacterial luciferases is not as limited as previously thought. In this study, the α,β -unsaturated aldehydes with chain length of 8, 10, 12 and 14 carbon atoms were synthesized in a three step synthesis approach. To elucidate the conversion of these potential substrates, an *in vitro* assay was developed. The four synthesized, unsaturated aldehydes **5a-d**, as well as their saturated analogs **6a-d** were analyzed with luciferases from three different genera (*P. leiognathi*, *V. harveyi*, *A. fischeri*). The results indicate, that all of them are accepted by the enzymes and show reasonable to low light emission. Comparing the different potential substrates, tetradecanal (**6a**) exhibits the highest light emission yield, while three other substrates (**5a**, **6b**, **6c**) reached only about 54-75 % of the best performing tetradecanal (**6a**). This study comprises the first comparison of these eight aldehydes (**5a-d**, **6a-d**) as substrates for bacterial luciferases. Having a closer look at the time course of light emission, the different kinetics in the onset as well as decay of light emission for tetradecanal (**6a**) and (*E*)-tetradec-2-enal (**5a**) were evident. Also, we have shown that luciferases from other bioluminescent bacteria show a similar pattern with regard to yield and kinetics of light emission. In summary, all eight substrates **5a-d** and **6a-d** were accepted by the luciferase leading to the conclusion that further investigations on substrate specificity and compatibility will lead to new insights into bacterial bioluminescence.

Author contribution

EB and JI synthesized the long chain aliphatic aldehydes, EB and CRT performed the bioluminescent analysis of these substrates, EB conducted the molecular docking and EB, JI, RB and PM wrote the manuscript.

Acknowledgments

This work was supported by the Austrian “Fonds zur Förderung der wissenschaftlichen Forschung” (FWF) to PM (P24189) and the PhD program “DK Molecular Enzymology” to PM and RB (W901). We would like to thank Johannes Niederhauser and Dr. Grit Straganz (Graz University of Technology) for their help with molecular docking experiments using Yasara.

Conflict of interest

The authors declare no conflict of interest.

2.7. References

- (1) Dunlap, P. In *Encyclopedia of Microbiology*; Schaechter, M., Ed.; Elsevier: Oxford, 2009; pp 45–61.
- (2) Strehler, B. L.; Cormier, M. J. *J. Biol. Chem.* **1954**, *211*, 213–225.
- (3) Strehler, B. L. *J. Am. Chem. Soc.* **1953**, *75*, 1264.
- (4) Strehler, B. L.; Cormier, M. J. *Arch. Biochem. Biophys.* **1953**, *47*, 16–33.
- (5) Hastings, J. W.; Gibson, Q. H. *J. Biol. Chem.* **1963**, *238* (7), 2537–2554.
- (6) Hastings, J. W.; Spudich, J.; Malnic, G. *J. Biol. Chem.* **1963**, *238* (9), 3100–3105.
- (7) Spudich, J.; Hastings, J. W. *J. Biol. Chem.* **1963**, *238* (9), 3106–3108.
- (8) Cormier, M. J.; Totter, J. R. *Biochim. Biophys. Acta* **1957**, *25*, 229–237.
- (9) Cormier, M. J.; Eley, M.; Abe, S.; Nakano, Y. *Photochem. Photobiol.* **1969**, *9*, 351–358.
- (10) Lee, J. *Biochemistry* **1972**, *11* (18), 3350–3359.
- (11) Shimomura, O.; Johnson, F. H.; Kohama, Y. *Proc. Natl. Acad. Sci. USA* **1972**, *69* (8), 2086–2089.
- (12) McCapra, F.; Hysert, D. W. *Biochem. Biophys. Res. Commun.* **1973**, *52* (1), 298–304.
- (13) Lee, J.; Murphy, C. L. *Biochemistry* **1975**, *14* (10), 2259–2268.
- (14) Shimomura, O.; Johnson, F. H.; Morise, H. *Proc. Natl. Acad. Sci. USA* **1974**, *71* (12), 4666–4669.
- (15) Macheroux, P.; Ghisla, S.; Hastings, J. W. *Biochemistry* **1993**, *32*, 14183–14186.
- (16) Dunlap, P. In *Bioluminescence: Fundamentals and Applications in Biotechnology - Volume 1*; Thouand, G., Marks, R., Eds.; Springer Berlin Heidelberg: Berlin, Heidelberg, 2014; Vol. 144, pp 37–64.
- (17) Fisher, A. J.; Raushel, F. M.; Baldwin, T. O.; Rayment, I. *Biochemistry* **1995**, *34*, 6581–6586.
- (18) Campbell, Z. T.; Weichsel, A.; Montfort, W. R.; Baldwin, T. O. *Biochemistry* **2009**, *48* (26), 6085–6094.
- (19) Fisher, A. J.; Thompson, T. B.; Thoden, J. B.; Baldwin, T. O.; Rayment, I. *J. Biol. Chem.* **1996**, *271* (36), 21956–21968.
- (20) Lin, L. Y.-C.; Sulea, T.; Szittner, R.; Vassilyev, V.; Purisima, E. O.; Meighen, E. A. *Protein Sci.* **2001**, *10* (8), 1563–1571.
- (21) Campbell, Z. T.; Baldwin, T. O.; Miyashita, O. *Biophys. J.* **2010**, *99* (12), 4012–4019.
- (22) Baldwin, T. O.; Christopher, J. A.; Raushel, F. M.; Sinclair, J. F.; Ziegler, M. M.; Fisher, A. J.; Rayment, I. *Curr. Opin. Struct. Biol.* **1995**, *5*, 798–809.
- (23) Chen, L. H.; Baldwin, T. O. *Biochemistry* **1989**, *28*, 2684–2689.
- (24) Li, Z.; Meighen, E. A. *Biochemistry* **1995**, *34*, 15084–15090.
- (25) Vervoort, J.; Muller, F.; O’Kane, D. J.; Lee, J. *Biochemistry* **1986**, *25*, 8067–8075.
- (26) Bergner, T.; Tabib, C. R.; Winkler, A.; Stipsits, S.; Kayser, H.; Lee, J.; Malthouse, J. P.; Mayhew, S.; Müller, F.; Gruber, K.; Macheroux, P. *Biochim. Biophys. Acta BBA - Proteins Proteomics* **2015**, *1854* (10), 1466–1475.
- (27) Morokutti, A.; Lyskowski, A.; Sollner, S.; Pointner, E.; Fitzpatrick, T. B.; Kratky, C.; Gruber, K.; Macheroux, P. *Biochemistry* **2005**, *44* (42), 13724–13733.
- (28) de Groot, B. L.; van Aalten, D. M. F.; Scheek, R. M.; Amadei, A.; Vriend, G.; Berendsen, H. J. C. *Proteins Struct. Funct. Genet.* **1997**, *29*, 240–251.
- (29) Morris, G. M.; Goodsell, D. S.; Halliday, R. S.; Huey, R.; Hart, W. E.; Belew, R. K.; Olson, A. J. *J. Comput. Chem.* **1998**, *19* (14), 1639–1662.
- (30) Trott, O.; Olson, A. J. *J. Comput. Chem.* **2009**, 455–461.
- (31) List, B.; Doehring, A.; Fonseca, M. T. H.; Wobser, K.; van Thienen, H.; Torres, R. R.; Galilea, P. L. *Adv. Synth. Catal.* **2005**, *347* (11-13), 1558–1560.

- (32) Kurfürst, M.; Ghisla, S.; Hastings, J. W. *Proc. Natl. Acad. Sci. USA* **1984**, *81*, 2990–2994.
(33) Lei, B.; Cho, K. W.; Tu, S.-C. *J. Biol. Chem.* **1994**, *269* (8), 5612–5618.

Highlights

- α , β -unsaturated aldehydes were synthesized in a three-step approach
- (un-)saturated aldehydes were investigated as potential substrates for luciferases
- saturated aldehydes showed higher light emission than unsaturated aldehydes
- light emission increases with longer aldehyde chain length, i.e. C14>C12>C10>C8
- unsaturated aldehydes display slower kinetics of light emission

2.8. Supplementary Data

Table S.1: List of used substrates for the *in vitro* assay. Substrate names, numbers, molecular formula, molecular weight and density are listed together with the calculated μmol s used in the substrate-buffer suspension and their molar solubility.

Substrate	Molecular formula	Molecular weight (g/mol)	Density (g/cm ³) (20°C, 760 Torr)	Moles (μmol)	Molar solubility [mol/L] (pH 7, 25°C)
tetradecanal (6a)	C ₁₄ H ₂₈ O	212.37	0.826	19.4	3.7E-5
(<i>E</i>)-tetradec-2-enal (5a)	C ₁₄ H ₂₆ O	210.36	0.839	19.9	1.0E-4
dodecanal (6b)	C ₁₂ H ₂₄ O	184.32	0.823	22.3	1.8E-4
(<i>E</i>)-dodec-2-enal (5b)	C ₁₂ H ₂₂ O	182.30	0.837	23.0	5.2E-4
decanal (6c)	C ₁₀ H ₂₀ O	156.27	0.818	26.2	9.8E-4
(<i>E</i>)-dec-2-enal (5c)	C ₁₀ H ₁₈ O	154.25	0.835	27.1	2.8E-3
octanal (6d)	C ₈ H ₁₆ O	128.21	0.811	31.6	5.4E-3
(<i>E</i>)-oct-2-enal (5d)	C ₈ H ₁₄ O	126.20	0.832	33.0	0.015

Table S.2: Results of the total light emission of the eight substrates investigated *in vitro*. List of eight aldehydes with structure, name and number that were analyzed with the luciferase of *P. leiognathi* in an *in vitro* assay. Their total light emission was measured and calculated in per cent, thereby setting the result of tetradecanal (**6a**) to 100 %.

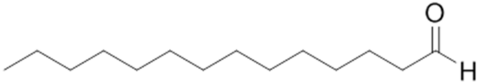
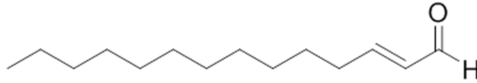
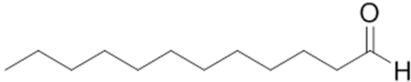
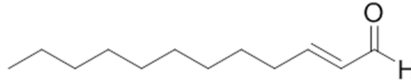
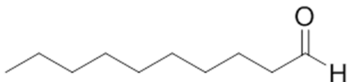
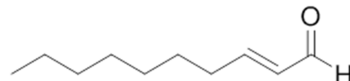
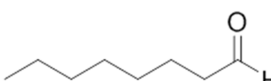
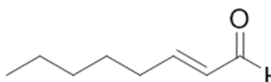
Number	Substrate		total light emission [%]
6a	tetradecanal		100
5a	(<i>E</i>)-tetradec-2-enal		54
6b	dodecanal		75
5b	(<i>E</i>)-dodec-2-enal		4
6c	decanal		64
5c	(<i>E</i>)-dec-2-enal		0,22
6d	octanal		19
5d	(<i>E</i>)-oct-2-enal		0,02

Figure S.1: ^1H and ^{13}C NMR spectra of ethyl (*E*)-oct-2-enoate (3d)

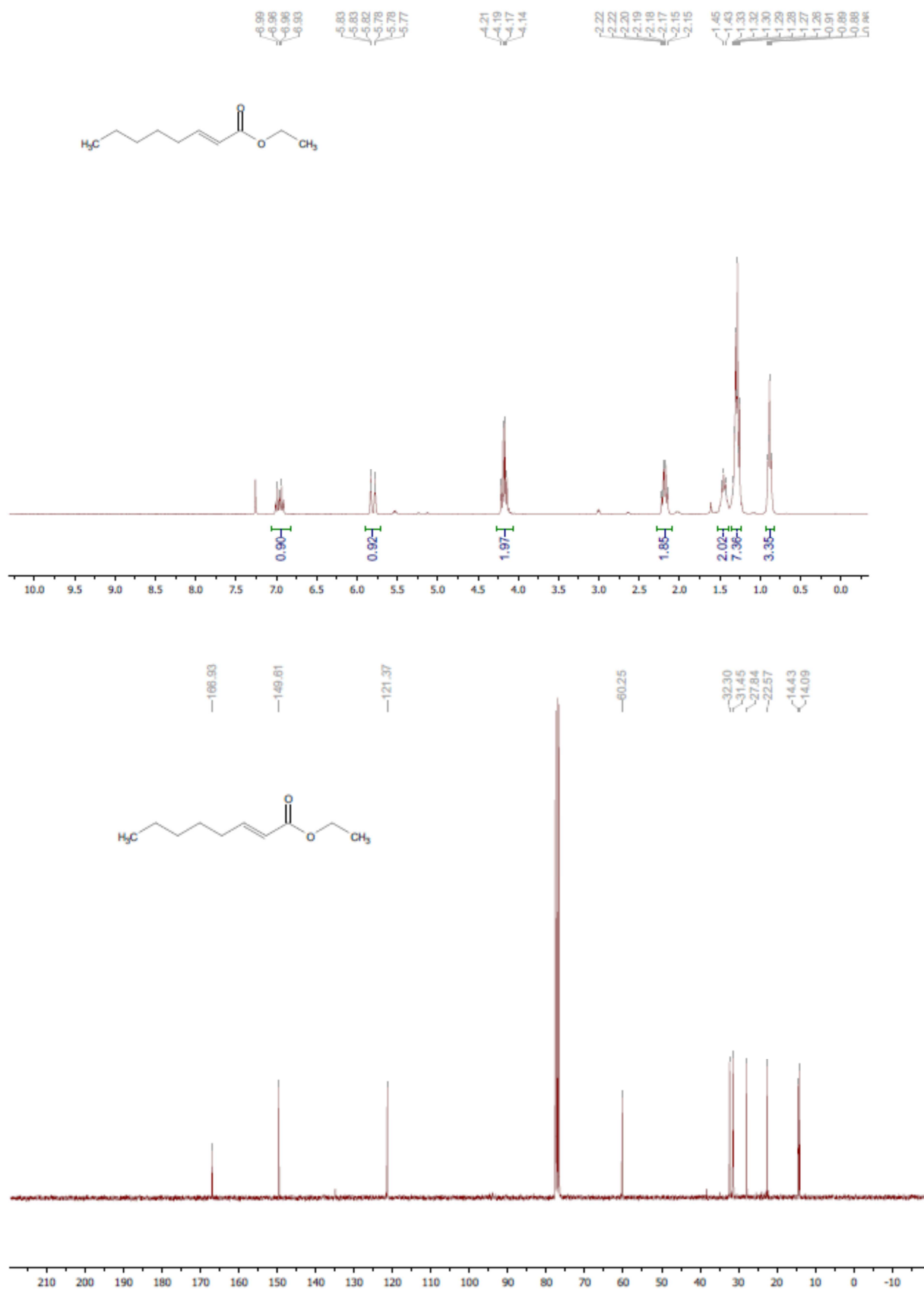


Figure S.2: ^1H and ^{13}C NMR spectra of ethyl (*E*)-dec-2-enoate (3c)

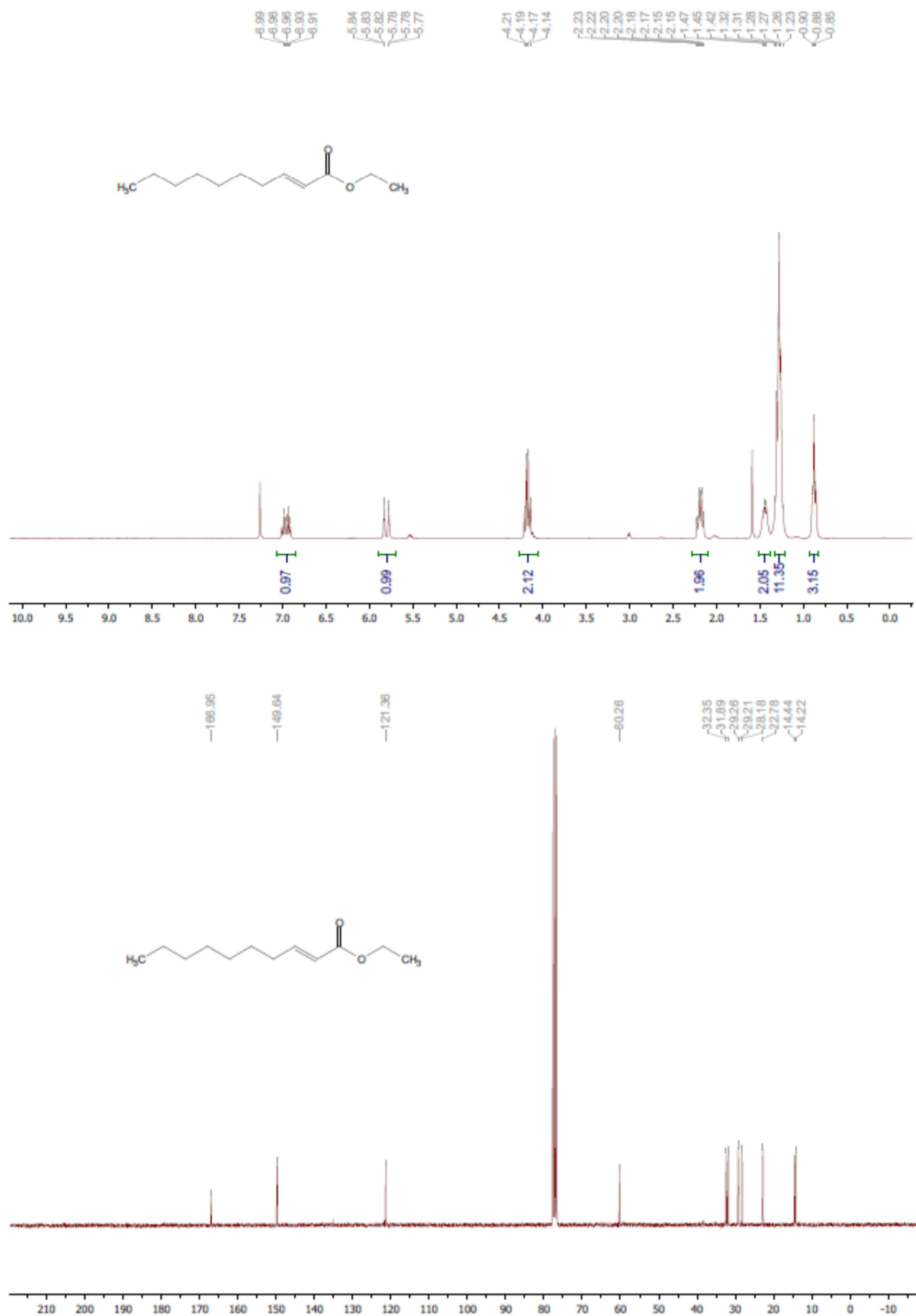


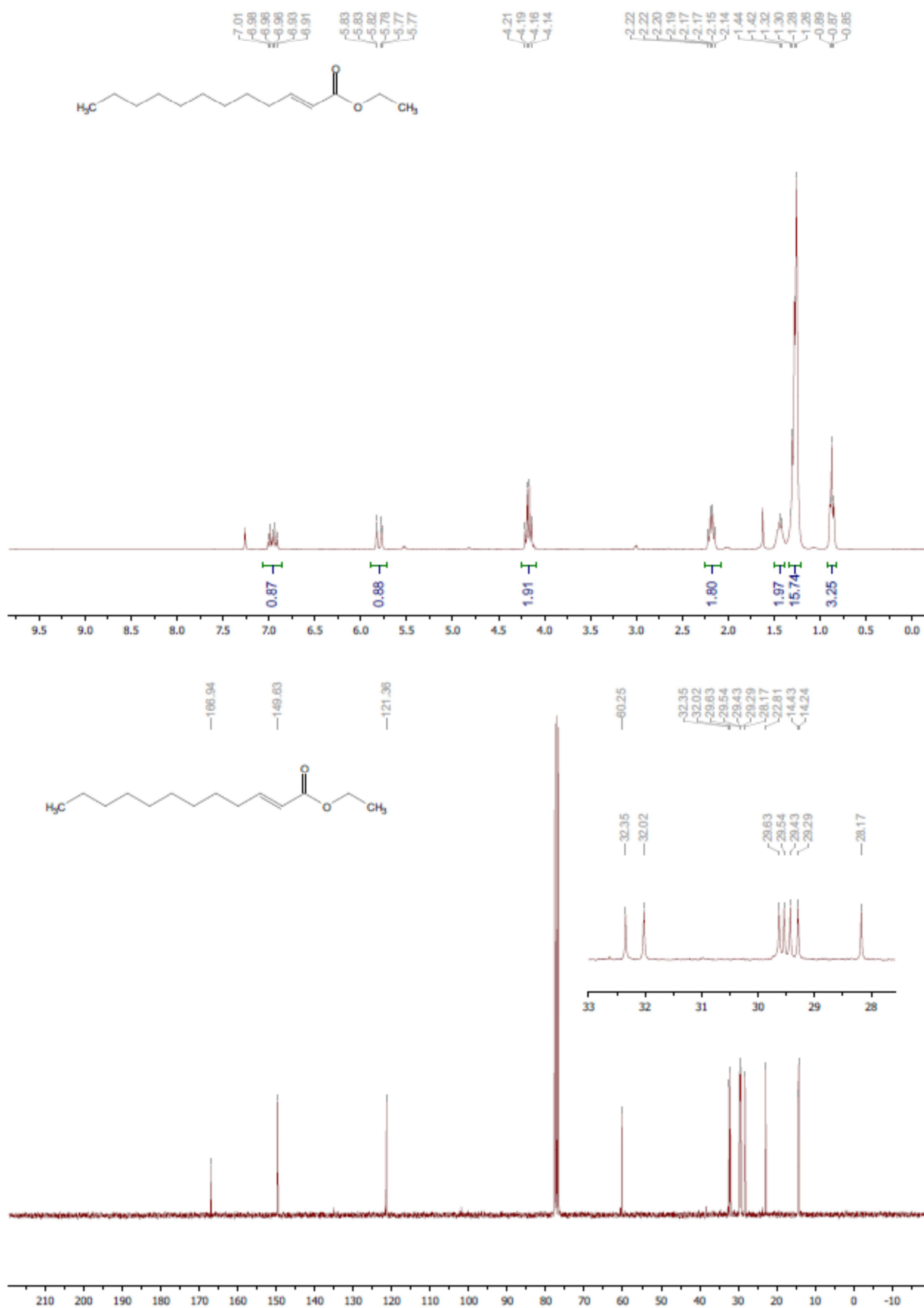
Figure S.3: ^1H and ^{13}C NMR spectra of ethyl (*E*)-dodec-2-enoate (3b)

Figure S.4: ^1H and ^{13}C NMR spectra of ethyl (*E*)-tetradec-2-enoate (3a)

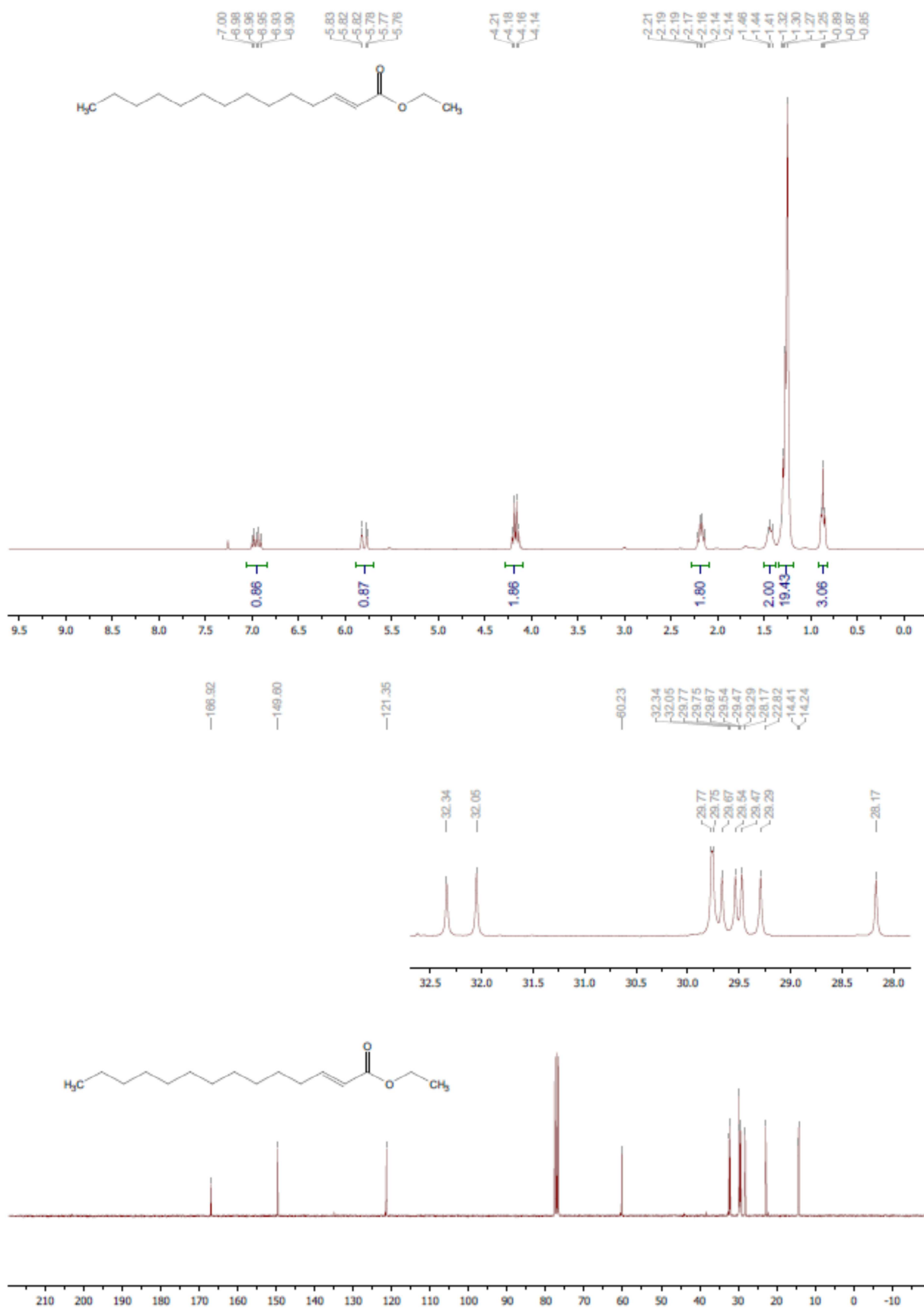


Figure S.5: ^1H and ^{13}C NMR spectra of ethyl (*E*)-oct-2-en-1-ol (4d)

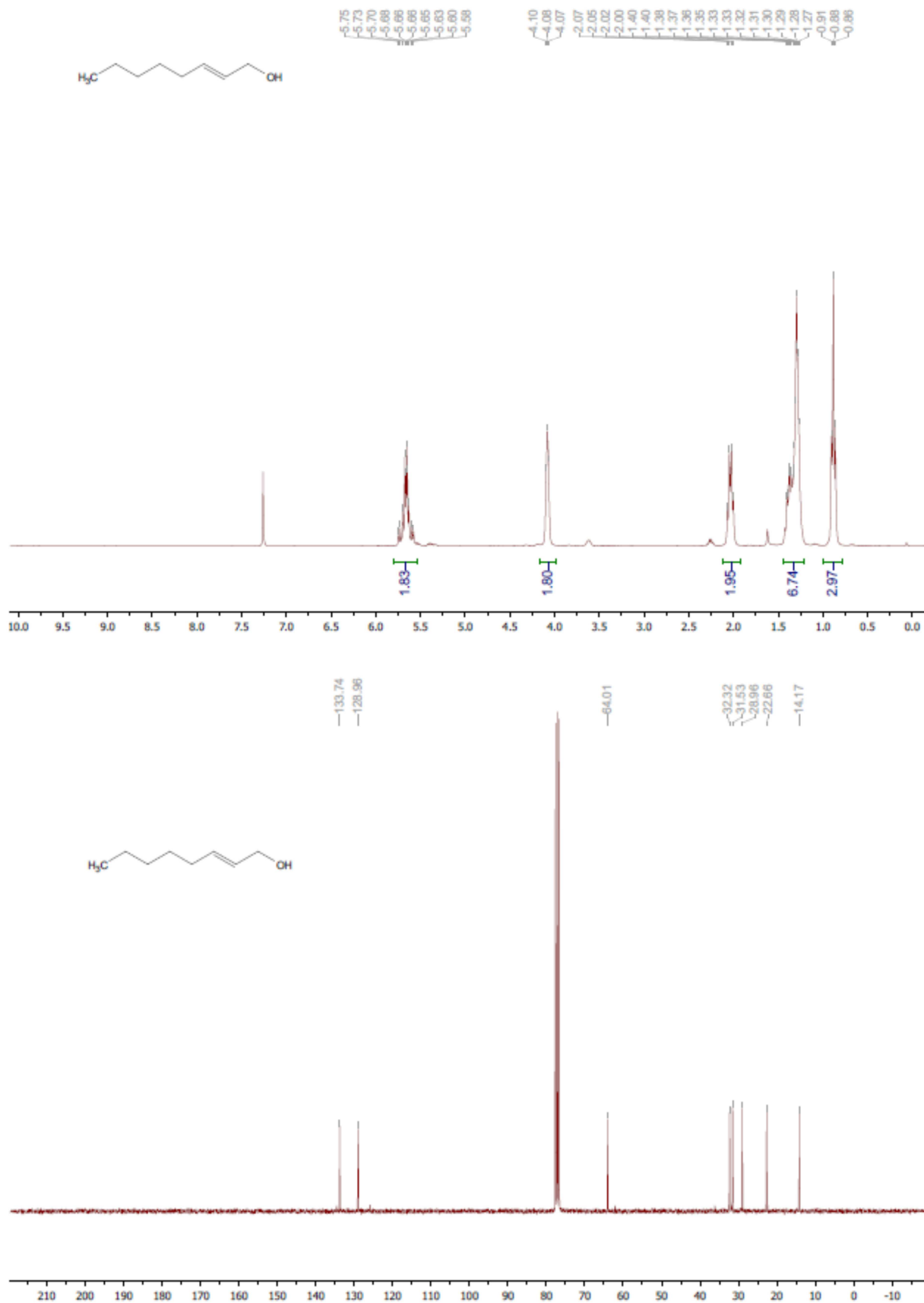


Figure S.6: ^1H and ^{13}C NMR spectra of ethyl (*E*)-dec-2-en-1-ol (4c)

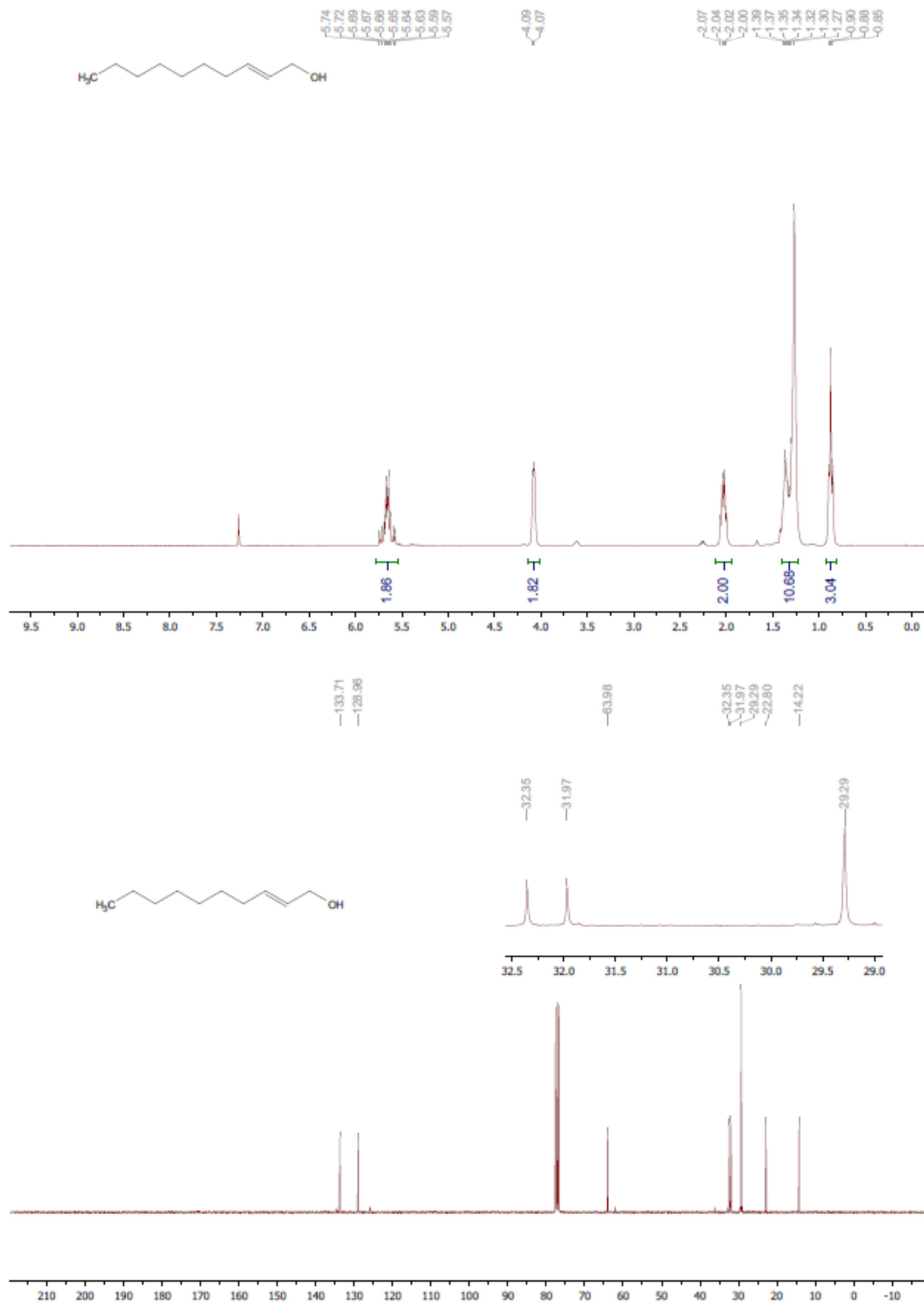


Figure S.7: ^1H and ^{13}C NMR spectra of ethyl (*E*)-dodec-2-en-1-ol (**4b**)

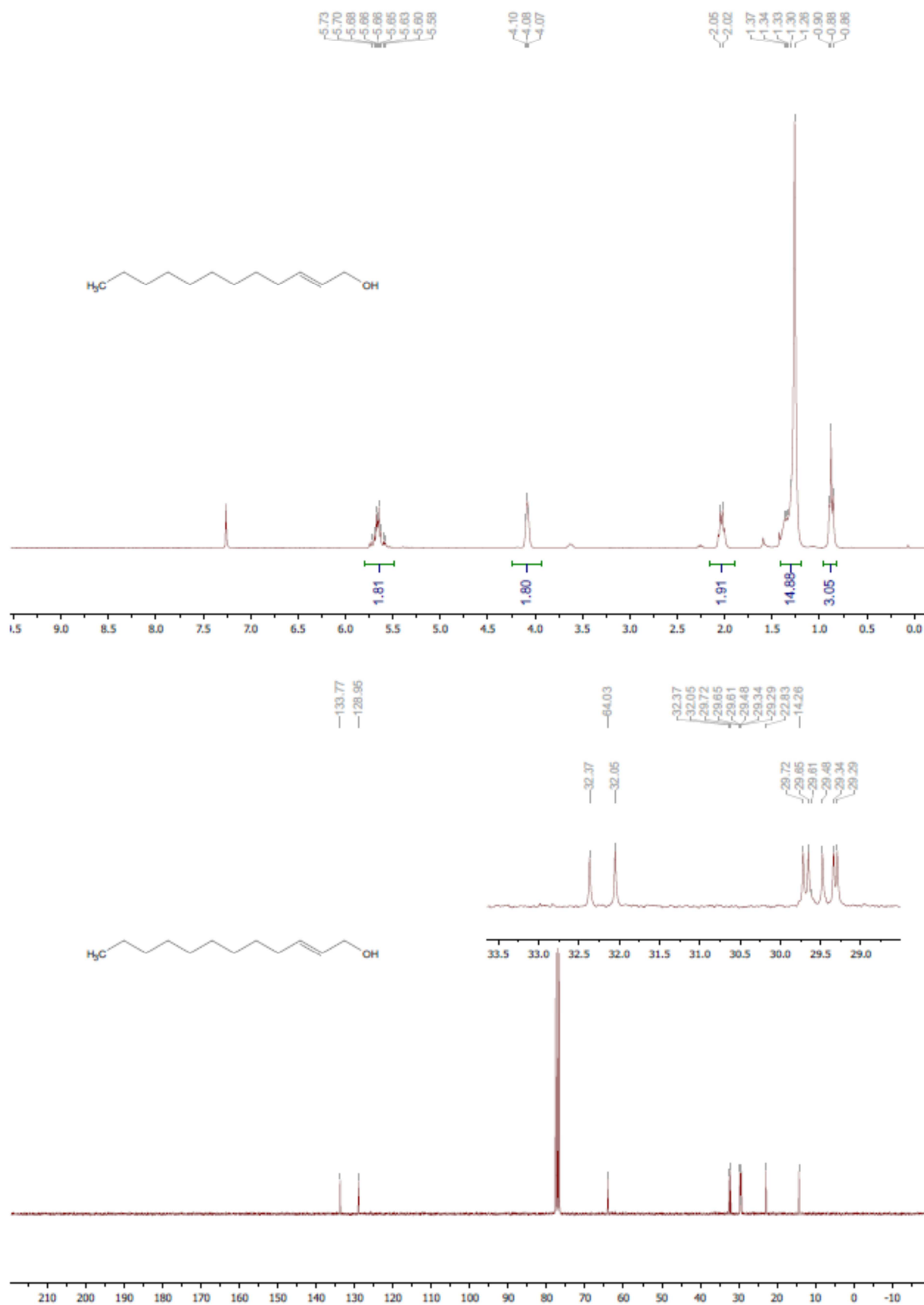


Figure S.8: ^1H and ^{13}C NMR spectra of ethyl (*E*)-tetradec-2-en-1-ol (4a)

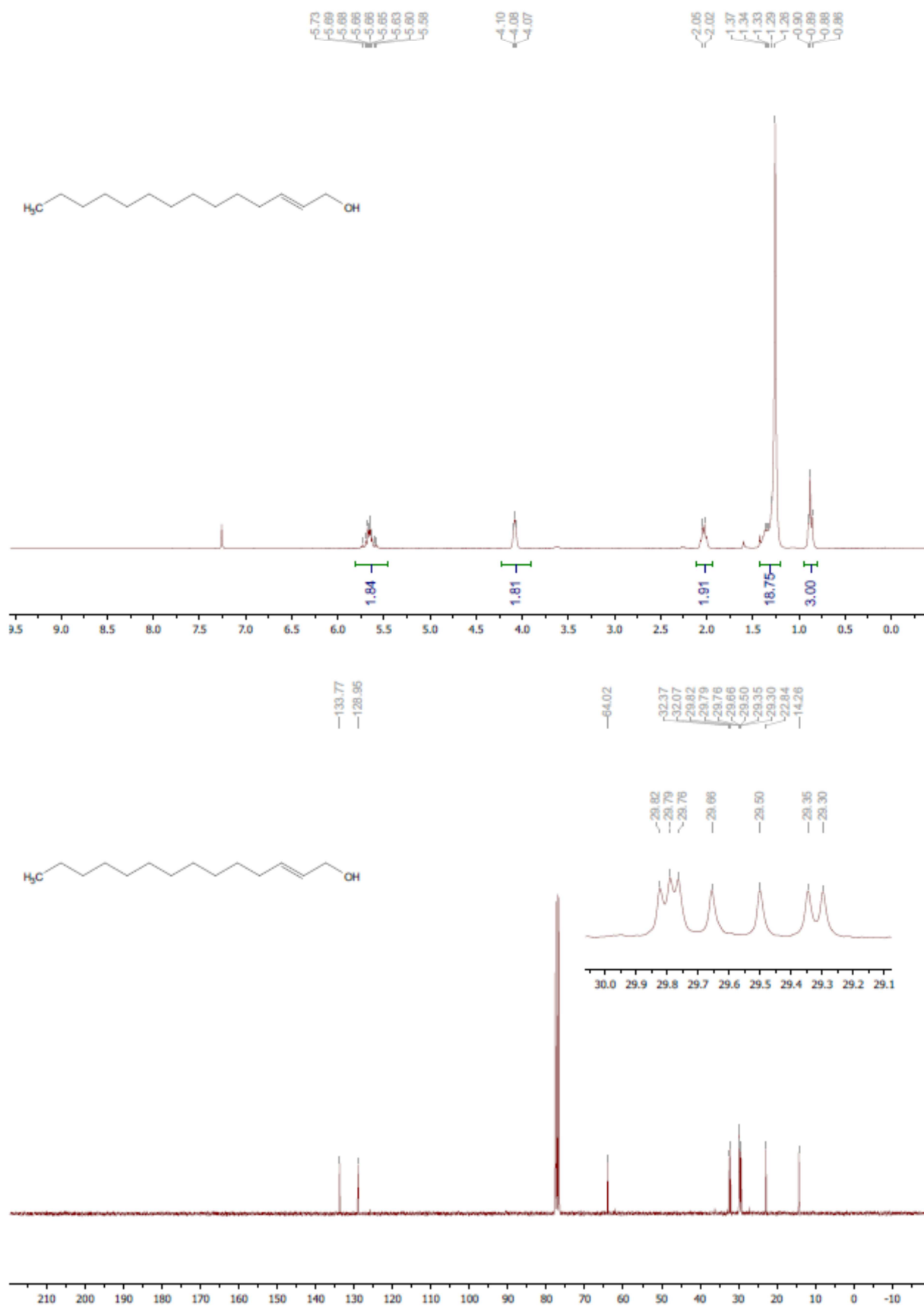


Figure S.9: ^1H and ^{13}C NMR spectra of (*E*)-oct-2-enal (5d)

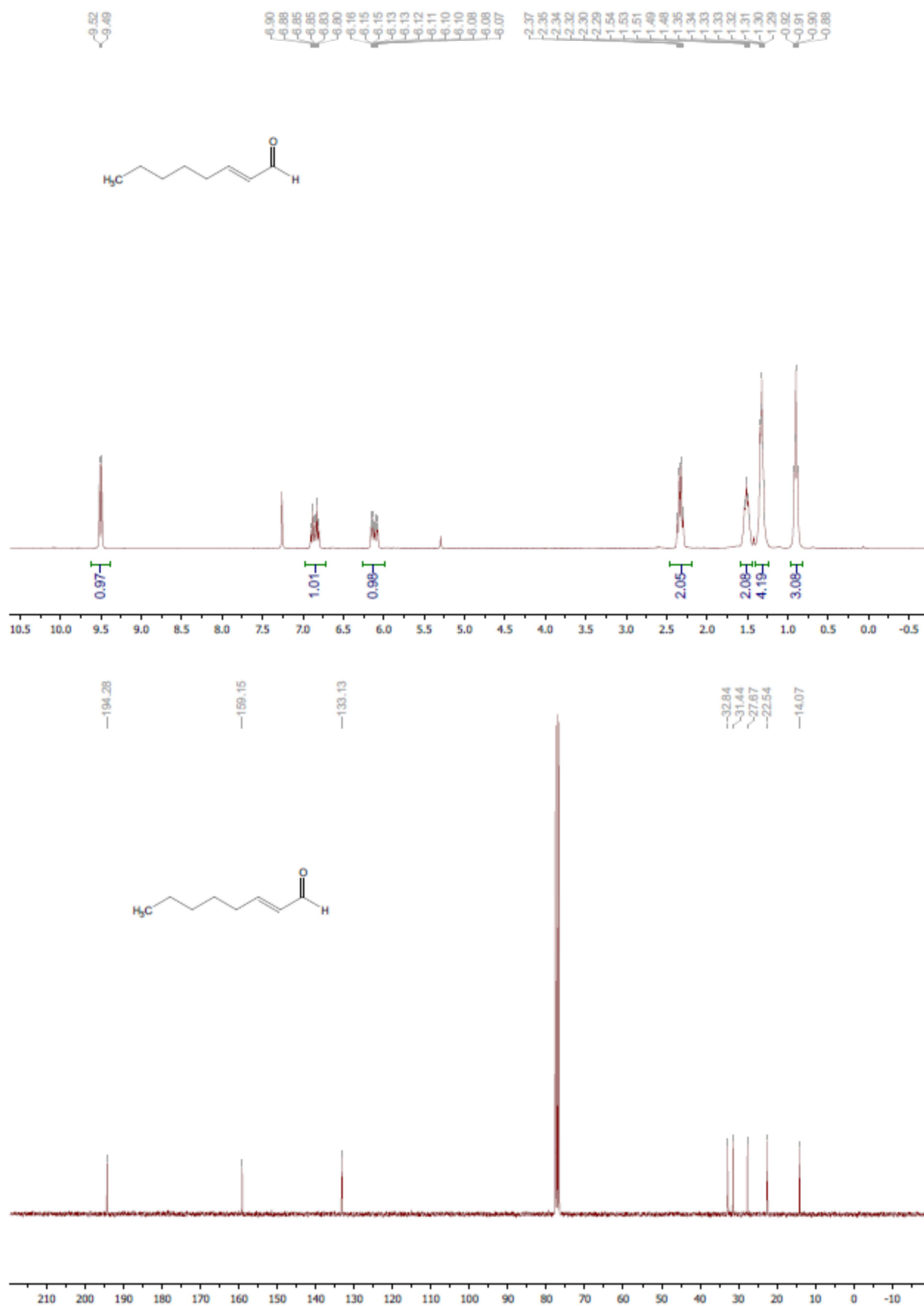


Figure S.10: ^1H and ^{13}C NMR spectra of (*E*)-dec-2-enal (5c)

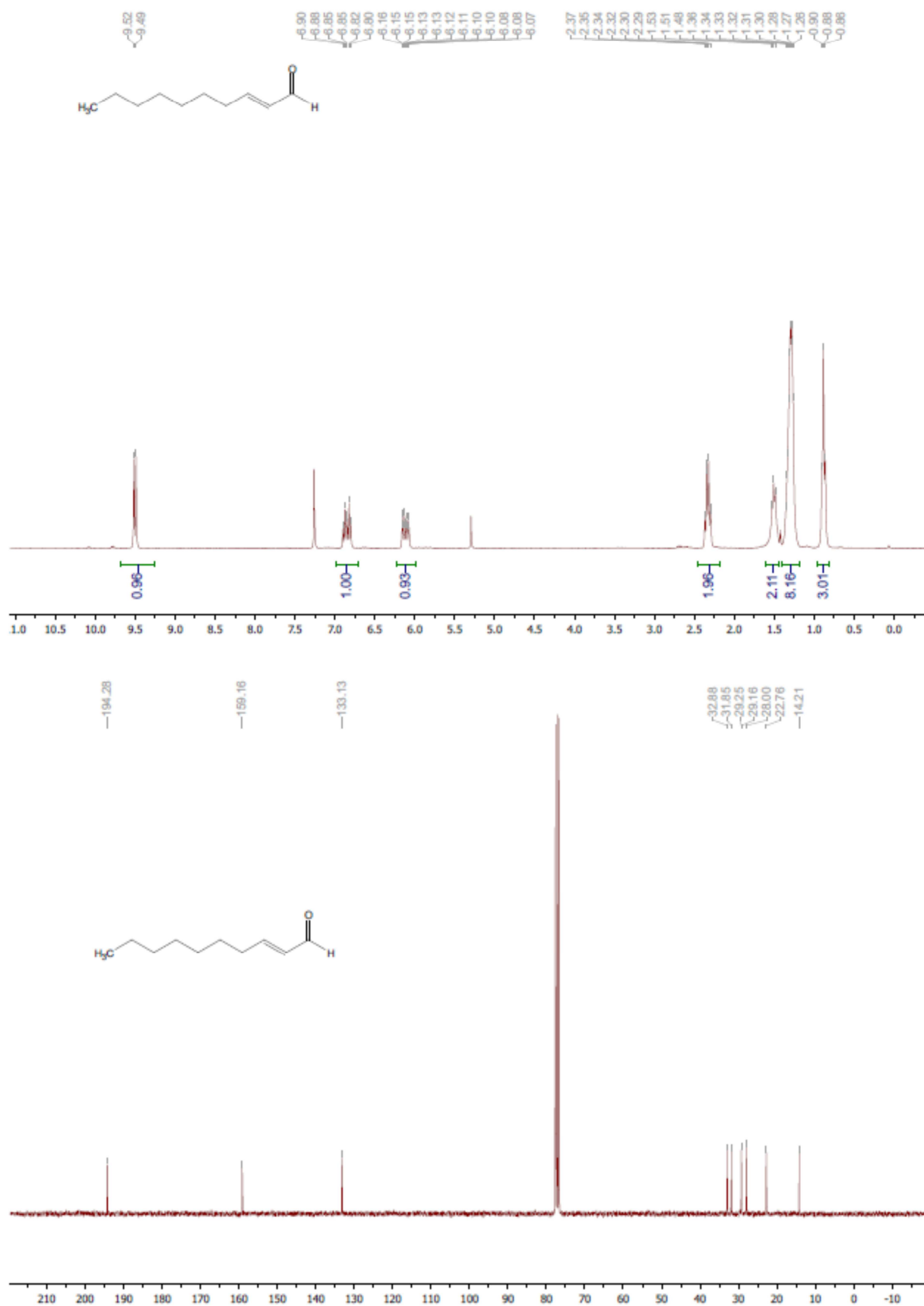


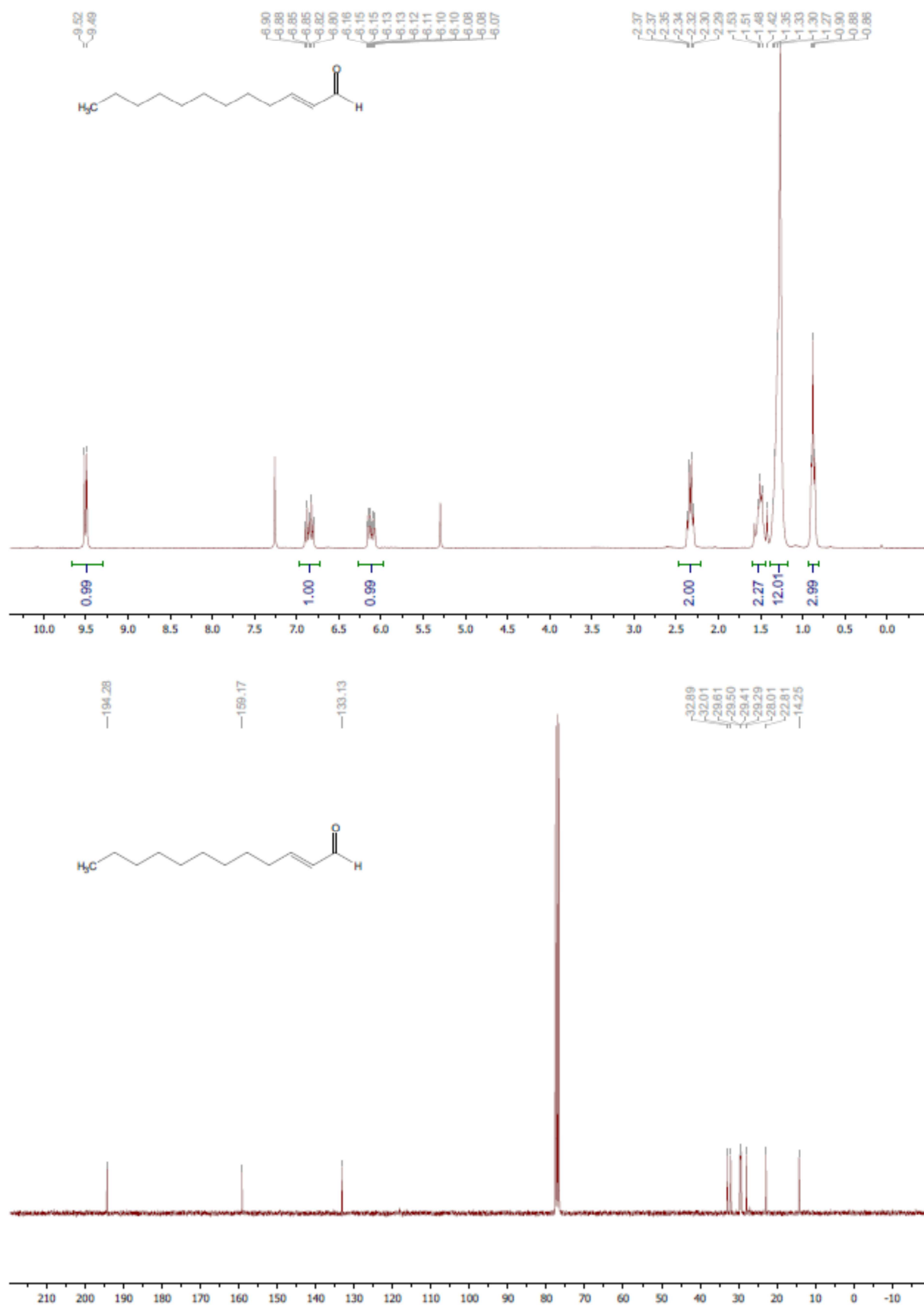
Figure S.11: ^1H and ^{13}C NMR spectra of (*E*)-dodec-2-enal (5b)

Figure S.12: ^1H and ^{13}C NMR spectra of (*E*)-tetradec-2-enal (5a)

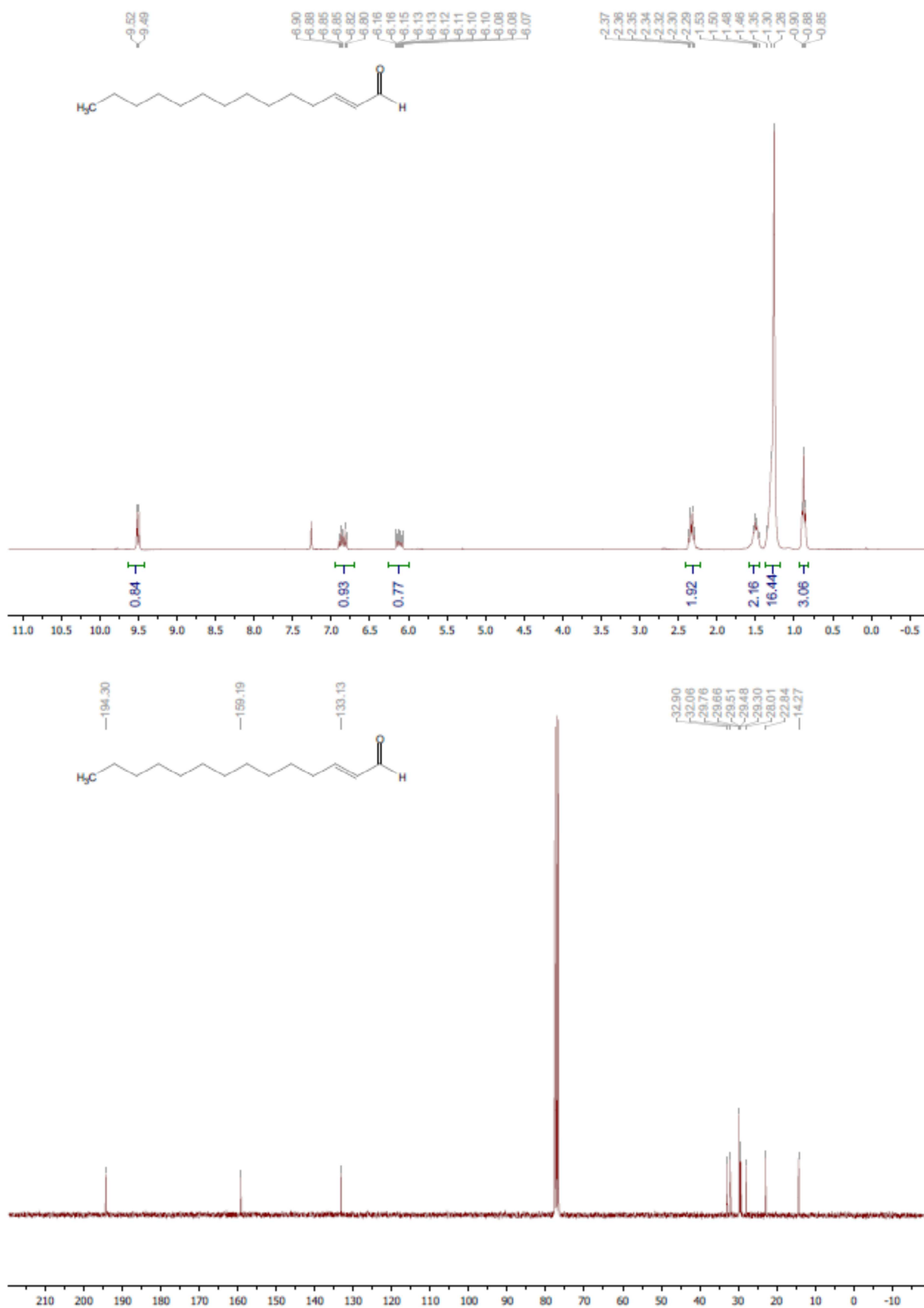


Figure S.13: Overlay of the molecular docking of octanal (6d, shown in cyan) and (*E*)-oct-2-enal (5d, shown in blue) into the active site of the luciferase of *Vibrio harveyi* with the flavin-4a-hydroperoxide intermediate (depicted in yellow). Additionally Trp250 is represented in the graph. The usual color code was applied, where oxygen is red, nitrogen is blue and phosphate is orange.

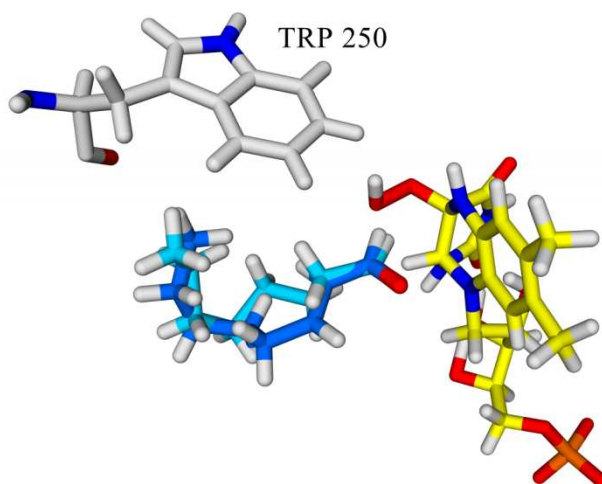


Figure S.14: Overlay of the molecular docking of decanal (6c, shown in cyan) and (*E*)-dec-2-enal (5c, shown in blue) into the active site of the luciferase of *Vibrio harveyi* with the flavin-4a-hydroperoxide intermediate (depicted in yellow). Additionally Trp250 is represented in the graph. The usual color code was applied, where oxygen is red, nitrogen is blue and phosphate is orange.

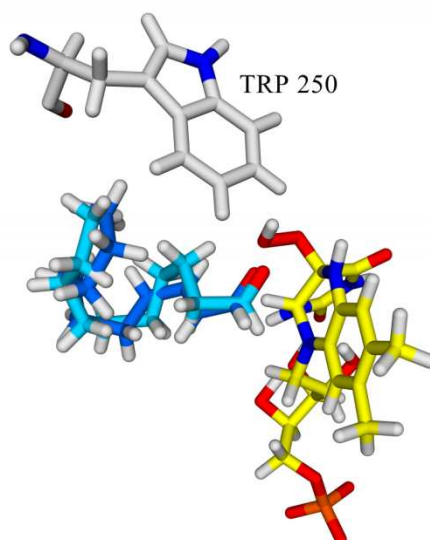


Figure S.15: Overlay of the molecular docking of dodecanal (6b, shown in cyan) and (*E*)-dodec-2-enal (5b, shown in blue) into the active site of the luciferase of *Vibrio harveyi* with the flavin-4a-hydroperoxide intermediate (depicted in yellow). Additionally Trp250 is represented in the graph. The usual color code was applied, where oxygen is red, nitrogen is blue and phosphate is orange.

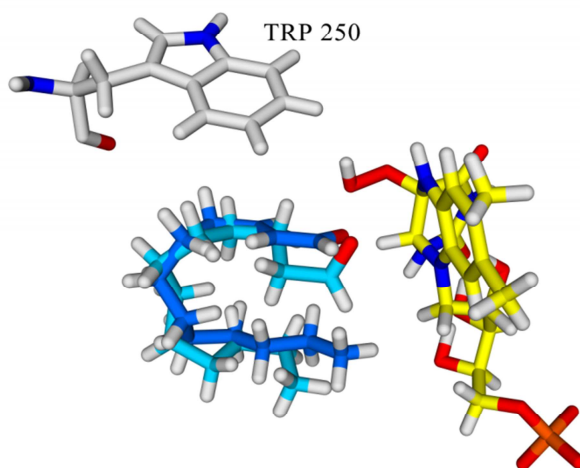


Table S.3: Evaluated distances of the C1 atom of the respective aldehyde substrate 5a-d and 6a-d to the distal oxygen atom of the flavin-4a-hydroperoxide intermediate given in angstrom.

	Substrate	distance O-C1 [Å]
6a	tetradecanal	3,637
5a	(<i>E</i>)-tetradec-2-enal	3,740
6b	dodecanal	4,696
5b	(<i>E</i>)-dodec-2-enal	3,751
6c	decanal	3,711
5c	(<i>E</i>)-dec-2-enal	3,708
6d	octanal	3,572
5d	(<i>E</i>)-oct-2-enal	3,577

Chapter III

Evidence for the generation of myristylated FMN by bacterial luciferase

This paper was published in the Journal of Molecular Microbiology, 104(6), pages 1027-1036, available online since April 19th, 2017 (doi:10.1111/mmi.13676).

III. Evidence for the generation of myristylated FMN by bacterial luciferase

Chaitanya R. Tabib*, Eveline Brodl* and Peter Macheroux+

Graz University of Technology, Institute of Biochemistry, Graz, Austria

*these authors contributed equally to this work

+To whom correspondence should be addressed:

Correspondence

Prof. Dr. Peter Macheroux, Graz University of Technology, Institute of Biochemistry, Petersgasse 12/II, A-8010 Graz, Austria; Email: peter.macheroux@tugraz.at

Keywords

myristylated FMN, bacterial bioluminescence, CIEEL mechanism, enzyme cascade, inhibition, *in vitro* assay.

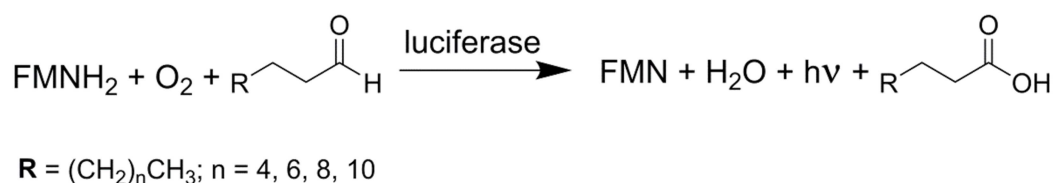
Running title: *Occurrence and generation of myrFMN*

3.1. Abstract

The genes responsible for the light production in bioluminescent bacteria are present as an operon, *luxCDABEG*. Many strains of *Photobacteria* carry an additional gene, termed *luxF*. X-ray crystallographic analysis of LuxF revealed the presence of four molecules of a flavin derivative, *i.e.* 6-(3'-(*R*)-myristyl) flavin adenine mononucleotide (myrFMN) non-covalently bound to the homodimer. In the present study, we exploited the binding of myrFMN to recombinant apo-LuxF to explore the occurrence of myrFMN in various bioluminescent bacteria. MyrFMN was detected in all bacterial strains tested including *Vibrio* and *Aliivibrio* indicating that it is more widely occurring in bioluminescent bacteria than previously assumed. We also show that apo-LuxF captures myrFMN and thereby relieves the inhibitory effect on luciferase activity. Thus, our results provide support for the hypothesis that LuxF acts as a scavenger of myrFMN in bioluminescent bacteria. However, the source of myrFMN remained obscure. To address this issue, we established a cofactor regeneration enzyme-catalyzed cascade reaction that supports luciferase activity *in vitro* for up to three days. This approach enabled us to unambiguously demonstrate that myrFMN is generated in the bacterial bioluminescent reaction. Based on this finding we postulate a reaction mechanism for myrFMN generation that is based on the luciferase reaction.

3.2. Introduction

Riboflavin, also known as vitamin B₂, serves as a precursor for the synthesis of flavin adenine dinucleotide (FAD) and flavin adenine mononucleotide (FMN), which share the same structural backbone, the isoalloxazine ring (Macheroux *et al.*, 2011). Flavoenzymes use either FMN or FAD to carry out a plethora of redox reactions that mostly revolve around the activation of dioxygen and the handling of one-electron or two-electron transfer reactions (Massey, 1994; Joosten and van Berkel, 2007; Teufel *et al.*, 2016). A prominent example for the utilization of dioxygen is the bacterial luciferase, which catalyzes the oxidation of long chain fatty aldehydes to their corresponding fatty acids, *e.g.* tetradecanal to myristic acid (Scheme 1).



Scheme 1: General reaction scheme for bacterial bioluminescence. Schematic representation of the luciferase catalyzed reaction, demonstrating the conversion of a long chain aldehyde (chain length from C8-C14) to the corresponding carboxylic acid where a FMNH₂ and an O₂ molecule are consumed in the process. Visible luminescence is emitted with a maximum at 490 nm.

In the course of the reaction, reduced FMN reacts with dioxygen to the FMN-C4a-peroxide, which subsequently reacts with the aldehyde to the FMN-4a-peroxyhemiacetal. The collapse of this intermediate generates the FMN-4a-hydroxide in an excited state, which relaxes to the ground state by emission of light centered at 490 nm. (Ulitzur and Hastings, 1979; Kurfürst *et al.*, 1984). Detailed studies on the reaction mechanism led to the suggestion that a radical mechanism, such as the chemically-induced electron exchange luminescence (CIEEL) mechanism, is responsible for the population of the excited state (Eckstein *et al.*, 1993).

The enzymes involved in bacterial bioluminescence are arranged in the form of an operon, with the typical gene organization being *luxCDABEG* as in *Photobacterium leiognathi* ATCC 25521 (Meighen, 1991). The *luxAB* genes encode for the heterodimeric protein luciferase consisting of a 40 kDa α -subunit and a 37 kDa β -subunit. The aldehyde required for the reaction is formed by a multi-enzyme complex consisting of a reductase (*luxC*), a transferase (*luxD*) and a synthetase (*luxE*). In addition, a NADH-dependent FMN reductase is encoded by *luxG* providing reduced FMN to the luciferase (Hastings *et al.*, 1969; Boylan *et al.*, 1985; Nijvipakul *et al.*, 2008). In many photobacterial strains (like TH1, S1 and ATCC 27561) an additional gene '*luxF*' was found in the operon inserted between *luxB* and *luxE* resulting in the new order, *luxCDABFEG* (Lee *et al.*, 1991; Dunlap, 2009; Bergner *et al.*, 2015). Interestingly, large quantities of LuxF were found in these bacteria. LuxF exists as a homodimer and shows an α/β barrel fold, similar to the β -subunit of the bacterial luciferase,

and therefore has presumably arisen by gene duplication of *luxB* (Moore and James, 1994). The exact role of LuxF is not yet known, however, it was hypothesized that the main function of LuxF is the binding of myristylated FMN (myrFMN), which is presumably a side product of the luciferase reaction. MyrFMN is thought to bind sufficiently tight in the active site of luciferase to inhibit the bioluminescent reaction (Moore and James, 1995). In fact, Wei and coworkers could demonstrate the inhibiting effect of myrFMN on the luciferase from *Vibrio harveyi* (Wei *et al.*, 2001).

The generation of myrFMN in the marine bacterial strains is a largely unexplored phenomenon. In our previous report, we have reported a method to isolate myrFMN from *Photobacterium leiognathi* S1 (Bergner *et al.*, 2015). Using isolated and purified myrFMN, we showed that it binds to recombinant apo-LuxF ($K_d = 80$ nM) fifty times more tightly than to luciferase from *P. leiognathi* ($K_d = 4$ μ M) by using isothermal titration calorimetry. This tight binding to LuxF is clearly due to the large hydrophobic surface area of the myristyl group, which is deeply buried in each binding site. As a consequence, it is extremely difficult to remove the bound flavin derivative from LuxF and therefore harsh denaturing conditions are required to extract myrFMN from LuxF, as described previously (Bergner *et al.*, 2015). Therefore, this tight binding of myrFMN to recombinant apo-LuxF was exploited to explore its occurrence in various bioluminescent bacterial strains (*luxF*⁺ and *luxF*) of *Photobacteria*. This analysis showed that myrFMN is present in all photobacterial strains tested, suggesting that its production is independent of the occurrence of *luxF*.

To better understand the occurrence and generation of myrFMN, we were interested in the relationship of bioluminescence intensity and the production of myrFMN in different bioluminescent bacterial genera, *i.e.* *Aliivibrio*, *Vibrio* and *Photobacteria*. These experiments suggested that total light production in bacteria correlates to myrFMN production and thus indicated that myrFMN is directly generated in the luciferase reaction. This insight prompted us to establish an enzyme driven cofactor regeneration system that sustains *in vitro* light emission for up to three days. We then utilized the apo-LuxF scavenging method to enrich and isolate any myrFMN produced in the experiment. This approach enabled us finally to unambiguously demonstrate that myrFMN is formed in the luciferase reaction.

3.3. Experimental procedures

3.3.1. Chemicals

Tetradecanal, IPTG, FMN, NADPH, glucose and all buffer components were from Chemos GmbH, Sigma-Aldrich, Peqlab and Roth. All these chemicals were used directly without further purifications. GDH (glucose dehydrogenase) was a gift from Dr. Wolfgang Kroutil, University of Graz.

3.3.2. Instrumentation

UV-Vis absorption spectra were recorded using a Specord 205/210 spectrophotometer (Analytic Jena, Jena, Germany). Both, *in vivo* (bacterial bioluminescence) and *in vitro* light emission (single and multiple turnover reactions), were measured using a Centro LB960 microplate luminometer (Berthold Technologies, Bad Wildbach, Germany). All protein purifications were primarily performed using a 5 mL HisTrap FF affinity column (GE Healthcare, UK) and later applied to a HiLoad 16/600 Superdex 200 prep grade gel filtration column on an ÄKTAexplorer 100 Pharmacia Biotech (GE Healthcare life sciences, UK).

HPLC analysis was performed with a semi-preparative Dionex UltiMate 3000 equipped with a Dionex UltiMate diode array detector. Separation over an Atlantis dC18 (4.6 x 250 mm, 5 μ m) column (Waters) was achieved using a gradient of 0.1 % TFA in water and acetonitrile at 25 °C and 1 mL min⁻¹ flow rate starting from 0% acetonitrile to 95% within 20 min, holding 95% for 5 min and going down to 0% within 5 min and holding 0% for another 10 min. For determination of the peaks the wavelengths at 280, 370 and 450 nm were used, respectively. For evaluation of the results, up to four references were measured having the following retention times and wavelength maxima: FAD: t_R = 9.1 min; maxima: 372/447 nm; FMN: t_R = 9.8 min; maxima: 371/446 nm; riboflavin: t_R = 10.4 min; maxima: 370/445 nm; myrFMN: t_R = 18.7 min; maxima: 386/442 nm. Fractions were collected from 18.0 to 24.0 min and fraction tubes were changed every 15 seconds. Those fractions containing myrFMN, according to the analysis at 370 nm, were combined and dried under reduced pressure. This sample was dissolved in methanol for HPLC-MS analysis.

HPLC-MS analysis was performed on an Agilent Technologies 1200 Series system equipped with a MWD SL multiple wavelength detector (deuterium lamp, 190-400 nm) and with a single quadrupole LCMS detector using electrospray ionization source (ESI). The samples were separated over an Agilent Poroshell 120 SB-C18 (3 x 100 mm, 2.7 μ m) column using the same gradient as mentioned above but with 0.01% FA in water and acetonitrile at 25 °C and 0.5 mL min⁻¹ flow rate. Determination of the peaks was achieved by analyzing the chromatograms at 210, 280, 370 and 450 nm, respectively and by using the mass spectrometer.

A negative ESI-Scan mode from m/z 100 to 800 was used to evaluate all the peaks and corresponding masses. The application 'XIC' (extracted ion chromatogram) of the HPLC-MS

software ChemStation was utilized for linking the peaks with the m/z values 601 (dephosphorylated 6'-(3'-(*R*)-myristyl FMN; $C_{31}H_{45}N_4O_8^-$; exact mass 601.31) and 681 (phosphorylated 6'-(3'-(*R*)-myristyl FMN; $C_{31}H_{46}N_4O_{11}P^-$; exact mass 681.29)). By using this function one defined m/z value (in this case 601 or 681) is searched within the negative ESI-scan mode from m/z 100 to 800 and drawn as separate chromatogram by the program.

3.3.3. Bioluminescent bacterial strains

The following bacterial strains were selected for our study: TH1, S1, ATCC 27561, ATCC 25521 and ATCC 25587 from genus *Photobacterium leiognathi*; ATCC 14126 from genus *Vibrio harveyi* and ATCC 7744 from genus *Aliivibrio fischeri*. Only TH1, S1 and ATCC 27561 contained *luxF* as reported previously (Bergner *et al.*, 2015). The bacteria were cultivated in 1 L flasks with 200 mL of 246-SWC media (246-sea water culture). The cells were grown at 25 °C with 130 rpm shaking for optimal aeration.

3.3.4. Cloning, gene expression and production of proteins

Production and purification of LuxAB and LuxF from *P. leiognathi* ATCC 27561 and of YcnD from *B. subtilis* was performed as described previously (Morokutti *et al.*, 2005; Bergner *et al.*, 2015). The protein concentrations were calculated using the molar extinction coefficients $82335 \text{ M}^{-1} \text{ cm}^{-1}$ (*P. leiognathi* LuxAB) and $26025 \text{ M}^{-1} \text{ cm}^{-1}$ (LuxF) at 280 nm and $12190 \text{ M}^{-1} \text{ cm}^{-1}$ (YcnD) at 450 nm, respectively.

Based on the DNA sequence available, a synthetic gene for LuxAB (from *V. harveyi* ATCC 14126 and *A. fischeri* ATCC 7744) was designed with a C-terminal octa-histidine tag and optimised for *E. coli* codon usage. The gene was then sub-cloned into a pET24b vector (Kan^R) and transformed into *E. coli* Rosetta strain (Cmp^R) for heterologous expression. The cells containing the construct were grown in LB media with kanamycin ($50 \mu\text{g mL}^{-1}$) and chloramphenicol ($20 \mu\text{g mL}^{-1}$) at 37 °C to an OD_{600} of ~ 0.6 . The protein production was then induced by addition of 0.1 mM IPTG and the cells were further grown for 16 h at 20 °C. The cells were then harvested by centrifugation (7000 g, 10 min, at 4 °C) and the wet cell pellets were stored at -20 °C until further use. The proteins were purified similar to the photobacterial luciferase as reported previously (Bergner *et al.*, 2015). The protein concentrations were calculated using the molar extinction coefficients $84230 \text{ M}^{-1} \text{ cm}^{-1}$ (*V. harveyi* LuxAB) and $83200 \text{ M}^{-1} \text{ cm}^{-1}$ (*A. fischeri* LuxAB) at 280 nm.

3.3.5. Analysis of bacterial strains for light emission vs myrFMN content

Assays were performed using the 96 well white assay plates. Light emission was measured using the luminometer. The OD of the cells was obtained by absorption measurements using an UV-Vis spectrophotometer at 660 nm (instead of 600 nm) to exclude the interference of artefacts due to bioluminescence.

To measure the light emission, 100 μ l of cells were pipetted into each well of the assay plate and after an initial delay of 1 s and rapid mixing of the plate for 0.1 s, the reading was taken for 1 s total time. The readings were taken for 24 h with time intervals 30/60 min. The light intensity (counts) at each time point was plotted. For comparison, the following bioluminescent bacterial strains were taken into consideration: *P. leiognathi* TH1, S1, ATCC 27561, ATCC 25587 and ATCC 25521; *V. harveyi* ATCC 14126; *A. fischeri* ATCC 7744.

For the quantification of myrFMN content, 10 g of wet cell pellet was taken for each strain mentioned above. The extraction of myrFMN *in vivo*, using recombinant apo-LuxF was performed precisely as described previously (Bergner *et al.*, 2015). The isolated product was analyzed with HPLC.

3.3.6. Inhibition assay

In this assay, the light emitted by the enzyme luciferase was measured using the luminometer. The reaction was performed similar to the *in vitro* assay described previously (Brodl *et al.*, 2017). The assay was performed in 96 well black assay plates using 100 mM potassium phosphate buffer with 300 mM NaCl, pH 7 as reaction buffer.

Briefly, the reaction mixture contained 200 nM luciferase, 300 nM YcnD, 300 nM FMN, 500 nM NADPH and the substrate-buffer suspension in the reaction buffer to make up the final volume to 250 μ L [due to the low solubility of aldehyde in the buffer, concentrated aldehyde suspensions were obtained by mixing 5 μ L of aldehyde with 10 mL of buffer using ultra-sonication]. Apo-LuxF was used in excess concentrations (up to 100 μ M) as a scavenger for myrFMN. The reactions were started by injecting NADPH to the master mix (after a delay of 5 s) and the readings were subsequently taken every second for 90 s total time.

Pure myrFMN sample in a concentration gradient from 0 to 50 μ M was used as the inhibitor in this assay (extracted and purified as reported previously in Bergner *et al.*, 2015). The concentration of myrFMN was calculated using the extinction coefficient of 11350 M⁻¹ cm⁻¹ at 396 nm. Three different sub-assay conditions were used to observe the inhibitory effect on the luciferase activity: First, in the absence of LuxF; second, in the presence of LuxF from the beginning of the reaction; and lastly when LuxF is added at a later stage of the reaction (after 90 s). All three conditions were tested for increasing myrFMN concentrations. Light emission was plotted against myrFMN concentration. The control reactions without myrFMN in each condition were considered as 100 %.

3.3.7. *In vitro* multiple turnover reaction

All enzymes and cofactors were diluted and prepared in 100 mM potassium phosphate buffer pH 7. For multiple turnover reactions the following components and concentrations were used: 100 μ M LuxAB, 150 μ M FMN, 150 μ M YcnD, 2 mM NADPH, 200 mg GDH (lyophilized powder), 1 M glucose and 100 μ l substrate-buffer solution. Due to low solubility of aldehydes in water, a substrate-buffer solution was obtained by adding 40 μ L of tetradecanal to a mixture of 1900 μ L reaction buffer and 100 μ L Triton X. This led to complete solubility of the substrate. All components were mixed to a final volume of 25 mL in a 50 mL enzyme reactor. The reaction was started by the addition of LuxAB and stirred at 4 °C for a maximum of 72 h. After 6 h, 200 μ M BSA was added to stabilize the enzymes.

For the workup, three main steps were performed analogous to the extraction of myrFMN *in vivo* (Bergner *et al.*, 2015). The reactions were stopped by adding 2.5 g guanidine-HCl and dropwise concentrated HCl to lower the pH to \sim 2. Three consecutive extractions were made with 15 mL each of an organic mixture of ethyl acetate:butanol (1:1). The organic phase was separated by centrifugation (4566 *g* at 4 °C for 30 min) and the collected, unified organic layers were dried in a vacuum evaporator at 56 °C under reduced pressure. The residual powder was dissolved in 20 mL lysis buffer (50 mM NaH₂PO₄, 300 mM NaCl, 10 mM imidazole, pH 8) and incubated with excess of recombinant histidine-tagged apo-LuxF for 30 minutes in the dark. The apo-LuxF with bound myrFMN was loaded on a 1 mL HisTrap FF/HP column (GE Healthcare) for purification. The column was washed with wash buffer (50 mM NaH₂PO₄, 300 mM NaCl, 20 mM imidazole, pH 8) and the fractions were eluted with elution buffer (50 mM NaH₂PO₄, 300 mM NaCl, 300 mM imidazole, pH 8). The eluent fractions were pooled and concentrated to 500 μ L. As a final purification step organic extraction was repeated again in small scale as described above. The dried samples were analyzed by HPLC.

3.4. Results

3.4.1. Analysis of bacterial strains for light emission and myrFMN content

In a previous study, we have shown that 6-(3'-(*R*)-myristyl)-FMN (myrFMN) is generated by various bacteria in the genera *Photobacterium* and does not correlate with the presence of *luxF*, a gene encoding a protein that specifically binds myrFMN (Bergner *et al.*, 2015). However, it remained unclear how myrFMN is generated and whether it affects the capability of bacteria to produce light. To address these issues, we have monitored the total light emission of various bioluminescent species and finally isolated myrFMN from the same bacterial cultures exploiting the high affinity of recombinant apo-LuxF as previously demonstrated (Bergner *et al.*, 2015). The extraction protocol as described in experimental procedures was designed to ensure that protein-bound myrFMN is released and thus becomes available for re-binding to the added recombinant apo-LuxF. The scavenged myrFMN was then co-purified with the histidine-tagged LuxF by means of affinity chromatography and eventually released from the purified protein for quantification via HPLC. The results of the total light emission and myrFMN determination in seven different bioluminescent marine bacteria are summarized in Figure 1. The highest total light emission and myrFMN content were found in *P. leiognathi* TH1 (this was set to 100 % for further comparison) followed by strains S1 and 27561, respectively. However, only trace amounts of myrFMN were detected in strains 25521 and 25587. It was also tested if myrFMN production is confined to the genus *Photobacteria* or also occurs in other genera, *i.e.* *Aliivibrio* and *Vibrio*. As is evident from Figure 1, the presence of myrFMN was demonstrated for *A. fischeri* and *V. harveyi* albeit in very small amounts in the case of the former species. These strains also produce less than 2 % of light compared to the best light-emitting strain TH1. Thus our results clearly indicate that generation of myrFMN occurs ubiquitously in bioluminescent bacteria and is not confined to *Photobacteria*. The presence of myrFMN extracted from the strains TH1 and S1 were further confirmed by HPLC-MS (Supporting Information). The amounts of myrFMN isolated from the other strains were below the detection limit for MS and therefore were not analysed in further detail. Furthermore, our findings suggest that myrFMN production and total light emission appear to be linked, suggesting that myrFMN is generated in the chemical processes leading to light emission, *i.e.* the oxidation of tetradecanal by bacterial luciferase. Interestingly, the best light emitters, *i.e.* *P. leiognathi* strains TH1, S1 and 27561 possess the *luxF* gene and thus produce LuxF, which may protect bacterial luciferase by scavenging myrFMN. In fact, we could recently demonstrate binding of myrFMN to photobacterial luciferase (Bergner *et al.*, 2015), however, it remained to be shown whether binding of myrFMN affects the activity of the enzyme.

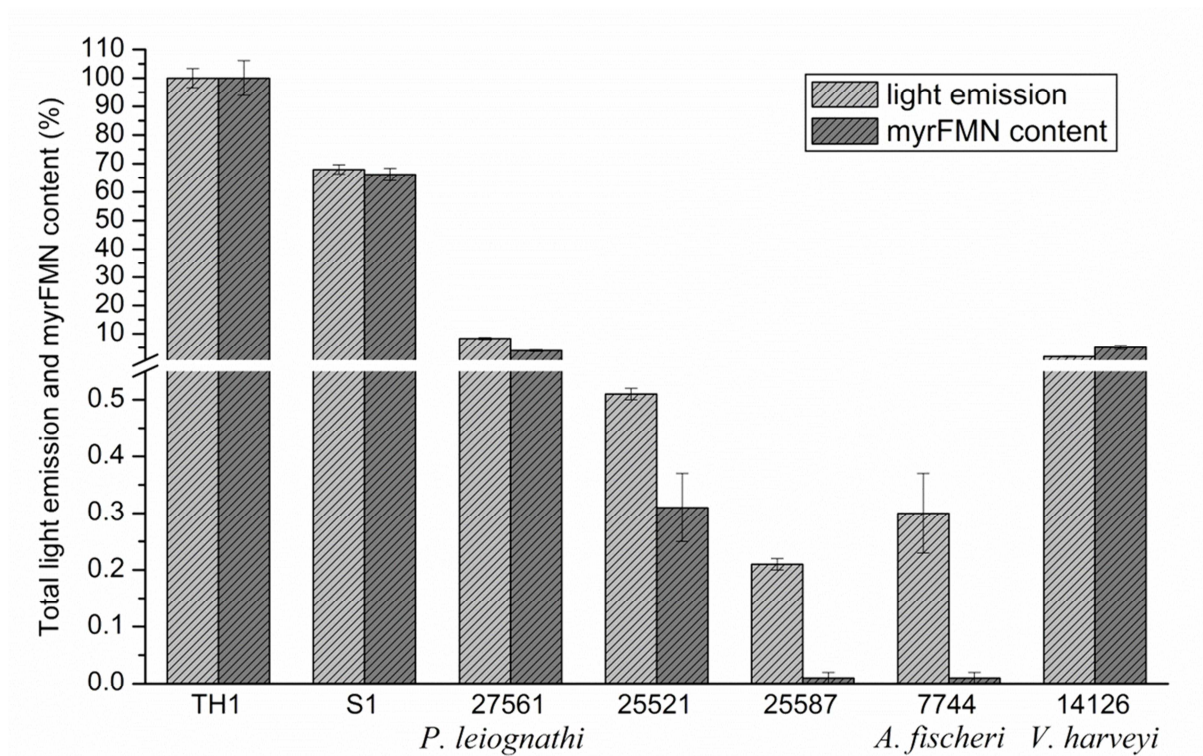


Figure 1: Correlation between light emission and myrFMN content: different bacterial strains compared for their light emission and myrFMN content. *Photobacterium leiognathi* TH1 exhibited maximum bioluminescence as well as produced maximum myrFMN (was set to 100 % for further comparison). It was subsequently followed by the S1 strain which we used as a reference strain. Nevertheless, trace amounts were also detected in all other tested photobacterial strains (ATCC 27561, ATCC 25521 and ATCC 25587). Furthermore, the last columns evidently show detectable amounts of light emission and myrFMN content in *V. harveyi* ATCC 14126 and *A. fischeri* ATCC 7744. [Number of experimental replicates, n=2.]

3.4.2. Inhibition of luciferase by myrFMN

Therefore, we set up an inhibition assay to evaluate the effect of myrFMN on the luciferase-catalyzed reaction. Briefly, purified myrFMN from *P. leiognathi* S1 was used in increasing concentrations (0–50 μM) in an assay with luciferase (200 nM) and other required components as mentioned in experimental procedures. The light emission over a period of 90 s was recorded. In Figure 2A, it was shown that as the concentration of myrFMN increased, the intensity of light emitted decreased (reaction 1 - black filled squares). A decrease in light emission indicates inhibition of luciferase activity as the active site is obstructed by myrFMN and prevents binding of FMNH_2 . However, addition of recombinant apo-LuxF to the same reaction (after a primary cycle of 90 s) scavenged myrFMN and thus allowed binding of FMNH_2 to be used in the bioluminescent reaction (reaction 1 + LuxF - red filled circles). In an additional reaction that more closely mimicked the situation *in vivo*, LuxF was added prior to initiating the reaction (reaction 2 - blue filled triangles). Increased light emission is observed at each concentration compared to the other two experiments suggesting that LuxF scavenged myrFMN before it bound to the luciferase in agreement with the 10-fold higher affinity to LuxF. This is also reflected by the IC_{50} for the inhibition as shown in Figure 2B. The concentration of myrFMN required to reduce the light emission to 50 % is approximately 2 μM , very close to the reported dissociation constant of myrFMN of 4 μM (Bergner *et al.*, 2015). However, to inhibit 50 % of the luciferase activity in the presence of LuxF, a six-fold higher concentration ($\sim 11 \mu\text{M}$) of myrFMN is required, thus demonstrating the protective effect of LuxF on the bioluminescent reaction.

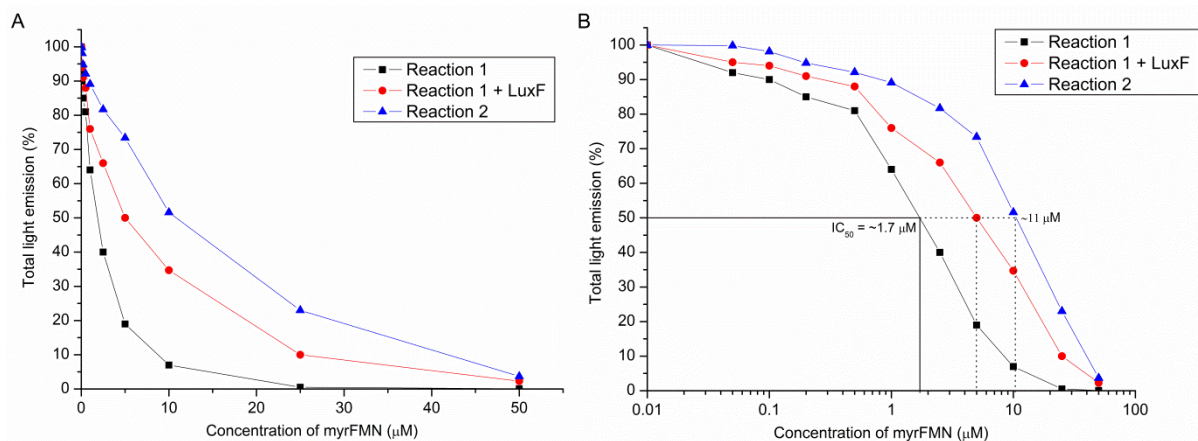
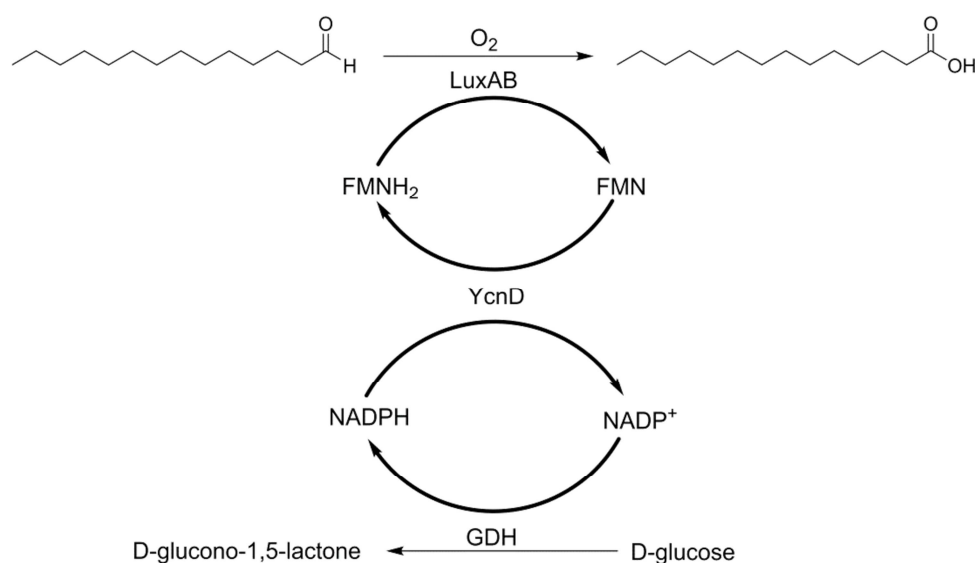


Figure 2: The Inhibition assays. **A:** Demonstrates inhibition of luciferase activity with increasing concentration of myrFMN. It is seen that as myrFMN concentration increases, the light emission decreases (reaction 1 - filled square). However, addition of LuxF to the same reaction (after primary cycle of 90 s) scavenges myrFMN allowing FMNH_2 to follow the normal reaction and produce light (reaction 1 + LuxF - filled round). A third condition, mimicking the *in vivo* situation, shows the inhibition effect of myrFMN in the presence of LuxF from the beginning of the reaction (reaction 2 - filled triangle). The peak maximum was plotted at each time point measured. **B:** Clearly shows the concentration of myrFMN at which luciferase still emits 50 % of light (IC_{50}), which is approximately 1.7 μM . However, to inhibit 50 % of the luciferase activity in the presence of LuxF, 6 fold higher concentration of myrFMN is required ($\sim 11 \mu\text{M}$), thus demonstrating the scavenging behavior of LuxF.

3.4.3. *In vitro* multiple turnover reaction

These findings point toward a direct link between light emission and myrFMN generation and thus we endeavored to provide direct proof that myrFMN is produced during the luciferase-catalyzed monooxygenation of long chain fatty aldehydes. Toward this goal, we developed an *in vitro* multiple turnover assay using the luciferase from *P. leiognathi*. This was achieved by coupling the bioluminescent reaction to YcnD, an oxidoreductase from *Bacillus subtilis* (Morokutti *et al.*, 2005) and glucose dehydrogenase (GDH). YcnD reduces FMN at the expense of NADPH and thus provides FMNH₂, which is stoichiometrically consumed in the luciferase-catalyzed reaction. On the other hand, GDH regenerates NADPH/H⁺ from NADP⁺ by oxidizing D-glucose, which is added at a concentration to ensure prolonged luciferase activity (Scheme 2). Detailed reaction conditions and reagent concentrations are described in experimental procedures. To rule out the possibility of artifacts, we performed the same experiment with several internal controls (*viz.* reaction with acid instead of aldehyde and without luciferase or oxygen) and none of the controls showed any myrFMN on the HPLC, therefore confirming that myrFMN is a product of the luciferase reaction and not a contaminant.



Scheme 2: Schematic representation of the multiple turnover *in vitro* assay. The luciferase employs molecular oxygen (O₂) and reduced FMN (FMNH₂) to oxidize, in this case, tetradecanal to tetradecanoic acid. For the reduced FMN a recycling system was established using the NADPH-dependent oxidoreductase YcnD from *Bacillus subtilis*. To recycle NADPH, glucose dehydrogenase (GDH) was applied.

The reactions were started by the addition of luciferase resulting in intense light emission, clearly visible in the darkroom. The light intensity decreased over time and the reactions were stopped when light emission ceased (typically after ca. 72 h). After quenching the reaction, recombinant apo-LuxF was employed as before to isolate any myrFMN produced during multiple luciferase turnovers. Recombinant histidine-tagged LuxF incubated with the

reaction mixture was then extracted by affinity chromatography and bound ligands were released by acid treatment and analyzed by a semi-preparative HPLC. As shown in Figure 3, the main compound released from LuxF has a retention time identical to an authentic myrFMN sample isolated from *P. leiognathi* S1 ($t_R = 18.8$ min). Moreover, the UV-Vis absorption spectrum is identical to the reference with absorption maxima at 386 and 441 nm (Figure 3, insert). MyrFMN samples were combined and dried under reduced pressure. The yield of myrFMN was approximately 0.18 nmol, thus only 0.005% of the FMN employed in our experiments was converted to myrFMN. The isolated and purified myrFMN was then subjected to HPLC-MS analysis using an Agilent Poroshell 120 SB-C18 column. Due to the usage of that column, the retention time of the myrFMN peak shifted to 14.2 minutes (Figure 4A). Phosphorylated and dephosphorylated myrFMN have exact molecular masses of 681.29 and 601.31, respectively, and therefore a negative ESI scan mode from 100 to 800 m/z was used. The extracted ion chromatogram (XIC) at m/z 681 showed a distinct peak at the same retention time as the chromatogram at 370 nm, verifying the result (Figure 4B). The mass spectrum confirms the formation of myrFMN (Figure 4B, insert) showing a distinct peak at m/z 681.3. Thus, the retention time observed in the HPLC system, the UV-Vis absorption properties and the determined mass of the isolated compound clearly show that myrFMN is generated in a luciferase multiple turnover reaction system.

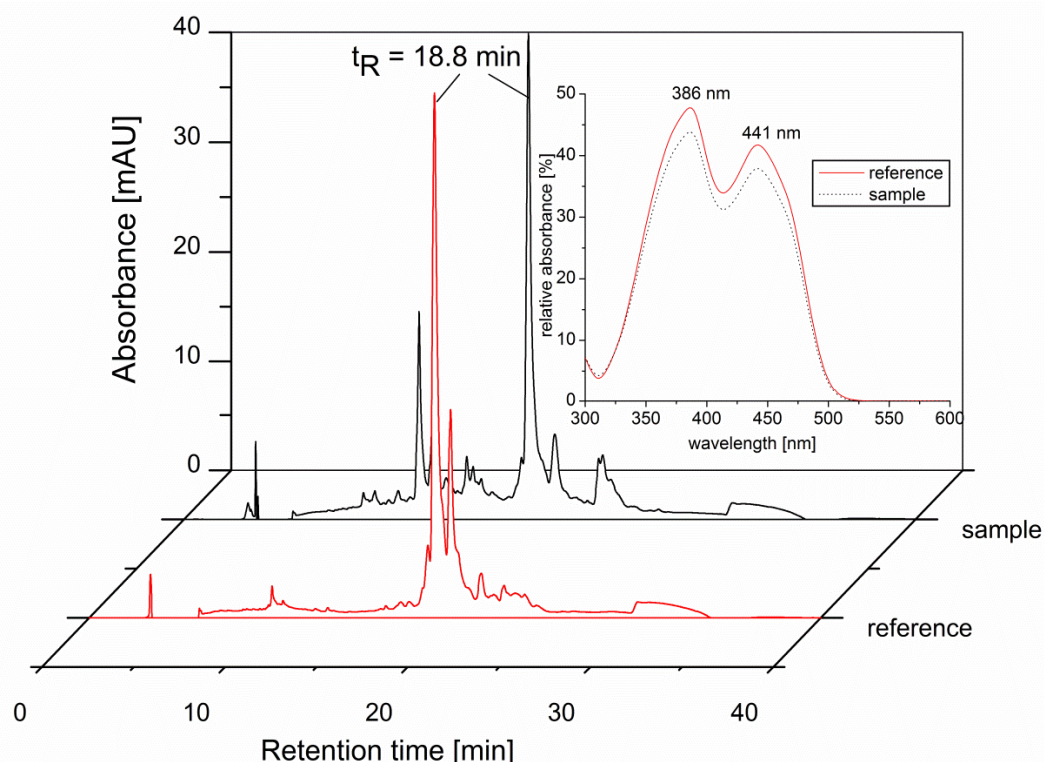


Figure 3: HPLC chromatograms of the myrFMN reference and the sample of the *in vitro* assay with the corresponding absorption spectra. After workup the sample of the *in vitro* assay (black line) was measured by HPLC with UV-Vis detection and compared to the reference sample of myrFMN (red line). The retention time for both samples is 18.8 minutes. The insert shows the overlay of the absorption spectra of the reference (red line) and the sample (black line) with the maxima of 386 nm and 441 nm.

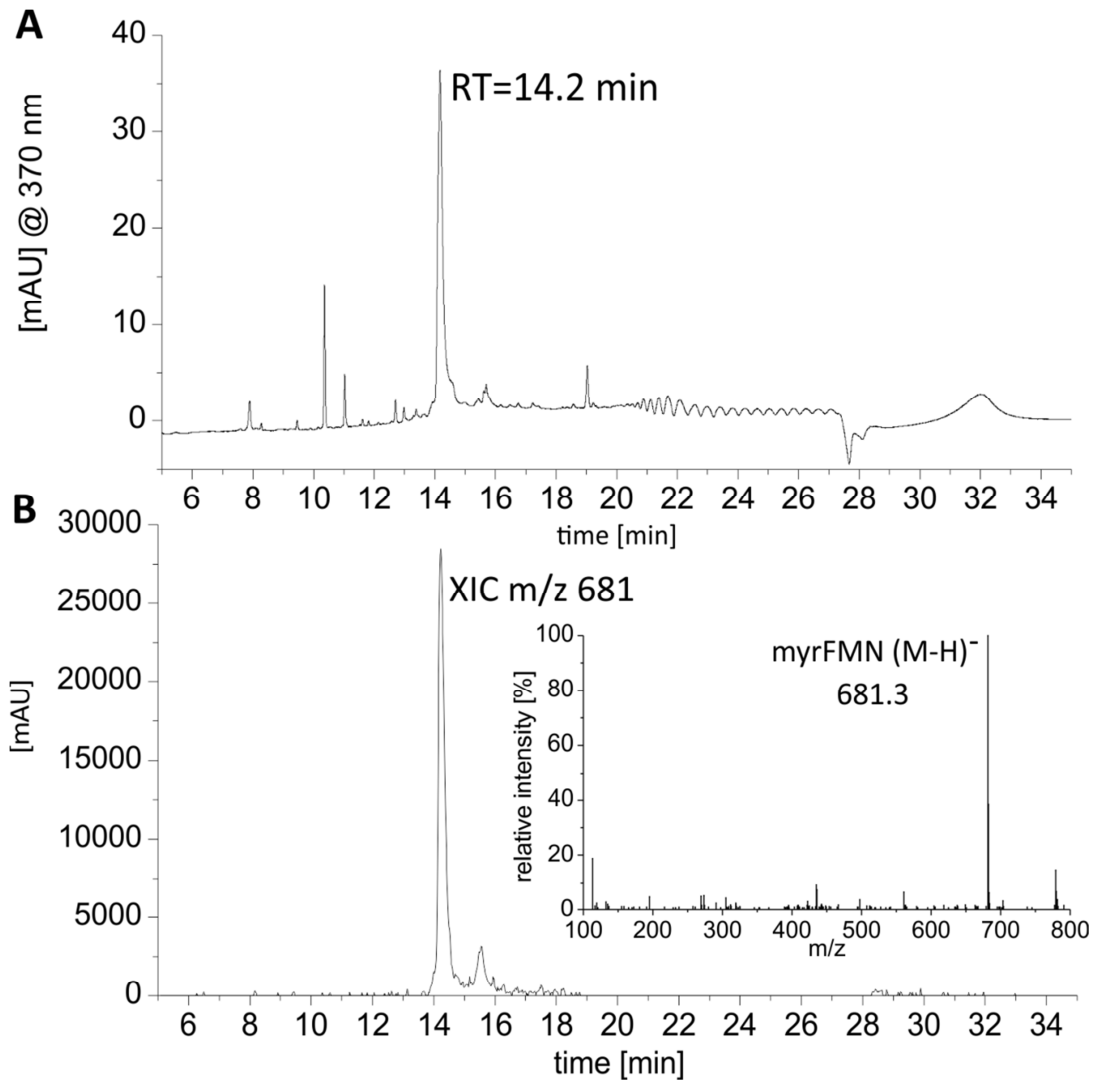


Figure 4: HPLC-MS measurement of the isolated myrFMN sample of the *in vitro* assay. A: HPLC chromatogram at 370 nm with a retention time of 14.2 min for the isolated and purified myrFMN sample. **B:** Extracted Ion Chromatogram (XIC) of m/z 681 in negative ESI mode. **B, insert:** MS-Spectrum at the retention time of 14.2 minutes corresponds to myrFMN with m/z 681 [M-H]⁻.

3.5. Discussion

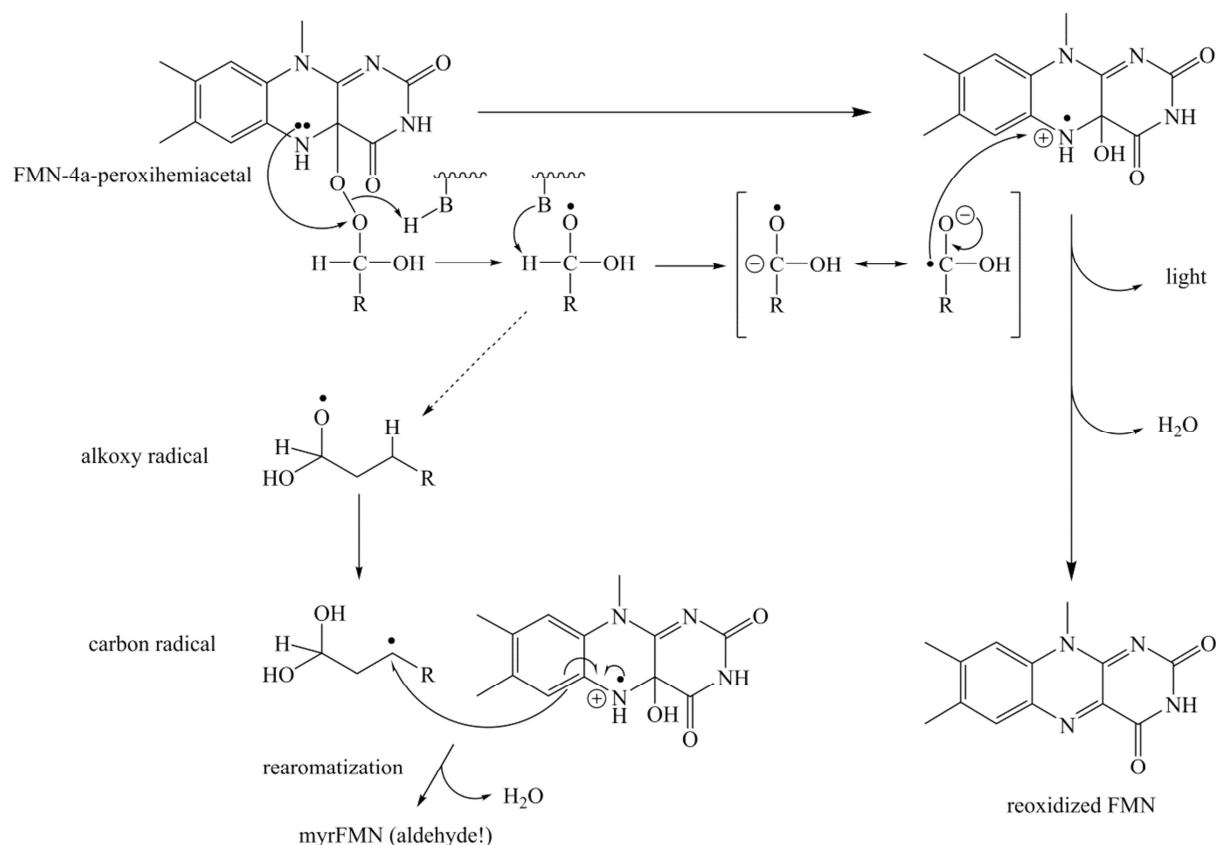
In our previous studies, we focused on the binding of myrFMN to LuxF and luciferase from *P. leiognathi* S1 (Bergner *et al.*, 2015). We have shown that myrFMN binds to LuxF and luciferase with a K_d of 80 nM and 4 μ M, respectively. Using this strong affinity toward LuxF, we showed that myrFMN is present in all photobacterial strains tested, irrespective of the presence or absence of *luxF*. In an extension of this work, we have demonstrated here that myrFMN is also produced in *Vibrio* and *Aliivibrio*. Furthermore, a quantitative analysis of light emission and myrFMN production showed a positive correlation suggesting that myrFMN is indeed generated as a consequence of luciferase activity (Figure 1). Interestingly, the best emitting strains, *i.e.* TH1, S1 and ATCC 27561, were those featuring *luxF* prompting the question whether LuxF is prerequisite to high and sustained luciferase activity *in vivo*. To address this question, we have conducted a series of *in vitro* luciferase assays to probe the potential of LuxF to relieve the inhibitory effect of myrFMN on luciferase activity. As shown in Figure 2, the presence of LuxF, tested in different experimental set-ups, unequivocally rescues luciferase activity in the presence of myrFMN and shifts the inhibition constant of myrFMN, as expressed by the IC_{50} , to higher concentrations. The IC_{50} of ~ 2 μ M, as deduced in Figure 2, is similar to the K_d of myrFMN to luciferase reported earlier, *i.e.* $K_d = 4$ μ M (Bergner *et al.*, 2015), which in turn is similar to the binding constant of FMNH₂ to luciferase, *i.e.* $K_d = 0.8$ μ M (Meighen and Hastings, 1971). Therefore, our results are in accordance with the relative affinities of myrFMN to LuxF and luciferase, respectively (Bergner *et al.*, 2015). The fact that preincubation with LuxF, mimicking the *in vivo* situation, leads to a substantially higher luciferase activity also suggests that dissociation of myrFMN from luciferase is a slow process compared to the binding to LuxF.

The obtained results clearly indicate a direct link between the formation of myrFMN and the luciferase catalyzed reaction. To provide a direct proof for this hypothesis, we designed an *in vitro* multi-enzyme, cofactor recycling system that sustained the luciferase reaction for at least 48-72 hours. This allowed us to isolate sufficient material for chromatographic, spectroscopic and mass spectrometric analysis and clearly provided evidence that myrFMN is produced in the *in vitro* luciferase reaction. This is the first direct experimental proof that myrFMN is formed in the luciferase catalyzed reaction.

3.5.1. Proposed mechanism for myrFMN formation

The demonstration that myrFMN is produced in the luciferase reaction invites the question how myrFMN generation can be rationalized based on the mechanism for the light-emitting process. It was shown that bacterial luciferase forms a stable FMN-4a-hydroperoxide intermediate, which subsequently reacts with the aldehyde substrate to form a FMN-4a-peroxyhemiacetal (Eberhard and Hastings, 1972; Kurfürst *et al.*, 1984; Macheroux *et al.*, 1993). The decomposition of this intermediate is the most critical step because it eventually leads to the population of the excited state of the FMN-4a-hydroxide intermediate (Scheme 3). The currently preferred models to explain the population of an excited-state FMN-4a-hydroxide are based on a radical mechanism, such as the chemically initiated electron exchange luminescence (CIEEL) process (Eckstein *et al.*, 1993; Tu, 2013). In this mechanism the decomposition of the FMN-4a-peroxyhemiacetal is initiated by the transfer of an electron from the N5 position of the flavin to the distal oxygen atom of the peroxyhemiacetal (Scheme 3). This triggers the cleavage of the O-O bond and the generation of an alkoxy radical. At this stage the proton from the C-1 carbon is abstracted and the resulting anionic radical transfers an electron back to the FMN-4a-hydroxy cation radical (Scheme 3, top line). This process is accompanied by the population of the excited state of the FMN-4a-hydroxide, which acts as the light-emitting luciferin.

Based on this radical mechanism we propose that the alkoxy radical rearranges to the carbon radical, as shown in Scheme 3, which then recombines with the FMN-4a-hydroxide radical cation to form a covalent bond between the C-3 carbon of the aldehyde and the C-6 carbon of the isoalloxazine ring. Rearomatization and cleavage of water will then lead to the formation of the flavin adduct. It should be noted that this leads to the formation of the myristylaldehyde linked to the flavin rather than myristic acid. Because aldehydes are prone to oxidation, we assume that this may occur spontaneously after formation of the flavin adduct. It is important to emphasize that this model rationalizes how a rather unreactive saturated carbon atom is activated to form a covalent carbon-carbon bond. Because no other mechanism put forward for the luciferase catalysed reaction has the potential to explain the formation of myrFMN, its very occurrence supports a radical mechanism for the luciferase reaction.



Scheme 3: Proposed mechanism for myrFMN formation: In the scheme above is shown the CIEEL mechanism for the luciferase catalyzed bioluminescence reaction. The reaction is initiated by the transfer of an electron from the N5 position of the flavin to the distal oxygen atom of the peroxide moiety. During the normal course of the reaction, the O-O bond cleavage leads to the formation of a radical anion, which transfers the electron back to the flavin generating an excited state of the flavin-4a-hydroxide. This excited state intermediate further goes on to emit light with a maximum at 490 nm. The mechanism we propose, for the formation of myrFMN suggests that a hydrogen rearrangement of the alkoxy radical leads to a C-3-carbon radical moiety. This then combines with the flavin-4a-hydroxide radical cation to form the covalent bond between the C-3 carbon of the aldehyde and the C-6 carbon of the isoalloxazine ring. After rearomatization and release of water, our stipulated product myrFMN is formed.

Given the very low yield of myrFMN obtained after up to 3 days of turnover *in vitro* we assume that the bioluminescent reaction efficiently outruns the formation of the side product. Nevertheless, our data show that bacterial strains that are capable of producing LuxF produce significantly more light apparently because LuxF scavenges myrFMN and thereby prevents the inhibition of the luciferase. Therefore, the creation of *luxF*, presumably by gene duplication of *luxB*, was an important evolutionary invention that provided an enormous advantage over other bioluminescent bacteria.

Author contributions

CRT and EB expressed and purified all proteins and cofactors. CRT designed the experiments, performed the assays and analyzed the data for the myrFMN vs light correlation in bacterial strains and determined the IC₅₀ for the inhibition assays. CRT and EB designed and performed the *in vitro* multiple turnover assays. EB analyzed the results for *in vitro* assays via HPLC. EB further confirmed the cofactor molecule on HPLC-MS. CRT, EB and PM wrote the manuscript.

Acknowledgements

This work was supported by the Austrian “Fonds zur Förderung der wissenschaftlichen Forschung” (FWF) to PM (P24189) and the PhD program “DK Molecular Enzymology” to PM (W901). We want to thank Dr. Wolfgang Kroutil, Institute of Organic and Bioorganic Chemistry, University of Graz, for providing us with GDH (glucose dehydrogenase). We would also like to thank Dr. Rolf Breinbauer, Institute of Organic Chemistry, Graz University of Technology, for granting access to HPLC-MS equipment. We want to thank Dr. Michael C. Pirrung (University of California at Riverside) and Dr. Silvia Wallner (Graz University of Technology) for the fruitful discussions.

Conflict of interest

The authors declare no conflict of interest.

3.6. References

- Bergner, T., Tabib, C.R., Winkler, A., Stipsits, S., Kaye, H., Lee, J., *et al.* (2015) Structural and biochemical properties of LuxF from *Photobacterium leiognathi*. *Biochim Biophys Acta* **1854**: 1466-1475.
- Boylan, M., Graham, A.F., and Meighen, E.A. (1985) Functional identification of the fatty acid reductase components encoded in the luminescence operon of *Vibrio fischeri*. *J Bacteriol* **163**: 1186-1190.
- Brodl, E., Ivkovic, J., Tabib, C.R., Breinbauer, R. and Macheroux, P. (2017) Synthesis of α,β -unsaturated aldehydes as potential substrates for bacterial luciferases. *Bioorg Med Chem* **25**: 1487-1495.
- Dunlap, P.V. (2009) Bioluminescence, microbial, In: *Encyclopedia of Microbiology*, 3rd edition. Schaechter, M. (ed). Oxford: Elsevier, pp. 45-61.
- Eberhard, A., and Hastings, J.W. (1972) A postulated mechanism for the bioluminescent oxidation of reduced flavin mononucleotide. *Biochem Biophys Res Commun* **47**: 348-353.
- Eckstein, J.W., Hastings, J.W., and Ghisla, S. (1993) Mechanism of bacterial bioluminescence: 4a,5-dihydroflavin analogs as models for luciferase hydroperoxide intermediates and the effect of substituents at the 8-position of flavin on luciferase kinetics. *Biochemistry* **32**: 404-411.
- Hastings, J.W., Weber, K., Friedland, J., Eberhard, A., Mitchell, G.W., and Gunsalus, A. (1969) Structurally distinct bacterial luciferases. *Biochemistry* **8**: 4681-4689.
- Joosten, V., and van Berkel, W.J. (2007) Flavoenzymes. *Curr Opin Chem Biol* **11**: 195-202.
- Kurfürst, M., Ghisla, S., and Hastings, J.W. (1984) Characterization and postulated structure of the primary emitter in the bacterial luciferase reaction. *Proc Natl Acad Sci U S A* **81**: 2990-2994.
- Lee, C.Y., Szittner R.B., and Meighen E.A. (1991) The *lux* genes of the luminous bacterial symbiont, *Photobacterium leiognathi*, of the ponyfish. Nucleotide sequence, difference in gene organization, and high expression in mutant *Escherichia coli*. *Eur J Biochem* **201**: 161-167.
- Macheroux, P., Ghisla, S., and Hastings, J.W. (1993) Spectral detection of an intermediate preceding the excited state in the bacterial luciferase reaction. *Biochemistry* **32**: 14183-14186.

Macheroux, P., Kappes, B., and Ealick, S.E (2011). Flavogenomics - a genomic and structural view of flavin-dependent proteins. *FEBS J* **278**: 2625-2634.

Massey, V. (1994) Activation of molecular oxygen by flavins and flavoproteins. *J Biol Chem* **269**: 22459-22462.

Meighen, E.A. (1991) Molecular biology of bacterial bioluminescence. *Microbiol Rev* **55**: 123-142.

Meighen, E.A., and Hastings, J.W. (1971) Binding site determination from kinetic data. Reduced flavin mononucleotide binding to bacterial luciferase. *J Biol Chem* **246**: 7666-7674.

Moore, S.A., and James, M.N.G. (1994) Common structural features of the luxF protein and the subunits of bacterial luciferase: Evidence for a ($\beta\alpha$)₈ fold in luciferase. *Protein Sci* **3**: 1914-1926.

Moore, S.A., and James, M.N.G. (1995) Structural refinement of the non-fluorescent flavoprotein from *Photobacterium leiognathi* at 1.60 Å resolution. *J Mol Biol* **249**: 195–214.

Morokutti, A., Lyskowski, A., Sollner, S., Pointner, E., Fitzpatrick, T.B., Kratky, C., *et al.* (2005) Structure and function of YcnD from *Bacillus subtilis*, a flavin-containing oxidoreductase. *Biochemistry* **44**: 13724-13733.

Nijvipakul, S., Wongratana J., Suadee C., Entsch B., Ballou D.P., and Chaiyen P. (2008) LuxG is a functioning flavin reductase for bacterial luminescence. *J Bacteriol* **190**: 1531-1538.

Teufel, R., Agarwal, V., and Moore, B.S. (2016) Unusual flavoenzyme catalysis in marine bacteria. *Curr Opin Chem Biol* **31**: 31-39.

Tu, S-C. (2013) Mechanisms of bacterial luciferase and related flavin reductases. In *Handbook of flavoproteins*. Hille, R., Miller, S.M., and Palfey, B. (eds). Berlin: De Gruyter, pp. 101-118.

Ulitzur, S., and Hastings, J.W. (1979) Evidence for tetradecanal as the natural aldehyde in bacterial bioluminescence. *Proc Natl Acad Sci U S A* **76**: 265-267.

Wei, C.J., Lei, B., and Tu, S.C. (2001) Characterization of the binding of *Photobacterium phosphoreum* P-flavin by *Vibrio harveyi* luciferase. *Arch Biochem Biophys* **396**: 199-206.

3.7. Supporting Information

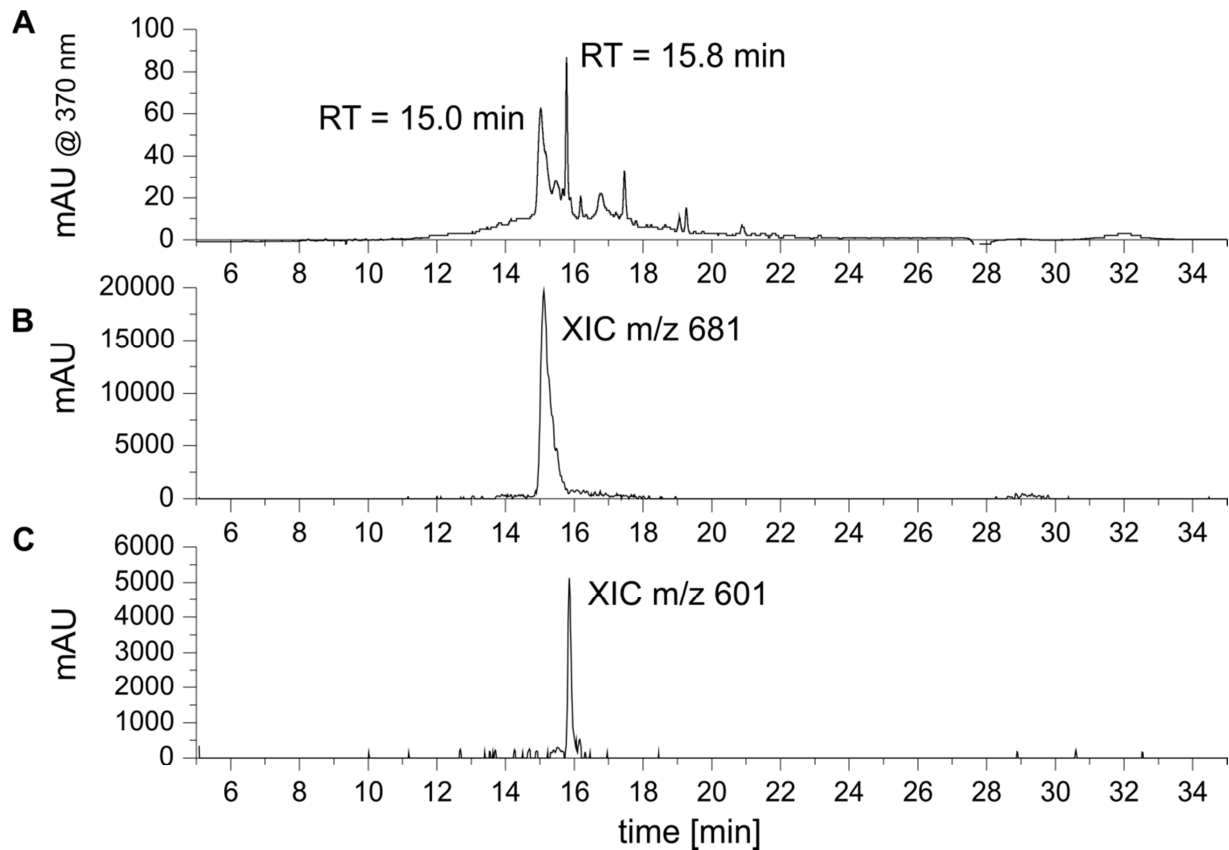


Figure 1_SupplInfo: HPLC-MS measurement of the isolated myrFMN sample of *Photobacterium leiognathi* S1. A: HPLC chromatogram at 370 nm with a retention time of 15.0 and 15.8 minutes for the isolated and purified myrFMN sample. **B:** Extracted Ion Chromatogram (XIC) of m/z 681 in negative ESI mode. **C:** Extracted Ion Chromatogram (XIC) of m/z 601 in negative ESI mode.

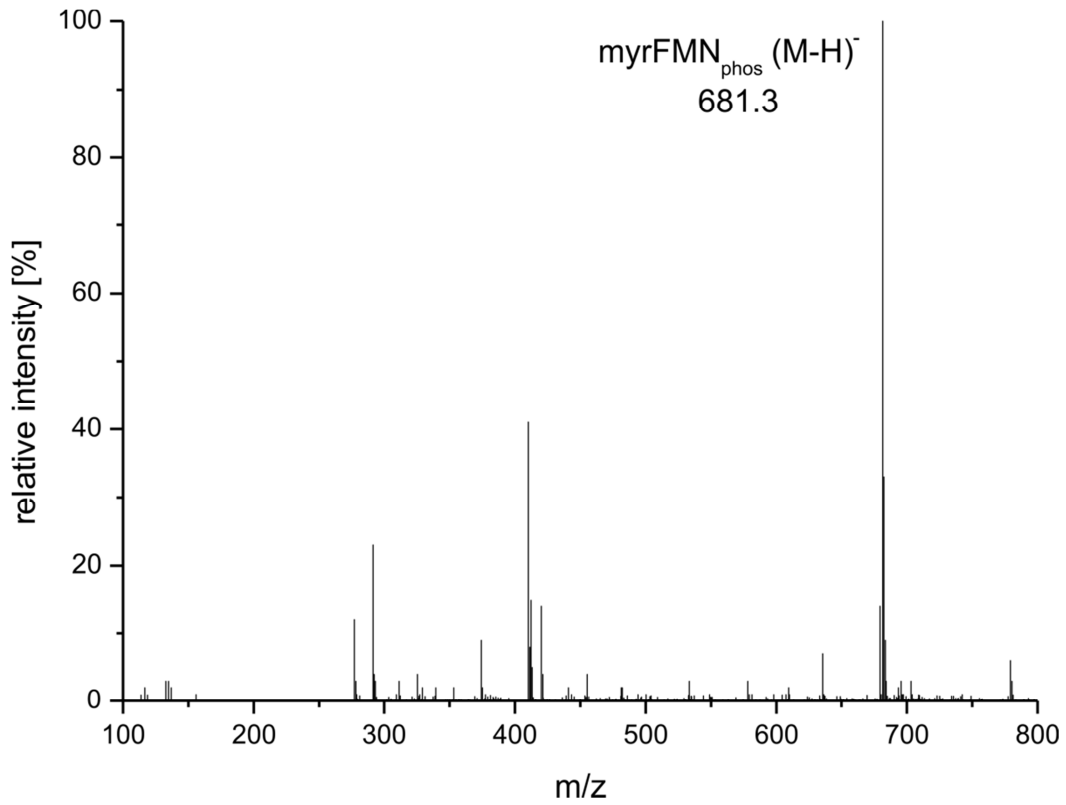


Figure 2_SupplInfo: MS-Spectrum at the retention time of 15.0 minutes corresponds to the phosphorylated myrFMN with m/z 681.3 [M-H]⁻.

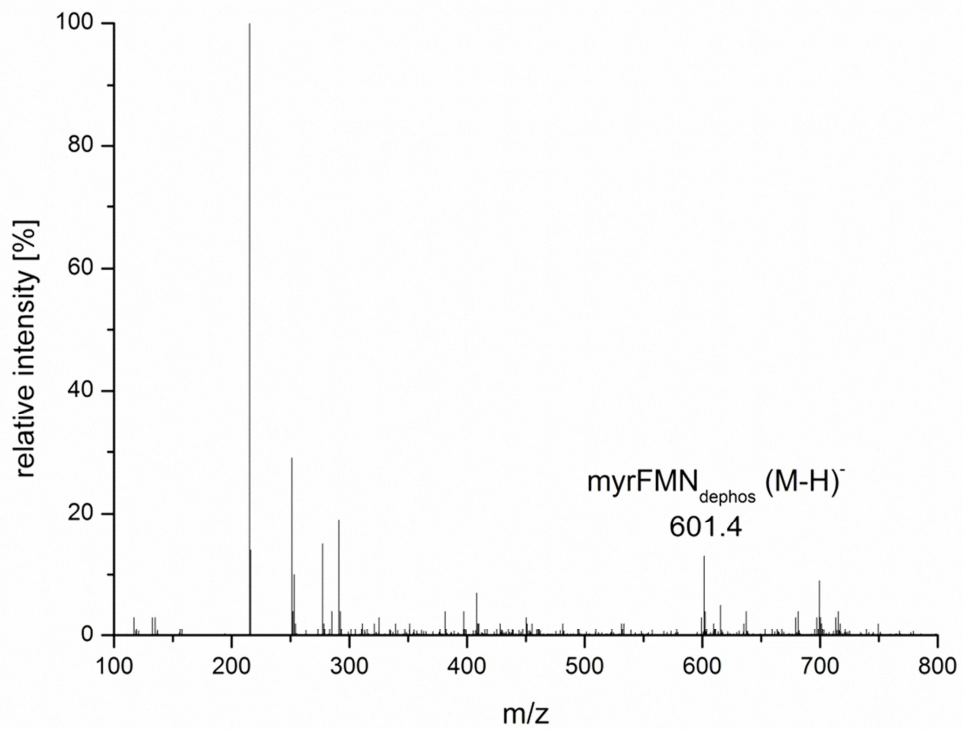


Figure 3_SupplInfo: MS-Spectrum at the retention time of 15.8 minutes corresponds to the dephosphorylated myrFMN with m/z 601.4 [M-H]⁻.

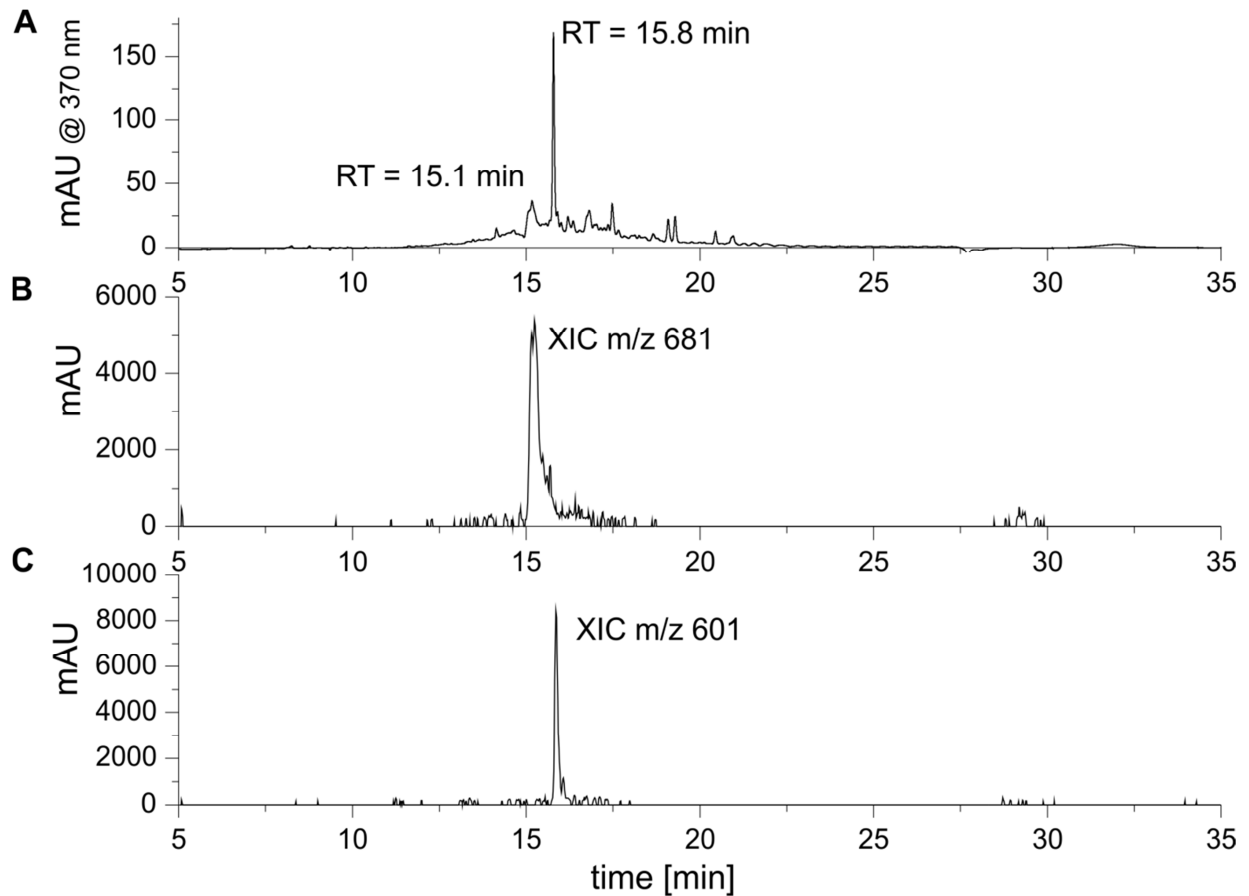


Figure 4_SupplInfo: HPLC-MS measurement of the isolated myrFMN sample of *Photobacterium leiognathi* TH1. **A:** HPLC chromatogram at 370 nm with a retention time of 15.1 and 15.8 minutes for the isolated and purified myrFMN sample. **B:** Extracted Ion Chromatogram (XIC) of m/z 681 in negative ESI mode. **C:** Extracted Ion Chromatogram (XIC) of m/z 601 in negative ESI mode.

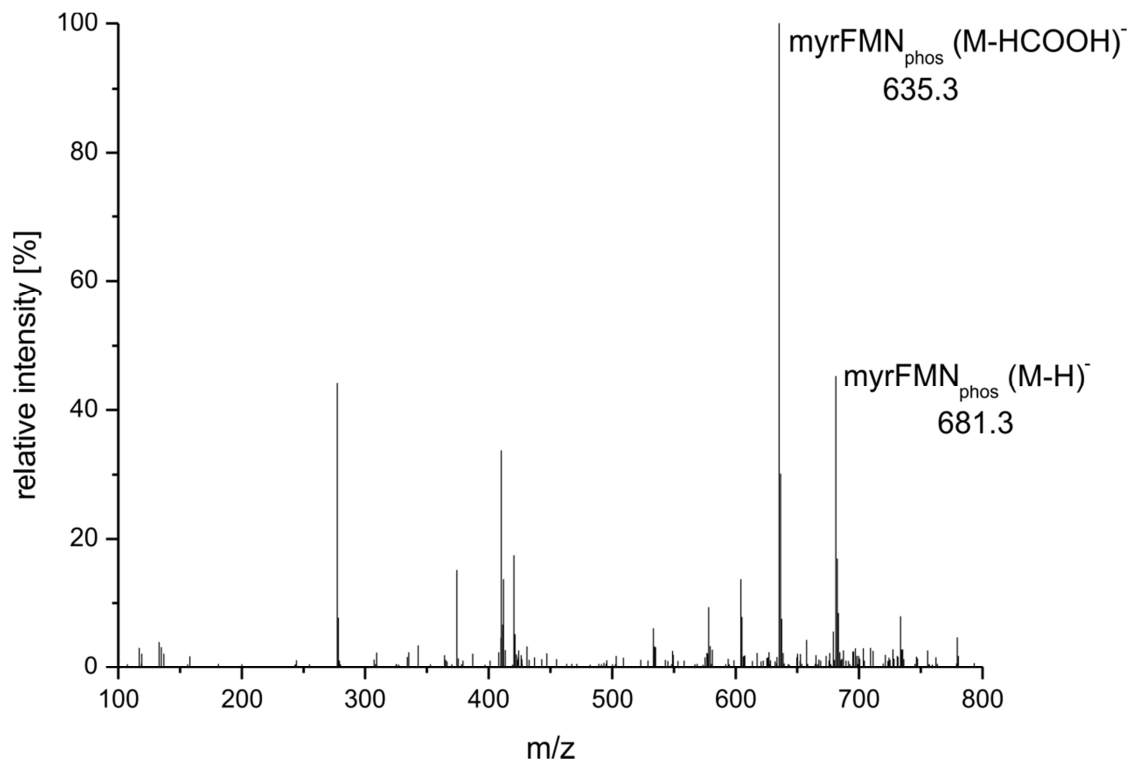


Figure 5_SupplInfo: MS-Spectrum at the retention time of 15.1 minutes corresponds to the phosphorylated myrFMN with m/z 681.3 [M-H]⁻ and to one main fragment with m/z 635.3 [M-HCOOH]⁻.

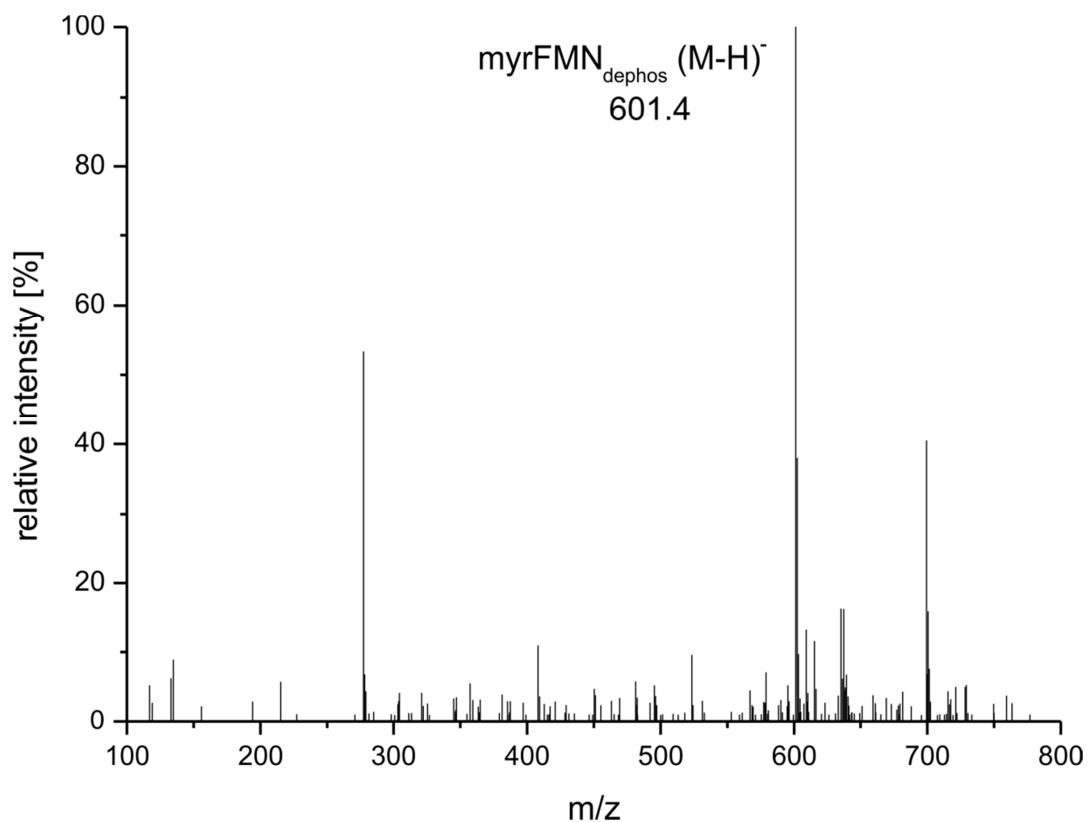


Figure 6_SupplInfo: MS-Spectrum at the retention time of 15.8 minutes corresponds to the dephosphorylated myrFMN with m/z 601.4 [M-H]⁻.

Chapter IV

***In situ* measurement and correlation of cell density and light emission of bioluminescent bacteria**

This paper was published as video article in the Journal of Visualized Experiments, e57881, available online since June 26th, 2018 (<https://www.jove.com/video/57881>; doi:10.3791/57881).

IV. *In Situ* Measurement and Correlation of Cell Density and Light Emission of Bioluminescent Bacteria

Eveline Brodl¹, Johannes Niederhauser¹, Peter Macheroux¹

¹Institute of Biochemistry, Graz University of Technology, Graz, Austria

Corresponding author

Peter Macheroux (peter.macheroux@tugraz.at); Tel: +43 (316) 873 – 6450

Keywords

Bioluminescence, *Escherichia coli*, Gibson cloning, growth curve, luciferase, *lux* operon, marine bacteria, quorum sensing, plate reader assay

SUMMARY

Bioluminescent bacteria regulate light production through a variety of mechanisms, such as quorum sensing. This novel method allows the *in situ* investigation of bioluminescence and the correlation of light emission to cell density. An artificial bioluminescent *Escherichia coli* system allows the characterization of *lux* operons, Lux proteins and their interplay.



Please find the video version of this manuscript published in the Journal of Visualized Experiments, e57881, (<https://www.jove.com/video/57881>), in the above added QR code.

4.1. Abstract

There is a considerable number of bacterial species capable of emitting light. All of them share the same gene cluster, namely the *lux* operon. Despite this similarity, these bacteria show extreme variations in characteristics like growth behavior, intensity of light emission or regulation of bioluminescence. The method presented here is a newly developed assay that combines recording of cell growth and bioluminescent light emission intensity over time utilizing a plate reader. The resulting growth and light emission characteristics can be linked to important features of the respective bacterial strain, such as quorum sensing regulation. The cultivation of a range of bioluminescent bacteria requires a specific medium (e.g., artificial sea water medium) and defined temperatures. The easy to handle, non-bioluminescent standard-research bacterium *Escherichia coli* (*E. coli*), on the other hand, can be cultivated inexpensively in high quantities in laboratory scale. Exploiting *E. coli* by introducing a plasmid containing the whole *lux* operon can simplify experimental conditions and additionally opens up many possibilities for future applications. The expression of all *lux* genes utilizing an *E. coli* expression strain was achieved by construction of an expression plasmid via Gibson cloning and insertion of four fragments containing seven *lux* genes and three *rib* genes of the *lux-rib* operon into a pET28a vector. *E. coli* based *lux* gene expression can be induced and controlled via Isopropyl- β -D-thiogalactopyranosid (IPTG) addition resulting in bioluminescent *E. coli* cells. The advantages of this system are to avoid quorum sensing regulation restrictions and complex medium compositions along with non-standard growth conditions, such as defined temperatures. This system enables analysis of *lux* genes and their interplay, by the exclusion of the respective gene from the *lux* operon, or even addition of novel genes, exchanging the *luxAB* genes from one bacterial strain by another, or analyzing protein complexes, such as *luxCDE*.

4.2. Introduction

The emission of light by living organisms (bioluminescence) is a fascinating process found in bacteria, fungi, insects, nematodes, fish and squids¹. Bioluminescent light emission emerges from a chemiluminescent reaction in which chemical energy is (partially) transformed into light energy ("cold light"). In bioluminescent bacteria, the heterodimeric enzyme luciferase catalyzes the monooxygenation of long chain, aliphatic aldehydes, such as tetradecanal, to the corresponding acids accompanied by light emission with a maximum at 490 nm^{2,3}.

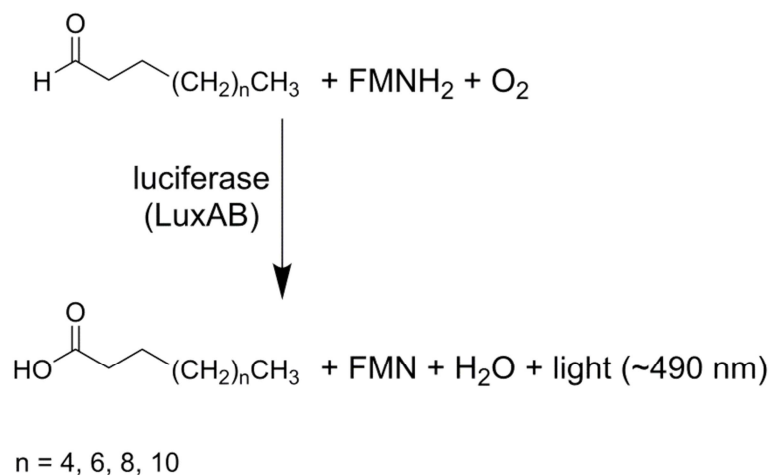


Figure 1: General reaction scheme of bacterial luciferase. The bacterial luciferase (LuxAB) catalyzes the monooxygenation of long chain aldehydes ($\text{CH}_3(\text{CH}_2)_n\text{CHO}$) by utilizing reduced flavin mononucleotide (FMNH_2) and molecular oxygen (O_2), yielding the products long chain acids ($\text{CH}_3(\text{CH}_2)_n\text{COOH}$), flavin mononucleotide (FMN), water (H_2O) and the emission of light centered at 490 nm.

The energy released during this oxidation causes an excited state FMN-4a-hydroxide, which serves as the light emitting luciferin⁴. The proteins involved in bacterial bioluminescence, namely LuxCDABEG, are encoded by the *lux* operon and are highly conserved over various bacterial strains^{2,5}. The genes *luxA* and *luxB* encode the heterodimeric luciferase; *luxC*'s, *luxD*'s, and *luxE*'s gene products are components of a fatty acid reductase complex; and *luxG* encodes a flavin reductase⁶. A number of bioluminescent *Photobacteria* (e.g., *Photobacterium mandapamensis* 27561) carry the additional *luxF* gene. It was reported that LuxF is a homodimeric protein that binds the unusual flavin derivative 6-(3'-(*R*)-myristyl)-FMN (myrFMN)⁷⁻¹². Additional genes have been identified that are responsible for riboflavin synthesis (e.g., *ribEBH*) and furthermore regulatory genes have been reported, that play a role in quorum sensing regulation of bioluminescence, especially for *Vibrio fischeri* and *Vibrio harveyi*^{6,13}. Despite the highly conserved gene order, bioluminescent bacteria show high variations in characteristics like growth behavior, intensity of light emission, or regulation of bioluminescence^{2,5,14}.

Several modified strains or plasmids containing parts or whole *lux* operons are known, exploiting bioluminescence as reporter systems. Various applications such as determining promoter activity, monitoring of bacterial contaminations in environment or food samples, Bioluminescence Resonance Energy Transfer (BRET), *in vivo* imaging of infections in eukaryotic organisms, pyrosequencing, and so forth were established¹⁵⁻¹⁷. Interestingly, the three most frequently used bioluminescent reporter systems are derived from the North American firefly (*Photinus pyralis*), the enteric pathogen of nematodes (*Photorhabdus luminescens*) and the sea pansy (*Renilla reniformis*). None of those systems has a bacterial origin, but the use of *lux* genes and operons from bacterial origins is gaining more interest for applied research¹⁶. The less abundant application of bioluminescence proteins from bacterial sources is mainly due to lower stability and longevity of bacteria derived luminescent proteins which can be related to their marine habitats. Bioluminescent bacteria of marine habitats are not cultivable under standard lab conditions. These bacteria require specific growth media and conditions, such as artificial sea water medium and lower growth/incubation temperatures (e.g., 28 °C).

To simplify comparison of *lux* operon characteristics or single *lux* genes of a range of different bioluminescent bacterial strains, a method to standardize *lux* operon expression and analysis is a prerequisite. Thus, the idea of integrating the whole *lux-rib* operon into the standard-research bacterium *Escherichia coli* (*E. coli*) emerged. For this purpose, Gibson assembly proved to be a useful tool to integrate multiple linear, overlapping fragments into one expression vector without the need for specific restriction sites. This method is also suitable when DNA inserts are too large (e.g., *P. mandapamensis* 27561 *luxCDABFEG-ribEBH*; ~ 9 kb operon size) to be amplified via PCR. A *lux* operon can be separated into multiple overlapping fragments, then be assembled into one expression plasmid and finally the sequence verified assembly product can be directly transformed into an appropriate *E. coli* system for high yield protein expression¹⁸⁻²⁰. In addition to the easy to handle *E. coli* based *lux* gene expression, a simple method combining recording of cell growth and bioluminescent light emission remained to be established. The method described here allows the *in situ* measurement and correlation of cell density and light emission of bioluminescent bacteria.

The analysis of *lux* genes and *lux* operon order and regulation of various bioluminescent bacteria with, on the one hand, an artificial bioluminescent *E. coli* system containing the whole *lux-rib* operon of *P. mandapamensis* 27561 and, on the other hand, a newly developed plate reader assay combining the *in situ* recording of cell density and light emission, helps to gain more information on the various bacterial *lux* systems. This fundamental characterization and comparison of luciferases and related enzymes may lead to alternatives to the already established reporter systems with enhanced stability and activity.

4.3. Protocol

1. Design, Preparation, and Expression of the *lux* Operon in *Escherichia coli*

Note: See **Table of Materials** for information on commercial kits used in this section.

1.1. For transferring the *lux* operon into *E. coli* choose a standard pET vector with appropriate restriction sites and antibiotic resistance gene of interest (*e.g.*, pET28a; NcoI, XhoI, kanamycin).

1.2. Design the fragments and overlapping primers for Gibson assembly based on the DNA sequence of *Photobacterium mandapamensis* 27561 (GenBank: DQ988878.2).

1.3. Set up a standard PCR reaction with the designed primers and the isolated genomic DNA of *Photobacterium mandapamensis* 27561 as template (see **Supplemental Material** for primers and conditions).

Note: Isolation of genomic DNA of the respective bacterial strain enhances PCR efficacy.

1.4. Purify the PCR product via spin-column purification.

1.5. Perform a restriction digestion of the isolated pET28a vector with NcoI and XhoI at 37 °C for 45 min.

1.6. Purify the linearized vector and the PCR fragments via agarose gel electrophoresis and subsequent spin-column purification.

1.7. Determine the DNA concentration of each fragment and the linearized vector and calculate the optimal quantities for the assembly according to the protocol^{20,21}.

Note: Efficacy of assembly depends on fragment size and number and has to be adjusted according to manufacturer's protocol^{20,21}.

1.8. After combining all fragments and the buffer in a PCR tube, incubate the assembly mixture in a PCR machine at 50 °C for 1 h.

1.9. Transform the assembled vector product according to standard transformation protocols for *E. coli* bacterial plasmid transformation into an appropriate *E. coli* system for high yield plasmid replication (*e.g.*, *E. coli* TOP10 or XL-1).

1.10. Pick colonies from the transformation plate and streak on new plates for DNA isolation.

1.11. Isolate plasmid DNA according to standard protocols.

1.12. To verify the correct assembly of the plasmid including all fragments, first perform a colony PCR according to standard protocols using primers specific for every assembled fragment.

1.13. Additionally to the colony PCR and subsequent agarose gel electrophoresis, prepare all isolated assembly vectors for DNA sequencing to verify the correct assembly and the correct DNA sequences.

1.14. Transform the verified plasmid according to standard transformation protocols for *E. coli* bacterial plasmid transformation into an appropriate *E. coli* system for high yield protein production (e.g., *E. coli* BL21).

Note: Continue directly with expression protocol below. For longer storage, the preparation of a glycerol stock is recommended.

2. Expression of Modified *E. coli* Strains

2.1 Prepare an overnight culture (ONC) for expression by inoculation of an appropriate volume of LB medium (e.g., 100 mL) with the previously prepared glycerol stock of the *E. coli* BL21 cells transformed with the assembled plasmid or directly from a transformation plate. Add 100 μ L of kanamycin (50 mg/mL; antibiotic resistance gene of pET28a) and incubate the ONC at 37 °C and 120 rpm in an incubator shaker overnight.

2.2. Inoculate the main expression culture (e.g., 800 mL of LB medium) with 8 mL of the ONC and add 800 μ L of kanamycin (50 mg/mL).

2.3. Incubate the main culture at 37 °C and 120 rpm in an incubator shaker until the cell density reaches an OD₆₀₀ of 0.6-0.8 (approximately 2.5 h).

2.4. Reduce the incubation temperature to 28 °C.

2.5. Induce protein expression by adding IPTG to a final concentration of 0.1 mM.

Note: Empirical tests showed that the reduction of the temperature to 28 °C gave the highest light intensity.

2.6. Observe bacterial cell culture until they start shining (approximately 1 h).

Note: Depending on the purpose of the expression, the cells are grown until the next day and are then harvested, or the cells can be kept shaking as long as they are shining (maximum 48 h). Harvesting the cells and purification of any proteins can be done according to standard procedures.

3. Expression of Bacterial Bioluminescent Strains

Note: Bacterial bioluminescent strains require specific growth medium/artificial sea water medium for growth and light production.

3.1 Prepare artificial sea water medium, composed of two separately prepared medium components.

Note: The preparation of the artificial sea water medium was adapted from the original protocol²². The following amounts are for 1 L liquid medium or 1 L agar medium.

3.1.1. For artificial sea water medium, weigh in the following salts: 28.13 g NaCl, 0.77 g KCl, 1.60 g CaCl₂ · 2 H₂O, 4.80 g MgCl₂ · 6 H₂O, 0.11 g NaHCO₃, 3.50 g MgSO₄ · 7 H₂O.

3.1.2. Add 1 L of distilled water and dissolve all components.

3.1.3. For LB medium, weigh in the following ingredients: 10 g yeast extract, 10 g peptone and for agar plates additionally 20 g agar.

3.1.4. Add 250 mL of tap water and dissolve components.

3.1.5. Autoclave both prepared media separately at 121 °C for 20 min.

3.1.6. For agar plates, combine 250 mL of LB medium with 750 mL of artificial sea water medium directly after autoclaving and prepare plates.

3.1.7. For liquid medium, combine 250 mL of LB medium with 750 mL of artificial sea water medium either directly after autoclaving or when cooled down.

Note: The artificial sea water medium may get turbid through salt precipitation.

3.2. Streak the bacterial bioluminescent strains on artificial sea water medium agar plates and incubate overnight at 24 – 30 °C.

Note: Long time storage of bacterial strains is normally achieved through freezing glycerol stocks of the bacterial culture. Strains should always be streaked on agar plates first to assure uniform starting conditions for all strains, prior to usage for liquid cultures, due to a lag phase in growth after thawing.

3.3. Prepare an ONC by inoculating 100 mL artificial sea water medium with a single colony from the plate. Incubate the ONC at 24 – 30 °C and 120 rpm in an incubator shaker overnight.

3.4. Inoculate 800 mL of artificial sea water medium with 8 mL of ONC.

3.5. Incubate the bacterial cells at 24 – 30 °C and 120 rpm in an incubator shaker.

Note: The light intensity profile of bioluminescent bacteria strongly varies with temperature. Depending on the regulatory mechanisms of the light production of the respective bacterial strain, light emission may start after approximately 1-6 h.

3.6. Observe bacterial cell culture until they start shining (approximately 1-6 h).

Note: Depending on the purpose of the expression, the cells are grown until the next day and are then harvested, or the cells can be kept shaking as long as they are shining. Harvesting the cells and purification of any proteins can be done according to standard procedures.

4. *In Vivo* Activity Assay for Bacterial Bioluminescent Strains and Modified *E. coli* Strains

Note: Long time storage of strains is normally achieved through freezing glycerol stocks of the bacterial culture. Strains should always be streaked on agar plates first to assure uniform starting conditions for all strains, prior to usage for liquid cultures, due to a lag phase in growth after thawing.

4.1. Streak the desired bioluminescent bacterial strain or modified *E. coli* strain on an agar plate and incubate at 28 °C overnight.

Note: The incubation temperature can vary from strain to strain and has to be evaluated empirically. To be able to compare bioluminescent bacterial strains and modified *E. coli* strains, growth conditions have to be identical.

4.2. Inoculate 3 mL of medium with the respective strain with a single colony from an agar plate and incubate the cells at 28 °C and 180 rpm in an incubator shaker for approximately 1-2 h.

4.3. Measure the cell density of a 1:10 dilution of the liquid culture at 650 nm. Calculate the ratio and volume for 1 mL culture with an OD₆₅₀ of 0.05.

Note: The subsequent plate reader assay will determine the cell density at 650 nm to avoid interference by the light emission of the strains.

4.4. Pipette the calculated volume of culture and medium into a 24-well black-walled plate with glass bottom. For the modified *E. coli* strain, add 1 µL of kanamycin (antibiotic resistance of pET28a vector) and 1 µL of IPTG (induction of gene expression) to the samples. Place a lid on the plate to avoid evaporation during the measurements.

Note: To assure that the pET28a vector containing the whole *lux* operon does not get lost by the *E. coli* culture, kanamycin must be added to each *E. coli* sample in the plate wells and to assure that light production of the *E. coli* cells can be measured, the gene expression must be induced by IPTG. To avoid crosstalk and measurement interference, black-walled well plates with glass bottom and transparent lid showed best results. Nevertheless, crosstalk can be observed and well positions have to be chosen carefully.

4.5. Start the measurement in a plate reader.

Note: The plate reader protocol is based on a script specially developed for this assay (see **Supplemental Material**) that combines two measurements, absorbance and bioluminescence. Data points are collected every 10 min with permanent shaking between the measurements and a constant temperature of 28 °C.

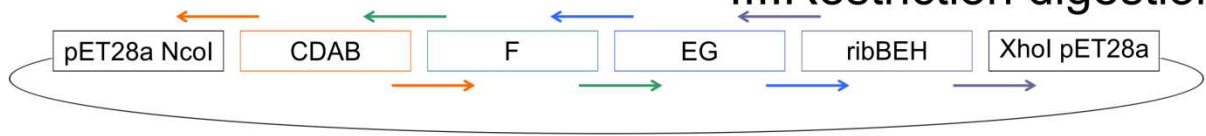
4.4. Representative Results

The gene order of the *lux* operon – *luxCDABFEG* - is highly conserved over various strains^{2,5,14}. For the design of the plasmid, the sequence information was taken from the bioluminescent bacterial strain *Photobacterium mandapamensis* 27561 and its gene order was kept the same, and, also, noncoding sequences between single genes were considered. A schematic overview of the applied Gibson cloning strategy is depicted in **Figure 2**. Four fragments in total, *luxCDAB*, *luxF*, *luxEG* and *ribEBH*, with 20-40 base pair overlapping sequences were generated. After following all steps of the Gibson assembly²⁰, DNA sequencing confirmed the correct assembly of the plasmid, including all fragments. The vector map of the final assembly product pET28a containing the *lux-rib* operon is depicted in **Figure 3**. A significant advantage of this modified pET28a vector is the utilization of standardized *E. coli* growth conditions and controlled induction with IPTG.

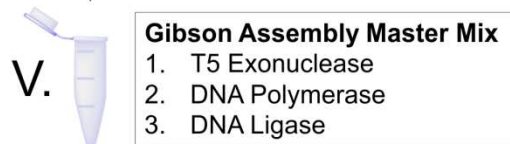
I. Primer design

II. PCR

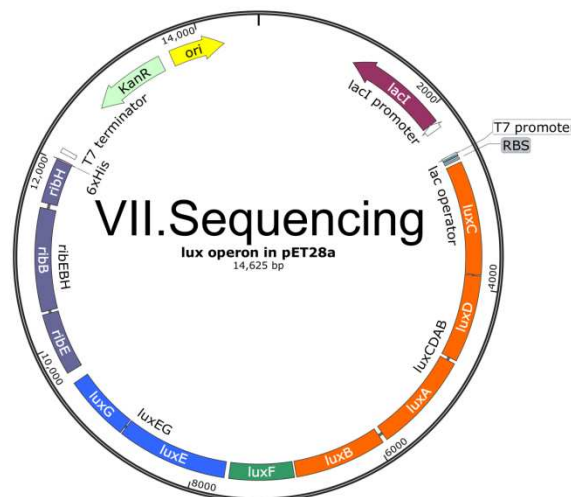
III. Restriction digestion



IV. DNA concentration



VI. Plasmid transformation and replication



VII. Sequencing

Figure 2: Schematic representation of the applied Gibson cloning strategy. **Step (I):** Overlapping primers (colored arrows; ca. 20-40 base pair overlap) are designed. Overlapping primers contain annealing sequences consisting of the respective 5' and 3' region of one fragment and the respective 3' and 5' region of the adjacent segment. **Step (II):** The designed fragments for assembly are generated via standard PCR reactions. **Step (III):** The target vector is linearized by restriction digestion (e.g., NcoI, XhoI). **Step (IV):** The DNA concentrations of all fragments and the linearized vector have to be determined to adjust concentration appropriate for Gibson assembly (according to the manufacturer's protocol). **Step (V):** All fragments and the linearized vector with optimized DNA concentrations are combined with the Gibson assembly master mix (T5 exonuclease, DNA polymerase, and DNA ligase) and are incubated at 50 °C for 1 h. **Step (VI):** The assembly product is transformed according to standard protocols into an appropriate *E. coli* strain for high yield plasmid replication (e.g., *E. coli* TOP10 or XL-1). **Step (VII):** To verify the correct assembly of the plasmid, DNA sequencing of the assembled plasmid has to be performed.

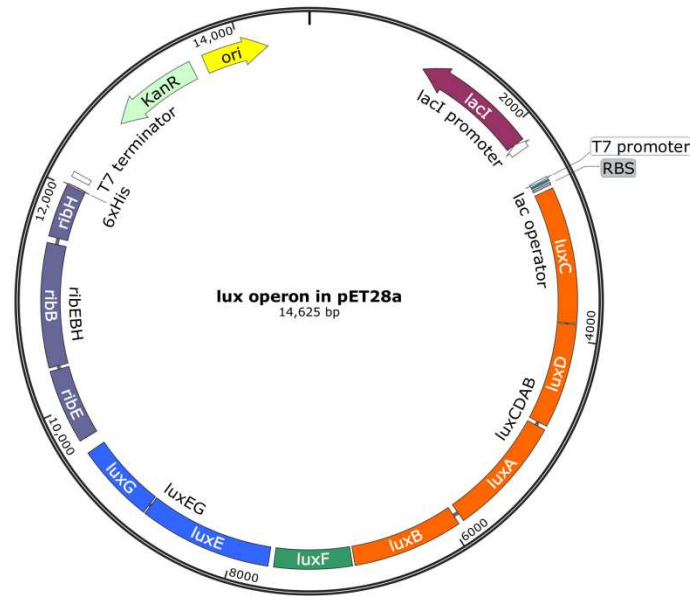


Figure 3: Vector map of pET28a containing the *lux-rib* operon. The *lux-rib* operon of *P. mandapamensis* 27561 is inserted in the multiple cloning site of pET28a in the original gene order (*luxCDABFEG-ribEBH*). Restriction sites used for cloning are NcoI and XhoI. Fragments used for Gibson assembly of the operon are *luxCDAB* in orange, *luxF* in green, *luxEG* in blue and *ribEBH* in lavender; genes within a fragment are shown as a separate box. Noncoding sequences between each gene of the operon are included in the applied cloning strategy. The final plasmid size of pET28a containing the whole *lux-rib* operon is 14,625 base pairs.

To measure light emission of bioluminescent bacteria and the respective cell density, a plate reader based method was developed. The method for the plate reader was generated combining single measurement scripts for light intensity and cell density. This novel script enabled the measurement of OD₆₅₀ and light intensity every 10 min for a user defined time frame, which has to be adjusted to the generation time of the bacteria used for the respective analysis (e.g., 10 h). The measurement of the optical density was performed at 650 nm to avoid interference with the light emission. As a proof of concept and to assure the health and the correct growth behavior of the *E. coli* cells, reference measurements were performed. In **Figure 4** the comparison of *E. coli* BL21 cells, *E. coli* BL21 cells containing an empty pET28a vector and *E. coli* BL21 cells containing the pET28a vector with the *lux-rib* operon insert are presented. For the latter strain, no IPTG was added to analyze the light emission due to the leakiness of the T7 promoter. All three reference measurements show a sigmoidal growth curve with three growth phases (lag, exponential, and stationary phase). Only the *E. coli* BL21 cells containing the pET28a vector with the *lux-rib* operon insert start to emit light, but in contrast to the measurements where expression is induced by addition of IPTG and light is emitted after 30 min, the non-induced cells only start to shine after approximately 5 h and show a much lower light emission (ca. 4-fold) compared to the induced system.

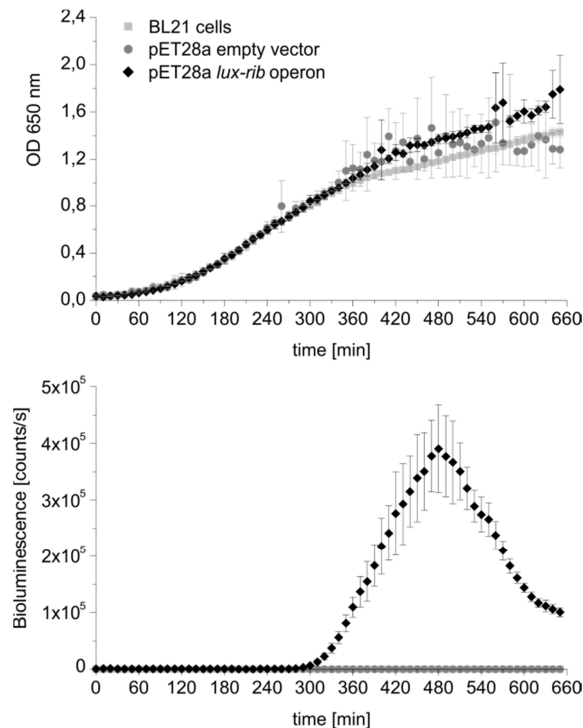


Figure 4: Comparison of growth curves and light intensities of reference strains. The OD at 650 nm and the bioluminescence intensity in counts per second were measured every 10 min over 10 h at 28 °C. All measurements are mean values of three biological replicates with four technical replicates each. Error bars represent standard deviations. *E. coli* BL21 cells (grey squares), *E. coli* BL21 cells containing an empty pET28a vector (grey circles), and *E. coli* BL21 cells containing the pET28a vector with the *lux-rib* operon insert (black diamond) were analyzed to assure correct growth behavior of our *E. coli* cells.

Figure 5 gives a comparison of growth curves and light intensities of the *lux* operon expressed in *E. coli* and the bioluminescent bacterial strain *P. mandapamensis* 27561, either in LB medium or in artificial sea water medium, using the novel established *in situ* method. To compare these bacteria, the measurements were performed at an incubation temperature of 28 °C. This temperature decreases the growth rate of the modified *E. coli* strain in LB medium as well as artificial sea water medium, but for bioluminescent bacterial strains lower temperatures are crucial. This temperature dependence is visible in **Figure 5A**, as *P. mandapamensis* 27561 shows a much higher cell density than *E. coli*. Furthermore, while for *E. coli* strains, LB medium allows generation of higher cell densities, for natural bioluminescent bacterial strains, artificial sea water medium is preferred and essential for bioluminescence. The recorded cell densities correlate with the respective light intensities, as shown in **Figure 5B**. Noteworthy, the bioluminescent *E. coli* cells reach similar light emission maxima in both LB medium as well as artificial sea water medium, although the highest intensities were recorded at different time points. In contrast to this observation, *P. mandapamensis* 27561 is viable with highly reduced growth rates in LB medium, but the bacterial cells did not emit light at all (**Figure 5B**). In artificial sea water medium, *P. mandapamensis* 27561 shows a maximum of light emission at around 1×10^4 counts per second, which is nearly a factor of 200 lower than *E. coli*. **Figure 5C** represents relative light

units where the bioluminescence is normalized by the OD. These results confirm that not only was the insertion of a plasmid containing the *lux* operon into *E. coli* successful and functional, but also that this modified *E. coli* strain is a valid alternative with even higher light emission yields and without the limitation of bacterial bioluminescence of marina bacteria, such as a complex seawater medium and lower temperatures.

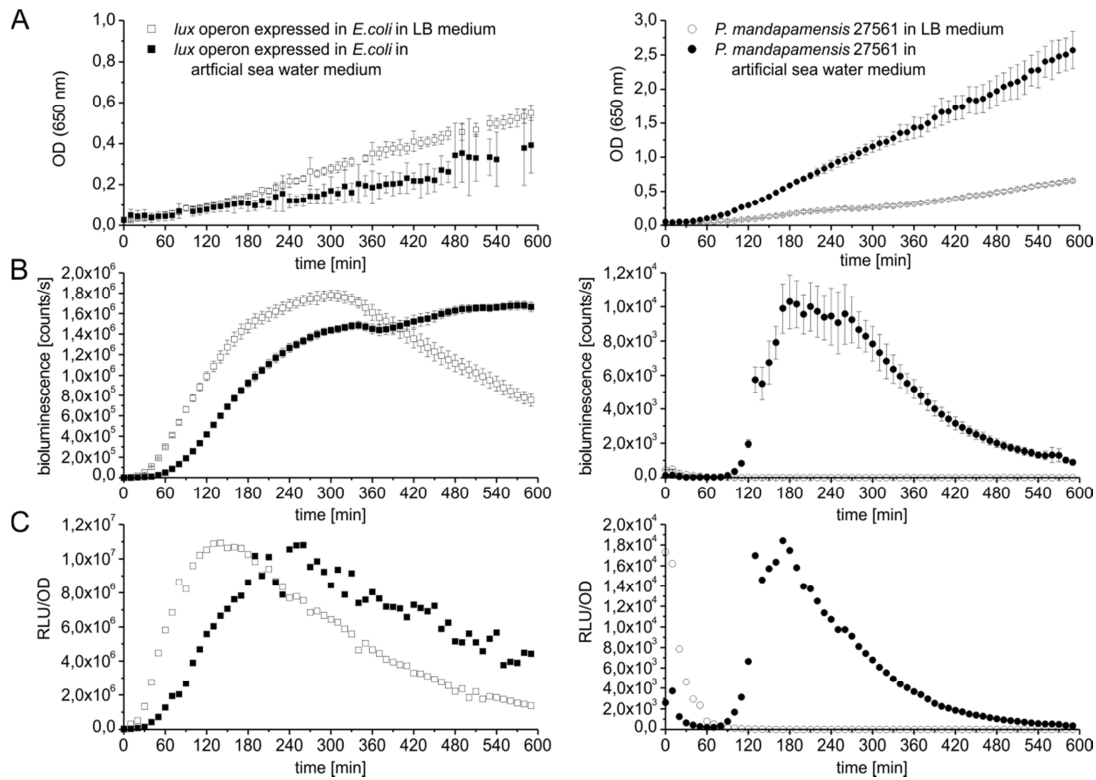


Figure 5: Comparison of growth curves and light intensities of the *lux* operon expressed in *E. coli* (squares) and *P. mandapamensis* 27561 (circles) in LB medium (open symbols) or artificial sea water medium (filled symbols). All measurements are mean values of three biological replicates with four technical replicates each. Error bars represent standard deviations. All experiments were performed at an incubation temperature of 28 °C. **(A)** Optical density (OD) measurements at 650 nm were performed every 10 min for 10 h. *E. coli* *lux* operon expression (left panel) is compared to *P. mandapamensis* 27561 (right panel) in LB medium and artificial sea water medium. Cell densities are determined at 650 nm to avoid bioluminescence-interference. **(B)** Measurement of light intensity (bioluminescence [counts/s]) was performed every 10 min for 10 h. *E. coli* *lux* operon expression (left panel) is compared to *P. mandapamensis* 27561 (right panel) in LB medium and artificial sea water medium. **(C)** Relative light intensities (RLU/OD) of the *lux* operon expressed in *E. coli* (left panel) and *P. mandapamensis* 27561 (right panel) are determined by normalizing bioluminescence to cell density.

Additionally, a long-term measurement of the *E. coli* based *lux-rib* gene expression over 24 h was performed to analyze the longevity of the light emission (**Figure 6**). Light emission lasted for 19.5 h, much longer than the bacterial strains (e.g., *P. mandapamensis* 27561) where a gradual decrease was observed resulting in very low light emission after 10 h.

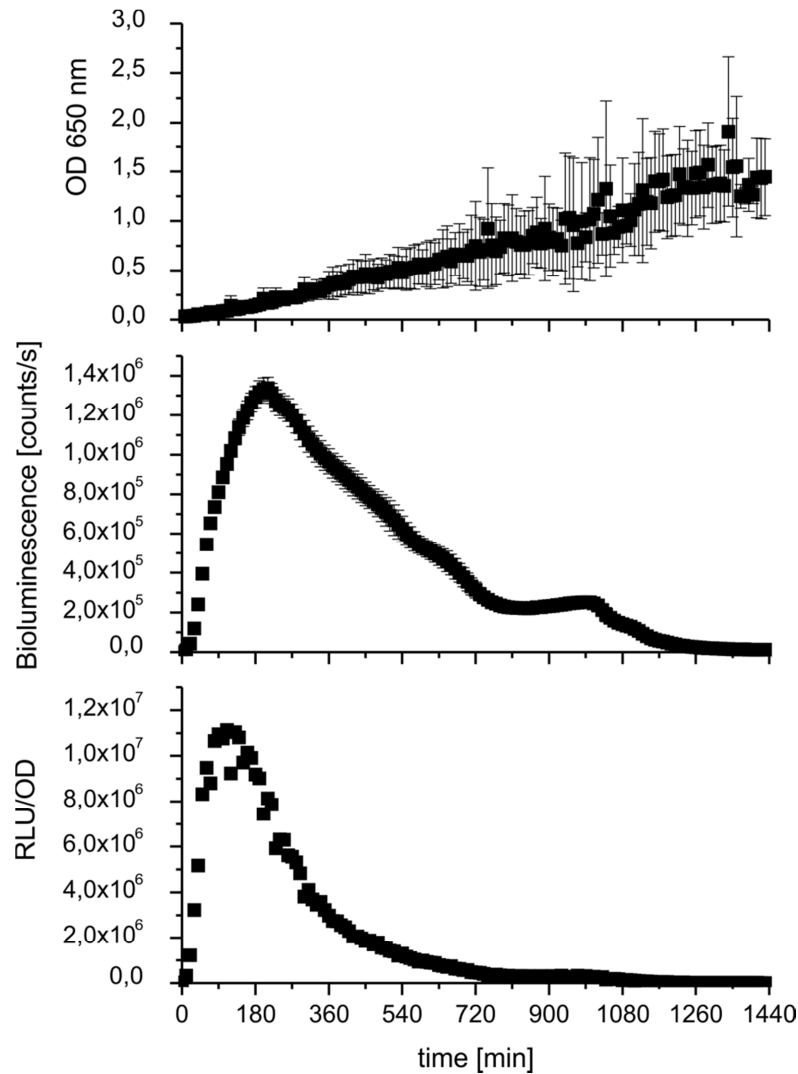


Figure 6: Comparison of growth curves and light intensities of *E. coli* based *lux* gene expression for 24 h. The OD at 650 nm and the bioluminescence intensity in counts per second were measured every 10 min over 24 h at 28 °C. All measurements are mean values of three biological replicates with four technical replicates each. Error bars represent standard deviations. Additionally, the relative light intensities (RLU/OD) where bioluminescence is normalized by cell density are represented.

To illustrate the limitations of the developed assay, **Figure 7** shows the measurement results of three bioluminescent bacterial strains, namely *Photobacterium mandapamensis* S1, *Photobacterium mandapamensis* TH1 and *Vibrio harveyi* 14126. For the first strain (S1), the method works very well and shows a maximal bioluminescence intensity of nearly 2×10^6 . For the other two strains (TH1 and 14126), the maximal light intensity cannot be determined because the light intensity generated by both exceeded the detection limit of the used instrument settings. The gain value defined for the developed method (script) for these two strains was set too high. Nevertheless, the onset of bioluminescence activity can be compared with each other. *P. mandapamensis* TH1 and *P. mandapamensis* S1 start shining after approximately 1 h and an OD₆₅₀ value of 0.1-0.2, respectively. In contrast, *V. harveyi* 14126 starts to emit light after approximately 5.5 h at an OD₆₅₀ value of 1.0. The observed onset of light emission is accompanied by an exponential increase in OD as well as

bioluminescence. It is known that bioluminescence of *V. harveyi* 14126 underlies quorum sensing regulation and therefore a specific cell density allowing the activation of the *lux* operon, which can be clearly observed in **Figure 7**¹³. This result demonstrates that with this novel *in situ* plate reader assay it is possible to easily compare bioluminescent bacteria and also roughly define a regulatory mechanism of these strains by determining whether a quorum sensing regulation can be observed or not.

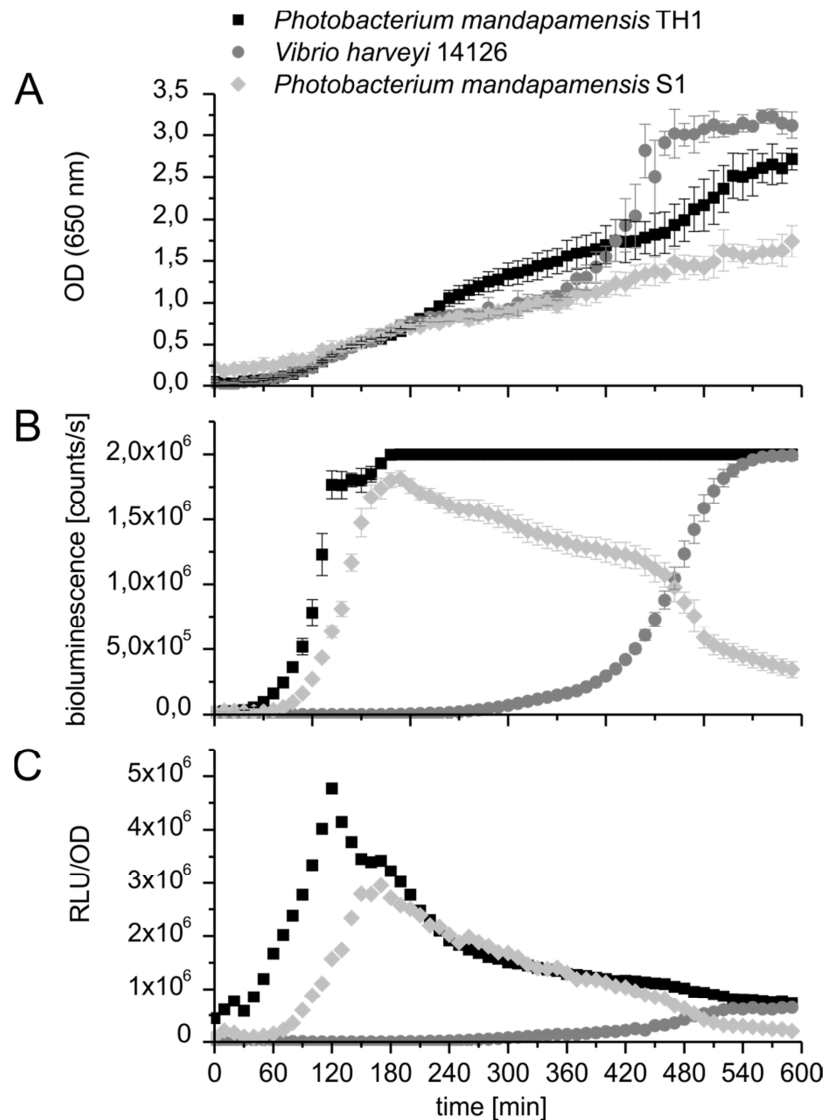


Figure 7: Comparison of bioluminescent bacteria to evaluate potential quorum sensing regulation. Light emission and cell density are measured every 10 min for 10 h and represent mean values of three biological replicates with four technical replicates each. Error bars represent standard deviations. Measurements of *Photobacterium mandapamensis* TH1 (black squares), *Vibrio harveyi* 14126 (grey circles) and *Photobacterium mandapamensis* S1 (grey diamonds) were compared to each other; **(A)** depicts the optical density (OD) at 650 nm, **(B)** the light intensity (bioluminescence [counts/s]), and **(C)** relative light intensities (RLU/OD).

Figure 8 shows an example of an expression culture of *E. coli* BL21 cells harboring the assembled pET28a plasmid containing the *lux* operon after induction with IPTG. After approximately one h after induction, the *E. coli* cells start shining with a blue-green color. **Figure 8A** shows the *E. coli* expression culture photographed in the light and **Figure 8B** gives the same culture in the dark. **Figure 8C** depicts an agar plate of artificial sea water medium with *P. mandapamensis* S1 glowing in the dark in the same blue-green color characteristic for bacterial bioluminescence.



Figure 8: Bioluminescence in liquid media and on agar plates. (A) 5 L flask with 2 L LB medium inoculated with *E. coli* BL21 cells expressing the pET28a *lux* operon plasmid photographed in light. **(B)** The same culture as in (A) photographed in the dark. Pictures A and B were taken approximately 2 h after induction of expression. **(C)** Artificial sea water medium agar plate with streaked culture of *P. mandapamensis* S1 photographed in the dark.

4.5. Discussion

The construction of an expression plasmid containing four fragments composing the whole *lux-rib* operon of *P. mandapamensis* 27561 was achieved via Gibson cloning. This *E. coli* based *lux* gene expression enables *E. coli* cells to emit light. Avoiding quorum sensing regulation and non-standard growth conditions are substantial advantages of this system.

The advantages of using Gibson cloning strategy are the easy assembly of multiple linear DNA fragments, high flexibility and no need for specific restriction sites¹⁸⁻²⁰. This method allows to easily change a *lux* operon, excluding single genes or gene clusters or introducing new genes or exchanging genes from one strain with another. A prerequisite for the application of this method is the availability of the respective *lux* operon gene sequence. Only for a small number of bioluminescent bacteria is the complete DNA sequence of the respective *lux* operon known and/or available. Many of these sequences are fragmented because they were generated using shotgun sequencing. In the case of the investigated *P. mandapamensis* 27561 the complete DNA sequence of the *lux* operon is known and available from the NCBI gene database (GenBank: DQ988878.2).

One critical step in the protocol of the Gibson assembly is the calculation of the DNA concentration of the single fragments. In the assembly protocol of the manufacturer it was recommended to use 0.2-0.5 pmols and a total volume of 20 μ L for 4-6 fragments^{20,21}. In our case, where *luxCDABFEG-ribEBH* is comprised of 4 fragments, the concentrations and total volumes were 0.1 pmol and 45 μ L, respectively, depending on the yield of PCR products. On the one hand, the concentration had to be reduced and on the other hand, the volume had to be increased. Nevertheless, the assembly worked very well and DNA sequencing confirmed the correct insertion at the first attempt. This finding confirmed Gibson assembly as a robust and appropriate method for our investigations, which can easily be modified¹⁸⁻²⁰.

The newly established plate reader assay is an easy to handle method. It enables a simple primary analysis of new or (un-)known bioluminescent bacterial strains and gives already a first hint on the regulatory mechanism of light production (*e.g.*, lag in luminescence at low cell densities). Additionally, growth conditions in combination with light production can easily be evaluated by simply changing growth medium or temperature.

The measurements with the plate reader were performed at 28 °C. The reason for this unusual setting is the temperature sensitivity of bioluminescent bacterial strains, where temperatures above 30 °C lead to less or even no growth and/or light emission. Note, that the plate reader is capable of keeping a defined temperature over time with the limitation of a missing active cooling system. Therefore, the ambient temperature has to be below the temperature of the measurement.

As a proof of concept, the comparison of the *E. coli* construct with the bioluminescent strain *P. mandapamensis* (**Figure 5**) on the one hand and the reference measurements (**Figure 4**) on the other hand were performed and confirm the reliability of this newly established system. Additionally, the long-term measurement assured the longevity of the light emission (**Figure 6**). But one has to consider that OD values are not reliable above a certain optical density, depending on the characteristics of the used measurement device (approximately 15 h in the present case) where an appropriate dilution would be needed for a measurement in the linear range of the detector. These high variances in OD values make these long time measurements not reliable. Therefore, shorter measurements such as 10 h are recommended using the experimental setup reported here.

Limitations of the established plate reader assay can be seen in **Figure 7**. The difficulty is to find an appropriate setting of the measurement. The 'gain value' adjusts the sensitivity of the photo multiplier tube (PMT). The gain is the amplification of the signal in the PMT, meaning that a higher gain factor will increase the signal. If the gain is set too low, the signal to noise ratio becomes bigger and light intensities of "low" shining bioluminescent bacteria cannot be measured any more (signals close to zero, data not shown). The challenge in a bioluminescent assay is to set the gain so the measurement results for all bacterial strains stay within the range of the instrument. Additionally, the measurement range for luminescence depends on the measurement interval time (e.g., maximum of 2,000,000 for 1 s).

The gain was set to 2800, which was empirically tested and chosen for the specific plate reader used for the establishment of this method. The used gain setting allows the recording of maximum emitted light by the bioluminescent *E. coli* system, *P. mandapamensis* 27561, and *P. mandapamensis* S1 without an overflow, but for the strains *P. mandapamensis* TH1 and *V. harveyi* 14126 the gain was too high. Therefore, these latter strains exceed the detection limit and the real maximal light intensity cannot be measured. This technical limitation might prevent the comparison of bioluminescent bacteria, which show high variations in maximum light emission, although growth conditions and cell densities might be comparable.

Positioning of the analyzed bacterial strains within the used well plates has to be evaluated empirically. Although black well plates with glass bottoms were used, crosstalk between the samples was observed. The light intensity of specific strains is so high, that all neighboring wells will show false positive light emissions (e.g., blank). Therefore, it is important to measure two different strains either separately or with a certain spatial separation to each other.

There are already many modified *E. coli* strains known that contain parts of the *lux* operon and are mainly application-oriented¹⁵⁻¹⁷. The methods described here, aim at fundamental research, for example the possibility of analyzing each *lux* gene separately. Although

research of bioluminescence has a long history, there are still many open questions. By excluding or introducing genes from the *lux* operon, exchanging the *luxAB* genes with genes from another strain, or analyzing protein complexes, embedded in the easy to handle *E. coli* system and further application of the plate reader assay, it might be possible to gain more information on regulatory processes and the functions of *lux* genes.

Author contribution

EB and JN designed the constructs and experiments. EB performed the experiments, analysis and data evaluation. EB and PM wrote the manuscript. EB, JN and PM participated in the video shoot.

Acknowledgments

We want to thank Wladislaw Maier (BMG Labtech GmbH) for his support in establishing the self-written script for the plate reader. This work was supported by the Austrian “Fonds zur Förderung der wissenschaftlichen Forschung” (FWF) to PM (P24189) and the PhD program “DK Molecular Enzymology” (W901) to PM.

Disclosures

The authors have nothing to disclose.

4.6. References

1. Widder, E.A. Bioluminescence in the Ocean: Origins of Biological, Chemical, and Ecological Diversity. *Science*. **328** (5979), 704–708 (2010).
2. Dunlap, P. Bioluminescence, Microbial. *Encycl Microbiol*. 45–61 (2009).
3. Ulitzur, S., Hastings, J.W. Evidence for tetradecanal as the natural aldehyde in bacterial bioluminescence. *Proc Natl Acad Sci USA*. **76** (1), 265–267 (1979).
4. Kurfürst, M., Ghisla, S., Hastings, J.W. Characterization and postulated structure of the primary emitter in the bacterial luciferase reaction. *Proc Natl Acad Sci USA*. **81**, 2990–2994 (1984).
5. Dunlap, P. Biochemistry and genetics of bacterial bioluminescence. *Biolumin Fundam Appl Biotechnol - Vol 1*. **144**, 37–64 (2014).
6. Meighen, E.A. Bacterial Bioluminescence: Organization, regulation, and application of the *lux* genes. *FASEB J*. **7**, 1016–1022 (1993).
7. Moore, S.A., James, M.N.G., O’Kane, D.J., Lee, J. Crystallization of *Photobacterium leiognathi* non-fluorescent flavoprotein with limited sequence identity to bacterial luciferase. *J Mol Biol*. **224**, 523–526 (1992).
8. Moore, S.A., James, M.N.G., O’Kane, D.J., Lee, J. Crystal structure of a flavoprotein related to the subunits of bacterial luciferase. *EMBO J*. **12** (5), 1767–1774 (1993).
9. Moore, S.A., James, M.N.G. Common structural features of the *luxF* protein and the subunits of bacterial luciferase: Evidence for a ($\beta\alpha$)₈ fold in luciferase. *Protein Sci*. **3**, 1914–1926 (1994).
10. Moore, S.A., James, M.N.G. Structural refinement of the non-fluorescent flavoprotein from *Photobacterium leiognathi* at 1.60 Å resolution. *J Mol Biol*. **249**, 195–214 (1995).
11. Kita, A., Kasai, S., Miyata, M., Miki, K. Structure of flavoprotein FP390 from a luminescent bacterium *Photobacterium phosphoreum* refined at 2.7 Å resolution. *Acta Crystallogr Sect D Biol Crystallogr*. **52** (1), 77–86 (1996).
12. Bergner, T. *et al.* Structural and biochemical properties of LuxF from *Photobacterium leiognathi*. *Biochim Biophys Acta - Proteins Proteomics*. **1854** (10), 1466–1475 (2015).
13. Defoirdt, T., Boon, N., Sorgeloos, P., Verstraete, W., Bossier, P. Quorum sensing and quorum quenching in *Vibrio harveyi*: Lessons learned from *in vivo* work. *ISME J*. **2** (1), 19–26 (2008).
14. Meighen, E. Genetics of bacterial bioluminescence. *Annu Rev Genet*. **28**, 117–139 (1994).

15. Kelkar, M., De, A. Bioluminescence based *in vivo* screening technologies. *Curr Opin Pharmacol.* **12** (5), 592–600 (2012).
16. Waidmann, M.S., Bleichrodt, F.S., Laslo, T., Riedel, C.U. Bacterial luciferase reporters: The Swiss army knife of molecular biology. *Bioeng Bugs.* **2** (1), 8–16 (2011).
17. Wilson, T., Hastings, J.W. *Bioluminescence living lights, lights for living.* Harvard University Press. (2013).
18. Gibson, D.G., Young, L., Chuang, R.Y., Venter, J.C., Hutchison, C.A., Smith, H.O. Enzymatic assembly of DNA molecules up to several hundred kilobases. *Nat Methods.* **6** (5), 343–345 (2009).
19. Gibson, D.G., Smith, H.O., Hutchison, C.A., Venter, J.C., Merryman, C. Chemical synthesis of the mouse mitochondrial genome. *Nat Methods.* **7** (11), 901–903 (2010).
20. Gibson, D.G. Enzymatic assembly of overlapping DNA fragments. *Methods Enzymol.* **498**, 349–361 (2011).
21. NEB NEBuilder HiFi DNA Assembly Reaction (E2621) (2015).
22. Atlas, R.M. *Handbook of Microbiological Media, Third Edition.* CRC Press. (2004).

4.7. Supplemental material

Table S1: Primers used for PCR of *lux-rib* operon fragments of *Photobacterium mandapamensis* 27561

Oligo name	Sequence 5'-3'
CDAB_fwd	TGTTTAACTTTAAGAAGGAGATATA ATGATTA AAAAAGATCCCACTG
CDAB_rev	TCCATTTTGTGCAT TTTTATTATCCTGTTATTTATTATTATAGATTTTT C
F_fwd	CAGGATAATAAAAA ATGACAAAATGGAATTATGGC
F_rev	TGACTTAACTGAA TTAGTTAAGGTTGTGTTCTTTTC
EG_fwd	CAACCTTAACTAA TTCAAGTTAAGTCAATTTAAATTTAAAAC
EG_rev	GAATGATTTTTAA CTACATATAACTAAACGCATCAG
rib_fwd	TAGTTATATGTAG TTAAAAATCATTTCATTATTTATG
rib_rev	ATCTCAGTGGTGGTGGTGGTGGTGGTGGT TTAAGGCTCGATTTCTGC

Primer names are according to the respective *lux* genes amplified during PCR, the red letters indicate the gene specific primers, the black letters the annealing sequence of the adjacent fragment.

Table S2: PCR reaction used prior to Gibson Assembly.

Phusion Polymerase	
1 x rxn	total 20µL
5x Phusion Buffer	4 µL
dNTPs (2mM)	2 µL
Primer fwd (10mM)	2 µL
Primer rev (10mM)	2 µL
DNA Template	ca. 140 ng
Phusion Polymerase (2U/µL)	0.5 µL
ddH ₂ O	8 µL

Table S3: PCR program used for amplification of *lux-rib* operon fragments

PCR program		
	98°C	30 s
x35	98°C	10 s
	56°-58°C	30 s
	72°C	2.5 min
	72°C	10 min
	4°C	hold

gradient in PCR machine

Script for plate reader FLUOStar (BMG Labtech)

;Script generated by script wizard (Omega V5.11 R3)

;Protocol Names:

st1:="BIOLUMI"

st2:="OD650"

st3:="SHAKE"

;Plate ID:

ID1:=""

;Number of readings (number of kinetic cycles):

NumberOfReadings:=66

R_Temp 28

wait for temp>=27.9

=====

for Reading:=1 to NumberOfReadings do begin ;kinetic loop

ID2:="Wizard script 'LumiOD650', Prot.1"

R_Run "<st1>" ;execute first test protocol

;merge horizontal (kinetic):

if Reading>1 then begin

Call "MergeReadings.exe <DataPath> <User> H ID2"

end;

ID2:="Wizard script 'LumiOD650', Prot.2"

R_Run "<st2>" ;execute second test protocol

;merge horizontal (kinetic):

if Reading>1 then begin

Call "MergeReadings.exe <DataPath> <User> H ID2"

end;

ID2:="Wizard script 'LumiOD650', Prot.3"

R_Run "<st3>" ;execute third test protocol

end; ;end of kinetic loop

;end of script

Table S4: List of required materials and equipment

Name of Material/ Equipment	Company	Catalog Number	Comments/Description
NEBuilder High-Fidelity DNA Assembly Cloning Kit	New England Biolabs Inc.	E2621S	for 10 rxn/ dx.doi.org/10.17504/protocols.io.cwaxad
Phusion Polymerase	Thermo Scientific	F530S	
Q5 High Fidelity DNA Polymerase	New England Biolabs Inc.	M0491S	
GeneJet Genomic DNA Purification Kit	Thermo Scientific	K0721	for 50 rxn
restriction enzymes and buffer (NcoI, XhoI)	New England Biolabs Inc.	R3193S/R0146S	
Wizard SV Gel and PCR Clean-Up kit	Promega	A9282	for 250 rxn
Monarch DNA Gel Extraction Kit	New England Biolabs Inc.	#T1020S	for 50 rxn
GeneJet Plasmid Miniprep Kit	Thermo Scientific	K0503	for 250 rxn
GoTaq® G2 DNA Polymerase	Promega	M7841	
24-well black sensoplate with glass bottom	Greiner Bio One	662892	
FLUOStar Omega plate reader	BMG Labtech		

Chapter V

The impact of LuxF on light intensity in bacterial bioluminescence

This chapter summarizes the last experiments and analyses of my PhD combined to a short manuscript.

V. The impact of LuxF on light intensity in bacterial bioluminescence

Eveline Brodl^a, Christina Horn^a, Hansjörg Weber^b, Johannes Niederhauser^a and Peter Macheroux^{a,*}

^aGraz University of Technology, Institute of Biochemistry, Petersgasse 12/2, 8010 Graz, Austria

^bGraz University of Technology, Institute of Organic Chemistry, Stremayrgasse 9, 8010 Graz, Austria

*Corresponding author: Prof. Dr. Peter Macheroux, Graz University of Technology, Institute of Biochemistry, Petersgasse 12/2, 8010 Graz, Austria. Email: peter.macheroux@tugraz.at

Keywords:

bacterial bioluminescence; luciferase; LuxF; light intensity; flavin derivatives; *lux* operon in *E. coli*; plate reader assay

5.1. Abstract

The enzymes involved in bacterial bioluminescence are encoded in the *lux* operon with a conserved gene order of *luxCDABEG*. Some photobacterial strains carry an additional gene, termed *luxF*, whose function and influence on bacterial bioluminescence is still uncertain. The *luxF* encoded and equally termed protein LuxF binds the flavin derivative 6-(3'-(*R*)-myristyl)-flavin mononucleotide (myrFMN), which is generated as a side product in the luciferase-catalyzed reaction. This study utilizes an *E. coli* based *lux-rib*-operon expression system where the *lux-rib* operon of *Photobacterium leiognathi* subsp. *mandapamensis* 27561, namely *luxCDAB(F)EG-ribEBH*, was cloned into a single expression vector. Exclusion of *luxF* from the *lux* operon enabled novel insights into the role of LuxF in light emission. *E. coli* cultures harboring and expressing the genes of the *lux-rib* operon including *luxF* emit 1.5-times more light than without *luxF*. Furthermore, isolation of the tightly bound flavin derivative revealed the presence of at least three different flavin derivatives. Analysis by UV/Vis absorption and NMR spectroscopy as well as mass spectrometry showed that the flavin derivatives bear fatty acids of various chain lengths. This distribution of FMN derivatives is vastly different to what was found in bioluminescent bacteria and indicates that the luciferase is supplied with a range of aldehyde substrates in *E. coli*.

5.2. Introduction

In bacterial bioluminescence the enzyme luciferase catalyzes the monooxygenation of a long-chain aliphatic aldehyde to the corresponding fatty acid [1,2]. It employs reduced flavin mononucleotide (FMNH₂) and molecular oxygen and generates water and light centered at 490 nm [3,4]. The enzymes needed for this complex bioluminescent machinery are encoded in a single operon under the control of a promoter with the gene order *luxCDABEG* [4]. LuxCDE constitute the fatty acid reductase complex providing the long-chain aliphatic aldehydes. *luxG* encodes a flavin reductase supplying the reduced FMN. LuxA and LuxB form the α - and β -subunit of the luciferase, respectively.

Earlier purification efforts of photobacterial luciferases were accompanied by another protein that was difficult to remove from luciferase preparations. Mitchell and coworkers called it light-inducible protein carrying a flavin-type chromophore designated “B” [5]. The protein has a low fluorescence efficiency and therefore has been later renamed non-fluorescent protein (NFP) [6,7]. Another name given to this protein was flavoprotein FP₃₉₀ due to its absorption maximum at 390 nm [8–11]. Initially, the gene was called *luxG(N)* [12–14] and later renamed *luxF* [15]. Nowadays, the gene and protein share the same notation, namely *luxF* and LuxF, respectively. The amino acid sequence of LuxF shows up to 30 % identity to the β -subunit and below 20 % identity to the α -subunit of bacterial luciferases of *Photobacterium leiognathi* or *Photobacterium phosphoreum* [6,16,17]. Therefore, it was assumed that *luxF* arose through a gene duplication event of *luxB* in an ancestor of *Photobacterium*, which was subsequently lost again from the genomes of several descendants. The identification of *luxF* and its position within the *lux* operon led to the gene order *luxCDABFEG* [12,13,15,16] and the differentiation of *Photobacterium leiognathi* into the subgroups *Photobacterium leiognathi* subsp. *leiognathi* (*luxF*⁻) and *Photobacterium leiognathi* subsp. *mandapamensis* (*luxF*⁺). Therefore, only *Photobacterium leiognathi* subsp. *mandapamensis* and *Photobacterium phosphoreum* contain *luxF* [18,19]. Further phenotypic characterization revealed that *P. leiognathi* subsp. *leiognathi* shows higher light intensities at low salt concentrations in an intense blue color, while *P. leiognathi* subsp. *mandapamensis* emits more light at high salt concentrations in a blue-green color [18].

LuxF is a homodimeric protein forming a seven stranded β/α fold. During the structural characterization of the protein, a flavin derivative was discovered that was tightly bound to the protein. In keeping with the observed electron density, this molecule was designated as 6-(3'-(*R*)-myristyl)-FMN (myrFMN). Each LuxF monomer binds two flavin derivatives; one is situated in the dimer interface and the other in the vicinity of the N-termini at the molecular surface (PDB 1FVP/1NFP/4J2P). Nevertheless, release of this molecule was only achieved under harsh conditions [6–9,17,20,21].

With this early discovery, first speculations on the function of this unknown protein and non-covalently bound molecule were postulated. The bound chromophore showed flavin-like properties and might have been formed during the bioluminescent reaction as side product in low quantities [5,22,23]. Kita and coworkers found two different flavin derivatives

in the crystal structure of FP₃₉₀; 6-(3'-(*R*)-myristyl)-FMN and 6-(4'-(*R*)-myristyl)-FMN leaving the possible function of the flavin derivative and of LuxF unanswered [8,9]. Others postulated that myrFMN may bind to the luciferase and acts as an inhibitor leading to the loss of luciferase activity [5,22,23]. More recently, some of these early hypotheses could be confirmed. It was reported that LuxF is important to prevent inhibition of the luciferase by myrFMN and thus it was proposed that LuxF acts as a scavenger of myrFMN [21,24]. During phylogenetic analyses of photobacterial strains, natural occurring nonsense mutations in *luxF* were discovered. They revealed that the strains carrying this inactivated *luxF* are luminous but to a lower degree [25]. This observation is in fact in accordance with the proposed role of LuxF as a scavenger of the inhibiting myrFMN. In this study, the incorporation of the *lux-rib* operon of *Photobacterium leiognathi* subsp. *mandapamensis* 27561 into a single expression vector for an *E. coli* based *lux* gene expression system was exploited to enable *in vivo* and *in vitro* analysis of LuxF. Furthermore, isolation of the produced alkylated FMN derivatives followed by a detailed analysis by means of UV/Vis absorption and NMR spectroscopy as well as mass spectrometry revealed that at least three different FMN derivatives are generated with varying side chains attached to the C6-position of the isoalloxazine ring.

5.3. Materials and methods

5.3.1. Reagents

All commercially available reagents, solvents, components for buffers, flavin mononucleotide (FMN), isopropyl- β -D-thiogalactopyranosid (IPTG) were from Sigma-Aldrich (Merck), Thermo Fisher Scientific or VWR, and were used without further purification.

5.3.2. Instrumentations

In vivo activity assays were performed on a FLUOstar plate reader (BMG Labtech, Ortenberg, Baden-Wuerttemberg, Germany). To avoid crosstalk and measurement interference, black-walled 24-well plates with glass bottom (Greiner Bio-One, Kremsmünster, Austria) were utilized. A script particularly for this assay was developed that combines absorption (optical density at 650 nm) and bioluminescence [counts/s] measurements and data points were collected every 10 min over 10 hrs with permanent shaking between the measurements and a constant temperature of 28 °C (Supplement) [26].

HPLC analysis was performed on a semi-preparative Dionex UltiMate 3000 machine (Thermo Fisher Scientific, Waltham, Massachusetts, USA) equipped with a Dionex UltiMate diode array detector. Separation was achieved with an Atlantis dC18 (4.6 x 250 mm, 5 μ m) column (Waters Corporation, Milford, Massachusetts, USA) using 0.1% TFA in water and acetonitrile at 25 °C and 1 mL/min flow rate. The multistep gradient method starts from 0% acetonitrile to 95% within 20 min, holding 95% for 5 min and going down to 0% within 5 min and

holding 0% for another 5 min. Peak determination and evaluation was performed at 280, 370 and 450 nm, respectively. Four different references were measured having the following retention times and wavelength maxima: FAD: $t_R = 9.1$ min; maxima: 372/447 nm; FMN: $t_R = 9.8$ min; maxima: 371/446 nm; riboflavin: $t_R = 10.4$ min; maxima: 370/445 nm; myrFMN: $t_R = 18.7$ min; maxima: 386/442 nm (reference sample isolated from *P. leiognathi* S1) [21,24]. Fractions were collected from 18.0 to 24.0 min while fraction tubes were changed every 15 s. Those fractions containing myrFMN or other flavin derivatives, according to the analysis at 370 nm, were dried under reduced pressure. All samples were dissolved in MeOH (HPLC grade) for HPLC-MS analysis.

HPLC-MS measurements were performed with an Agilent Technologies 1200 Series system (Agilent Technologies, Santa Clara, California, USA) equipped with a MWD SL multiple wavelength detector (deuterium lamp, 190-400 nm) and with single quadrupole LC-MS detector using electrospray ionization source (ESI). Separation over an Agilent Poroshell 120 SB-C18 (3 x 100 mm, 2.7 μ m) column was achieved using the same gradient as mentioned above but with 0.01% FA in water and acetonitrile at 25 °C and 0.5 mL/min flow rate. The determination and evaluation of peaks was achieved by analyzing the chromatograms at 210, 280, 370 and 450 nm, respectively, using mass spectrometry. A negative ESI-Scan mode from m/z 100 to 800 was used.

A Varian INOVA 500 MHz NMR spectrometer (Agilent Technologies, Santa Clara, California, USA) and the VNMRJ 2.2D software were used for all NMR measurements. ^1H NMR spectra (499.98 MHz) were measured on a 5 mm indirect detection PFG-probe, while a 5 mm dual direct detection probe with z-gradients was used for ^{13}C NMR spectra (125.71 MHz).

5.3.3. Bacterial strain and growth conditions

Bacterial bioluminescent strains require a specific growth medium for growth and light production. In this case the composition of the artificial sea water medium 246 for liquid medium as well as agar plates was used [26,27]. This medium is composed of two separately prepared media components. The following composition equals 1 L liquid media or 1 L agar media. For the artificial sea water component 28.13 g NaCl, 0.77 g KCl, 1.60 g $\text{CaCl}_2 \times 2 \text{H}_2\text{O}$, 4.80 g $\text{MgCl}_2 \times 6 \text{H}_2\text{O}$, 0.11 g NaHCO_3 , 3.50 g $\text{MgSO}_4 \times 7 \text{H}_2\text{O}$ were dissolved in 1000 mL distilled water. For the LB component 10 g yeast extract, 10 g peptone and for agar plates additionally 20 g agar were combined in 250 mL distilled water. Both components were separately autoclaved at 121 °C for 20 minutes. For agar plates as well as for liquid medium, 250 mL of LB with 750 mL of artificial sea water were directly combined after autoclaving. To assure uniform starting conditions, bacterial bioluminescent strains should always be streaked on artificial sea water medium agar plates first and incubated overnight at 24-30 °C, prior to usage for liquid cultivation (depending on the bacterial bioluminescent strains, different temperatures lead to the best growth conditions and highest light intensities). *Photobacterium leiognathi* subsp. *mandapamensis* 27561 was incubated at 28 °C overnight. For a standard overnight culture (ONC), 4 mL of artificial sea water medium were inoculated with one colony from the agar plate and incubated at 28 °C at 200 rpm overnight.

5.3.4. Design and expression of the *lux-rib* operon in *E. coli*

The aim was to design a pET28a vector containing the *lux-rib* operon of *Photobacterium leiognathi* subsp. *mandapamensis* 27561, namely *luxCDAB(F)EG-ribEBH*, either containing the *luxF* gene or without *luxF*. Therefore, Gibson cloning was applied using the NEBuilder High-Fidelity DNA Assembly Master Mix (New England Biolabs, Ipswich, Massachusetts, USA) [28]. The design and cloning strategy for these *E. coli* constructs was described earlier [26]. Shortly, overlapping primers were designed for four fragments, namely CDAB, F, EG and ribEBH embedded into a pET28a vector (Supplement, Table S1). PCR with the ordered primers and isolated genomic DNA of *Photobacterium leiognathi* subsp. *mandapamensis* 27561 was performed according to standard procedures (Supplement, Table S2 and S3). All isolated and purified fragments, the linearized and purified vector (pET28a restriction digested with NcoI and XhoI) and the NEBuilder High-Fidelity DNA Assembly Master Mix were incubated for one hour at 60 °C. After transformation in chemically competent *E. coli* Top10 cells and isolation of the new plasmid, sequencing results confirmed the two newly designed vectors (Supplement, Figure S1).

For overnight cultures (ONC), 4 mL of LB medium with kanamycin (50 µg/mL) were inoculated with one colony from the agar plate and incubated at 37 °C at 200 rpm overnight. The main culture consisting of 800 mL LB/kanamycin medium was inoculated with 8 mL of ONC. Cultures were grown at 37 °C to an OD₆₀₀ of around 0.6. The heterologous protein expression/light production was then induced by addition of 0.1 mM IPTG and the cells were further grown for approximately 44 hrs at 28 °C (temperature for highest and longest light emission for up to 48 hrs). The cells were then harvested by centrifugation (4500 g, 10 min, at 4 °C) and the wet cell pellets were stored at -20 °C until further use.

5.3.5. Extraction of myrFMN and other flavin derivatives

The frozen cell pellets were thawed at room temperature and suspended in lysis buffer (50 mM NaH₂PO₄, 300 mM NaCl, 10 mM imidazole, pH 8) and a spatula tip of lysozyme was added (approximately 10 mg). The cell suspension was stirred at room temperature for 30 min followed by further cell lysis via ultra-sonication (120 Watt) for 3 min (repeated three times with 3 min of cooling between sonication) using a Rosetta cell in an ice water bath. The lysed cells were centrifuged at 38500 g at 4 °C for 30 min to remove large debris and insoluble proteins and aggregates. The supernatant was used for further isolation steps.

For the extraction, three main steps were performed analogous to the extraction of myrFMN *in vivo* [21]. 2.5 g guanidine-HCl were added to the supernatant followed by dropwise addition of concentrated HCl to lower the pH to 2. Three consecutive extractions were performed with 15 mL each of an organic mixture of ethyl acetate:butanol (1:1). The organic phase was separated by centrifugation (4566 g at 4 °C for 30 min) and the unified organic layers were dried in a vacuum evaporator at 56 °C under reduced pressure. The residual powder was dissolved in 20 mL lysis buffer and incubated with an excess of recombinant histidine-tagged apo-LuxF for 30 min in the dark. The apo-LuxF with bound flavin derivative

was loaded on a 5 mL HisTrap FF/HP column (GE Healthcare, Chicago, Illinois, USA) for affinity-tag-purification. The column was washed with wash buffer (50 mM NaH₂PO₄, 300 mM NaCl, 20 mM imidazole, pH 8) and the fractions were eluted with elution buffer (50 mM NaH₂PO₄, 300 mM NaCl, 300 mM imidazole, pH 8). The eluent fractions were pooled and concentrated to 500 µL. As a final purification step organic extraction was repeated again in small scale with 400 µL of organic solvent as described above. The dried samples were analyzed by HPLC.

5.3.6. *In vivo* activity assay for bacterial bioluminescent strains and modified *E. coli* strains

The plate reader assay combines two methods (bioluminescence emission measurement [counts/s] and cell density measurement at 650 nm) by using a customized script combining these measurement types. The exact sample preparation steps and the utilized methods and script mode were described previously [26]. The measurement of the optical density was performed at 650 nm to avoid crosstalk or interference with the light emission.

The bioluminescent bacterial strain or modified *E. coli* strain were streaked on agar plates and incubated at 28 °C overnight. To be able to compare bioluminescent bacterial strains and modified *E. coli* strains, the temperature and the medium should be the same. An overday culture (ODC) of 4 mL of either artificial sea water medium or LB medium was inoculated with a single colony from the corresponding agar plate (for the modified *E. coli* strain the addition of the antibiotic kanamycin (50 µg/mL) is necessary) and incubated at 28 °C, 180 rpm for approximately three hours. The cell density of a 1:10 dilution of the ODC at 650 nm was determined. The dilution factor was calculated to reach a final starting OD₆₅₀ of 0.05 in a volume of 1 mL medium. The determined volume of culture and medium were directly pipetted into a 24-well black-walled plate with glass bottom (Greiner Bio-One, Kremsmünster, Austria) and the measurement using a FLUOstar plate reader (BMG Labtech, Ortenberg, Baden-Wuerttemberg, Germany) was initiated. For each strain three biological replicates with four technical replicates each were analyzed. Blank measurements utilizing not-inoculated medium were always implemented. Data analysis was performed via the MARS analysis software, Excel and Origin. Blank values were subtracted from measurement values followed by calculation of the mean value and standard deviation of each biological replicate.

5.4. Results

Recent studies in our laboratory have provided evidence that myrFMN is generated during the luciferase reaction and exhibits inhibitory properties on the luciferase [21,24]. Since LuxF was found to bind four molecules of myrFMN per homodimeric LuxF, we reasoned that the function of LuxF might be the scavenging of myrFMN to prevent inhibition of the luciferase. In order to investigate this potential function of LuxF, we generated an *E. coli* based gene

expression system containing the whole *lux-rib* operon with the added advantage to simplify modifications of the *lux-rib* operon, *i.e.* investigate the function of LuxF by deleting *luxF* in the *lux-rib* operon. For the primary design of the *lux-rib* operon embedded in the pET28a vector, the sequence information from the bioluminescent bacterial strain *Photobacterium leiognathi* subsp. *mandapamensis* 27561 was used. Gibson assembly has shown to be a suitable cloning strategy for larger vector constructs with a high number of genes [29–31]. The conserved gene order of the *lux-rib* operon was maintained as found in the original sequences. Therefore, also original noncoding sequences between single genes were added to the operon constructs. Several fragments (with and without *luxF*) *luxCDAB*, *luxF*, *luxEG* and *ribEBH* with 20-40 base pair overlapping sequences were generated. Utilization of a Gibson assembly master mix allowed the easy fusion of all fragments and vector in the correct order [28]. The vector maps of the final constructs are depicted in the supplement (Figure S1). These pET28a vectors harboring complete *lux-rib* operons enabled controlled induction of gene expression using IPTG under standard growth conditions. Furthermore, this strategy allows the deletion or exchange of a single gene within a *lux-rib* operon opening up new possibilities for diverse studies comparing different gene variants within the various *lux* operons. In this study, we focused on the *luxF* gene, the protein LuxF and its potential influence on the intensity of bioluminescence.

A previously established and reported plate reader assay was used to measure light intensity of modified *E. coli* cultures and the respective cell density [26]. A customized plate reader script combined both measurements and collected data points every 10 min over 10 hrs (see Supplementary Information). Reference and blank measurements were performed to exclude unusual growth behavior of *E. coli* cells or basal (not induced) gene expression and the corresponding light emission. *E. coli* BL21 cells, *E. coli* BL21 cells containing an empty pET28a vector and *E. coli* BL21 cells containing the pET28a vector with the *lux-rib* operon (*luxF*⁺ and *luxF*) but without induction (no IPTG was added) were analyzed. The growth rates of the *E. coli* cultures were not influenced and showed the expected sigmoidal behavior. In the case of *E. coli* BL21 cells, harboring the *lux-rib* operon, bioluminescence was observed even without induction. This background bioluminescence appeared due to leakiness of the T7 promoter. But the onset of light emission occurred at 4.5 hrs and with very low light intensity (ca. 4-fold less) compared to the induced system (Supplement, Figure S2).

The comparison of the *E. coli* based *lux-rib* gene expression system, with and without *luxF*, confirmed the hypothesis that LuxF is beneficial for the bioluminescence intensity. As shown in Figure 1, *luxF* exhibited no influence on the growth behavior of the *E. coli* cells (Figure 1, panel A), but the maximal light intensity of *luxF*⁺ expression cultures was higher compared to those lacking *luxF* (Figure 1, panel B). Figure 1, panel C represents relative light units (RLU/OD) where the bioluminescence is normalized to the optical density, displaying the same tendency as panel B. These results further substantiate earlier observations that LuxF has a positive impact on bioluminescence emission. Our approach enabled us to demonstrate that within an *E. coli* based *lux-rib* gene expression system the presence of *luxF* enhances light intensity by a factor of 1.5 (Fig 1).

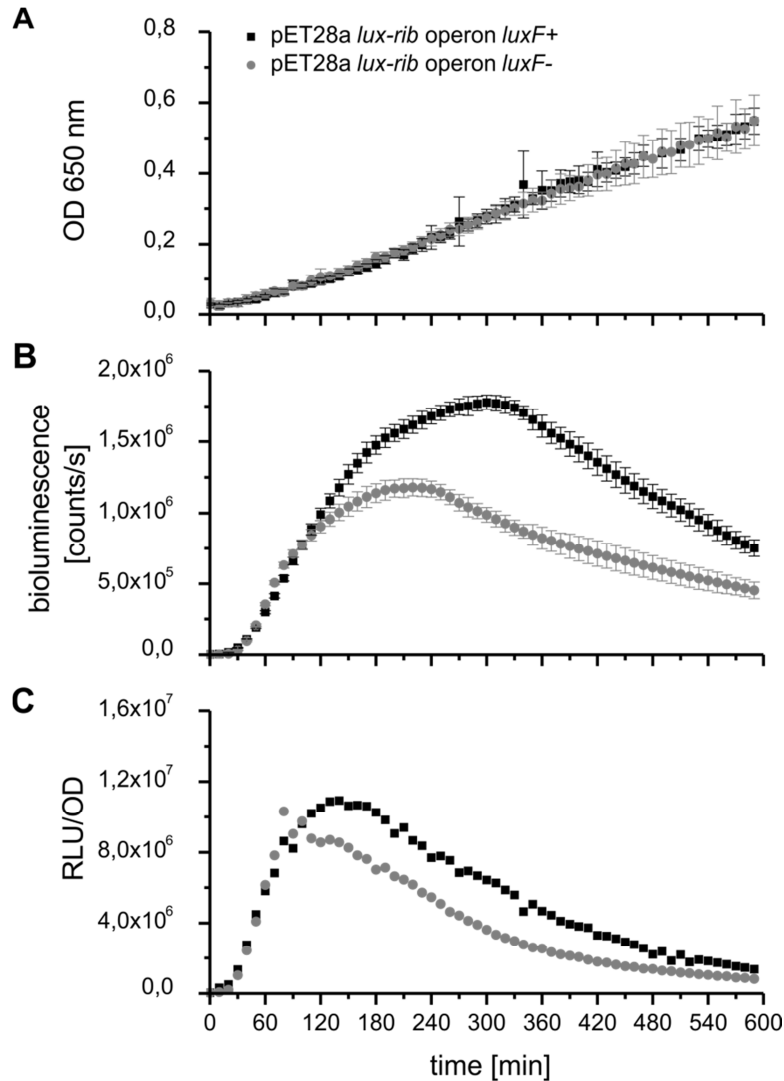


Figure 1: Comparison of growth curves and light intensities of *E. coli* based *lux-rib* gene expression system in LB medium. The OD₆₅₀ and the bioluminescence intensity [counts/s] were measured every 10 min over 10 hrs at 28 °C. All measurements are mean values of three biological replicates with four technical replicates each. Error bars represent standard deviations. *E. coli* BL21 cells containing the pET28a vector with the *lux-rib* operon insert with *luxF* (*luxF+*; black squares) and without *luxF* (*luxF-*; grey circles) were analyzed. **A:** Comparison of the optical densities at 650 nm. **B:** Comparison of bioluminescent light intensities [counts/s]. **C:** Comparison of relative light intensities (RLU/OD; bioluminescence normalized to cell density).

In our previous studies, the generation and properties of the unusual byproduct of the bioluminescent reaction and inhibitor of the luciferase, 6-(3'-(*R*)-myristyl)-FMN (myrFMN), was the focus of our interest [21,24]. Therefore, the question arose, if this flavin derivative is also formed in our *E. coli* based *lux-rib* gene expression system. To address this question, we have performed large-scale expressions using the *lux-rib* operon expression system. In order to analyze flavin derivatives generated during bioluminescence in *E. coli* host cells, a previously reported isolation protocol, combining organic extraction and exploiting the binding affinity to histidine-tagged apo-LuxF, was utilized [21,24]. Surprisingly, our analysis

revealed not only the existence of myrFMN but also two other flavin derivatives. As shown in Fig. 2A, the three flavin derivatives featured similar retention times and similar UV/Vis absorption properties (inserts in Fig. 2B-D). Following preparative HPLC separation the combined fractions containing either peak 1, 2 or 3 (Fig. 2A) were subjected to mass spectrometry. The obtained m/z values were determined as 681.3, 695.3 and 737.3, respectively, for the molecular weight minus one hydrogen atom in negative scan mode. As a first assumption, the UV/Vis absorption properties as well as the masses would fit nicely to different fatty acid chains attached to the C-6 position of the isoalloxazine system (indicated as structure as insert in Fig. 2A).

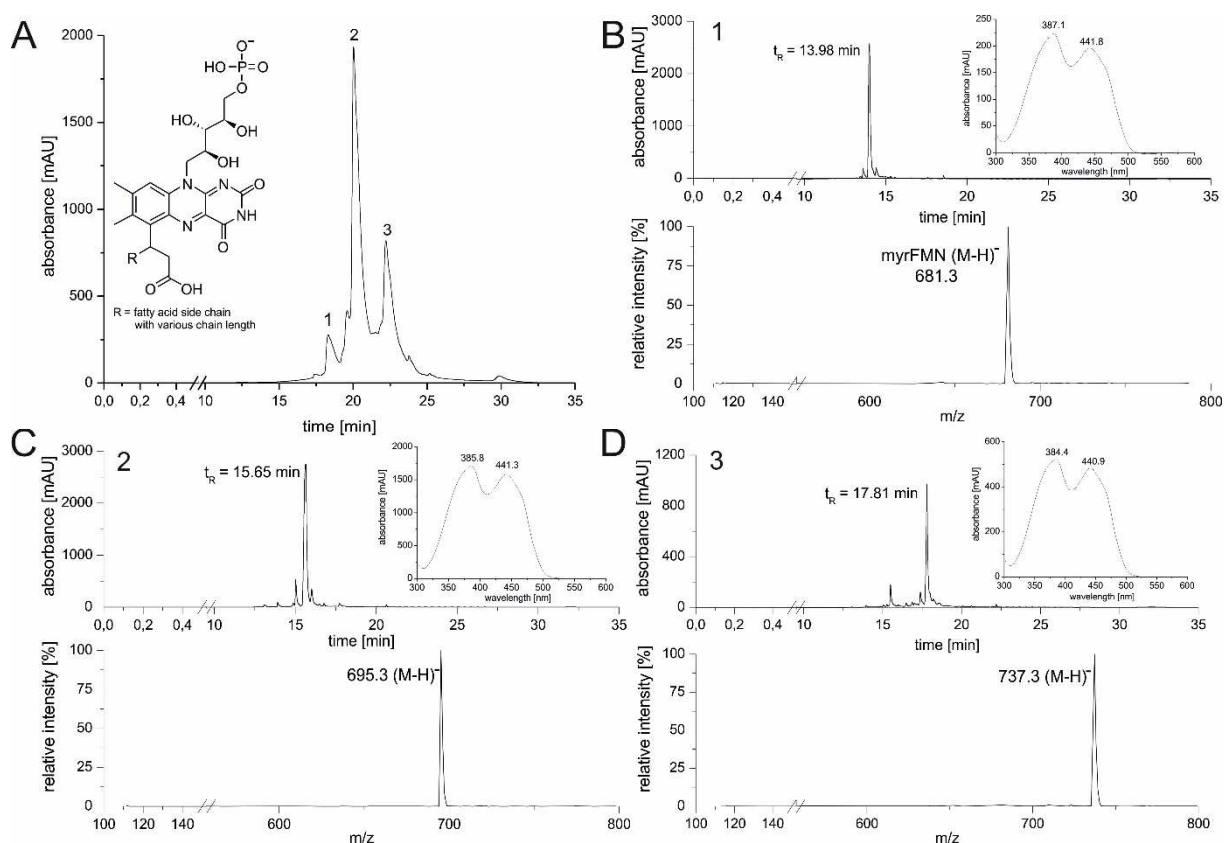


Figure 2: HPLC-UV/Vis and HPLC-MS analysis of isolated flavin derivatives as side products of the bioluminescent reaction. A: HPLC analysis of possible products of the bioluminescent reaction after applied isolation protocol. Three flavin derivatives (1, 2 and 3) were detected. The postulated general structure is depicted in panel A. **B:** HPLC-MS analysis of myrFMN showed a retention time of 13.98 min (upper panel) and spectral maxima at 387.1 and 442.8 nm (insert in upper panel) and a mass to charge ratio of 681.3 (molecular mass minus one hydrogen; lower panel). **C:** HPLC-MS analysis of compound 2 showed a retention time of 15.65 min (upper panel) and spectral maxima at 385.8 and 441.3 nm (insert in upper panel) and a mass to charge ratio of 695.3 (molecular mass minus one hydrogen; lower panel). **D:** HPLC-MS analysis of compound 3 showed a retention time of 17.81 min (upper panel) and spectral maxima at 384.4 and 440.9 nm (insert in upper panel) and a mass to charge ratio of 737.3 (molecular mass minus one hydrogen; lower panel).

To get an idea of the molecular structures of the potential new flavin derivatives, NMR measurements were performed. Owing to the low yield of the derivatized flavins only the major fraction (compound 2) could be analyzed by one and two-dimensional NMR spectroscopy (see Figure 3 and Supplementary Figures S4-S6). Nevertheless, NMR measurements of all three isolated flavin derivatives showed the same pattern, for example a signal for the proton at the C-6 position was only detected in FMN (used as reference) confirming the position of the attachment of the aliphatic acid. The two methyl groups at positions 7 and 8 of the isoalloxazine ring were detected in all compounds. Due to the low concentrations of the isolated flavin derivatives, other protons could not be assigned. A clear difference between FMN and the isolated flavin derivatives was the presence of the fatty acid side chain, however, the exact number of hydrogen atoms and therefore the length and composition of the side chain could not be determined.

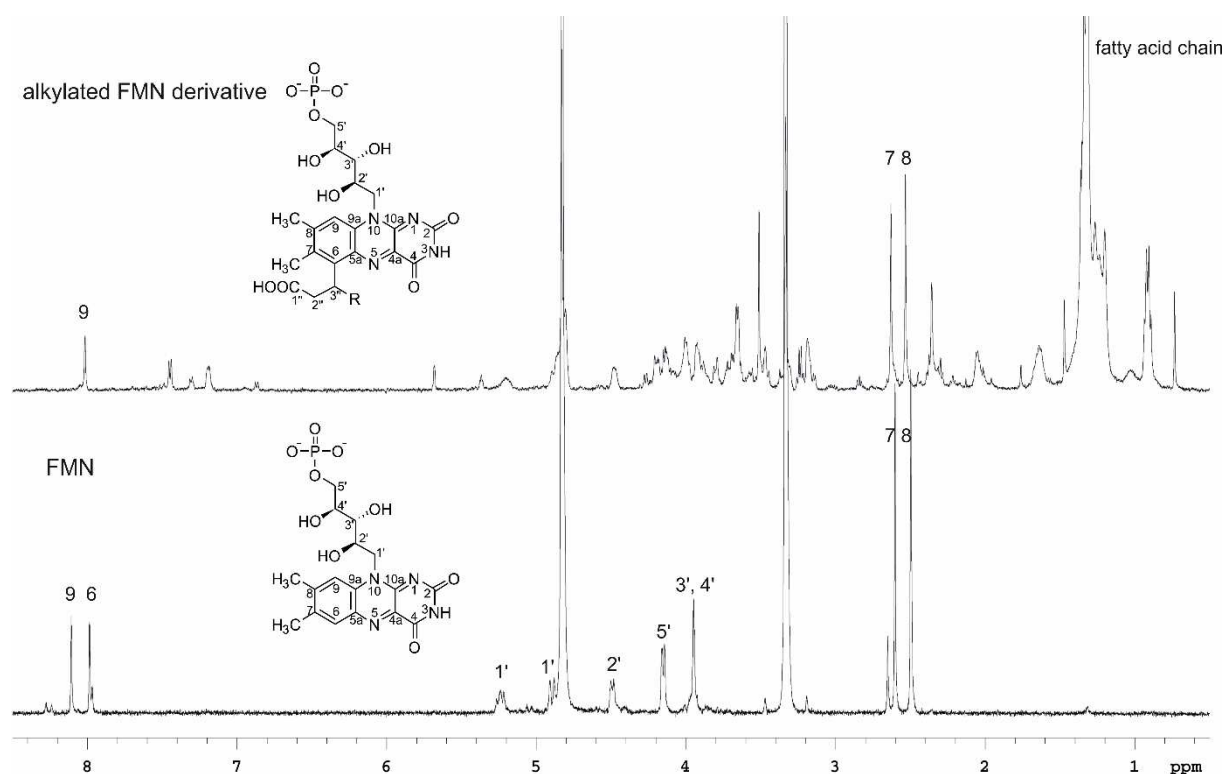


Figure 3: Comparison of the $^1\text{H-NMR}$ -spectra of alkylated FMN derivative (compound 2) and FMN. For both measurements the most prominent peaks were assigned with the corresponding number of the atom position of the chemical structure, depicted as insert.

5.5. Discussion

Functional studies of genes and the encoded proteins by genetic deletion or insertion have not been reported for bioluminescent bacteria probably because many species in the genera *Vibrio* and *Photobacterium* possess multiple resistances against many commonly used antibiotics. Furthermore, basic genetic tools like specific plasmids and transformation protocols for bioluminescent bacteria are not available and they are difficult to transform with vectors designed for *Escherichia coli* and other genetic model organisms. Therefore, we have adopted the inverse approach to gain more insight into the role of *luxF* by transforming *E. coli* with the *lux-rib* operon of *P. leiognathi* subsp. *mandapamensis* 27561 [26]. This bears several advantages such as the availability of ready-to-use plasmids for heterologous gene expression and easy manipulation of the plasmid in terms of the composition of genes being expressed. Furthermore, the expression is inducible and not under the control of specific mechanisms, such as quorum sensing typically found in bioluminescent bacteria [32]. In addition, *E. coli* is easy to cultivate and therefore the handling and growth does not depend on complex media (*i.e.* sea water or alternatives thereof).

Our results have shown that LuxF had a significant influence on the maximal light intensity by a factor of 1.5. This indicates that the presence of LuxF leads to the removal of myrFMN from the bioluminescence light production machinery and hence prevents the inhibition of the luciferase. We were able to track this inhibitory relieving effect in our experiments, while measuring the light emission over time. In these experiments we detected an effect of LuxF on light intensity which occurred first after approximately two hours. This observation suggests that the amount of myrFMN accumulates slowly over time and the inhibitory relieving effect of LuxF can primarily be detected after the amount of myrFMN in the cells reaches a critical concentration leading to luciferase inhibition and thereby to a decrease of total light emission. Whether myrFMN is directly transferred to LuxF from the active site of the luciferase or is scavenged by LuxF after release from the luciferase remains to be investigated.

In a previous study we have shown that myrFMN is produced as a side product of the bioluminescent reaction *in vivo* as well as *in vitro* [21,24]. In the present study, HPLC-UV/Vis, HPLC-MS and NMR measurements confirmed the structure of myrFMN. Additionally, two other flavin derivatives were detected as side products of the bioluminescent reaction in *E. coli* and their structure was also examined by the same combination of methods. Since the generation of the FMN derivative was shown to occur in the bioluminescent reaction, *i.e.* in the oxidation of the long-chain fatty aldehyde to the corresponding acid, we propose that the other two FMN derivatives are also produced in the active site of the luciferase. From this it follows that not only myristoyl aldehyde but also other aldehydes are provided as substrates for the luciferase, which was shown to accept a variety of aldehydes with different chain lengths [1,2,33–35]. In bioluminescent bacteria the major source for the long-chain fatty aldehyde substrate is the fatty acid synthase (FAS) complex from which the LuxCDE complex downloads myristoyl-CoA for further reduction to the aldehyde at the

expense of NADPH [4,36–45]. Thus, the finding that various flavin derivatives are produced raises the question of the source of aldehydes in bioluminescent *E. coli*. The relative low abundance of myrFMN may indicate that the LuxCDE complex does not preferentially download myristoyl-CoA from the FAS but reduces free fatty acid CoA derivatives available in the cell. Due to the mass difference determined by HPLC-MS analysis, compared to FMN or myrFMN, we first assumed pentadecanoylFMN and stearoylFMN, respectively, to be the two newly identified flavin derivatives (compound 2 and 3). In other words, pentadecanal and octadecanal would be the substrates converted by the luciferase and accounting for the production of new flavin derivatives. According to a fatty acid composition analysis in *E. coli* cells under various growth conditions and temperatures, the amounts of myristic acid are always below 10% while those for octadecenoic acid were around 30-35% and pentadecanoic acid was not even detected [46]. Therefore, it is unlikely that the *E. coli* FAS provides pentadecanoyl-CoA leading to the production of pentadecanal, which obviously seemed to be the substrate mostly turned over by the luciferase as judged from the prevalence of compound 2.

Due to the low yield of isolated flavin derivatives and detailed one and two-dimensional NMR spectroscopy of only one of the three compounds, no further conclusions and structural information could be drawn from these measurements. Therefore, the exact molecular structures of these flavin derivatives remain subject of speculations. Further in-depth analyses are needed to elucidate not only the nature of these compounds but also their function and formation mechanism.

5.6. Conclusion

Introduction of the complete *lux-rib* operon of a bioluminescent bacterial strain into a single expression vector enables an *E. coli* based *lux-rib* gene expression system. This setup allows fast and easy exchange of either single or multiple genes of the *lux* operon within the expression system. This method can be exploited to analyze the interplay of Lux proteins and their effects on light intensity [26]. In this study, we focused on investigating the *lux-rib* operon of *Photobacterium leiognathi* subsp. *mandapamensis* 27561 especially in terms of light production and as a function of *luxF*. This was achieved by comparing *lux-rib* operon expression systems with and without *luxF*. Plate reader assays combining the measurements of light intensity and growth curves revealed that the *luxF* gene had no influence on the growth behavior but a significant impact on the maximal light intensity. The presence of LuxF during the bioluminescent reaction increases the maximum light emission of the *E. coli* expression system by a factor of 1.5. Thus, our results further support the hypothesis that LuxF supports luciferase activity by alleviating the inhibition caused by myrFMN. In addition, the *E. coli* based *lux-rib* gene expression system was analyzed concerning the ability to produce flavin derivatives, *i.e.* 6-(3'-(*R*)-myristyl)-FMN. Analysis by UV/Vis absorption spectroscopy and mass spectrometry revealed the presence of three different flavin derivatives. Subsequent NMR measurements confirmed the assumption that these three

compounds are alkylated FMN derivatives, but could not elucidate the molecular structure in detail. Therefore, the exact formula as well as the possible function of these newly detected molecules remains elusive.

Author contribution

EB and JN designed the constructs and experiments. EB and CH performed the plate reader assays and isolated the flavin derivatives. EB performed all HPLC measurements and analyzed the data. HW performed NMR measurements. EB, JN and PM wrote the manuscript.

Acknowledgments

This work was supported by the Austrian “Fonds zur Förderung der wissenschaftlichen Forschung” (FWF) through the PhD program (Doktoratskolleg) “Molecular Enzymology” to PM (W901).

Conflict of interest

The authors declare no conflict of interest.

5.7. References

- [1] Hastings JW, Spudich J, Malnic G. The influence of aldehyde chain length upon the relative quantum yield of the bioluminescent reaction of *Achromobacter fischeri*. J Biol Chem 1963;238:3100–5.
- [2] Ulitzur S, Hastings JW. Evidence for tetradecanal as the natural aldehyde in bacterial bioluminescence. Proc Natl Acad Sci USA 1979;76:265–7.
- [3] Kurfürst M, Ghisla S, Hastings JW. Characterization and postulated structure of the primary emitter in the bacterial luciferase reaction. Proc Natl Acad Sci USA 1984;81:2990–4.
- [4] Meighen EA. Bacterial bioluminescence: organization, regulation, and application of the lux genes. FASEB J 1993;7:1016–22.
- [5] Mitchell GW, Hastings JW. Light-Induced Bioluminescence. Isolation and Characterization of a Specific Protein Involved in the Absorption and Delayed Emission of Light. Biochemistry 1970. doi:10.1021/bi00815a018.
- [6] Moore SA, James MNG, O’Kane DJ, Lee J. Crystallization of *Photobacterium leiognathi* non-fluorescent flavoprotein with limited sequence identity to bacterial luciferase. J Mol Biol 1992;224:523–6.
- [7] Moore SA, James MNG, O’Kane DJ, Lee J. Crystal structure of a flavoprotein related to the subunits of bacterial luciferase. EMBO J 1993;12:1767–74.
- [8] Kita A, Kasai S, Miyata M, Miki K. Structure of flavoprotein FP390 from a luminescent bacterium *Photobacterium phosphoreum* refined at 2.7 Å resolution. Acta Crystallogr Sect D Biol Crystallogr 1996;52:77–86. doi:10.1107/S0907444995009796.
- [9] Kita A, Kasai S, Miki K. Crystal structure determination of a flavoprotein FP390 from a luminescent bacterium, *Photobacterium phosphoreum*. J Biochem 1995;117:575–8.
- [10] Kasai S, Matsui K, Nakamura T. Purification and some properties of FP390 from *P. phosphoreum*. In: Edmondson DE, McCormick DB, editors. Flavins and Flavoproteins, Berlin/New York: Walter de Gruyter; 1987, p. 647–50.
- [11] Kasai S, Fujii S, Miura R, Odani S, Nakaya T, Matsui K. Structure of FP390 including its prosthetic group (Q-flavin): physiological significance of light emitting reaction in luminous bacteria. In: Curti B, Ronchi S, Zanetti G, editors. Flavins and Flavoproteins, Walter de Gruyter; 1991, p. 285–8.
- [12] Raibekas AA. Green flavoprotein from *P. leiognathi*: Purification, characterization and identification as the product of the *lux G(N)* gene. J Biolumin Chemilumin 1991:169–76.
- [13] Illarionov BA, Blinov VM, Donchenko AP, Protopopova M V, Karginov VA, Mertvetsov NP, et al. Isolation of bioluminescent functions from *Photobacterium leiognathi*: analysis of *luxA*, *luxB*, *luxG* and neighboring genes. Gene 1990;86:89–94.

- [14] Baldwin TO, Devine JH, Heckel RC, Lin JW, Shadel GS. The complete nucleotide sequence of the *lux* regulon of *Vibrio fischeri* and the *luxABN* region of *Photobacterium leiognathi* and the mechanism of control of bacterial bioluminescence. *J Biolumin Chemilumin* 1989;4:326–41. doi:10.1002/bio.1170040145.
- [15] Mancini JA, Boylan M, Soly RR, Graham AF, Meighen EA. Cloning and expression of the *Photobacterium phosphoreum* luminescence system demonstrates a unique *lux* gene organization. *J Biol Chem* 1988;263:14308–14.
- [16] Soly RR, Mancini JA, Ferri SR, Boylan M, Meighen EA. A new *lux* gene in bioluminescent bacteria codes for a protein homologous to the bacterial luciferase subunits. *Biochem Biophys Res Commun* 1988;155:351–8.
- [17] Moore SA, James MNG. Common structural features of the luxF protein and the subunits of bacterial luciferase: Evidence for a ($\beta\alpha$)₈ fold in luciferase. *Protein Sci* 1994;3:1914–26.
- [18] Ast JC, Dunlap P V. Phylogenetic analysis of the *lux* operon distinguishes two evolutionarily distinct clades of *Photobacterium leiognathi*. *Arch Microbiol* 2004;181:352–61. doi:10.1007/s00203-004-0663-7.
- [19] Lee CY, Szittner RB, Meighen EA. The *lux* genes of the luminous bacterial symbiont, *Photobacterium leiognathi*, of the ponyfish: Nucleotide sequence, difference in gene organization, and high expression in mutant *Escherichia coli*. *Eur J Biochem* 1991. doi:10.1111/j.1432-1033.1991.tb16269.x.
- [20] Moore SA, James MNG. Structural refinement of the non-fluorescent flavoprotein from *Photobacterium leiognathi* at 1.60 Å resolution. *J Mol Biol* 1995;249:195–214.
- [21] Bergner T, Tabib CR, Winkler A, Stipsits S, Kayer H, Lee J, et al. Structural and biochemical properties of LuxF from *Photobacterium leiognathi*. *Biochim Biophys Acta - Proteins Proteomics* 2015;1854:1466–75. doi:10.1016/j.bbapap.2015.07.008.
- [22] Kasai S. Preparation of P-flavin-bound and P-flavin-free luciferase and P-flavin-bound β -subunit of luciferase from *Photobacterium phosphoreum*. *J Biochem* 1994;115:670–4.
- [23] Wei C-J, Lei B, Tu S-C. Characterization of the binding of *Photobacterium phosphoreum* P-flavin by *Vibrio harveyi* luciferase. *Arch Biochem Biophys* 2001;396:199–206. doi:10.1006/abbi.2001.2612.
- [24] Tabib CR, Brodl E, Macheroux P. Evidence for the generation of myristylated FMN by bacterial luciferase. *Mol Microbiol* 2017;104:1027–36. doi:10.1111/mmi.13676.
- [25] Kaeding AJ, Ast JC, Pearce MM, Urbanczyk H, Kimura S, Endo H, et al. Phylogenetic diversity and cosymbiosis in the bioluminescent symbioses of “*Photobacterium mandapamensis*.” *Appl Environ Microbiol* 2007;73:3173–82. doi:10.1128/AEM.02212-06.

- [26] Brodl E, Niederhauser J, Macheroux P. *In Situ* Measurement and Correlation of Cell Density and Light Emission of Bioluminescent Bacteria. *J Vis Exp* 2018. doi:10.3791/57881.
- [27] Atlas RM. Handbook of microbiological media, third edition. Third Edit. CRC Press; 2004.
- [28] NEB. NEBuilder HiFi DNA Assembly Reaction (E2621) 2015. doi:dx.doi.org/10.17504/protocols.io.cwaxad.
- [29] Gibson DG, Smith HO, Hutchison CA, Venter JC, Merryman C. Chemical synthesis of the mouse mitochondrial genome. *Nat Methods* 2010;7:901–3. doi:10.1038/nmeth.1515.
- [30] Gibson DG, Young L, Chuang RY, Venter JC, Hutchison CA, Smith HO. Enzymatic assembly of DNA molecules up to several hundred kilobases. *Nat Methods* 2009;6:343–5. doi:10.1038/nmeth.1318.
- [31] Gibson DG. Enzymatic assembly of overlapping DNA fragments. *Methods Enzymol* 2011;498:349–61. doi:10.1016/B978-0-12-385120-8.00015-2.
- [32] Miller MB, Bassler BL. Quorum sensing in bacteria. *Annu Rev Microbiol* 2001. doi:10.1146/annurev.micro.55.1.165.
- [33] Hastings JW, Gibson QH. Intermediates in the bioluminescent oxidation of reduced flavin mononucleotide. *J Biol Chem* 1963;238:2537–54.
- [34] Cormier MJ, Totter JR. Quantum efficiency determinations on components of the bacterial luminescence system. *Biochim Biophys Acta* 1957;25:229–37.
- [35] Cormier MJ, Eley M, Abe S, Nakano Y. On the requirement and mode of action of long-chain aldehydes during bacterial bioluminescence. *Photochem Photobiol* 1969;9:351–8.
- [36] Ferri SR, Meighen EA. A *lux*-specific myristoyl transferase in luminescent bacteria related to eukaryotic serine esterases. *J Biol Chem* 1991;266:12852–7.
- [37] Janßen HJ, Steinbüchel A. Fatty acid synthesis in *Escherichia coli* and its applications towards the production of fatty acid based biofuels. *Biotechnol Biofuels* 2014. doi:10.1186/1754-6834-7-7.
- [38] Carey LM, Rodriguez A, Meighen E. Generation of fatty acids by an acyl esterase in the bioluminescent system of *Photobacterium phosphoreum*. *J Biol Chem* 1984;259:10216–21.
- [39] Lawson DM, Derewenda U, Serre L, Wei Y, Derewenda ZS, Ferri S, et al. Structure of a myristoyl-ACP-specific thioesterase from *Vibrio harveyi*. *Biochemistry* 1994;33:9382–8. doi:10.1021/bi00198a003.
- [40] Wall L, Meighen EA. Subunit structure of the fatty acid reductase complex from *Photobacterium phosphoreum*. *Biochemistry* 1986;25:4315–21. doi:10.1021/bi00363a021.

- [41] Soly RR, Meighen EA. Identification of the acyl transfer site of fatty acyl-protein synthetase from bioluminescent bacteria. *J Mol Biol* 1991;219:69–77. doi:10.1016/0022-2836(91)90858-4.
- [42] Wall L, Rodriguez A, Meighen E. Intersubunit transfer of fatty acyl groups during fatty acid reduction. *J Biol Chem* 1986;261:15981–8.
- [43] Lee CY, Meighen EA. Cysteine-286 as the site of acylation of the Lux-specific fatty acyl-CoA reductase. *Biochim Biophys Acta - Protein Struct Mol Enzymol* 1997;1338:215–22. doi:10.1016/S0167-4838(96)00203-8.
- [44] Rodriguez A, Riendeau D, Meighen E. Purification of the acyl coenzyme A reductase component from a complex responsible for the reduction of fatty acids in bioluminescent bacteria. *J Biol Chem* 1983;258:5233–7.
- [45] Fujita Y, Matsuoka H, Hirooka K. Regulation of fatty acid metabolism in bacteria. *Mol Microbiol* 2007. doi:10.1111/j.1365-2958.2007.05947.x.
- [46] Marr AG, Ingraham JL. Effect of temperature on the composition of fatty acids in *Escherichia coli*. *J Bacteriol* 1962. doi:10.1038/npre.2008.1909.1.

5.8. Supplement

Table S1: Primers used for PCR of *lux-rib* operon fragments of *Photobacterium leiognathi* subsp. *mandapamensis* 27561 with and without *luxF* (adapted from Brodl et al, JoVE 2018 [26])

Oligo name	Sequence 5'-3'
27561_CDAB_fwd (luxF+)	TGTTAACTTTAAGAAGGAGATATA ATGATTA AAAAAGATCCCACTG
27561_CDAB_rev (luxF+)	TCCATTTTGTGCAT TTTTATTATCCTGTTATTTATTAT ATAGATTTTTC
27561_F_fwd (luxF+)	CAGGATAATAAAAA ATGACAAAATGGAATTATGGC
27561_F_rev (luxF+)	TGACTTAACTGAAT TAGTTAAGGTTGTGTTCTTTTC
27561_EG_fwd (luxF+)	CAACCTTAACTAA TCAGTTAAGTCAATTTAAATTA AAAC
27561_EG_rev (luxF+)	GAATGATTTTAA CTACATATAACTAAACGCATCAG
27561_rib_fwd(luxF+)	TAGTTATATGTAG TAAAAATCATT CATCTCATTATTTATG
27561_rib_rev (luxF+)	ATCTCAGTGGTGGTGGTGGTGGTGGT GCTTAAGGCTCGATT TCTGC
27561_CDAB_fwd (luxF-)	TGTTAACTTTAAGAAGGAGATATA ATGATTA AAAAAGATCCCACTG
27561_CDAB_rev (luxF-)	GCCACACTGCCAT TTTTATTATCCTGTTATTTATTAT ATAGATTTTTC
27561_EG_fwd (luxF-)	CAGGATAATAAAAA ATGGCAGTGTGGCTTCTTAC
27561_EG_rev (luxF-)	GAATGATTTTAA CTACATATAACTAAACGCATCAGA AATAC
27561_rib_fwd(luxF-)	TAGTTATATGTAG TAAAAATCATT CATCTCATTATTTATG
27561_rib_rev (luxF-)	ATCTCAGTGGTGGTGGTGGTGGTGGT GCTTAAGGCTCGATT TCTGC

Primer names are according to the respective *lux* genes amplified during PCR, the red letters indicate the gene specific primers, the black letters the annealing sequence of the adjacent fragment.

Table S2: PCR reaction used prior to Gibson Assembly (adapted from Brodl et al, JoVE 2018 [26])

Phusion Polymerase	
1 x rxn	total 20 μ L
5x Phusion Buffer	4 μ L
dNTPs (2mM)	2 μ L
Primer fwd (10mM)	2 μ L
Primer rev (10mM)	2 μ L
DNA Template	ca. 140 ng
Phusion Polymerase (2U/ μ L)	0.5 μ L
ddH ₂ O	8 μ L

Table S3: PCR program used for amplification of *lux-rib* operon fragments (adapted from Brodl et al, JoVE 2018 [26])

	98°C	30 s	
x35	{ 98°C 56°-58°C 72°C	10 s	gradient in PCR machine
		30 s	
		2.5 min	
	72°C	10 min	
	4°C	hold	

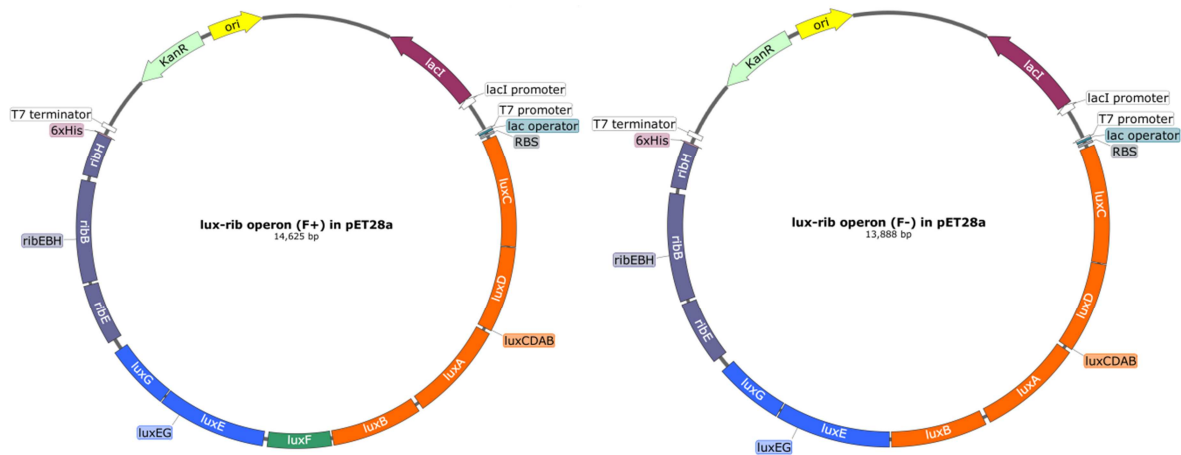


Figure S1: Vector maps of *lux-rib* operon of *Photobacterium leiognathi* subsp. *mandapamensis* 27561 integrated into a pET28a vector via Gibson Assembly; adapted from Brodl et al, JoVE 2018 [26].

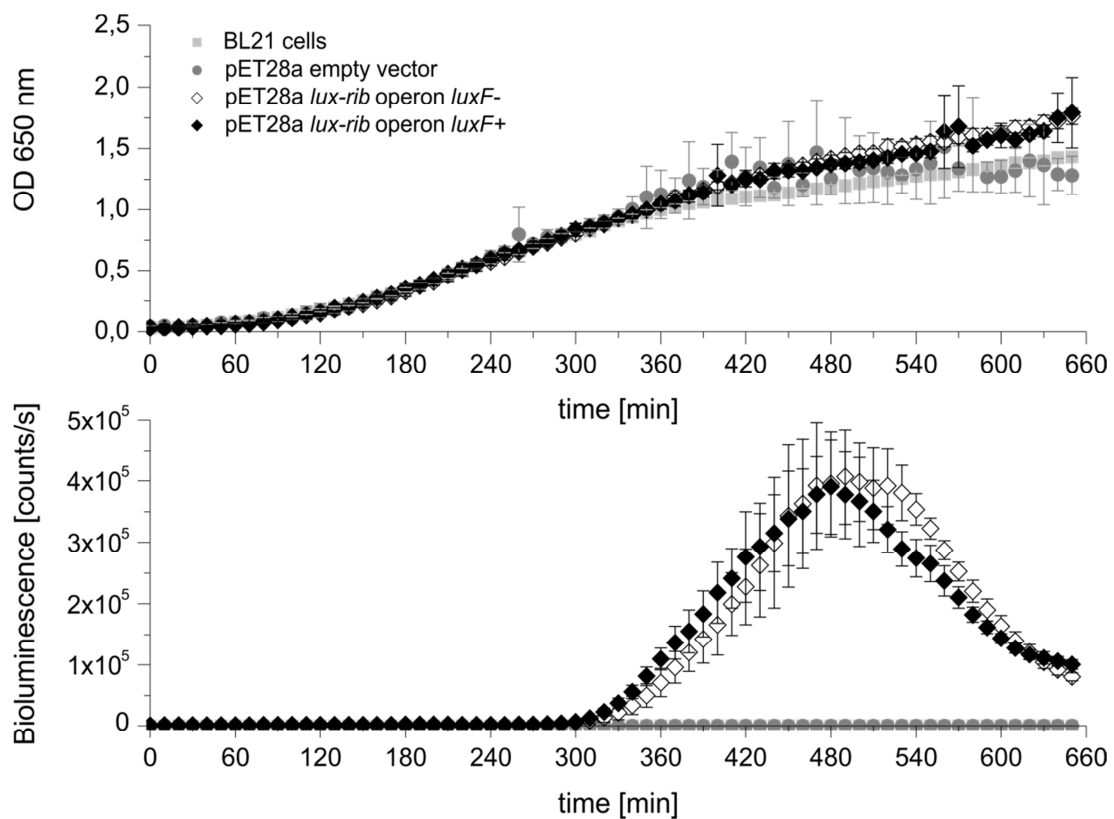


Figure S2: Comparison of growth curves and light intensities of reference strains; adapted from Brodl et al, JoVE 2018 [26]. The OD at 650 nm and the bioluminescence intensity [counts/s] were measured every 10 min over 10 hours at 28 °C. All measurements are mean values of three biological replicates with four technical replicates each. Error bars represent standard deviations. *E. coli* BL21 cells (grey squares), *E. coli* BL21 cells containing an empty pET28a vector (grey circles) and *E. coli* BL21 cells containing the pET28a vector with the *lux-rib* operon insert but without *luxF* (white diamond) and *E. coli* BL21 cells containing the pET28a vector with the *lux-rib* operon insert with *luxF* (black diamonds) were analyzed to assure correct growth behavior of the *E. coli* cells. For the latter two cultures no IPTG was added and observed light emission after 5 hours corresponds to the leakiness of the T7 promoter.

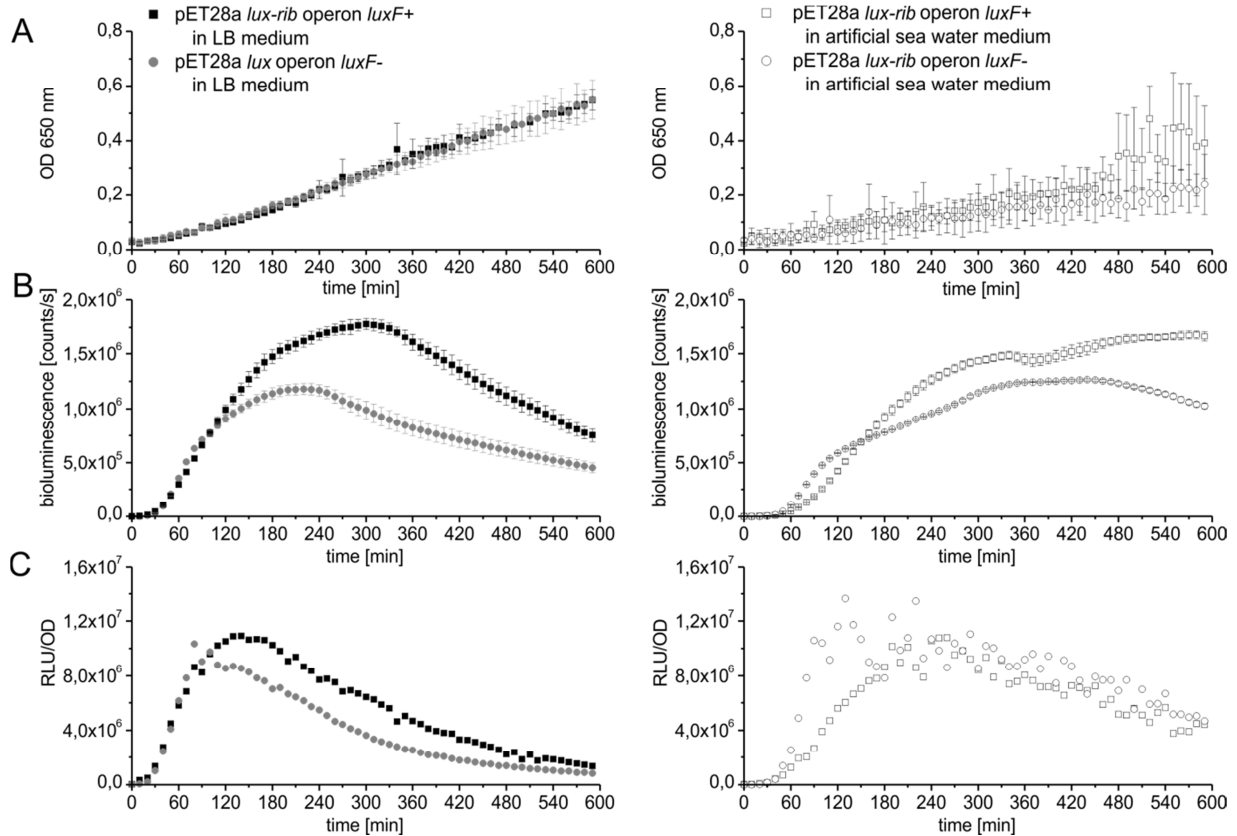


Figure S3: Comparison of growth curves and light intensities of *E. coli* based *lux-rib* gene expression system in LB and artificial sea water medium. The OD at 650 nm and the bioluminescence intensity [counts/s] were measured every 10 min over 10 hours at 28 °C. All measurements are mean values of three biological replicates with four technical replicates each. Error bars represent standard deviations. *E. coli* BL21 cells containing the pET28a vector with the *lux-rib* operon insert once with *luxF* (*luxF+*) (squares) and once without *luxF* (*luxF-*) (circles) were compared with each other in LB medium (filled) and artificial sea water medium (open). **A:** Comparison of the optical densities at 650 nm for the *lux-rib* expression system in *E. coli*. LB medium shows higher cell densities up to 0.6 (left panel, filled squares and circles), while for the artificial sea water medium lower cell densities and higher scattering was observed (right panel, open squares and circles). **B:** Comparison of bioluminescent light intensities [counts/s] for the *lux-rib* expression system in *E. coli*. In both media, *E. coli* cells containing the pET28a vector with the *lux-rib* operon with *luxF* (*luxF+*) (squares) showed higher light intensities than without *luxF* (circles) with a factor of approximately 1.3-1.5, respectively. **C:** Comparison of relative light intensities (RLU/OD; bioluminescence normalized to cell density). For LB medium (left panel, filled squares and circles), the trend determined in panel B was confirmed. For artificial sea water medium (right panel, open squares and circles), again scattering was observed.

Script for plate reader FLUOStar (BMG Labtech) [26]

;Script generated by script wizard (Omega V5.11 R3)

;Protocol Names:

st1:="BIOLUMI"

st2:="OD650"

st3:="SHAKE"

;Plate ID:

ID1:=""

;Number of readings (number of kinetic cycles):

NumberOfReadings:=66

R_Temp 28

wait for temp>=27.9

;;=====

for Reading:=1 to NumberOfReadings do begin ;kinetic loop

ID2:="Wizard script 'LumiOD650', Prot.1"

R_Run "<st1>" ;execute first test protocol

;merge horizontal (kinetic):

if Reading>1 then begin

Call "MergeReadings.exe <DataPath> <User> H ID2"

end;

ID2:="Wizard script 'LumiOD650', Prot.2"

R_Run "<st2>" ;execute second test protocol

;merge horizontal (kinetic):

if Reading>1 then begin

Call "MergeReadings.exe <DataPath> <User> H ID2"

end;

ID2:="Wizard script 'LumiOD650', Prot.3"

R_Run "<st3>" ;execute third test protocol

end; ;end of kinetic loop

;end of script

Figure S4: ^1H NMR of FMN (reference; bottom) and alkylated FMN derivatives with various fatty acid side chains (from top to bottom: myristoylFMN with a mass of 681.3 (M-H) $^-$; alkylated FMN derivative 3 with a mass of 737.3 (M-H) $^-$; alkylated FMN derivative 2 with a mass of 695.3 (M-H) $^-$). The corresponding postulated molecular structures are depicted as inserts. For all four measurements the most prominent peaks were assigned with the corresponding number of the atom position.

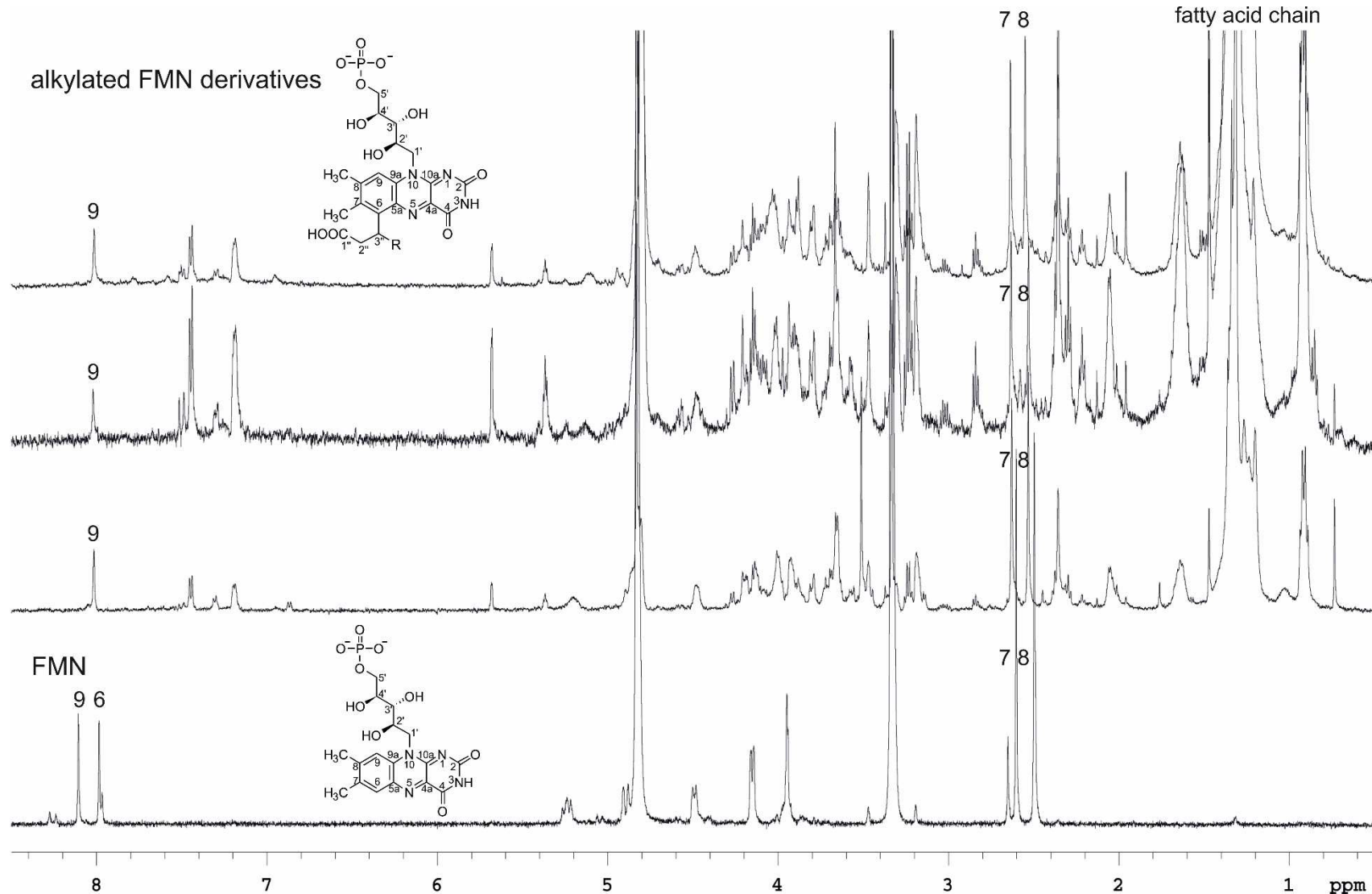


Figure S5: Heteronuclear Single Quantum Coherence (HSQC) measurement (^1H and ^{13}C) of FMN as reference. The corresponding molecular structure is depicted as insert. The annotation follows the corresponding number of the atom position.

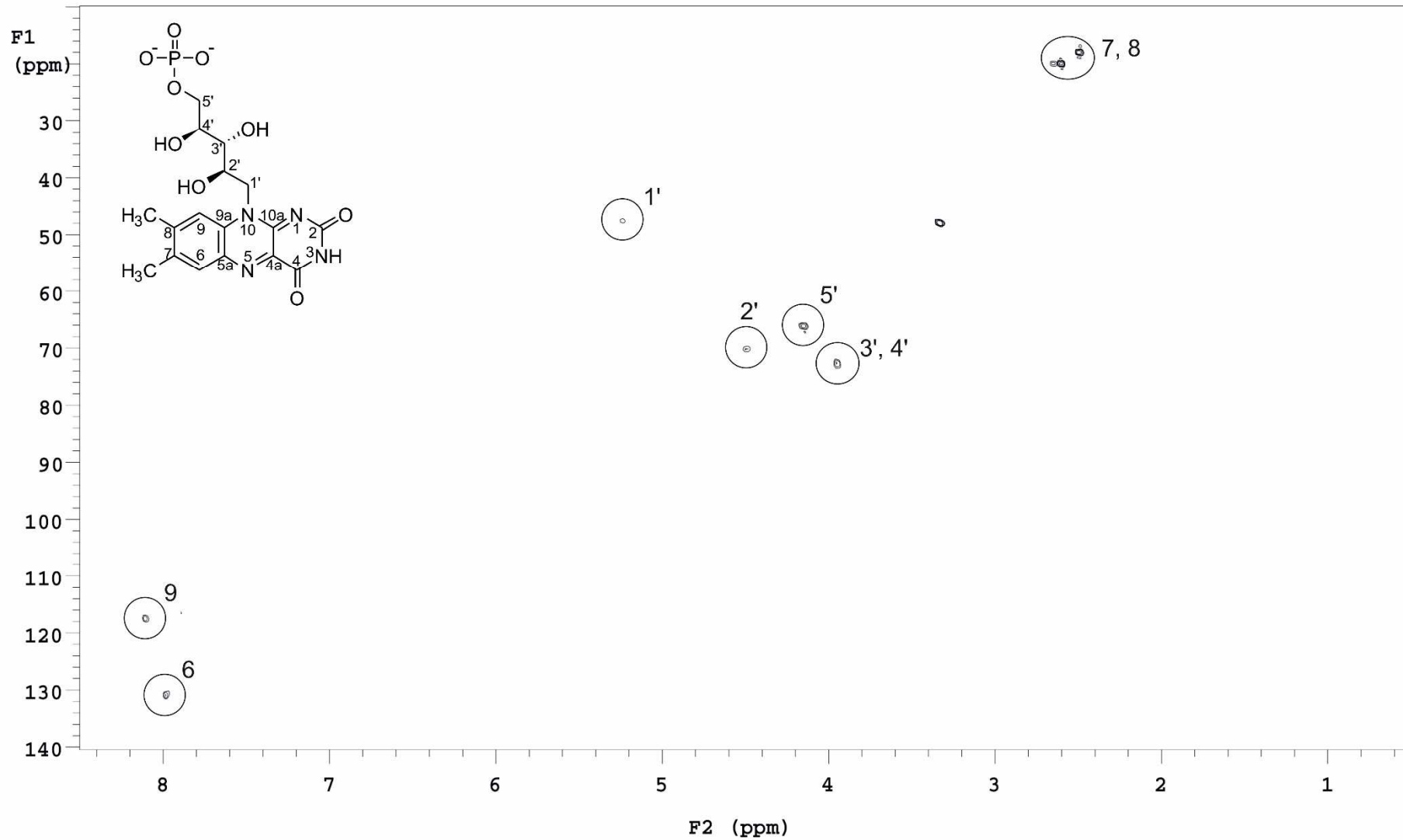
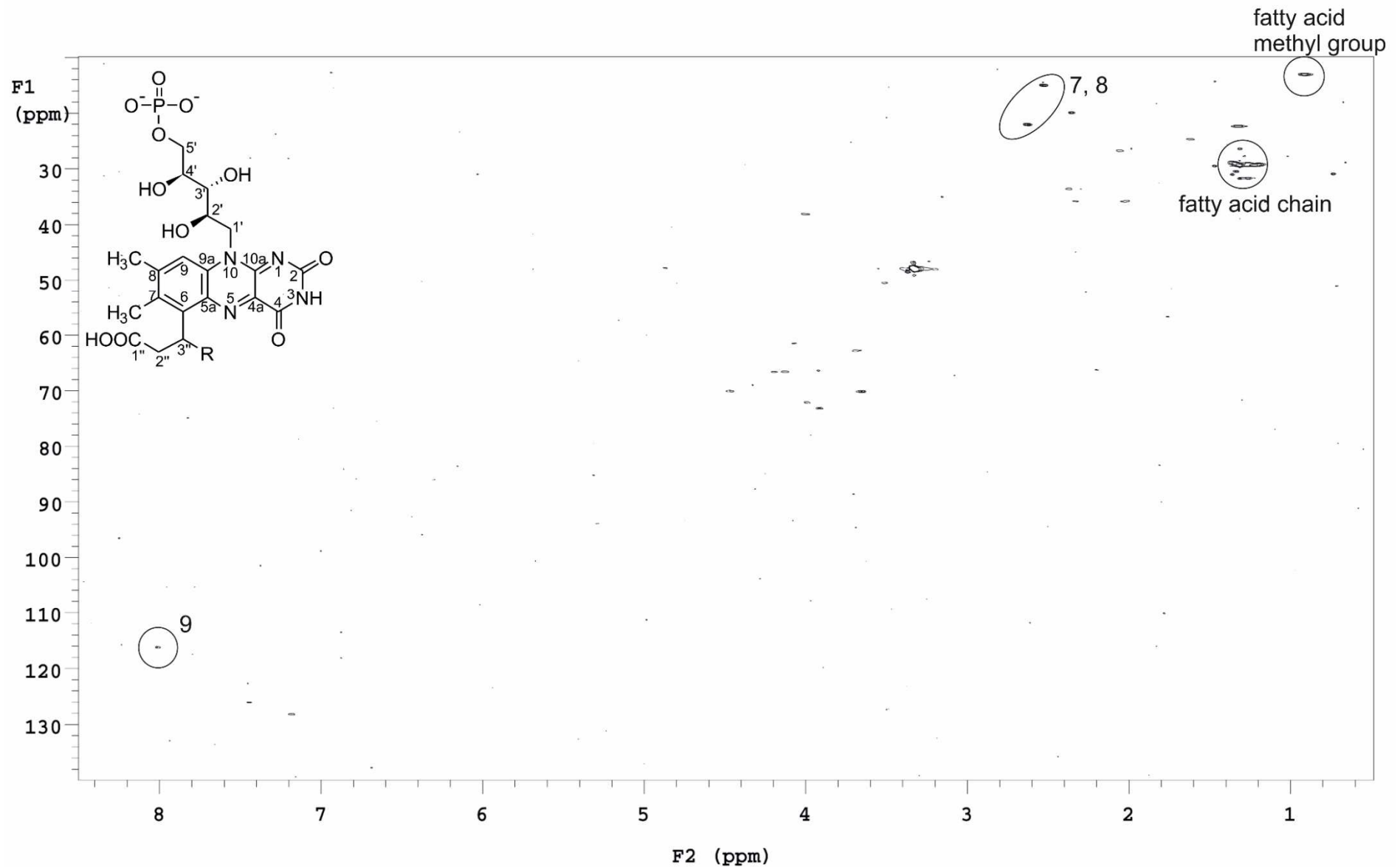


Figure S6: Heteronuclear Single Quantum Coherence (HSQC) measurement (^1H and ^{13}C) of alkylated FMN derivative 2 with the corresponding mass of 695.3 (M-H) $^-$. The proposed molecular structure is depicted as insert. The annotation follows the corresponding number of the atom position.



VI. Conclusion and Outlook

The main focus of my PhD thesis was the elucidation of the function and influence of the protein LuxF and its tightly bound flavin derivative myrFMN on the bacterial bioluminescent reaction and the corresponding enzyme machinery. As a first step we analyzed long-chain α,β -unsaturated aldehydes as possible substrates for the luciferase. These unsaturated aldehydes have an activated C3-carbon atom that could hypothetically explain the formation of the unusual bond of myrFMN between the C3 of the aliphatic acid and the C6 of the isoalloxazine ring. The α,β -unsaturated aldehydes ranging from chain lengths of 8, 10, 12 or 14 carbon atoms were accepted as substrates yielding very low conversions. Supplementary docking studies utilizing the crystal structure of LuxAB of *Vibrio harveyi* (PDB 3FGC) and an *in silico* bound flavin-4a-hydroperoxide intermediate together with various long-chain saturated and unsaturated aldehydes revealed that the spacious active site of the luciferase allows a variety of different binding modes [1]. Although we learned more about the active site of the luciferase and the potentially accepted substrates, the findings we collected during these experiments did not explain the production of the side product myrFMN.

In our next study, we tried to combine *in vivo* and *in vitro* studies to elucidate the role of LuxF in bacterial bioluminescence. Comparison of different bioluminescent bacterial strains revealed that the formation of myrFMN is independent of *luxF* occurrence. Furthermore, myrFMN has a high affinity to the luciferase and tightly binds to the active site thereby inhibiting the bioluminescent reaction. In our lab, we were able to demonstrate that LuxF has an even higher affinity to myrFMN than the luciferase. This characteristic enables LuxF to scavenge myrFMN away from the luciferase thereby preventing the inhibition. A newly developed *in vitro* assay with cofactor recycling system proved that luciferase is responsible for this side product formation and that myrFMN is produced during the bioluminescent reaction. So far, the molecular structure of this flavin derivative was not confirmed although it was already reported three decades ago [2,3]. We were now able to confirm the existence of the myrFMN molecule via HPLC-MS measurement [4]. These results gave first hints on the function of the protein LuxF and the flavin derivative myrFMN.

To determine the effect of LuxF on the bacterial bioluminescent reaction mechanism in greater detail, a method that would simplify experimental setups was implicitly needed. Hence, an *E. coli* based *lux* gene expression system was established. Therefore, the whole *lux-rib* operon was inserted in an expression vector for *E. coli* leading to *E. coli* cultures exhibiting a bioluminescent reaction upon expression-induction. Furthermore, a plate reader assay combining measurements of cell density and light intensity was developed. These novel tools do not only allow exerting an easy and fast analysis of the growth behavior and light emission characteristics of bioluminescent bacterial strains in general, but also to analyze the effect of a single gene being present or absent within the *lux* operon, in our specific case *luxF*. We demonstrated that the presence of *luxF* within the *lux* operon leads to higher light emission compared to *E. coli* cultures containing the vector with the *lux* operon lacking *luxF*. Moreover, we were able to isolate myrFMN from these *E. coli* expression cultures as well as two formerly unknown flavin derivatives. Consequently, the structures of

these three side products were investigated via HPLC and NMR analysis which led to the determination of myrFMN but left the nature of the other two flavin derivative side chains unanswered [3; unpublished manuscript]. Our experimental efforts allowed us to anticipate the role of LuxF and therefore we postulated a synthesis pathway for myrFMN. Nevertheless, the exact interaction or mechanism behind this elevated light emission and the role of LuxF stays obscure.

An interesting aspect, which is still unknown, is the process behind the scavenging of myrFMN from the luciferase by LuxF. A question that arose during our studies was a possible protein-protein complex formation between LuxAB and LuxF. To elucidate this interaction, a stable heterodimeric luciferase is a prerequisite allowing kinetic studies as well as analysis of protein-protein interplay. Alternatively, *in silico* studies using available protein sequences and corresponding structural information allow to hypothetically clarify luciferase active site compositions, charges on the surface of the protein and binding affinities of substrates, cofactors and products. *In silico* would greatly support *in vitro* experimental investigations and help us gain insight in the interplay of Lux proteins. Applying crystallographic methods could further help us to resolve the various mechanisms behind bacterial bioluminescence. Unfortunately, the number of available crystal structures is limited to a very low number of proteins of the *lux* operon, namely LuxAB (*Vibrio harveyi*) (PDB 1LUC/1BRL/3FGC) [6–8], LuxD (*Vibrio harveyi*) (PDB 1THT) [9] and LuxF (*Photobacterium leiognathi*) (PDB 1NFP/1FVP/4J2P) [2,3,10].

The aforementioned structural elucidation of various different bacterial luciferases would help in gaining further insights in the reaction mechanism. Co-crystallization with reaction intermediates would take the knowledge one step further. The bacterial luciferases are unstable proteins which are prone to aggregation during heterologous protein expression. In our crystallization trials mainly the inactive beta-homodimer and not the LuxAB α - β -heterodimer was formed which led to the structural determination of the LuxB₂-complex, which has also been reported earlier (PDB 1XKJ/1BSL) [11,12]. Further trials to crystallize the active bacterial luciferase of *Vibrio harveyi*, which showed highest stability among the various investigated luciferases and a trustworthy experimental ratio of alpha and beta subunit, resulted in solving another beta-homodimer structure (PDB 6FRI). Hence, only the structure of one single bacterial luciferase of *Vibrio harveyi* is known today.

Currently, a master thesis project in our lab is focused on finding a route to the stable expression of α - β -heterodimeric luciferase from *Photobacterium*, *Vibrio* and *Aliivibrio* species. We assume that most likely the less stable α -subunit is degraded during purification steps, which are required for protein crystallization. The beta-homodimer, which showed high stability, accumulates, leading to aggregate formation and subsequently to crystallization of the homo-dimeric complex. This results in a heterologously expressed and *in vitro* used protein sample that contains only a small amount of active enzyme. To circumvent the loss of LuxA during affinity-tag purification, we aim to use a dual tag vector, containing one Streptavidin tag on the N-terminus of the alpha subunit and a Histidine tag on the C-terminus of the beta subunit. Purification only via the first or only via the second

tag or the combination of both tags should allow isolation of an active luciferase with equal distribution of alpha and beta subunits in a heterodimeric complex.

Due to the low stability and thereby decreased activity of our luciferase preparations, kinetic studies were not feasible. Furthermore, the substrates for the bioluminescent reaction, long-chain aliphatic aldehydes, have a very low solubility in buffer systems and thus only suspensions could be prepared. Addition of a defined volume of these suspensions result in an unknown substrate concentration within the reaction mixture [1]. To accurately dissolve long-chain aliphatic aldehydes an organic solvent (*e.g.* methanol) is required. Luciferase protein-preparations proved to not be tolerant to any experimentally investigated organic solvent.

A stable expressed and purified bacterial luciferase would allow further biochemical and structural characterizations such as kinetic assays, interaction studies (LuxAB with LuxG or LuxF or LumP or YFP) and co-crystallization with reaction intermediates. The even more challenging anaerobic crystallization of the luciferase would be feasible with a stable protein-complex. Co-crystallization potentially allows the trapping of reaction intermediates like reduced FMN or the hemiacetal intermediate. If this is even feasible, considering also the need for molecular oxygen to be able to form this latter intermediate, is open for discussion.

Investigation and isolation of the unusual flavin derivatives was possible due to our isolation protocol. The low yields of isolated flavin derivatives were problematic especially during HPLC-MS and further NMR analyses. Although the isolation protocol was established for this purpose, loss of huge amounts of the target molecules along each step of the purification was determined via HPLC-UV/Vis measurements (data not shown). Optimizing this procedure would allow higher yields of isolated flavin derivatives which could be used for in-detail analyses of the molecules, especially the two so far not identified FMN derivatives, as well as for novel protein-activity assays.

The field of bacterial bioluminescence fascinated researches all over the world already over one century. With the discovery of the green fluorescent protein (GFP) and the following Nobel Prize in Chemistry in 2008 to Osamu Shimomura, Roger Tsien and Martin Chalfie the bioluminescent field attracted attention [13]. In a broader perspective this research area has developed in many diverse directions. At the International Conference on Bioluminescence and Chemiluminescence 2018 in Nantes, France, I got a glimpse on the scientific community and their interests. From biologists interested in the bioluminescence of sharks or mushrooms, to analysts and engineers developing new imaging techniques and detection tools based on bioluminescence, basic research focusing on the details of each reaction step in a chemi- or bioluminescent process to kinetic and biochemical analysis of luciferases and luciferins, are just a few examples of this broad field. Although scientists have investigated bioluminescence already over decades, there are still many open questions that need to be answered and this research field will fascinate many more researches in the future.

- [1] Brodl E, Ivkovic J, Tabib CR, Breinbauer R, Macheroux P. Synthesis of α,β -unsaturated aldehydes as potential substrates for bacterial luciferases. *Bioorganic Med Chem* 2017;25. doi:10.1016/j.bmc.2017.01.013.
- [2] Moore SA, James MNG. Structural refinement of the non-fluorescent flavoprotein from *Photobacterium leiognathi* at 1.60 Å resolution. *J Mol Biol* 1995;249:195–214.
- [3] Kita A, Kasai S, Miyata M, Miki K. Structure of flavoprotein FP390 from a luminescent bacterium *Photobacterium phosphoreum* refined at 2.7 Å resolution. *Acta Crystallogr Sect D Biol Crystallogr* 1996;52:77–86. doi:10.1107/S0907444995009796.
- [4] Tabib CR, Brodl E, Macheroux P. Evidence for the generation of myristylated FMN by bacterial luciferase. *Mol Microbiol* 2017;104:1027–36. doi:10.1111/mmi.13676.
- [5] Brodl E, Niederhauser J, Macheroux P. *In Situ* Measurement and Correlation of Cell Density and Light Emission of Bioluminescent Bacteria. *J Vis Exp* 2018. doi:10.3791/57881.
- [6] Fisher AJ, Thompson TB, Thoden JB, Baldwin TO, Rayment I. The 1.5 Å resolution crystal structure of bacterial luciferase in low salt conditions. *J Biol Chem* 1996;271:21956–68. doi:10.1074/jbc.271.36.21956.
- [7] Fisher AJ, Rayment I, Raushel FM, Baldwin TO. Three-dimensional structure of bacterial luciferase from *Vibrio harveyi* at 2.4 Å resolution. *Biochemistry* 1995;34:6581–6. doi:10.1021/bi00020a002.
- [8] Campbell ZT, Weichsel A, Montfort WR, Baldwin TO. Crystal structure of the bacterial luciferase/flavin complex provides insight into the function of the β subunit. *Biochemistry* 2009;48:6085–94. doi:10.1021/bi900003t.
- [9] Lawson DM, Derewenda U, Serre L, Wei Y, Derewenda ZS, Ferri S, et al. Structure of a myristoyl-ACP-specific thioesterase from *Vibrio harveyi*. *Biochemistry* 1994;33:9382–8. doi:10.1021/bi00198a003.
- [10] Bergner T, Tabib CR, Winkler A, Stipsits S, Kayer H, Lee J, et al. Structural and biochemical properties of LuxF from *Photobacterium leiognathi*. *Biochim Biophys Acta - Proteins Proteomics* 2015;1854:1466–75. doi:10.1016/j.bbapap.2015.07.008.
- [11] Tanner JJ, Miller MD, Wilson KS, Tu SC, Krause KL. Structure of bacterial luciferase β 2 homodimer: Implications for flavin binding. *Biochemistry* 1997;36:665–72. doi:10.1021/bi962511x.
- [12] Thoden JB, Holden HM, Fisher a J, Sinclair JF, Wesenberg G, Baldwin TO, et al. Structure of the beta 2 homodimer of bacterial luciferase from *Vibrio harveyi*: X-ray analysis of a kinetic protein folding trap. *Protein Sci* 1997;6:13–23.
- [13] The Nobel Prize in Chemistry 2008. <https://www.nobelprize.org/prizes/chemistry/2008/press-release/>.

VII. List of abbreviations

AA	acrylamide
ACP	acyl carrier protein
APDO	5-amino-6-(D-ribitylamino)uracil
ATCC	American Type Culture Collection
BFP	blue fluorescent protein
BLAST	Basic Local Alignment Search Tool
CaCl ₂	calcium chloride
CaH ₂	calcium hydride
CIEEL	chemically initiated electron exchange luminescence
DAPO	2,5-diamino-6-(5'-phosphoribosylamino)-4-pyrimidineone
DCM	dichloromethane
DHBP	3,4-dihydroxyl-2-butanone 4-phosphate
DIBALH	diisobutylaluminum hydride
dist. H ₂ O/ dd. H ₂ O	deionized water
DMAP	4-(dimethylamino)-pyridine
DMF	N,N-dimethylformamide
DNA	deoxyribonucleic acid
dNTP	deoxynucleoside triphosphate
DTT	dithiothreitol
<i>E. coli</i>	<i>Escherichia coli</i>
EDTA	ethylenediaminetetraacetic acid
FAD	flavin adenine dinucleotide
FMN	flavin mononucleotide
FMNH ₂	reduced flavin mononucleotide
FMNHOOH	flavin mononucleotide -4a-hydroperoxide
FMNHOH	hydroxyflavin mononucleotide
FRET	Förster resonance energy transfer
g	gram
GTP	guanosine triphosphate
h	hour
HCl	hydrogen chloride
HGT	horizontal gene transfer
HPLC	high performance liquid chromatography
HPLC-MS	HPLC-mass spectrometry
IPTG	isopropyl β-D-1-thiogalactopyranoside
ITC	isothermal titration calorimetry
K _d	dissociation constant
K _i	inhibition constant
K _m	Michaelis-Menten constant
KCl	potassium chloride
kDa	kilo Daltons
LB	Lysogeny broth
lumazine	6,7-dimethyl-8-ribityllumazine
LumP	lumazine protein
LuxAB	bacterial luciferase
LuxC	NADPH-dependent acyl protein reductase

LuxD	acyl-transferase
LuxE	acyl-protein synthetase
LuxF	scavenger of flavin derivatives (<i>e.g.</i> myrFMN)
LuxG	NAD(P)H-dependent flavin reductase
MALDI	matrix assisted laser desorption ionization
MeOH	methanol
MgCl ₂	magnesium chloride
MgSO ₄	magnesium sulfate
min	minute
mL	milliliter
mM	milli-molar
MnO ₂	manganese(IV) oxide
MS	mass spectrometry
myrFMN	6-(3'-(<i>R</i>)-myristyl)-FMN
m/z	mass to charge
NaCl	sodium chloride
NaHCO ₃	sodium bicarbonate
NaH ₂ PO ₄	sodium dihydrogen phosphate
NCBI	National Center for Biotechnology Information
NiSO ₄	nickel-sulfate
OD ₆₀₀	optical density at 600 nm
ODC	overday culture
ONC	overnight culture
P ₄ O ₁₀	phosphorus pentoxide
PAGE	polyacrylamide gel electrophoresis
PCR	polymerase chain reaction
PDB	protein data base
PMT	photo multiplier tube
rep-PCR	repetitive element palindromic PCR
RibA	GTP cyclohydrolase II
RibB	DHBP synthetase
RibE	riboflavin synthetase
RibF	riboflavin kinase
RibH	lumazine synthetase
rpm	rounds per minute
SDS	sodium-dodecyl-sulfate
SDS-PAGE	SDS-polyacrylamide gel electrophoresis
stearylFMN	octadecanoyl FMN
TEMED	tetramethylethylenediamine
TFA	trifluoroacetic acid
THF	tetrahydrofuran
TLC	thin layer chromatography
Tris	2-amino-2-(hydroxymethyl)propane-1,3-diol
UV-Vis	ultraviolet-visible
XIC	extraction ion chromatogram
YFP	yellow fluorescent protein

VIII. Contributions

Chapter I: Molecular Mechanisms of Bacterial Bioluminescence

For this review, I performed extensive BLAST searches on NCBI of known *lux* operon sequences of bioluminescent bacteria. Starting from *Photobacterium leiognathi* subsp. *mandapamensis* ATCC 27561, where the gene sequence of the whole *lux-rib* operon is known, all obtainable bioluminescent bacterial strains with the core genes *luxCDABE* were identified. All obtained strains were reanalyzed in order to determine all related sequences. After thorough evaluation, 49 bioluminescent bacterial strains were compiled and summarized in Supplementary Table 1 building the basis for sequence alignments to calculate conservation scores. Furthermore, I concentrated on the chapters introduction, ecology, phylogeny, the *lux* operon, enzymes and reaction mechanisms in bacterial bioluminescence, genes associated with the *lux* operon and conclusion. I described the gene order of the *lux* operons and explained all enzymes and their general reaction mechanisms in bacterial bioluminescence. I give an overview on genes associated with the *lux* operon, such as the *rib* genes and give an introduction to change in color of light emission. I prepared all figures in those subchapters mentioned above, supplementary table 1 and all schemes.

Chapter II: Synthesis of α,β -unsaturated aldehydes as potential substrates for bacterial luciferases

I contributed to this work by synthesizing four different long chain unsaturated aldehydes, together with JAKOV IVKOVIC. Furthermore, I heterologously expressed and affinity-purified bacterial luciferases from three different strains. Together with CHAITANYA R. TABIB, I evaluated these newly synthesized unsaturated aldehydes and commercially available saturated aldehydes as substrates for the three purified bacterial luciferases and compared their enzymatic activity and light intensities. Additionally, molecular dockings of the bacterial luciferase from *Vibrio harveyi* with the reaction intermediate flavin-4a-hydroperoxide and various long chain aliphatic aldehydes were performed by me. The paper was mainly written by me with the contribution of JAKOV IVKOVIC for the synthesis part and help and revision of ROLF BREINBAUER and PETER MACHEROUX.

Chapter III: Evidence for the generation of myristylated FMN by bacterial luciferase

For this paper, my contribution was expression and purification of all proteins and cofactors. CHAITANYA R. TABIB performed biochemical assays and analyzed the formation of myrFMN versus light emission in various bioluminescent bacterial strains. Furthermore, he determined the IC_{50} value of myrFMN and the bacterial luciferase of *Photobacterium leiognathi* S1. CHAITANYA R. TABIB and I optimized and performed the *in vitro* multiple turnover assays. I isolated and analyzed the reaction products of these assays via HPLC. I further confirmed the cofactor molecule via HPLC-MS. CHAITANYA R. TABIB, PETER MACHEROUX and I wrote the manuscript. I focused on material methods and results for the HPLC analyses (figures 3 and 4; schemes 1 and 2) and prepared the complete supplementary information.

Chapter IV: *In situ* measurement and correlation of cell density and light emission of bioluminescent bacteria

JOHANNES NIEDERHAUSER and I designed an *E. coli* based *lux* operon expression system. I performed the genetic experiments, heterologously expressed and analyzed the *lux* operon's gene products *in vivo*. I designed a plate reader assay together with a script for this specific measurement and performed all measurements with different strains and media. I wrote the manuscript and prepared all figures and the protocol with supervision of PETER MACHEROUX. Additionally, I performed the complete revision, prepared the film script and organized all preparations for the film day. JOHANNES NIEDERHAUSER, PETER MACHEROUX and I participated in the video shoot while all experiments during video recordings were performed by me.

Chapter V: The impact of LuxF on light intensity in bacterial bioluminescence

JOHANNES NIEDERHAUSER and I designed an *E. coli* based *lux* operon expression system. I performed the initial genetic experiments and the heterologous expression leading to light emission of modified *E. coli* strains. Together with CHRISTINA HORN, we analyzed light intensities and growth curves of these newly designed expression systems. Furthermore, we isolated the side products of the bioluminescent reaction and analyzed them on HPLC and HPLC-MS. HANSJÖRG WEBER performed the NMR measurements of these isolated side products. I wrote the manuscript and prepared all figures with the support of JOHANNES NIEDERHAUSER and PETER MACHEROUX.

IX. List of publications

Publications in peer-reviewed journals

- Brodl, E., Winkler, A., Macheroux, P., Molecular Mechanism of Bacterial Bioluminescence, CSBJ, 2018, accepted.
- Brodl, E., Ivkovic, J., Tabib, C., Breinbauer, R., Macheroux, P., Synthesis of α,β -unsaturated aldehydes as potential substrates for bacterial luciferases, *Bioorg. Med. Chem.*, 2017, 25, 4, 1487-1495.
- Tabib, C., Brodl, E., Macheroux, P., Evidence for the generation of myristylated FMN by bacterial luciferase, *Mol. Microbiol.*, 2017, 104, 6, 1027–1036.
- Brodl, E., Niederhauser, J., Macheroux, P. *In Situ* Measurement and Correlation of Cell Density and Light Emission of Bioluminescent Bacteria. *J. Vis. Exp.*, e57881, doi:10.3791/57881 (2018).

Lecture on an international conference

- 20th International Symposium on Bioluminescence and Chemiluminescence: LuxF: a rescue factor in bacterial bioluminescence? Nantes, France, 31.05.2018

Lectures within the DK program Molecular Enzymology

- 19th Doc Day NAWI Graz Doctoral Schools Molecular Biosciences and Biotechnology: Teaching *E. coli* to shine, Graz, Austria, 09.02.2018
- Graduate Seminar: *luxF*: a rescue factor in bacterial bioluminescence? Graz, Austria, 30.06.2017
- Graduate Seminar: Role of enzymes involved in Bacterial Bioluminescence, Graz, Austria, 07.01.2016

Poster presentations on international conferences

- Gordon Research Seminar and Conference: Enzymes, Coenzymes and Metabolic Pathways (GRS/GRC): LuxF and its various roles in bacterial bioluminescence, Waterville Valley, NH, USA, 21.7.-27.7.2018
- 19th International Symposium on Flavins and Flavoproteins: Genomic integration of *luxF* into the *Vibrio harveyi lux* operon, Groningen, Netherlands, 02.-06.07.2017
- 8th International Congress on Biocatalysis (Biocat) 2016: *In vitro* bioluminescence: an enzyme cascade producing myrFMN, Hamburg, Germany, 28.08.-01.09.2016
- 2015 International Chemical Congress of Pacific Basin Society (Pacifichem): The role of luciferase in myrFMN formation, Honolulu, Hawaii, 15.-20.12.2015
- 12th International Symposium on Biocatalysis and Biotransformations (Biotrans) 2015: The mystery of myrFMN production by bioluminescent bacteria, Vienna, Austria, 26.-31.7.2015

Poster presentations within the DK program Molecular Enzymology

- 17th Doc Day NAWI Graz Doctoral Schools Molecular Biosciences and Biotechnology: Bacterial bioluminescence: the *in vitro* formation of myrFMN, Graz, Austria, 03.02.2017
- Joint DK Meeting: Towards *in vitro* bioluminescence: exploiting bacterial luciferases, Semmering, Austria, 29.-30.9.2016
- 8th ÖGMBT Annual Meeting: Towards *in vitro* bioluminescence: exploiting bacterial luciferases, Graz, Austria, 12.-14.09.2016
- 16th Doc Day NAWI Graz Doctoral Schools Molecular Biosciences and Biotechnology, New insights in bacterial bioluminescence: *in vitro* myrFMN production, Graz, Austria, 07.07.2016
- 14th Doc Day NAWI Graz Doctoral Schools Molecular Biosciences and Biotechnology, The mystery of myrFMN production by bioluminescent bacteria, Graz, Austria, 06.07.2015

Science communication

- 15th Doc Day NAWI Graz Doctoral Schools Molecular Biosciences and Biotechnology, Member of the organizing committee Graz, Austria, 05.02.2016

X. Curriculum Vitae

Name Eveline Brodl, BSc MSc
Address Theodor Körnerstraße 169, 8010 Graz
Date of Birth 12.08.1990, Deutschlandsberg, Austria
E-Mail eveline.brodl@gmail.com
Telephone +43 681 81578779



Education

- Sep 2014 – Jan 2019 **PhD in Biochemistry**
 Institute of Biochemistry, Graz University of Technology
 DK Molecular Enzymology
 Supervisor: Univ.-Prof. Dr. rer. nat. Peter Macheroux
 PhD-Thesis: A short story of living lights: Functional studies on the role of LuxF and flavin derivatives in bacterial bioluminescence
Methodology: standard cloning methods, heterologous expression and purification of proteins, protein biochemistry (enzymatic biocatalytic transformations, activity assays, FPLC, plate reader assays, UV/Vis spectroscopy), bioinformatics, product analysis (HPLC-MS and NMR analysis), basic crystallization techniques
- Feb 2012 – Jul 2014 **Master of Science in Biochemistry and Molecular Biomedicine**
 NAWI Graz: Graz University of Technology and University of Graz
 Master-Thesis: *Study of the S-Methyltransferase Botmt*
 Supervisor: Dipl.-Ing. Dr.tech. Mandana Gruber
 Institute of Organic Chemistry, Graz University of Technology
Methodology: organic synthesis of modified cofactors, enzymatic biocatalytic transformations, heterologous expression and purification of proteins, GC, TLC, HPLC and NMR analysis
- Jan 2013 – Jul 2013 **Erasmus stay** in Stavanger, Norway
 Universitetet i Stavanger
 Topics: Protein Biochemistry, Food Microbiology and Organic Retrosynthesis
- Oct 2008 – Feb 2012 **Bachelor of Science in Chemistry**
 NAWI Graz: Graz University of Technology and University of Graz
 Bachelor-Thesis: *Synthese von Inhibitoren der Adipose Triglyceride Lipase (ATGL)*
 Institute of Organic Chemistry, Graz University of Technology
Methodology: chemical synthesis of molecules under inert atmosphere, GC, TLC, HPLC and NMR analysis
- Sep 2000 – Jun 2008 **Matura (A-levels)**, graduated with honors
 Bischöfliches Gymnasium Graz

Soft skills

Apr 2018	Managing Cross-Cultural Conflicts
Apr 2018	Leading Diverse Teams
May – Jun 2017	Managing (Research)-Projects – Project Management

Work experience

Sep 2016 – Jan 2019	University assistant at the Institute of Biochemistry Lecturer and supervising tutor in various lab courses at the Institute of Biochemistry Supervisor of Bachelor and Master students
Aug 2013 – Dec 2013	ACIB Graz Laboratory project assistant and researcher during master thesis <i>heterologous expression and purification of proteins, biochemical characterization</i>

Qualifications

Language skills	German (native) English (fluent spoken and written) French (basic) Norwegian (basic)
Computational skills Bioinformatic tools	MS Office, CorelDraw (basic) Yasara (basic) Pymol (basic) Origin ChemiBioDraw MestReNova

Interests

Sports	Swimming, Skiing, Badminton, Dancing
Travelling	Exploring new countries